University of Hamburg

Doctoral Thesis

The B7 protein family as ligands for Killer Cell Immunoglobulin-like Receptors (KIRs)

Author:
Nils Dominik Lonken

Supervisor:
Prof. Dr. Marcus Altfeld

A thesis submitted in fulfilment of the requirements
for the degree of DOCTOR RERUM NATURALIUM (Dr. rer. nat.)

in the

Research Group of Virus Immunology
Department of Biology

Hamburg, February 2024

The following evaluators recommended the admission of the dissertation:

First supervisor: **Prof. Dr. Marcus Altfeld**, Research Department Virus Immunology, Leibniz Institute of Virology, Hamburg, Germany

Second supervisor: **Prof. Dr. Thomas Dobner**, Research Department Viral Transformation, Leibniz Institute of Virology, Hamburg, Germany

First reviewer: **Prof. Dr. Tobias Lenz**, Research Department Evolutionary Immunogenomics, University of Hamburg UHH, Hamburg, Germany

Second reviewer: **Prof. Dr. Julia Kehr**, Research Department Molecular Plant Genetics, University of Hamburg UHH, Hamburg, Germany

Submitted by: Nils Dominik Lonken

Submitted on: 17.02.2024

Date of disputation: 15.07.2024

Abstract

Nils Dominik Lonken

The B7 protein family as ligands for Killer Cell Immunoglobulin-like Receptors (KIRs)

Killer cell immunoglobulin-like receptors (KIRs) were first described on NK cells and CD8 T cells but are known to be present on more immunological subsets [1–5]. Interestingly, all 15 known *KIR* genes are encoded in the *MHC* region and are extensively characterised besides *KIR3DL3* [6–9]. *KIR3DL3* which was long considered to be a pseudogene, as no protein was detectable on the cell surface nor intracellularly, is evolutionarily conserved among humans [10]. Besides of its lacking proof of expression KIR3DL3 was considered an orphan receptor until recently B7-H7 (HHLA2) was identified as ligand for KIR3DL3 [11]. The B7 protein family itself, first described as receptors of B cells, contains a collection of important immunological molecules such as B7-1 (CD80), B7-2 (CD86) and B7-H1 (PD-L1) which are known regulators of T cells of the adaptive immune response [12–15]. Furthermore, the family contains NK cell regulators such as B7-H6 for the NK cell activating receptor NKp30 [16]. The thesis therefore tries to identify potential additional KIR B7 protein interactions through the methods of a protein based high throughput screen (HTS) and follows up on potential new interaction partners with cell-based binding and cytotoxicity assays to investigate a possible biological relevance. The distribution of identified interaction partners in humans are assessed through compartment studies. Overall, the HTS identified the known interaction partners of KIR3DL3 & B7-H7, NKp30 & B7-H6 and a novel interaction of KIR3DL2 & B7-H1 (PD-L1) which could not be validated on a cellular basis. The follow up experiments focusing on the KIR3DL3 & B7-H7 interplay confirmed the inhibitory nature of the interaction on a cellular level. Furthermore, peripheral blood is a compartment in which both receptors are present and could interact. In summary, the presented dissertation points out that the function of the KIR3DL3 receptor remains poorly understood and characterised. Furthermore, the key role within the human immune system is not solved. Future work will have to focus on potential effects of KIR3DL3 knock outs to shed light on the question why the gene is evolutionarily conserved, yet only scarcely expressed on different tissues and cell systems in different individuals. Additionally, it is of interest to understand the role of the KIR3DL3 & B7-H7 axis in infectious diseases as both molecules are

present on important immune cells. B7-H7 is highly overexpressed in multiple tumours such as renal cell carcinoma, acute lymphoblastic leukaemia, non-small lung cancer, gallbladder, and stomach cancer [11, 17–26]. Some answers to the elusive interaction might also come from clinical trials as a novel checkpoint antigen. The ongoing clinical phase I trials of the monoclonal antibodies NPX267 and HBM1020 targeting the KIR3DL3 & B7-H7 axis may help to shed light on the significance of the interaction.

Zusammenfassung

Nils Dominik Lonken

Die B7 Proteinfamilie als Liganden für Killerzell-Immunglobulin-ähnliche Rezeptoren (KIRs)

Killerzell-Immunglobulin-ähnliche Rezeptoren (KIRs) wurden zuerst auf NK Zellen und CD8 T Zellen nachgewiesen. Heute weiß man jedoch, dass sie auch auf anderen Immunzellen vorhanden sind [1–5]. Interessanterweise sind alle 15 bekannten *KIR* Gene in der *MHC* Region codiert und bis auf *KIR3DL3* ausführlich charakterisiert [6–9]. *KIR3DL3*, welches lange Zeit als Pseudogen behandelt wurde, da man keine Proteinexpression auf der Zelloberfläche oder innerhalb der Zelle nachweisen konnte, ist in allen Menschen konserviert [10]. Ein zusätzlicher Grund, weshalb *KIR3DL3* als Pseudogen behandelt wurde, war das kein Ligand bekannt war, bis kürzlich B7-H7 (HHLA2) als solcher identifiziert wurde [11]. Die B7 Proteinfamilie, welche zuerst auf B Zellen beschrieben wurde, umfasst eine Reihe von wichtigen immunologischen Rezeptoren. Darunter B7-1 (CD80), B7-2 (CD86) and B7-H1 (PD-L1), welche alle für ihre T Zellregulation der adaptiven Immunantwort bekannt sind [12–15]. Zusätzlich enthält die Familie NK Zell Rezeptoren wie B7-H6, welcher NK Zellen via des NKp30 Rezeptors aktivieren kann [16]. Die vorgelegte Dissertation versucht zusätzliche Interaktionen von KIR und B7 Protein mittels eines proteinbasierten Hochdurchsatzscreens zu identifizieren (HTS). Weiterhin werden gefundene Interaktionspartner durch zellbasierte Bindungsexperimente und Zelltoxizitätsexperimente auf ihre biologische Funktion hin untersucht. Im letzten Schritt werden die Interaktionspartner im humanen System auf ihre Interaktion hin untersucht. Insgesamt konnte mit dem HTS die bereits bekannten Interaktionen von KIR3DL3 & B7-H7, sowie NKp30 & B7-H6 und eine neue Interaktion zwischen KIR3DL2 & B7-H1 (PD-L1) identifiziert werden, wobei letztere auf zellulärer Basis nicht bestätigt werden konnte. Die folgenden Experimente fokussierten sich daher auf das Zusammenspiel von KIR3DL3 & B7-H7 und bestätigten die inhibitorische Funktion der Interaktion. Zusätzlich konnte Blut als humanes Kompartiment identifiziert werden, in dem beide Rezeptoren vorhanden sind. Zusammenfassend stellt die Dissertation dar, dass die Funktion des KIR3DL3 Rezeptors und der ihn exprimierenden Zellen immer noch nahezu unverstanden ist. Zudem ist nicht zu erkennen, warum der Rezeptor evolutionär

konserviert ist, obwohl er nahezu nicht auf der Oberfläche präsentiert wird. Zukünftige Arbeiten werden sich damit befassen müssen, welche Auswirkungen ein Verlust des KIR3DL3 Rezeptors hat. Zudem wird es von besonderer Bedeutung sein, die Rolle der KIR3DL3 & B7-H7 Interaktion in viralen oder bakteriellen Krankheiten zu verstehen, da beide Rezeptoren auf wichtigen immunologischen Zellgruppen vorhanden sind. Bisher weiß man lediglich, dass B7-H7 in diversen Krebsarten überexprimiert wird, wie zum Beispiel in Nierenkrebs, akut lymphatischer Leukämie, nicht-kleinzelligen Lungen- karzinomen, Gallenblasenkrebs und Magenkrebs und dies meist unabhängig vom immunologischen Checkpoint Molekül B7-H1 (PD-L1), welches schon lange in erfolgreich in der Krebstherapie eingesetzt wird [11, 17–26]. Ein paar der Antworten zu eben jenen Fragen, werden auch durch klinische Studien beantwortet werden, wie zum Beispiel die Phase I Studien zu den monoklonalen Antikörpern NPX267 und HBM1020, die sich gegen die KIR3DL3 & B7-H7 Interaktion richten.

Acknowledgements

After a long journey, I want to take the opportunity to warmly thank:

Marcus Altfeld for providing the dissertation topic and his supervision together with excellent scientific advice and continuous support throughout the entire project.

Thomas Dobner for additional input on the project and his expertise on human adenoviruses. Invitations to your group meetings gave me lots of fruitful thoughts for the project.

Benedetta and **Pia** for their day-to-day expertise, the many fruitful scientific discussions, and the help to find my way around in the new lab when I started my journey in Hamburg.

Mareike, Maria, and Sreejith who kept me motivated and cheered me up when I wanted to quit academia more than once. Now you can focus your effort on someone else.

Paloma and **Wingi** who helped me out multiple times with virus stocks and pep talks for work, which finally not got published.

Heike Hildebrandt and **Christin Illig** for their technical support and reminder E-Mails. You are the reason the lab organization is flawless.

My family for their support and never doubting me even though I did.

I warmly thank all other **colleagues** I met at the Leibniz Institute of Virology. The three years passed way too quick.

This thesis was supported through research funding by the **European research council (ERC)**.

The style template for the dissertation was adapted from **Steve Gunn** and **Sunil Patel** and licensed by overleaf under the number CC BY-NC-SA 3.0 [27]. Emblems of the university and institute were kindly provided by the **Leibniz Institute of Virology** and **Lucas Rieder** [28].

Contents

List of Figures

List of Tables

List of Abbreviations

2ndary	Secondary IgG Antibody
AA	Amino Acid
ADCC	Antibody Dependent Cell Cytotoxicity
AIDS	Acquired Immunodeficiency Syndrome
AML-2	Acute Myeloid Leukemia Protein 2
AKT	Protein kinase B
APC	Allophycocyanin
APCs	Antigen Presenting Cells
β2m	β2-Microglobulin
β2m-KO-Jurkat	JurkatE6.1-$\Delta\beta$m
BCR	B Cell Receptor
CAR	Chimeric Antigen Receptor
CCL	C-C Motif Ligand
CCR	C-C Chemokine Receptor
CD	Cluster of Differentiation
CD28H	Cluster of Differentiation 28 Homolog
cDNA	Complementary DNA
CLP	Common Lymphoid Progenitor
CMP	Common Myeloid Progenitor
CMV	Cytomegalovirus
CTL	Cytotoxic Lymphocyte
CTLA-4	Cytotoxic T Lymphocyte Associated Antigen 4
CV	Coefficient Of Variance
CXCL	C-X-C Motif Ligand
CXCR	C-X-C Chemokine Receptor
DAMPs	Damage-Associated Molecular Patterns
DC	Dendritic Cell
DMEM	Dulbecco's Modified Eagle's Medium
DMSO	Dimethyl Sulfoxide
DNA	Deoxyribonucleic Acid
ECM	Extracellular Matrix
Eppi	Eppendorf Cup
ER	Endoplasmic Reticulum
ERK	Extracellular-Signal Regulated Kinases
FACS	Fluorescence-Activated Cell Sorting
FasL	Fas Ligand
FBS	Fetal Bovine Serum
FC	Flow Cytometry
Fcγ Rs	Fc-Gamma Receptors
FcRL3	Fc Receptor Ligand 3
FMO	Fluorescence Minus One
FSC	Forward Scatter

GWAS	Genome-Wide Association Study
h	Hours
HAdV	Human Adenoviruses
HHLA2	Human-Endogenous-Retroviruses–H Long-Terminal Repeat Associating 2 (HHLA2)
HIV	Human Immunodeficiency Virus
HLA	Human Leukocyte Antigen
HTS	High Throughput Screen
IFN	Interferon
IFN-γ	Interferon Gamma
Ig	Immunoglobulin
IGPR-1	Immunoglobulin-Containing And Proline-Rich Receptor-1
IL	Interleukin
ITAM	Immunoreceptor Tyrosine-Based Activating Motif
ITIM	Immunoreceptor Tyrosine-Based Inhibition Motif
JAK	Janus Kinase
kBp	Kilo Base Pairs
KIR	Killer Cell Immunoglobulin-Like Receptor
KO	Knock Out
LFA-1	Lymphocyte Function-Associated Antigen 1
LPS	Lipopolysaccharide
MAD	Median Absolute Deviation
MAP	Mitogen-Activated Protein
MAPK	Mitogen-Activated Protein Kinase
MdFI	Median Fluorescence Intensity
MFI	Mean Fluorescence Intensity
MHC	Major Histocompatibility Complex
Min	Minutes
miRNA	Micro RNA
mRNA	Messenger Ribonucleic Acid
mTOR	Mammalian Target Of Rapamycin
NCAM	Neural Cell Adhesion Molecule
NCR	Natural Cytotoxicity Receptor
NFkB	Nuclear Factor “Kappa Light Chain Enhancer” Of Activated B-Cells
NGS	Next Generation Sequencing
NK	Natural Killer
NKD	Natural Killer Cell Immunodeficiency
NKG2	Natural Killer Group 2 Member Receptor
NSCLC	Non-Small-Cell Lung Cancer
P	Page
PAMPs	Pathogen-Associated Molecular Patterns
PBMC	Peripheral Blood Mononuclear Cell
PBS	Phosphate Buffered Saline
PD-1	Programmed Cell Death 1
PE	R-Phycoerythrin
PFA	Paraformaldehyde
PI3K	Phosphoinositide 3-Kinases
PKC	Protein Kinase C
PLC	Peptide-Loading Complex
PMT	Photomultiplier Tube

PRRs	Pattern Recognition Receptors
PVR	Poliovirus Receptor
R10	Roswell Park Memorial Institute Media + 10 % Fetal Bovine Serum
RAS	Rat Sarcoma Kinase
RAF	Rapidly Growing Fibrosarcoma Protein
RNA	Ribonucleic Acid
RPMI	Roswell Park Memorial Institute
RT	Room Temperature
SHP-1	Src Homology 2 Domain-Containing Protein Tyrosine Phosphatase 1
SHP-2	Src Homology 2 Domain-Containing Protein Tyrosine Phosphatase 2
SH2B3	Src Homology 2-B Adaptor Protein 3
siRNA	Small Interfering RNA
SPR	Surface Plasmon Resonance
SSC	Side Scatter
STAT	Signal Transducers And Activators Of Transcription
STAT4	Signal Transducer And Activator Of Transcription 4
TGF	Transforming Growth Factor
Th	T Helper
Th1	CD4 T Helper Cells Type 1
TLR	Toll-Like Receptor
TMD	Trans Membrane Domain
TNF	Tumor Necrosis Factor
TNF-α	Tumor Necrosis Factor- Trail
TRAIL	Tumor Necrosis Factor Related Apoptosis-Inducing Ligand
UKE	University Medical Center Hamburg-Eppendorf
UTR	Untranslated Region
VISTA	V-Domain Ig Suppressor Of T Cell Activation
VSV	Vesicular Stomatitis Virus
VSVG	Vesicular Stomatitis Virus Glycoprotein

To Matthias, hopefully someone
else will be more successful in
research so it was not all in vain.

1 Introduction

1.1 The structure and components of the human immune system

Throughout evolution, humans have been under constant selection pressure from invasive pathogens, which through various replication and dissemination strategies threatened the survival of the species and lead to the development of defense mechanisms [29]. In general, the developed mechanisms form the two arms of the human immune system: the innate immune response and the adaptive immune response [30, 31]. The innate immune response is the first responder, whenever a pathogen tries to enter the human body and is genetically encrypted in the germline, recognizing molecular patterns which are not naturally present in the mammalian host [30, 31]. The adaptive immune response is the second line of defence and consists of a small set of specialised cells, which, through genetic rearrangement, assemble antigen-binding molecules with unique specificity for diverse foreign structures and create a long lasting memory [30–32]. Both systems fundamentally rely on the ability to distinguish between intrinsic so-called "self" and external "non-self" molecules which was a concept first developed by Burnet *et al.* [31, 33, 34]. The concept describes the aversion of the immune system to any molecule which can not be intrinsically produced. The theory was later on extended by Janeway *et al.* who hypothesised that pathogens are recognised by germline encoded receptors which are primed for molecular signatures of foreign species not present in the host [34, 35].

The innate immune system consists of physical, mechanical, and chemical barriers, and a biochemical component including the complement system as well as myeloid and lymphoid cells, such as dendritic cells (DCs), granulocytes, innate lymphoid cells (ILCs), mast cells, monocytes/macrophages and natural killer (NK) cells (Figure 1.1) [31, 32, 36–39]. All mentioned cells contain so-called pattern recognition receptors (PRRs) which are encoded in the germline and recognise pathogen associated molecular patterns (PAMPs) and damage associated molecular patterns (DAMPs), while tolerating host molecules [32, 33, 36, 40, 41]. Upon binding of PAMPs and DAMPs to the PRRs, the cells of the innate immune system can activate and engage in phagocytosis of pathogens [32, 42–48]. The phagocytosis allows for parts of the digested pathogens to be presented on cell surface receptors, such as human leukocyte antigen (HLA) molecules, by macrophages and dendritic cells, linking the innate immunity

with the adaptive immunity [49]. On the other hand, the adaptive immunity stimulates the cells of the innate immune system, through the release of cytokines and opsonisation of pathogens through antibodies which enhance the ability of phagocytosis [50, 51].

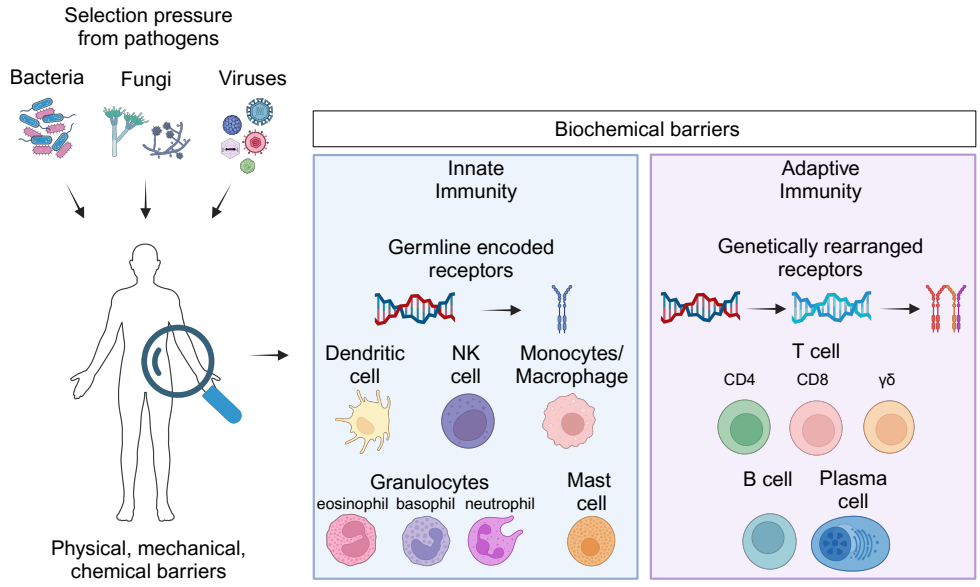

FIGURE 1.1: Overview of the immune system. Constant selection pressure from invasive pathogens lead to the development of an adaptive immune system. Shown are the cells of the innate and adaptive arm of the immune system. NK cells, monocytes/macrophages, granulocytes, and mast cells react in an unspecific manor. T cells and B cells alike allow for a specific pathogen response through genetically rearranged receptors and memory cells. This figure was adapted from Janeway *et al.* and Rodriguéz *et al.* and was created with BioRender.com [29, 48].

The innate immune receptors change over time through small germline mutations. Viruses and bacteria tolerate more mutations and have shorter generation times which allow them to escape immune system recognition [52–54]. Hence, the adaptive immune system developed as another branch of the immune system which countered the seemingly unlimited number of pathogens with a wide variety of highly specified receptors [33]. Key players of the adaptive immunity, which undergo a life-long training, are T cells and B cells with their respective T cell receptor (TCR) and B cell receptor (BCR) [32, 48]. Interestingly, each individual T cell and B cell can generate its own individual TCR or BCR through immunoglobulin chain rearrangement, V(D)J segment recombination and V(D)J segment hyper-mutation, matching the seemingly unlimited number of pathogens with a seemingly infinite number of unique receptors [32, 55–58]. The large number of receptors comes with the threat of auto-reactive T cells and B cells which need to be eliminated from the immune system through positive and negative selection as well as clonal deletion which is conducted in the thymus and bone marrow [59]. Only the T and B cells, somatically selected with low avidity to host molecules and high avidity to pathogens, can be allowed to circulate

through the human body or persist in one of its many lymph nodes and lymph organs [60, 61].

The somatically selected B cells can get activated upon binding of foreign proteins (antigens), to the BCR. Afterwards B cells tend to proliferate and differentiate into plasma cells with the ability to secrete antibodies with a specificity against the encountered antigen [32, 48]. Depending on the type of antibody, e.g. IgM or IgG the pathogen can get neutralized through surface receptor blockage or agglutination, which can then be phagocytosed by cells of the innate immune system [62]. During the maturation of the B cells, the BCR undergoes additional hyper-mutations to create a perfectly fitting antibody for the pathogen, which then can get secreted [63]. As it is dificult to opsonise or neutralise all pathogens before they start infecting cells, these infected cells also need to be identified and eliminated. This is achieved through a B cell and T cell cross-talk initiated by B cells. The B cells can endocytose BCRs with bound peptide fragments of the pathogens (antigens) and can present them on HLA molecules to T cells [32, 64]. T cells on the other hand can be divided in multiple subclasses, e.g. CD4, CD8 and $\gamma\delta$ T cells, named after their expressed receptors [32, 65]. CD4 T cells can get activated via foreign peptides presented on HLA class II molecules and facilitate immunological cross-talk between antigen presenting cells (APCs) and CD8 T cells [66]. Furthermore, they can help to shape the entire immune response through the release of cytokines including interferons (IFNs) and interleukins (ILs) [32, 67–70]. On the other hand, CD8 T cells, also called cytotoxic T cells, can get activated via the recognition of foreign peptides presented on HLA class I molecules [71, 72]. The key role of CD8 T cells is to kill transformed or infected cells through the release of cytotoxic granules [32, 73–75]. $\gamma\delta$ T cells are the most recently discovered T cells which can mainly be found in tissues of the skin, lung and intestine [76]. Interestingly, they exhibit the ability to detect antigens in an HLA independent manner and can rapidly produce large quantities of cytokines which give them a unique role in inflammation responses as well as immune homeostasis [77, 78]. Furthermore, they exhibit both innate and adaptive immunity characteristics such as phagocytosis as well as memory phenotypes making them an interesting bridge between the two parts of the immune system [78, 79].

Taken together, the interplay between the two parts of the immune system might be the key to success [80]. As the production of antibodies, expansion of B and T cells and the formation of memory cells is slow, the innate immune system needs to take over until a highly specific adaptive immune response can follow [31, 32, 48]. In this way the manifestation of a chronic infection can be prevented [31, 81]. The key advantage of the adaptive immunity, which might have allowed humans to stay ahead of their microbiological foes, is that the created memory cells can persist in a dormant state and quickly reactivate in case of a reinfection, what can allow for a quick pathogen clearance [69, 82–85].

1.2 The role of NK cells in the human immune system

1.2.1 Discovery and characterisation of NK cells

Natural killer (NK) cells were first described by Kiessling *et al.* and Herbermann *et al.* who both independently from each other reported in 1975 a new type of cells which exhibited cytotoxic characteristics in non-immunised mice shortly after the exposure to a moloney leukaemia virus-induced lymphoma cell line YAC and other cancer cell lines [86, 87]. Not much later, cells with similar characteristics were described in humans [88, 89].

In the years that followed Lanier *et al.* tried to characterize NK cells through the presence of CD56 and CD57 and the absence of CD16 and CD3 receptors [90–92]. NK cells are characterized through the absence of CD3, CD14, CD19 and CD34 receptors and the presence of CD7, CD45 and CD56 receptors [31, 93]. Furthermore, they can be sub-divided into $CD56^{bright}$ and $CD56^{dim}$ populations depending on the amount of CD56 receptors on their cell surface and whether CD16 receptors are present [94]. While $CD56^{bright}$ populations do not tend to express the CD16 receptor but high amounts of CD56 they tend to produce higher amounts of cytokines than their $CD56^{dim}$ counterpart [31, 32, 94]. $CD56^{dim}$ NK cells on the other hand, tend to present high amounts of the CD16 receptor and killer cell immunoglobulin-like receptors (KIRs) on their cell surface and show enhanced cytotoxicity [94].

Overall, NK cells make up 5 - 15 % of all peripheral blood mononuclear cells (PBMCs), with an average 9:1 ratio between $CD56^{dim}$ and $CD56^{bright}$ NK cells [31, 32, 93–95].

1.2.2 NK cell effector functions

NK cells can engage on the forefront of infection control, clearance, and placentation of the trophoblast [96, 97]. This is achieved through two main effector functions: 1) the cytotoxic lysis of infected or abnormal cells and 2) through the release of inflammatory cytokines (Figure 1.2) [32, 98].

The first process of cytotoxic lysis is a highly regulated process and occurs in three steps upon chemotactic attraction of the NK cell. First, the infected or abnormal target cell is recognized, second an immunological synapse is formed and finally the target cell killed through degranulation [98]. To identify target cells, NK cells constantly screen their surrounding. If they notice the missing of host receptors ("missing-self") or recognize a foreign receptor ("non-self") which might pose a threat they might get activated (subsection 1.2.4, page 7) [99, 100]. This non-self-recognition can also be enhanced through antibody opsonised pathogens recognised via CD16 [31, 32, 101]. In the next step the NK cell can dock to the target cells through integrins and CD11 receptors [102]. Then the immunological synapse can be formed consisting of activated NK cell receptors, filamentous actin and granules filled with granzyme B, perforin, or

death receptor ligands (PD-Ls) [98, 102–104]. Upon a Ca^{2+} influx into the NK cell death receptor ligands can be released which bind e.g., the FAS or TRAIL receptor and trigger apoptosis via the caspase-cytochrome C pathway. Additionally, granzyme B and perforin can get released which trigger pore forming and the caspase pathway through cleavage of caspases or Bid protein [105–113]. An effective way to monitor NK cell degranulation was previously shown by our laboratory and includes the measurement and staining of CD107a, a receptor which is included in the cytotoxic granules and is displayed on the cell surface of NK cells after degranulation took place [114].

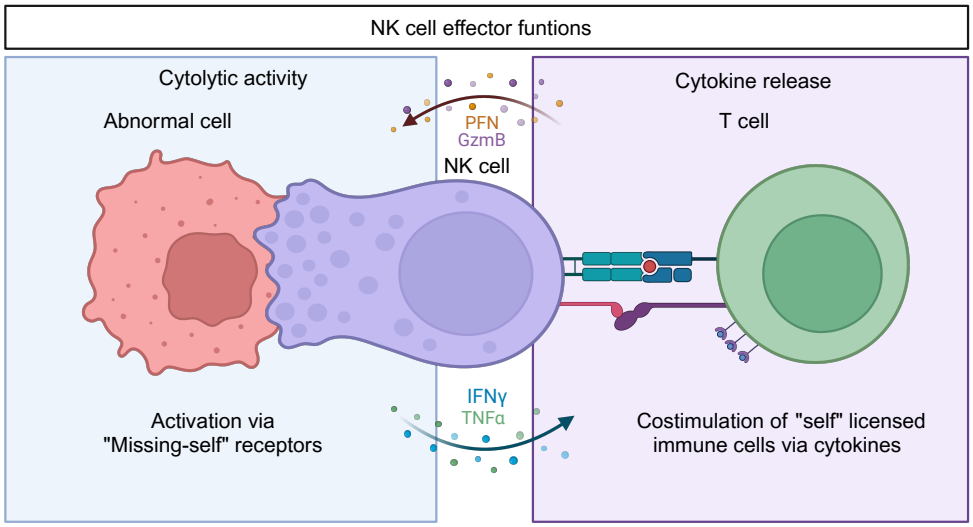

FIGURE 1.2: NK cell effector functions. NK cells can engage in infection control and clearance through cytotoxic lysis of abnormal cells and the release of inflammatory cytokines to activate additional players of the immune system. This figure was adapted from Abel *et al.* and was created with BioRender.com [98].

The release of inflammatory cytokines on the other hand is highly dependent on external stimuli and their activation kinetics are distinct [115, 116]. Cytokines and chemokines are mainly released by $CD56^{bright}$ NK cells [32, 117, 118]. Most cytokines belong to the T helper cell one (Th1) sub-group including interferons and homing factors which in turn can activate other cells of the immune system such as APCs and T cells [32, 96, 101, 119–122]. The combination of cytokines and chemokines, furthermore, released by NK cells, also allow for trophoblast recognition during placentation and uterine endothelial remodelling [97]. The absence of these biochemical signals can lead to poor placentation with stillbirth, miscarriage, preterm labor, fetal growth restriction, preeclampsia, and eclampsia [97, 123].

1.2.3 Examples of NK cell receptors and ligands

NK cells can express a variety of different receptors on the cell surface to allow for a tight control and regulation. They can be broadly divided into the five categories of activating, inhibiting, cytokine, chemotactic and adhesion receptors [96, 124]. While the activating receptors can trigger cytotoxicity of NK cells through degranulation,

inhibiting receptors might prevent NK cells from degranulating [96]. Cytokine receptors on the other hand, can allow for survival and co-stimulatory activation signals, e.g. IL-2 and chemotactic receptors can allow for recruitment of NK cells to locations of pathogen presence [96]. The adhesion receptors finally can allow the cell to stay in place while conducting their killing activity [96].

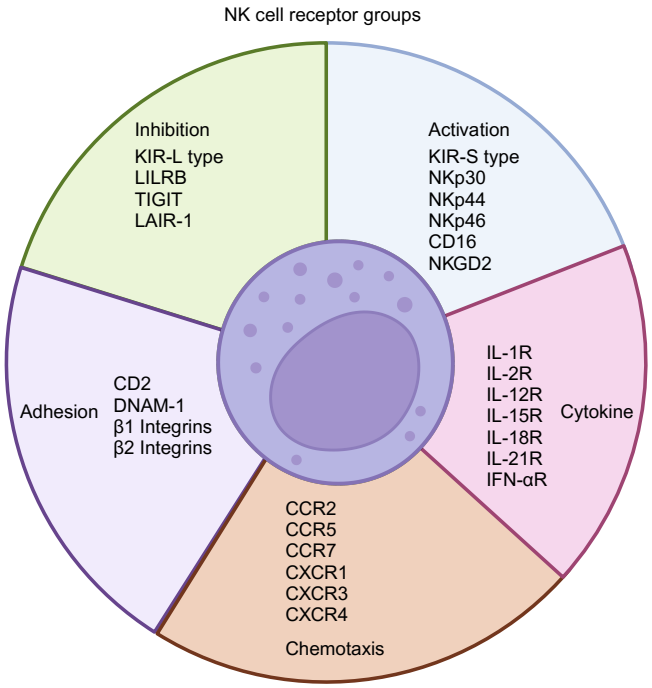

FIGURE 1.3: NK cell receptor groups. NK cells display a plethora of receptors on their cell surface which can be grouped into five main categories: activating receptors, cytokine receptors, chemokine receptors, adhesion receptors and inhibitory receptors. This figure was adapted from Vivier *et al.* and was created with BioRender.com [96, 124].

However, as this picture of receptor groups might be straight forward the details are more complex. The function of receptors can depend on the ligand bound. Due to different ligands one receptor can be activating or inhibiting. One example is NKp30 which upon binding of B7-H6 activates the NK cell but upon binding of Pp65 from cytomegalus virus (CMV) inhibits the NK cell [125]. Besides receptors which can act as an activating and inhibiting receptor NK cells can get both activating and inhibiting signals from different receptors, e.g. from different KIRs, at the same time which makes a proper signal integration necessary (subsection 1.3.1, page 9). Interestingly, inhibitory signals thereby always override activating signals making them an interesting target for novel drug developments [126, 127]. Additionally, NK cells can get activated through CD16 receptors via the constant region of antibodies which are bound to opsonised pathogens triggering an antibody dependent cellular cytotoxicity (ADCC) [31, 32, 128–130]. To add another layer of complexity to the NK cell receptors, not all individuals carry the same genes for NK cell receptors and the expression of receptors differs among NK cells of each individual [131]. As one NK cell within a

human might express high levels of KIR3DL1 protein on the cell surface while another cell might have completely silenced the gene. Henceforth, the diversity of NK cells and their receptors seems to resemble the manifold of pathogens they target.

1.2.4 Mechanisms of NK cell education and licensing for "self" tolerance and “missing-self” detection

After the principle of "self" and "non-self" detection introduced by Burnet *et al.* was widely accepted, the field could not explain experiments in which some target cells would be easily killed by NK cells but not by cytotoxic T cells and vice versa [132]. Later experiments found, that cells killed by cytotoxic T cells but not NK cells expressed a high amount of major histocompatibility complex (MHC)/HLA molecules on the cell surface while cells prone to kiling by NK cells did not show MHC/HLA molecules leading to the "missing-self" hypothesis [132–135]. The hypothesis centres around the idea that NK cells frequently monitor the peptides presented on HLA class I molecules through inhibitory receptors such as Killer cell Immunoglobulin-like Receptors (KIRs) [99, 100]. Viruses can cause HLA molecule downregulation. Once the ligands for the inhibitory NK cell receptors are missing the activating signals within NK cells can over weigh and the NK cells start killing the cells with "missing-self" HLA molecules [31, 32, 96, 136–138].

NK cells which are able to recognize "missing-self", are activated via co-stimulation of activating ligands and show the highest immune response to cells with "missing-self" are referred to as educated NK cells [139, 140]. They are the largest group of NK cells within humans and can also be inhibited through inhibitory receptors to keep an immunological balance [141]. Uneducated or unlicensed NK cells on the other hand do exist as well and are characterised by the missing of receptors for "missing-self" recognition or activation [31, 142, 143]. It is postulated that they originate from autoreactive NK cells [92, 143–146]. Unlike T cells and B cells which undergo somatic selection and can get killed when they are autoreactive, autoreactive or uneducated NK cells exist but tend to show a general hypo-responsiveness towards any kind of activating signal preventing autoimmune diseases [31, 142, 144, 147]. However, the mechanisms involved for this type of reaction remain poorly understood [96, 139, 141].

1.2.5 NK cell development and memory effects

Due to the high heterogeneity of NK cells multiple theories as to how they develop exist [148]. The linear model proposes that NK cells derive from a common lymphoid progenitor (CLP) and through multiple maturation steps lose their ability to become T cells and B cells until they are determined to be an NK cell upon loss of CD34 expression and the expression of lymphocyte function-associated antigen (LFA-1) as point-of-no-return [93]. Interestingly, the linear theory also defines $CD56^{dim}$ NK cells as the final step of NK cells which derive from $CD56^{bright}$ NK cells (Figure 1.4) [149–151]. Specifically, the final step is highly controversial and does not explain, how

NK cells can exist with many different sub-populations. Henceforth, in recent years the branch theory has emerged, that NK cells derive both from CLPs and common myeloid progenitors (CMPs) into multiple NK cell populations with different receptor repertoires [131, 152, 153]. According to the branch theory CD56^{bright} and CD56^{dim} would then derive from different progenitors [148, 154]. Furthermore, the branch theory suggests, that depending on the infection, different sub-populations expand during the clearance and contract at their end with small numbers of cells to stay behind [155].

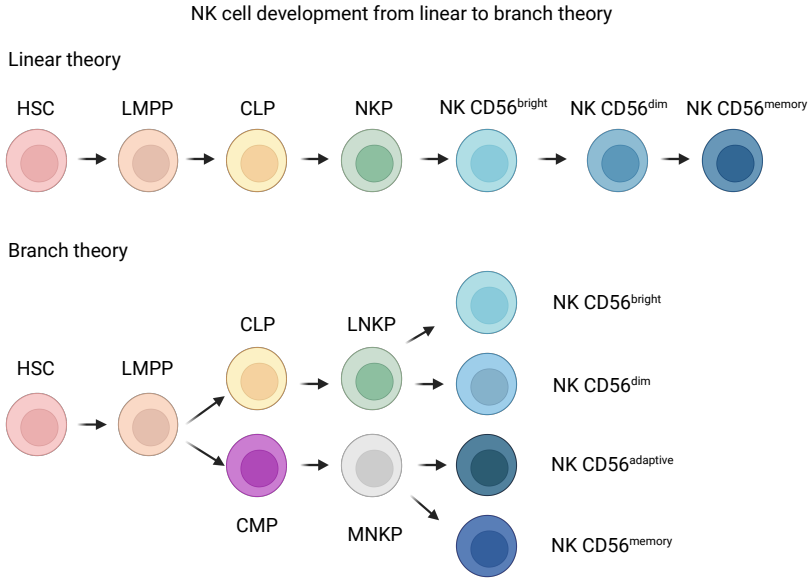

FIGURE 1.4: NK cell development. Two theories of NK cell development exist. While the linear theory sees CD56^{dim} as a developmental stage after CD56^{bright} cells the branch theory tracks them back to different progenitor cells. Henceforth, in the branch theory multiple NK cell sub-populations co-exist and can expand, while in the linear theory CD56^{bright} cells need to expand to create new CD56^{dim} cells. HSC = hematopoietic stem cell, LMPP = lymphoid myeloid primed progenitor, CLP = common lymphoid progenitor, CMP = common myeloid progenitor, LNKP = lymphoid NK cell progenitor, MNKP = myeloid NK cell progenitor. This figure was adapted from Cichoki *et al.* and was created with BioRender.com [148].

These small populations gave rise to the additional theory that memory NK cell exist, although they are not part of the adaptive immunity. The first hint in this direction was the observation that NK cells in mice can be sensitised by haptens and then persist for more than four weeks in the liver [156, 157]. Furthermore, a transfer of these NK cells into unsensitised mice allowed for hapten specific immunity [156, 157]. Similar results were found in macaques for Human-Immunodeficiency-Virus (HIV) proteins [158]. In humans the theory started to gain traction after cytomegalovirus (CMV) proteins were reported to shape the expression of NK cell receptors and allowed for NK cell expansion and persistence [159–162]. Multiple other research groups reported that memory-like NK cell states could also be induced via exposure to the cytokines

IL-12, IL-15 and IL-18 although the mechanisms behind remain elusive [163–165].

1.3 The role of Killer cell Immunoglobulin-like Receptors (KIRs) in the human immune system

1.3.1 Discovery and characterization of KIRs

Killer cell Immunoglobulin-like Receptors (KIRs) were first described by Harel- Bellan *et al.* and Moretta *et al.* in 1986 and 1990 as new surface markers for NK cells [1, 2]. It is proposed that they are not unique to NK cells but are also expressed by other lymphoid cells such as CD8 T cells [3–5, 166, 167].

Extensive genetic studies showed that in total 15 *KIR* genes and two *KIR* pseudogenes are encoded on chromosome 19q13.4 in the *MHC* region with a length of approximately 150 kBp and display many allelic polymorphisms due to extensive duplications and allele cross-overs (Figure 1.5) [6–9, 31]. The 15 genes are arranged in a head to tail fashion with 2 - 4 kBp spacer in between and can be grouped into the haplotypes A and B [168–170]. Haplotype A consists of the genes *KIR3DL3, KIR2DL3, KIR2DP1, KIR2DL1, KIR3DP1, KIR2DL4, KIR3DL1, KIR2DS4* and *KIR3DL2*. The haplotype B contains all others [90, 168]. The *KIRs* most likely derived from Ly49 genes 30 - 45 million years ago [171–173]. Besides being highly polymorphic, *KIR* genes show copy number variations and sequences of haplotypes can vastly differ [169]. Additionally, *KIR* genes can be completely absent, and each immune cell can show a unique *KIR* expression patterns increasing the complexity of NK cell biology [168, 170, 174].

KIRs are in general named and catalogued either after the cluster of differentiation (CD) nomenclature or according to their protein structures [170]. While the CD nomenclature allows for a global standardised identification according to the gene locus, it fails to represent the properties of sub-groups within the KIRs [172, 176]. For example, KIRs can be grouped by whether they contain two (2D) or three (3D) immunoglobulin-like (Ig-like) extracellular domains or a short (S) or a long (L) intracellular domain (Figure 1.5) [31, 177, 178]. Besides making KIR names more readable through protein structures like KIR3DL3 instead of CD158z they also allow for additional information for the reader. For example, KIR3D receptors contain D0-D1-D2 domains, while KIR2D receptors either contain D1-D2 (type I) or D0-D1 (type II) domains which imply different binding characteristics [169, 170, 179]. Furthermore, long intracellular domains (L) always come with immunoreceptor tyrosine-based inhibition motifs (ITIMs) making the entire receptor inhibitory while short intracellular domains (S) always come with immunoreceptor tyrosine-based activation motifs (ITAMs) making the entire receptor activating [31, 170, 180–184]. ITIMs can get phosphorylated via sarcoma (Src) tyrosine kinases. Afterwards they can recruit Src homology region 2-containing protein tyrosine phosphatase 1 & 2 (SHP-1&2) which dephosphorylates other signalling molecules inhibiting multiple receptor pathways [31, 48, 185–187]. ITAMs on the other hand, can be recruited through transmembrane proteins such

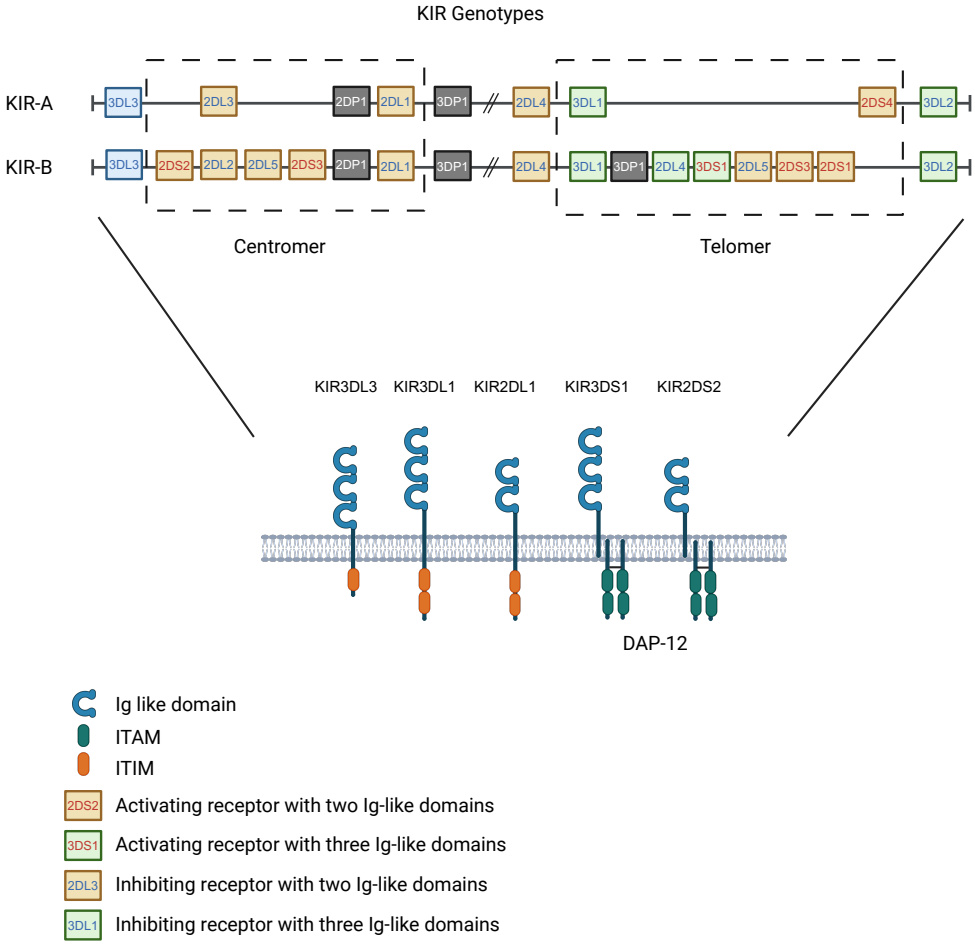

FIGURE 1.5: KIR loci and structures. In total 15 *KIR* genes and two *KIR* pseudogenes are encoded on chromosome 19q13.4 in the *MHC* region with a length of approximately 150 kBp. *KIR3DL3* is the only gene present in every human and is truncated in its transmembrane domain as well as its ITIMs. Activating KIRs with a short terminal domain recruit adapter proteins like DAP-12 for activating signals while inhibiting KIRs with a long terminal domain have ITIMs integrated in the receptor. This figure was adapted from Medjouel-Khlifi *et al.* and Parham *et al.* and was created with BioRender.com [97, 175].

as DAP-10 or DAP-12 which bind KIRs. Phosphorylated ITAMs can then in turn recruit tyrosine kinases such as PI3K-Grb2, Syk and ZAP-70 which activate the RAS-RAF-ERK, PIP2-PKC-NF-κB or PI3K/AKT pathway downstream leading to the activation of NK cells (Figure 7.7, page 142) [31, 48, 181, 188–193].

KIR3DL3 is a receptor consisting of three Ig-like extracellular domains (3D) linked to a long intracellular domain (L) with inhibitory ITIMs [10]. The free combination of extracellular and intracellular domains lead to 15 KIRs and in combination with lots of polymorphisms create a vast amount of different KIRs of which a more or less up to date gene and protein sequence can be found on the allele frequency net database website [194]. The high variety of KIRs causes that their ligands need to be diverse themselves. Looking at HLA receptors they do come in similar varieties and most

likely co-evolved with KIRs creating a perfect interaction tandem [123, 170, 171, 195].

1.3.2 Human Leukocyte Antigen (HLA) receptors as ligands for KIRs

Human Leukocyte Antigen (HLA) genes are located on chromosome 6p21.3 within the major histocompatibility complex (MHC) region and encode for so-called HLA class I and class II molecules [169, 196–201]. With more than 10,000 allele variants and polymorphisms they contain a plethora of unique receptors which can present different peptides to the cells of the immune system [169, 201–204]. While classical HLA class I receptors have long been known to bind KIRs, non-classical HLA class I and classical HLA class II molecules have only recently been described as KIR ligands [81, 124, 146, 169, 205–207]. HLA class I receptors mainly present proteins from the cytoplasm of nucleated cells and therefore potential pathogen particles from e.g., viruses while HLA class II receptors can present antigen fragments from endocytosed pathogens on APCs [169, 208–212].

Although KIRs as binding partners belong to the germline encoded receptors, they tend to show a sensitivity to the peptides presented on the HLA receptors and not just the presence or absence of HLA molecules [169, 213–218]. Henceforth, in this dissertation HLA receptors with specific peptide sequences will be used as positive controls for KIRs in the different experiments.

1.3.3 KIR3DL3: A unique KIR and mysterious receptor gets unravelled

Unlike multiple *KIRs*, which can be absent or present in human individuals depending on whether the gene is present or not, e.g. *KIR3DL1* or *KIR3DS1*, every human has exactly two gene copies of *KIR3DL3* which are located close to the centromere (Figure 1.5, page 10) [146, 219–223]. In fact *KIR3DL3* and the *KIR3DP1* pseudogene enclose the genes for the centromeric *KIR* section with *KIR2DS2, KIR2DL2/3, KIR2DL1, KIR2DS3* [7, 224]. Interestingly, the same location and similar sequences of *KIR3DL3* are evolutionarily highly conserved and can also be found in orang-utans, chimpanzees, gibbons and rhesus monkeys while other *KIRs* greatly differ [224–227]. Furthermore, only two splice variants are known which have no impact on the translated mRNA sequence [10]. Besides the predetermined gene allocation, *KIR3DL3* is highly polymorphic and heterozygous with more than 150 haplotypes especially in exon 1 - 5 while exons 7 - 9 show less variety [194, 223, 228]. The most frequent allotype in Europeans is *KIR3DL3*001* while globally *KIR3DL3*003*, **009* and **010* are the most prominent allotypes [223].

Previously, CD56^{bright} NK cells isolated from peripheral blood as well as decidual NK cells in pregnant woman were reported to express *KIR3DL3* mRNA at low levels [5, 10, 179, 219, 229]. Reasons for the low expression can be a high promotor methylation

which can be abolished through 96 h of 2 µM 5'2' deoxyazacytidine treatment, post-transcriptional miRNA silencing preferably through miRNA-26a-5p, miRNA-26b-5p and miRNA-185-5p and AML-2 inhibiting DNA binding factor [10, 230–232]. If the promoter hypermethylation gets abolished, the *KIR3DL3* promotor remarkably can show the highest activity of all *KIR* gene promotors in NK3.3 and HeLa cells [231, 233].

Besides the genetical and expressional uniqueness, KIR3DL3 also differs in its long intracellular domain which is truncated and contains only one ITIM due to a premature stop codon in exon 9 (Figure 1.5, page 10) [10, 219, 234]. Furthermore, the entire exon 6 which encodes the amino acids between the Ig-like domain and transmembrane domain is missing and this further shortens the receptor in comparison to other KIRs [219]. This truncation and the absence of protein for a long time has led to some speculation that the gene and receptor is not functional itself but co-exists as a pseudogene [10, 235]. On the other side, its evolutionary conservation, which also extends to its protein structure and two binding loops, has led to the hypothesis that KIR3DL3s ligand is likely to be an important immunological molecule which is equally conserved [223]. Additionally, KIR3DL3 receptors form dimers which still allow to recruit SHP-1 and 2 adapter proteins for an inhibitory signalling [223].

Due to the low expression levels of *KIR3DL3* it was not until 2005 that the KIR3DL3 protein was detected on the cell surface of NK92 cells [10]. Recently, KIR3DL3 protein was also detected on the NK-92MI cell line as well as on human CD4 and CD8 T cells isolated from peripheral blood after a 21-day stimulation by CD3 and CD28 via targeted antibody tetramers as well as on $\gamma\delta$ T cells and CD8 T cells in the digestive tract, peripheral blood, thymus and lungs [11, 17]. Interestingly, $\gamma\delta$ T cells and CD8 T cells in the lungs and peripheral blood can display a naïve phenotype while the ones in the intestine can show memory like features [17, 18]. In combination with the expression of Fc Receptor Ligand 3 (FcRL3) Palmer *et al.* postulated that KIR3DL3 is a cell surface marker of self-reactive and hyporesponsive tissue-resident T cells [17, 236]. Wei *et al.* on the other hand described these T cells as NK-like T cells [18]. Furthermore, some peripheral $CD56^{dim}$ NK cells isolated from peripheral blood were reported to express low levels of KIR3DL3 [18]. Additionally, KIR3DL3 cell surface expression seems to vary with different allele variants [17]. For example, *KIR3DL3*003* showed significant higher surface expressions than *KIR3DL3*039* although the mechanisms behind remain elusive [17].

Ligand investigations by Bhatt *et al.* in 2020 identified human-endogenous-retro viruses–H Long-terminal repeat associating 2 (HHLA2) protein also called B7-H5 in old nomenclatures and B7-H7 in new nomenclatures as ligand for KIR3DL3 [11]. This finding was confirmed by Palmer *et al.* and Wei *et al.* [17, 18]. The KIR3LD3 B7-H7 axis can signal independent of PD-1 via SHP-1 & 2 and can silence key players such as RAS-RAF-ERK, PIP2-PKC-NF-κB or PI3K/AKT pathway suggesting a new inhibitory pathway for cancer treatments [11, 18]. This interaction can be abolished

when tyrosine 382 of the ITIM is mutated into a phenylalanine [18]. Upon the interaction of KIR3DL3 and B7-H7, NK cells were unable to create immunological synapses with target cells [18]. As a result, NK cells and CD8 T cells showed reduced killing activity in killing assays which could be reversed via B7-H7 or KIR3DL3 blocking antibodies [11, 17, 18].

1.4 The role of the B7 protein family in the human immune system

1.4.1 Discovery and characterisation of B7 proteins

B proteins were first described during the process of B cell characterisation as APCs in the 1980s [12]. Shortly after the seventh protein, B7, was characterised as binding to CD28 and CTLA-4 in 1987 a protein with similar binding characteristics was described [12–14]. Henceforth, B7-1 (CD80), and B7-2 (CD86) were introduced. Later on more B7 proteins, defined through one Ig domain and similar biological functions on APCs but little structural and sequence similarities, were found so that the B7 protein family has grown substantially and now consists of nine receptors [12, 15]. In fact, only 17 % - 20 % of gene sequence similarity and 18 % - 20 % amino acid sequence similarity is found among the members of the family which are scattered among multiple chromosomes (Figure 1.6) [12, 15, 237]. B7 proteins are not only present on B cells but can also be expressed on dendritic cells, stroma cells of the decidua, monocytes/-macrophages and NK cells [15, 238–240]. B7 proteins which can be highly regulated on APCs during pregnancy, can support the rearrangement of the uterus mucosa and can prevent graft-versus-host reactions from T cells and macrophages [15, 241–246]. Besides the healthy expression on the previously mentioned cells B7 proteins are reported to be upregulated in multiple cancers such as gastric cancer, colorectal cancer, glioma, leukaemia, melanoma, renal cell carcinoma and non-small cell lung cancer [18, 247–251].

Since the approval of PD-L1 and CTLA-4 immunotherapies for clinics other B7 proteins have gained interest of researchers but their varying structure make drug development or ligand identification tedious [12, 252, 253]. The interest is represented by the more than 10,000 ongoing clinical trials for B7 proteins [254]. A small summary of current efforts is shown in Table 1.1 and highlights the ever growing importance of B7 proteins for medical treatments.

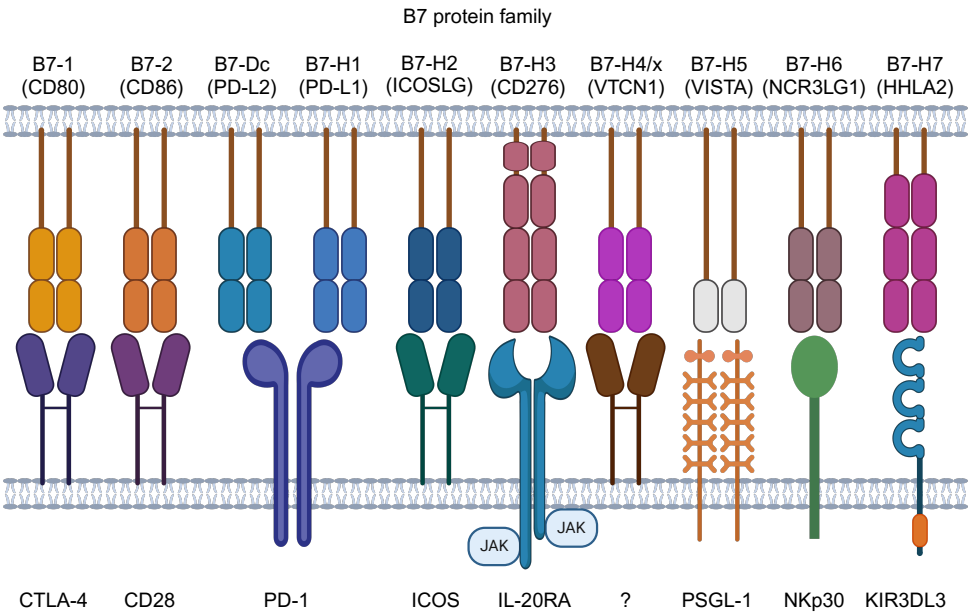

FIGURE 1.6: Overview of B7 protein family. The different B7 proteins and their known ligands are depicted. Shades of colours like blue and purple on the B7 protein side resemble the protein sequence homology between the B7 receptors and the number of boxes their respective V domains. This figure was adapted from Zhao *et al.* and West *et al.* and was created with BioRender.com [12, 15].

Table 1.1: Overview of B7 proteins and their clinical applications. The table was adapted from Khan *et al.*, West *et al.* and Zhao *et al.* [12, 15, 255].

B7 protein on APCs	**Alternative name**	**Chromosome location**	**Sequence similarity to B7-1**	**Binding partner**	**Receptor function**	**Clinical applications and current trials**
B7-1	CD80	3q13	100 %	CTLA-4, CD28	Co-stimulation	FDA approved Ipilimumab and Abatacept [256, 257]; AGEN1884, BMS-986218, IBI310 phase I ongoing trial for solid tumours; Cadonilimab phase II ongoing trials for solid tumours and many more [254, 258–263].
B7-2	CD86	3q21	25 %	CTLA-4, CD28	Co-inhibition	FDA approved Ipilimumab and Abatacept [256, 257]; AGEN1884, BMS-986218, IBI310 phase I ongoing trial for solid tumours; Cadonilimab phase II ongoing trials for solid tumours and many more [254, 258–263].
B7-Dc	PD-L2	9p24	18 %	PD-1	Co-inhibition	FDA approved Nivolumab, Cemiplimab, Pembrolizumab [256].

TABLE 1.1: Continued overview of B7 proteins and their medical applications. The table was adapted from Khan *et al.*, West *et al.* and Zhao *et al.* [12, 15, 255].

B7 protein on APCs	**Alternative name**	**Chromosome location**	**Sequence similarity to B7-1**	**Binding partner**	**Receptor function**	**Clinical applications and current trials**
B7-H1	PD-L1	9p24	18 %	PD-1	Co-inhibition	FDA approved Nivolumab, Cemiplimab, Pembrolizumab, Atezolizumab, Durvalumab, Avelumab [256, 264]; On going phase I trials of BMS-936559 for HIV patients and BGB-A333, HLX20 for solid tumours and many more [254, 262, 265].
B7-H2	ICOSLG	21p12	21 %	ICOS	Co-stimulation	-
B7-H3	CD276	15q24	23 %	IL-20RA	Co-stimulation, co-inhibition	Enoblituzumab phase I ongoing trials for melanoma, head neck cancers, non-small lung cancer, neuroblastoma, rhabdomyosarcoma and osteosarcoma [255].
B7-H4	VTCN1, B7x	1p11.1	17 %	-	Co-inhibition	SGN-B7H4V, FPA150, ABL103, GEN1047 and NC762 mab phase I ongoing clinical trials for solid tumours with severe metastasis [254, 266–272].

Table 1.1: Continued overview of B7 proteins and their medical applications. The table was adapted from Khan *et al.*, West *et al.* and Zhao *et al.* [12, 15, 255].

B7 protein on APCs	**Alternative name**	**Chromosome location**	**Sequence similarity to B7-1**	**Binding partner**	**Receptor function**	**Clinical applications and current trials**
B7-H5	VISTA	10q22.1	16 %	PSGL-1, VSIG3, HLA-F, HLA-E [273]	Co-inhibition	JNJ-61610588 phase I clinical trial aborted [254, 274].
B7-H6	NCR3LG1	11p15.1	18 %	NKp30	Co-stimulation	BI 765049 phase I clinical trial ongoing for colorectal cancer, non-small cell lung cancer, head-neck cancer, hepatocellular, gastric or pancreatic carcinoma [254, 275].
B7-H7	HHLA2	3q13.13	21 %	TMIGD2, KIR3DL3	Co-inhibition	NPX267 (KIR3DL3 mab) phase I ongoing trials for metastatic malignant neoplasms and solid tumours, HBM1020 (B7-H7 mab) Phase I ongoing trial for advanced solid tumours [254, 276–278].

1.4.2 B7-H7 a unique B7 protein

Identified in 2013, *B7-H7* also called *HHLA2* gene is located on chromosome 3q13.13 and is the only B7 member which does not have a homologous gene in mice although it is evolutionarily conserved in primates [19]. Together with B7-H3 and B7-H4 it forms a B7 sub-family defined by high protein sequence similarities of 30 % [18, 19, 279]. *B7-H7* is not silenced and frequently transcribed but can be post-transcriptionally regulated via miR-3116 and miR-6870–5p [280, 281].

The B7-H7 protein is the longest B7 protein with 414 amino acids and is the only B7 protein with three extracellular Ig domains [19, 282]. B7-H7 can be expressed on the cell surface of B cells, monocytes/macrophages, DC cells and exhausted T cells isolated from peripheral blood as well as on trophoblast tissue, small intestine epithelium, and multiple cancers such as renal cell carcinoma, acute lymphoblastic leukaemia, non-small lung cancer, gallbladder and stomach cancer [11, 17–26]. Specifically in tumour tissues, B7-H7 can be often expressed when B7-H1 (PD-L1) is absent, making it an attractive target for immunotherapies also given that these patients show decreased overall survival rates [18, 23, 24, 283–286]. In tumour tissues, it has also been shown, that infiltrating T cells can express B7-H7 as sign of T cell exhaustion upon extensive activation of the mammalian target of rapamycin (mTOR) pathway [25]. Furthermore, B7-H7 expression can be induced via inflammatory cytokines [19, 282, 287].

B7-H7 has long been known to bind transmembrane and immunoglobulin (Ig) domain containing 2 (TMIGD2) protein also called immunoglobulin-containing and proline-rich receptor-1 (IGPR-1) or CD28 homolog (CD28H) and recently has been described as binder to KIR3DL3 [11, 18, 287, 288]. The binding affinity between the two receptors differ greatly with a KD of 48.9 µM for KIR3DL3 & B7-H7 and a KD of 9 µM for TMIGD2 & B7-H7. B7-H7 ligand expression of KIR3DL3 and TMIGD2 seems to be mutually exclusive, henceforth no direct competition seems to occur [17, 18, 289]. Interestingly, the binding of B7-H7 to KIR3DL3 is mediated through the IgC-IgV2 domain on B7-H7 side and the D0 domain on KIR3DL3 side [18]. Upon binding of KIR3DL3 to B7-H7 T cell activation, proliferation and cytokine production is diminished via JAK/STAT, PI3K/AKT, MAPK-ERK and WNT pathways [19, 287, 290, 291].

1.5 Open questions between KIRs and B7 protein interactions

The general genetics, regulation, expression patterns and structures of KIRs and B7 proteins are well characterised. The specific interaction of KIR3DL3 & B7-H7 and their implications for the immune system still remain elusive. Furthermore, no direct interaction compartment for the two receptors has been identified. Additionally, it has not been investigated, whether other B7 proteins, due to their little sequence

similarity, are ligands for other KIRs. Henceforth, the dissertation tries to identify potential additional KIR & B7 protein interactions.

2 Hypothesis and aims of the research project

Given the variety of B7 family proteins and KIRs, the current study postulates that more B7 family proteins bind KIRs, giving them the ability to shape immune responses to viruses and other pathogens. The B7 protein family contains key players of the immune system such as CD80 (B7-1), CD86 (B7-2) and PD-L1 (B7-H1). Considering the genetic conservation of the KIR3DL3 receptor within the human species, the thesis tries to understand the functional role and cellular compartmentalization of these receptors together with their ligands (Figure 2.1).

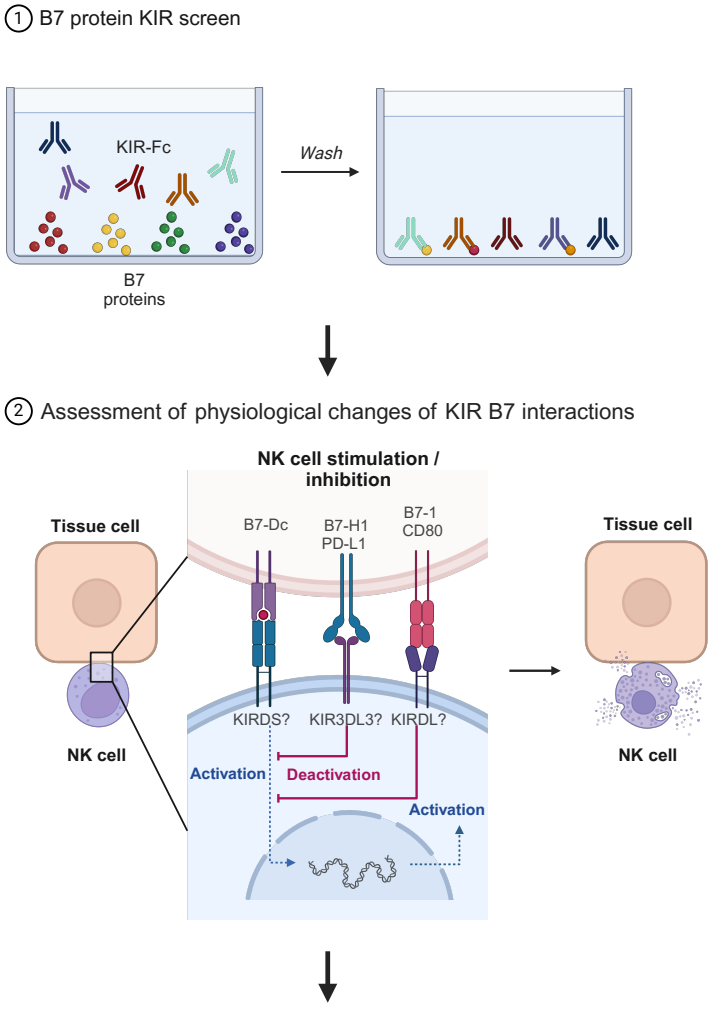

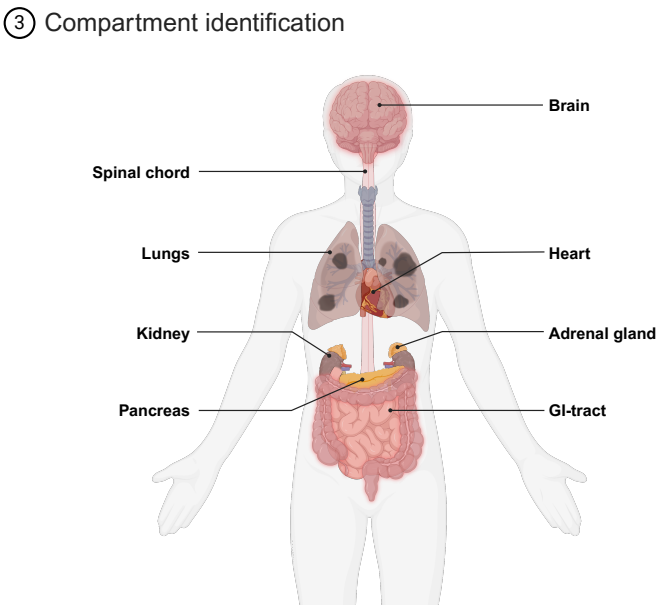

FIGURE 2.1: Working hypothesis. The presented thesis investigated whether more interactions between B7 proteins and KIR receptors are present giving them the ability to shape immune responses to viruses and other pathogens. Furthermore, the thesis tries to shed light on the functional role of the KIR3DL3 receptor and its B7-H7 ligand within the human system, and in which compartments they are generally present. This figure was adapted from Maruthamuthu *et al.*, Kumar *et al.* and created with BioRender.com [40, 292, 293].

To test this hypothesis and research aims the following steps were proposed:

- Screen all B7 proteins as ligands for KIRs.
- Assess KIR3DL3 & B7-H7 interactions and potential additional KIR binding partners for physiological outcomes.
- Identify the cellular compartmentalization of KIR3DL3 & B7-H7 and potential additional KIR binding partners.

3 Results

3.1 B7 protein KIR-Fc fusion construct protein screen

3.1.1 Setup of B7 protein and KIR-Fc fusion construct protein controls

In a high throughput screen (HTS) all B7 proteins tagged with biotin were tested for binding against all commercially available KIR-Fc fusion construct proteins (subsection 7.8.1, page 137). As described earlier by our laboratory, B7 proteins were coated on streptavidin pre-coated M-280 metal beads and then incubated with the respective KIR-Fc fusion construct protein before being stained with a secondary antibody targeted against the Fc part of the Fc fusion construct protein [90, 207].

In order to determine whether the streptavidin beads were coated successfully with B7 proteins, the coated beads were incubated with antibodies targeting respective B7 proteins followed by assessing the Median Fluorescence Instensity (MdFI). Biotin coated beads were used as control. A statistically significant MdFI shift for the B7 proteins on the beads was obtained for all B7 proteins with the following median MdFIs: B7-1 (CD80) 10476.50 ± 2487.50 $p<0.05$, B7-2 (CD86) 5013.00 ± 1683.00 $p<0.05$, B7-Dc (PD-L2) 25918.50 ± 582.00 $p<0.05$, B7-H1 (PD-L1) 17507.50 ± 3265.50 $p<0.05$, B7-H2 (ICOSLG) 33381.00 ± 2516.50 $p<0.05$, B7-H3 8244.50 ± 2015.00 $p<0.05$, B7-H4 (VTCN1) 17654.50 ± 2400.50 $p<0.05$, B7-H5 (VISTA) 15318.50 ± 4856.00 $p<0.05$, B7-H6 (NCR3LG1) 5661.50 ± 1087.00 $p<0.05$, B7-H7 (HHLA2) 2202.00 ± 87.00 $p<0.05$ (Table 3.1). An example of the primary data of B7 protein coating is shown in Figure 3.1 and the overall results in Figure 3.2.

Table 3.1: Median and MAD of the MdFIs obtained from the B7 beads incubated with the respective B7 mab ($n = 2$).

B7 protein	**Median MdFI**	**MAD MdFI**	**adjusted p-value compared to biotin control**
Biotin	261647.00	0.00	-
Biotin 2ndary only	981.00	90.00	<0.05
B7-1 (CD80) biotin	1218.00	136.00	-
B7-1 (CD80)	10476.50	2487.50	<0.05

TABLE 3.1: Continued median and MAD of the MdFIs obtained from the B7 beads incubated with the respective B7 mab (n = 2).

B7 protein	**Median MdFI**	**MAD MdFI**	**adjusted p-value compared to biotin control**
B7-2 (CD86) biotin	470.00	218.50	-
B7-2 (CD86)	5013.00	1683.00	<0.05
B7-Dc (PD-L2) biotin	46.20	3.80	-
B7-Dc (PD-L2)	25918.50	582.00	<0.05
B7-H1 (PD-L1) biotin	53.90	27.60	-
B7-H1 (PD-L1)	17507.50	3265.50	<0.05
B7-H2 (ICOSLG) biotin	51.40	1.25	-
B7-H2 (ICOSLG)	33381.00	2516.50	<0.05
B7-H3 biotin	43.90	2.50	-
B7-H3	8244.50	2015.00	<0.05
B7-H4 (VTCN1) biotin	50.75	1.95	-
B7-H4 (VTCN1)	17654.50	2400.50	<0.05
B7-H5 (VISTA) biotin	41.70	7.10	-
B7-H5 (VISTA)	15318.50	4856.00	<0.05
B7-H6 (NCR3LG1) biotin	58.45	0.65	-
B7-H6 (NCR3LG1)	5661.50	1087.00	<0.05
B7-H7 (HHLA2) biotin	442.00	6.50	-
B7-H7 (HHLA2)	2202.00	87.00	<0.05

Additionally, KIR-Fc fusion construct protein controls were prepared by coating of streptavidin beads with peptide loaded HLA receptors (Table 6.9, page 114), CD155, B7-H6 and B7-H7. After incubation of the HLA receptors and beads, coating was shown by incubating them with the respective mab targeted against the HLA receptors, CD155, B7-H6 and B7-H7. A statistically significant MdFI shift for the controls was obtained for all samples with the following median MdFIs: HLA-A 15819.00 ± 219.00 $p<0.05$, HLA-B 7835.50 ± 183.50 $p<0.05$, HLA-C 14788.00 ± 506.50 $p<0.05$, HLA-F 8010.00 ± 1508.00 $p<0.05$, HLA-G 8392.00 ± 3128.50 $p<0.05$, B7-H6 (NCR3LG1) 3309.00 ± 87.00 $p<0.05$, B7-H7 (HHLA2) 1949.50 ± 47.00 $p<0.05$, CD155 (PVR) 25550.00 ± 2096.00 $p<0.05$ (Table 3.2). An example of the primary data of HLA receptor coating is shown in Figure 3.3 and the overall results in Figure 3.4.

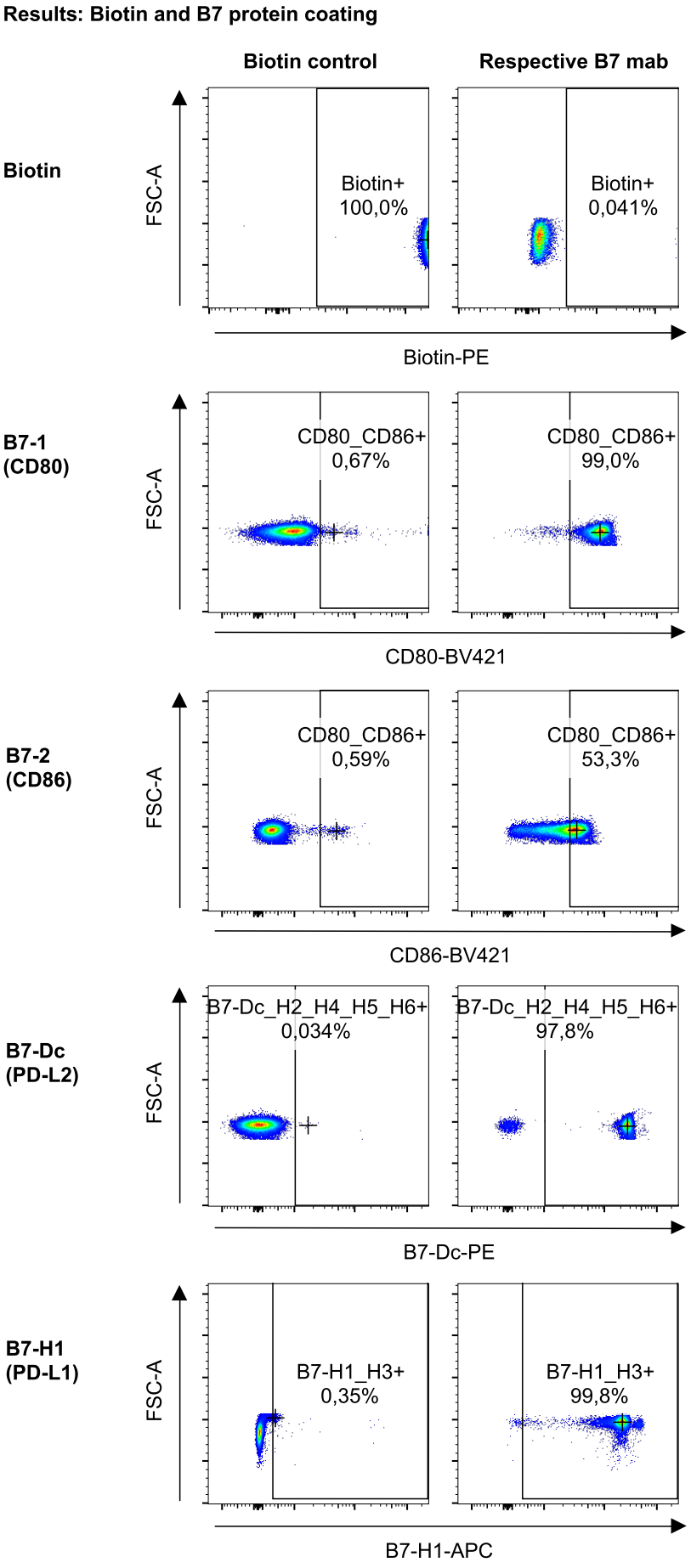
Results: Biotin and B7 protein coating
Biotin control
Respective B7 mab
Biotin
FSC-A
Biotin+
100,0%
Biotin+
0,041%
Biotin-PE
B7-1
(CD80)
CD80_CD86+
0,67%
CD80_CD86+
99,0%
CD80-BV421
B7-2
(CD86)
CD80_CD86+
0,59%
CD80_CD86+
53,3%
CD86-BV421
B7-Dc
(PD-L2)
B7-Dc_H2_H4_H5_H6+
0,034%
B7-Dc_H2_H4_H5_H6+
97,8%
B7-Dc-PE
B7-H1
(PD-L1)
B7-H1_H3+
0,35%
B7-H1_H3+
99,8%
B7-H1-APC

Continued results: Biotin and B7 protein coating

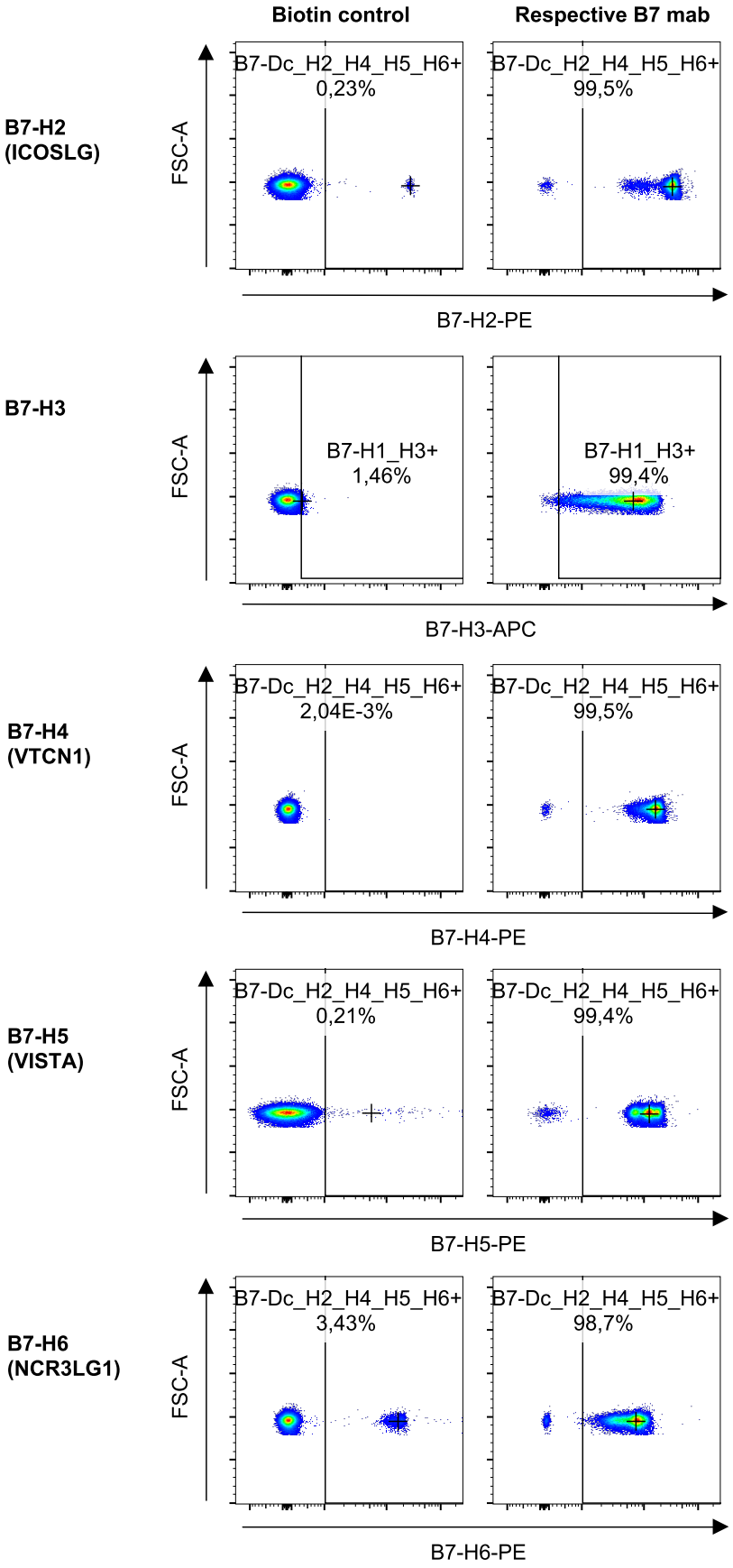

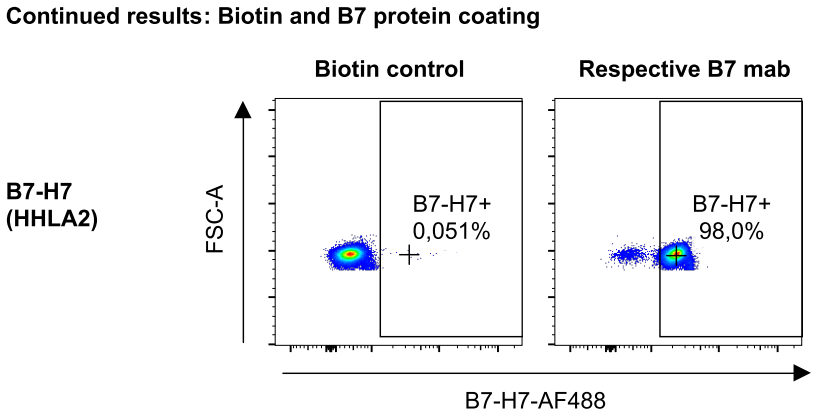

FIGURE 3.1: Primary data of streptavidin beads coated with B7 proteins, stained for respective B7 proteins shown for one technical triplicate (n = 1). All B7 proteins showed a mab signal confirming a successful coating of the streptavidin beads while beads only coated with biotin did not show any signal.

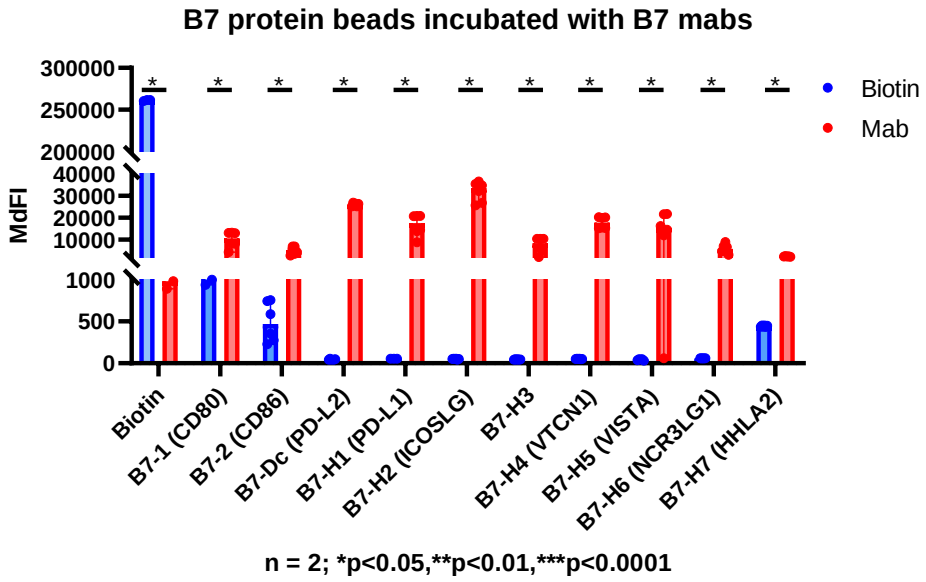

FIGURE 3.2: Results of streptavidin beads coated with B7 proteins, stained for respective B7 proteins shown for all biological replicates (n = 2). All B7 proteins showed a mab signal confirming a successful coating of the streptavidin beads while beads only coated with biotin did not show any signal: B7-1 (CD80) 10476.50 ± 2487.50 $p<0.05$, B7-2 (CD86) 5013.00 ± 1683.00 $p<0.05$, B7-Dc (PD-L2) 25918.50 ± 582.00 $p<0.05$, B7-H1 (PD-L1) 17507.50 ± 3265.50 $p<0.05$, B7-H2 (ICOSLG) 33381.00 ± 2516.50 $p<0.05$, B7-H3 8244.50 ± 2015.00 $p<0.05$, B7-H4 (VTCN1) 17654.50 ± 2400.50 $p<0.05$, B7-H5 (VISTA) 15318.50 ± 4856.00 $p<0.05$, B7-H6 (NCR3LG1) 5661.50 ± 1087.00 $p<0.05$, B7-H7 (HHLA2) 2202.00 ± 87.00 $p<0.05$. Analysed with Wilcoxon-paired tests corrected for multiple testing with Benjamini & Hochberg method [294].

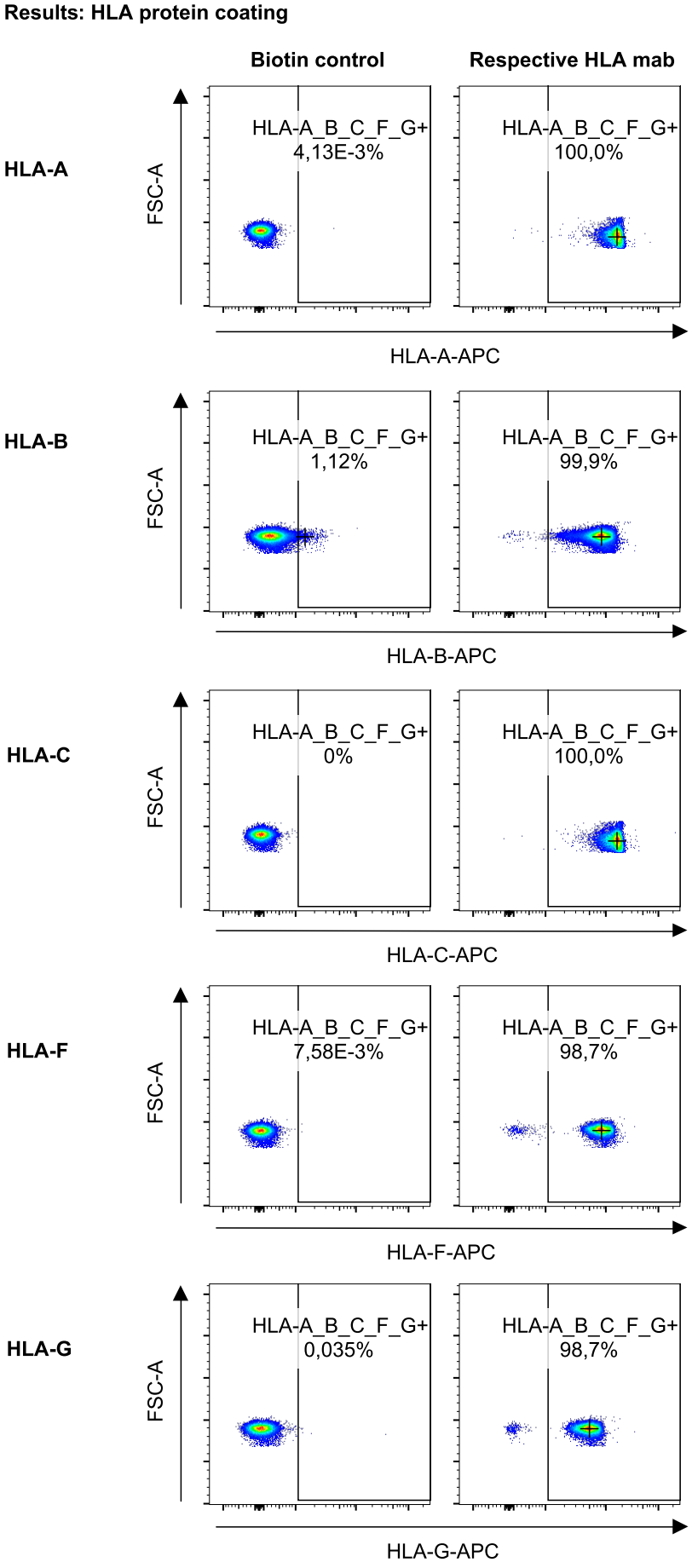
Results: HLA protein coating
Biotin control
Respective HLA mab
HLA-A
HLA-A_B_C_F_G+
4,13E-3%
HLA-A_B_C_F_G+
100,0%
FSC-A
HLA-A-APC
HLA-B
HLA-A_B_C_F_G+
1,12%
HLA-A_B_C_F_G+
99,9%
FSC-A
HLA-B-APC
HLA-C
HLA-A_B_C_F_G+
0%
HLA-A_B_C_F_G+
100,0%
FSC-A
HLA-C-APC
HLA-F
HLA-A_B_C_F_G+
7,58E-3%
HLA-A_B_C_F_G+
98,7%
FSC-A
HLA-F-APC
HLA-G
HLA-A_B_C_F_G+
0,035%
HLA-A_B_C_F_G+
98,7%
FSC-A
HLA-G-APC

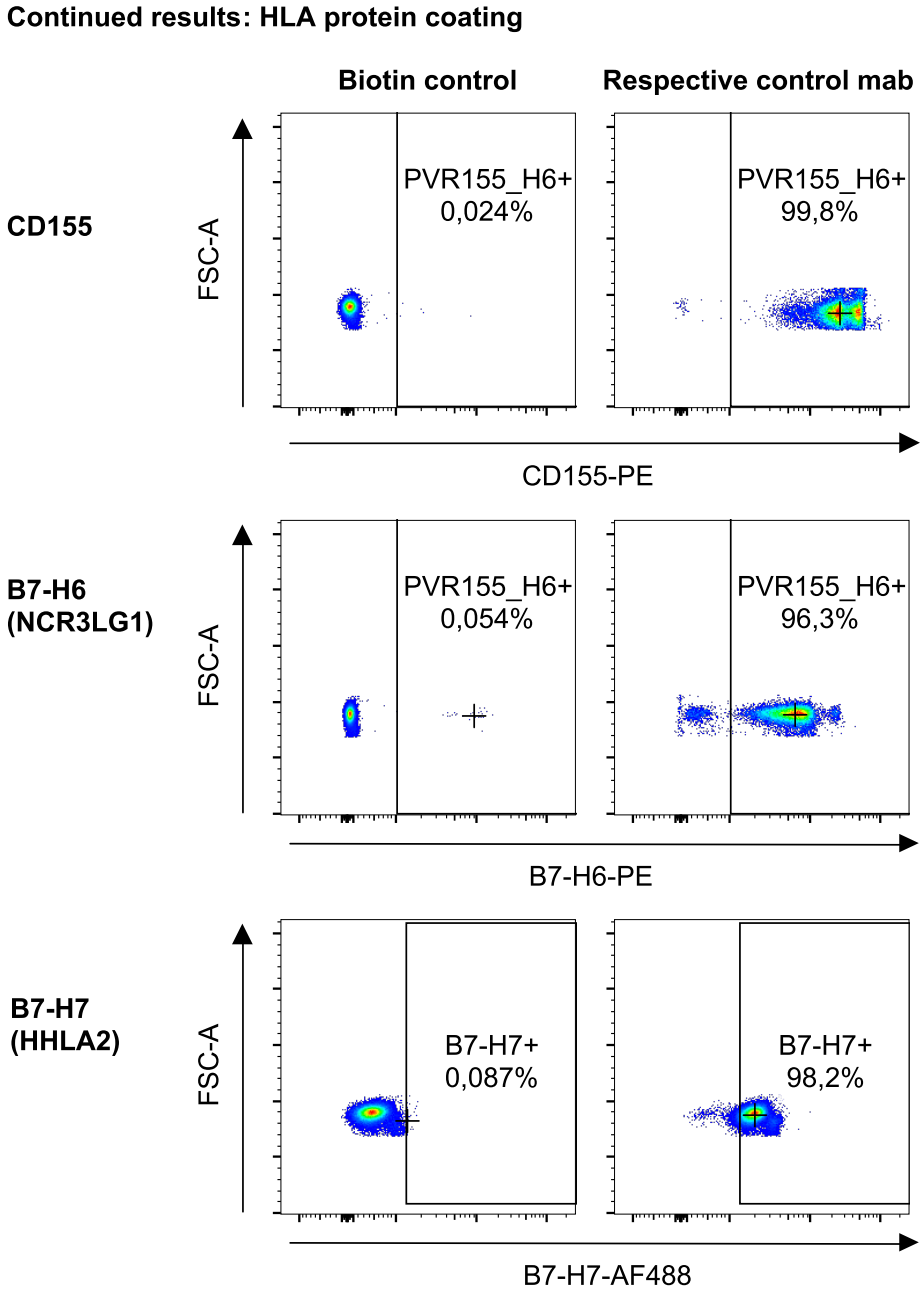

FIGURE 3.3: Primary data of streptavidin beads coated with HLA receptors, CD155, B7-H6 and B7-H7 stained for respective HLA receptors shown for one technical triplicate (n = 1). All control receptors showed a mab signal confirming a successful coating of the streptavidin beads while beads only coated with biotin did not show any signal.

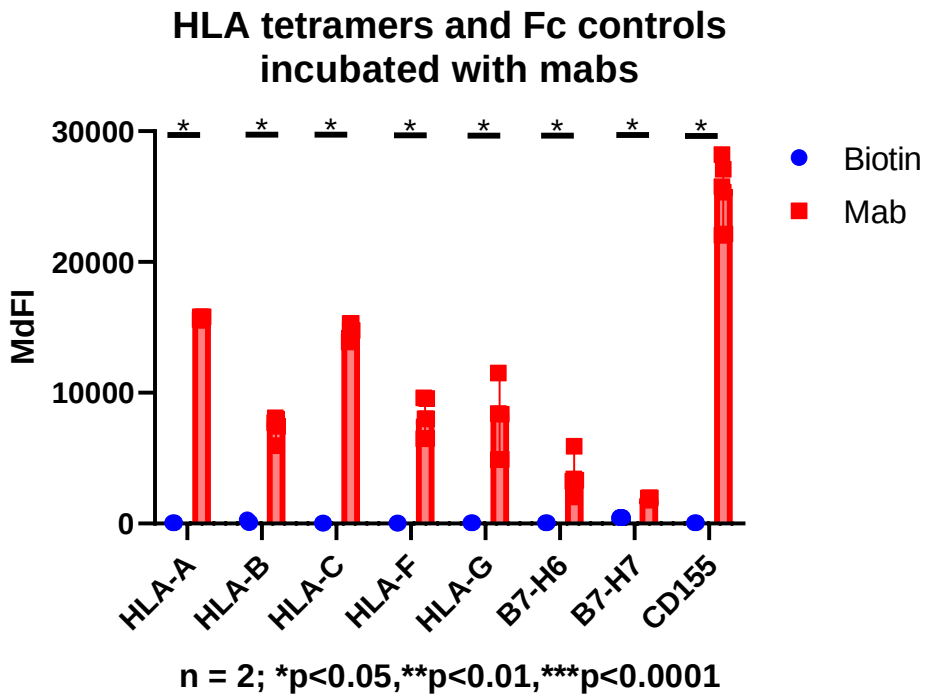

FIGURE 3.4: Results of streptavidin beads coated with HLA receptors, CD155, B7-H6 and B7-H7 stained for respective control receptors shown for all biological replicates (n = 2). All control receptors showed a mab signal confirming a successful coating of the streptavidin beads while beads only coated with biotin did not show any signal: HLA-A 15819.00 ± 219.00 $p<0.05$, HLA-B 7835.50 ± 183.50 $p<0.05$, HLA-C 14788.00 ± 506.50 $p<0.05$, HLA-F 8010.00 ± 1508.00 $p<0.05$, HLA-G 8392.00 ± 3128.50 $p<0.05$, B7-H6 (NCR3LG1) 3309.00 ± 87.00 $p<0.05$, B7-H7 (HHLA2) 1949.50 ± 47.00 $p<0.05$, CD155 (PVR) 25550.00 ± 2096.00 $p<0.05$. Analysed with Wilcoxon-paired tests corrected for multiple testing with Benjamini & Hochberg method [294].

TABLE 3.2: Median and MAD of the MdFIs obtained from the HLA beads and Fc control beads incubated with the respective mab (n = 2).

HLA/Control protein	**Median MdFI**	**MAD MdFI**	**adjusted p-value compared to biotin control**
HLA-A biotin	55.20	1.30	-
HLA-A	15819.00	219.00	<0.05
HLA-B biotin	63.55	20.55	-
HLA-B	7835.50	183.50	<0.05
HLA-C biotin	50.10	2.55	-
HLA-C	14788.00	506.50	<0.05
HLA-F biotin	50.10	2.30	-

TABLE 3.2: Continued median and MAD of the MdFIs obtained from the HLA beads and Fc control beads incubated with the respective mab (n = 2).

HLA/Control protein	**Median MdFI**	**MAD MdFI**	**adjusted p-value compared to biotin control**
HLA-F	8010.00	1508.00	<0.05
HLA-G biotin	55.20	0.50	-
HLA-G	8392.00	3128.50	<0.05
B7-H6 (NCR3LG1) biotin	59.75	0.65	-
B7-H6 (NCR3LG1)	3309.00	87.00	<0.05
B7-H7 (HHLA2) biotin	464.00	1.00	-
B7-H7 (HHLA2)	1949.50	47.00	<0.05
CD155 (PVR) biotin	59.10.00	1.30	-
CD155 (PVR)	25550.00	2096.00	<0.05

Furthermore, the functionality and the native conformation of the B7 proteins after coating on the streptavidin beads was assessed by incubating the B7 beads with known B7 ligands in their Fc fusion construct version (Table 6.10, page 115). As no ligands have yet been identified for B7-H4, it's functionality was not assessed. A statistically significant MdFI binding signal between the B7 proteins and their respective ligands was obtained for all B7 proteins besides the B7-H5 (VISTA) protein with the following median MdFIs: B7-1 (CD80) 4102.00 ± 358.00 $p<0.05$, B7-2 (CD86) 2274.50 ± 363.00 $p<0.05$, B7-Dc (PD-L2) 5020.50 ± 1074.00 $p<0.05$, B7-H1 (PD-L1) 8343.00 ± 93.00 $p<0.05$, B7-H2 (ICOSLG) 8148.50 ± 401.50 $p<0.05$, B7-H3 2329.00 ± 879.00 $p<0.05$, B7-H5 (VISTA) 184.00 ± 0.50 $p=1.00$, B7-H6 (NCR3LG1) 6873.50 ± 350.50 $p<0.05$, B7-H7 (HHLA2) 1016.00 ± 24.50 $p<0.05$ (Table 3.3). An example of the primary data to confirm the functionality of the extracellular domain of the B7 proteins is depicted in Figure 3.5 and the overall results in Figure 3.6.

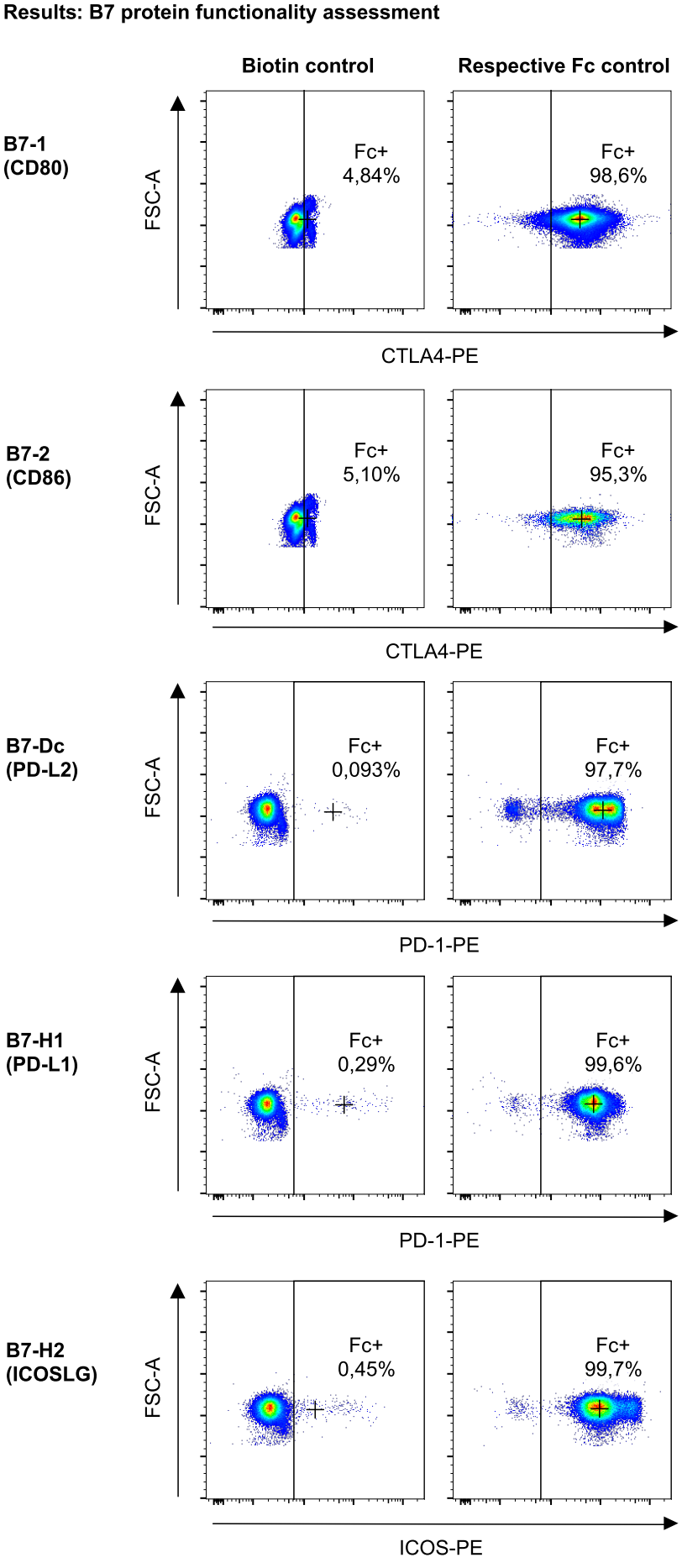
Results: B7 protein functionality assessment
Biotin control
Respective Fc control
B7-1
(CD80)
FSC-A
Fc+
4,84%
Fc+
98,6%
CTLA4-PE
B7-2
(CD86)
FSC-A
Fc+
5,10%
Fc+
95,3%
CTLA4-PE
B7-Dc
(PD-L2)
FSC-A
Fc+
0,093%
Fc+
97,7%
PD-1-PE
B7-H1
(PD-L1)
FSC-A
Fc+
0,29%
Fc+
99,6%
PD-1-PE
B7-H2
(ICOSLG)
FSC-A
Fc+
0,45%
Fc+
99,7%
ICOS-PE

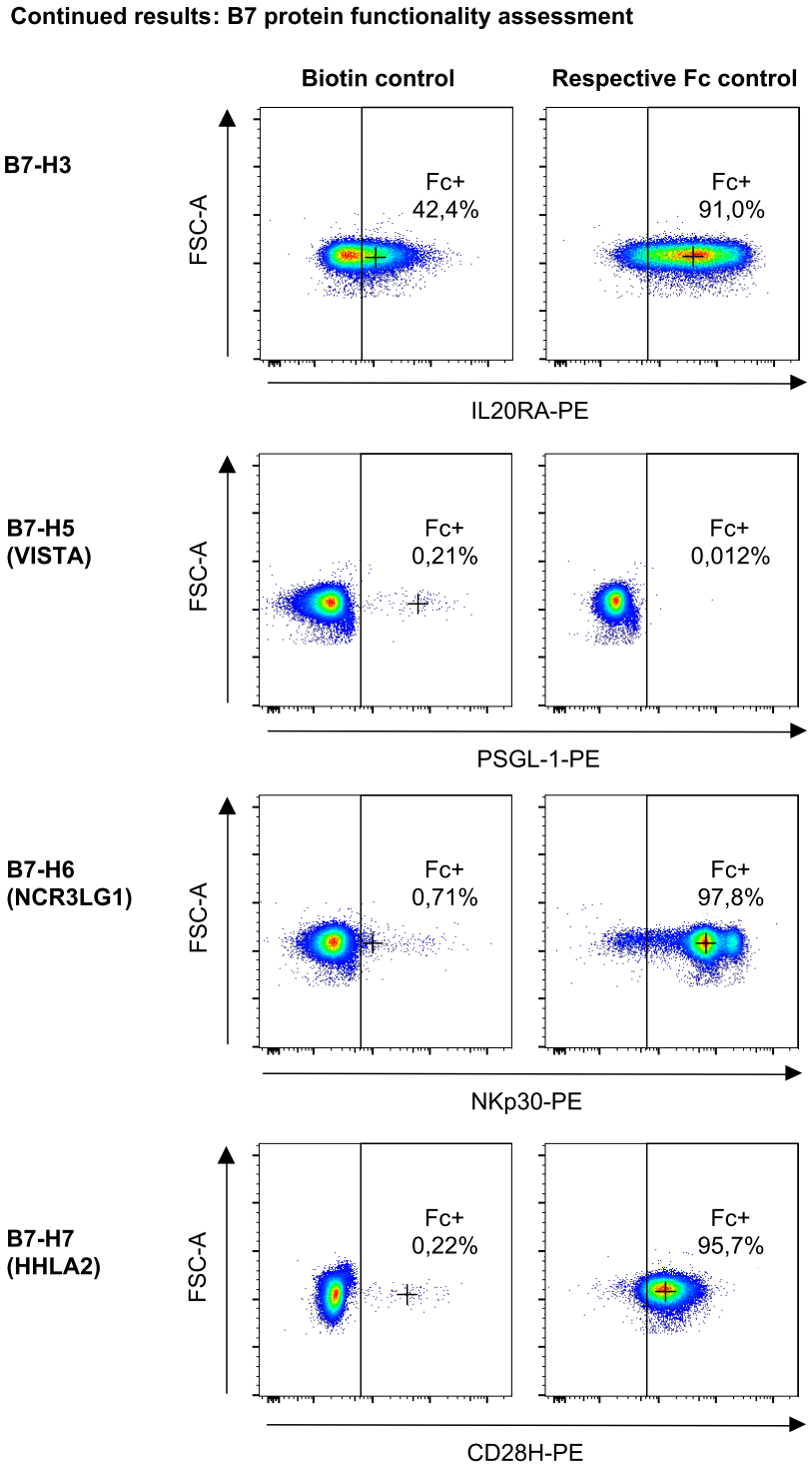

FIGURE 3.5: Primary data of streptavidin beads coated with B7 proteins incubated with known ligands and stained for respective Fc fusion construct proteins shown for one technical triplicate (n = 1). For B7-H4 no other ligand was known, henceforth no Fc control was included for the protein. Furthermore, all B7 proteins did bind their known interaction partner besides B7-H5 pointing towards an impaired extracellular domain.

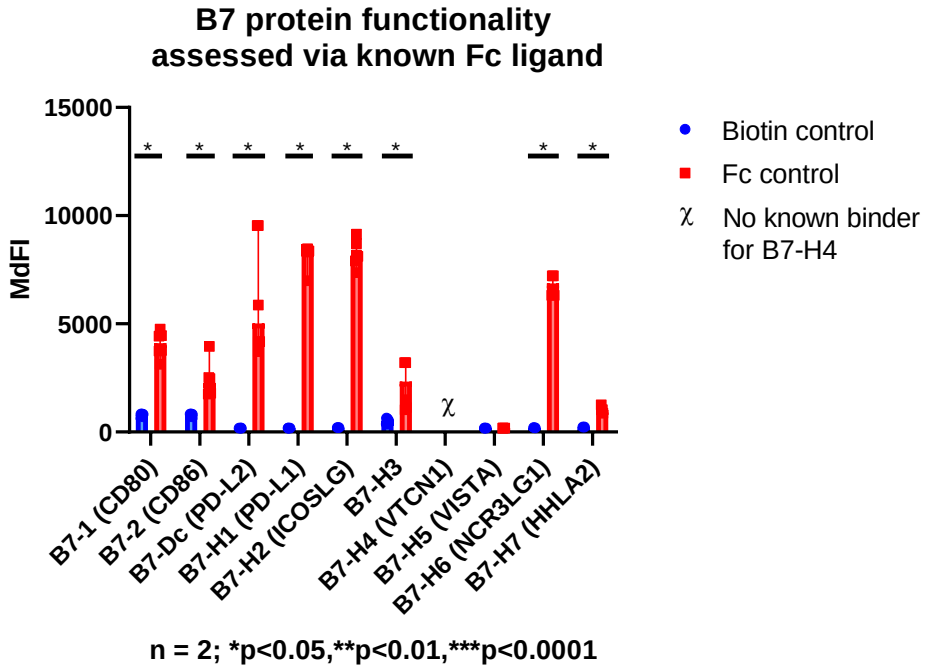

FIGURE 3.6: Results of B7 beads incubated with their known Fc ligands stained for respective Fc terminus shown for all biological replicates (n = 2). Besides B7-H4 and B7-H5 all B7 proteins did bind their known interaction partner demonstrating a functional extracellular domain. For B7-H4 no other ligand was known, henceforth no Fc control was included for the protein. Furthermore, all B7 proteins did bind their known interaction partner besides B7-H5 pointing towards an impaired extracellular domain: B7-1 (CD80) 4102.00 ± 358.00 $p<0.05$, B7-2 (CD86) 2274.50 ± 363.00 $p<0.05$, B7-Dc (PD-L2) 5020.50 ± 1074.00 $p<0.05$, B7-H1 (PD-L1) 8343.00 ± 93.00 $p<0.05$, B7-H2 (ICOSLG) 8148.50 ± 401.50 $p<0.05$, B7-H3 2329.00 ± 879.00 $p<0.05$, B7-H5 (VISTA) 184.00 ± 0.50 $p=1.00$, B7-H6 (NCR3LG1) 6873.50 ± 350.50 $p<0.05$, B7-H7 (HHLA2) 1016.00 ± 24.50 $p<0.05$. Analysed with Wilcoxon-paired tests corrected for multiple testing with Benjamini & Hochberg method [294].

TABLE 3.3: Median and MAD of the MdFIs obtained from the B7 beads incubated with their known Fc ligands (n = 2).

B7 protein	**Median MdFI**	**MAD MdFI**	**adjusted p-value compared to biotin control**
B7-1 (CD80) biotin	794.50	30.00	-
B7-1 (CD80)	4102.00	358.00	<0.05
B7-2 (CD86) biotin	794.50	30.00	-
B7-2 (CD86)	2274.50	363.00	<0.05
B7-Dc (PD-L2) biotin	183.00	0.50	-

TABLE 3.3: Continued median and MAD of the MdFIs obtained from the B7 beads incubated with their known Fc ligands (n = 2).

B7 protein	**Median MdFI**	**MAD MdFI**	**adjusted p-value compared to biotin control**
B7-Dc (PD-L2)	5020.50	1074.00	<0.05
B7-H1 (PD-L1) biotin	183.00	0.50	-
B7-H1 (PD-L1)	8343.00	93.00	<0.05
B7-H2 (ICOSLG) biotin	204.50	0.50	-
B7-H2 (ICOSLG)	8148.50	401.50	<0.05
B7-H3 biotin	515.00	107.00	-
B7-H3	2329.00	879.00	<0.05
B7-H4 (VTCN1)[1] biotin	-	-	-
B7-H4 (VTCN1)	-	-	-
B7-H5 (VISTA) biotin	183.50	0.50	-
B7-H5 (VISTA)	184.00	0.50	=1.00
B7-H6 (NCR3LG1) biotin	195.00	2.50	-
B7-H6 (NCR3LG1)	6873.50	350.50	<0.05
B7-H7 (HHLA2) biotin	228.00	1.00	-
B7-H7 (HHLA2)	1016.00	24.50	<0.05

The functionality and the native conformation of the KIR/NKp-Fc fusion construct proteins used for the B7-KIR-Fc screen was assessed once by incubating the HLA beads with the respective Fc fusion construct ligands. No statistically significant binding signal between the Fc fusion construct proteins and their respective ligands was obtained for any Fc fusion construct protein with the following median MdFIs: KIR2DL1-Fc 23965.00 ± 354.00 p>0.05, KIR2DL2-Fc 19811.00 ± 48.00 p>0.05, KIR2DL3-Fc 19811.00 ± 17262.00 p>0.05, KIR2DL4-Fc 1472.00 ± 4.00 p>0.05, KIR2DL5-Fc 1475.00 ± 3.00 p>0.05, KIR2DS4-Fc 2769.00 ± 26.00 p>0.05, KIR3DL1-Fc 36620.00 ± 30.00 p>0.05, KIR3DL2-Fc 36891.00 ± 5.30 p>0.05, KIR3DL3-Fc 12656.00 ± 4952.00 p>0.05, KIR3DS1-Fc 20399.00 ± 100.00 p>0.05, NKp30-Fc 23293.00 ± 24.50 p>0.05, NKp46-Fc 19523.00 ± 48.00 p>0.05 (Table 3.4). However, if more runs were simulated with normally distributed measurements around the obtained MdFIs with the same MAD all results besides the KIR2DL3-Fc fusion construct protein showed statistically significant binding signals (subsection 7.10.3). An example of the primary

[1]No values measured as no alternative binder as control protein was available.

data to confirm the functionality of the extracellular domain of the Fc fusion construct proteins is depicted in Figure 3.7 and the overall results in Figure 3.8.

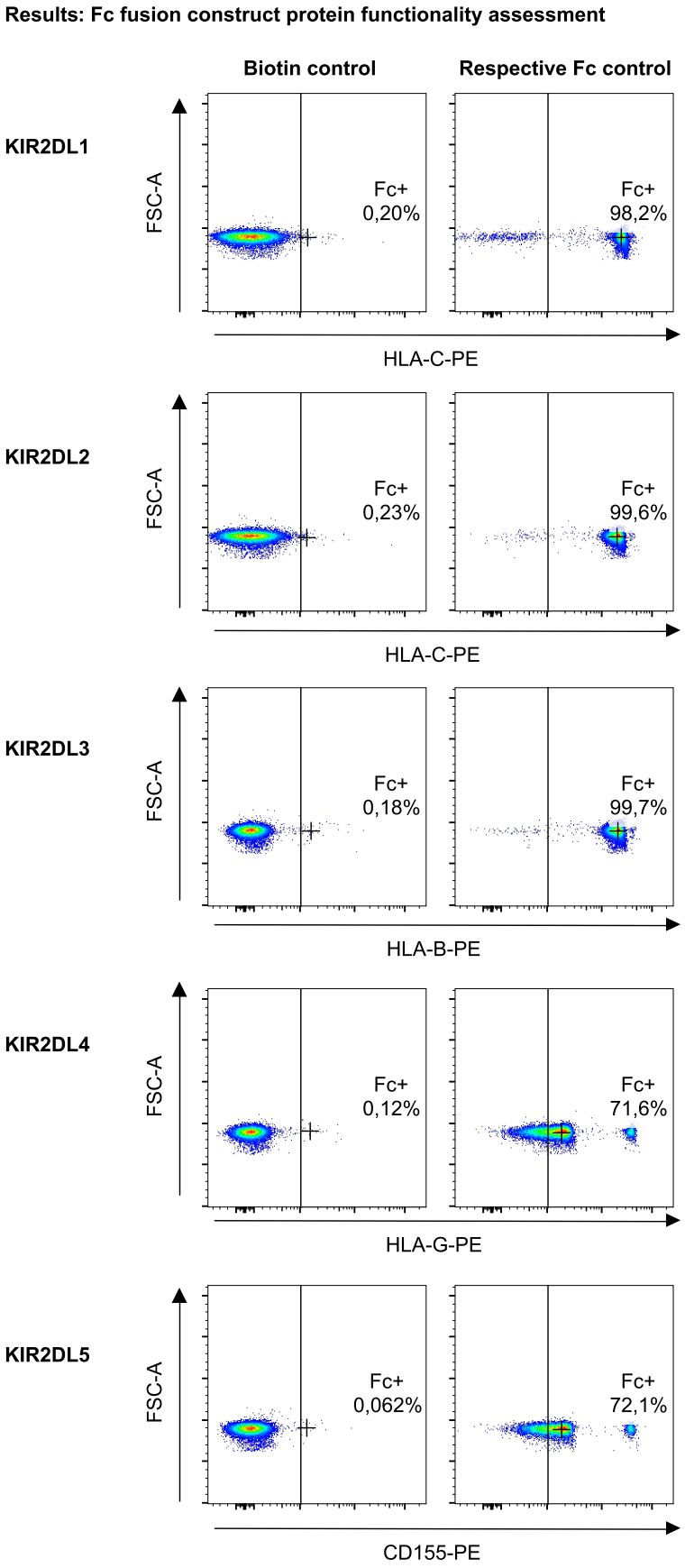

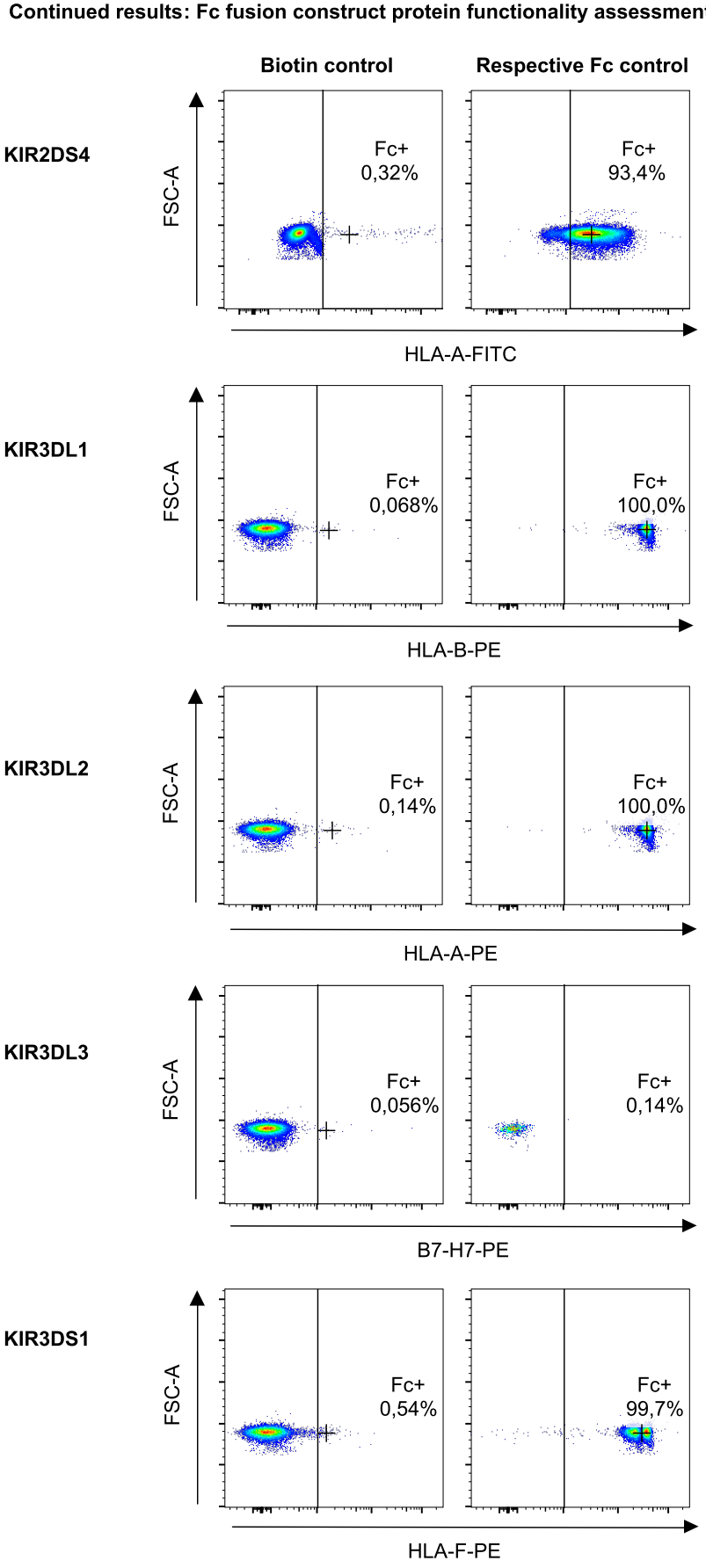
Continued results: Fc fusion construct protein functionality assessment
Biotin control
Respective Fc control
KIR2DS4
FSC-A
Fc+
0,32%
Fc+
93,4%
HLA-A-FITC
KIR3DL1
FSC-A
Fc+
0,068%
Fc+
100,0%
HLA-B-PE
KIR3DL2
FSC-A
Fc+
0,14%
Fc+
100,0%
HLA-A-PE
KIR3DL3
FSC-A
Fc+
0,056%
Fc+
0,14%
B7-H7-PE
KIR3DS1
FSC-A
Fc+
0,54%
Fc+
99,7%
HLA-F-PE

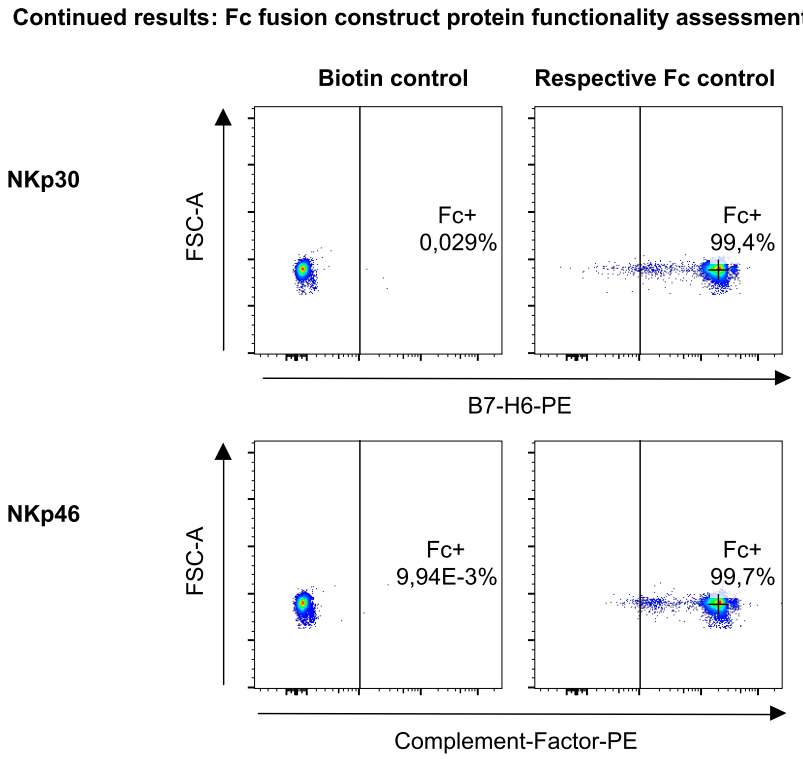

FIGURE 3.7: Primary data of KIR-Fc fusion construct proteins incubated with known ligands and stained for respective Fc tail shown for one technical triplicate (n = 1). All KIR-Fc fusion construct proteins did bind their known interaction partner.

TABLE 3.4: Median and MAD of the MdFIs obtained from the KIR-Fc fusion construct proteins incubated with their known ligands (n = 1).

KIR-Fc protein	**Median MdFI**	**MAD MdfI**	**adjusted p-value compared to biotin control**	**simulated adjusted p-value compared to biotin control**
KIR2DL1-Fc biotin	61.10	1.20	-	-
KIR2DL1-Fc	23965.00	354.00	>0.05	<0.05
KIR2DL2-Fc biotin	64.60	1.20	-	-
KIR2DL2-Fc	19811.00	48.00	>0.05	<0.05
KIR2DL3-Fc biotin	65.80	0.50	-	-
KIR2DL3-Fc	19811.00	17262.00	>0.05	>0.05
KIR2DL4-Fc biotin	65.80	0.60	-	-

TABLE 3.4: Continued median and MAD of the MdFIs obtained from the KIR-Fc fusion construct proteins incubated with their known ligands (n = 1).

KIR-Fc protein	Median MdFI	MAD MdfI	adjusted p-value compared to biotin control	simulated adjusted p-value compared to biotin control
KIR2DL4-Fc	1472.00	4.00	>0.05	<0.05
KIR2DL5-Fc biotin	65.80	0.60	-	-
KIR2DL5-Fc	1475.00	3.00	>0.05	<0.05
KIR2DS4-Fc biotin	444.00	1.00	-	-
KIR2DS4-Fc	2769.00	26.00	>0.05	<0.05
KIR3DL1-Fc biotin	67.50	4.70	-	-
KIR3DL1-Fc	36620.00	30.00	>0.05	<0.05
KIR3DL2-Fc biotin	62.30	0.00	-	-
KIR3DL2-Fc	36891.00	5.30	>0.05	<0.05
KIR3DL3-Fc biotin	76.70	1.70	-	-
KIR3DL3-Fc	12656.00	4952.00	>0.05	<0.05
KIR3DS1-Fc biotin	63.40	0.60	-	-
KIR3DS1-Fc	20399.00	100.00	>0.05	<0.05
NKp30-Fc biotin	63.40	0.50	-	-
NKp30-Fc	23293.00	24.50	>0.05	<0.05
NKp46-Fc biotin	62.80	4.50	-	-
NKp46-Fc	19523.00	48.00	>0.05	<0.05

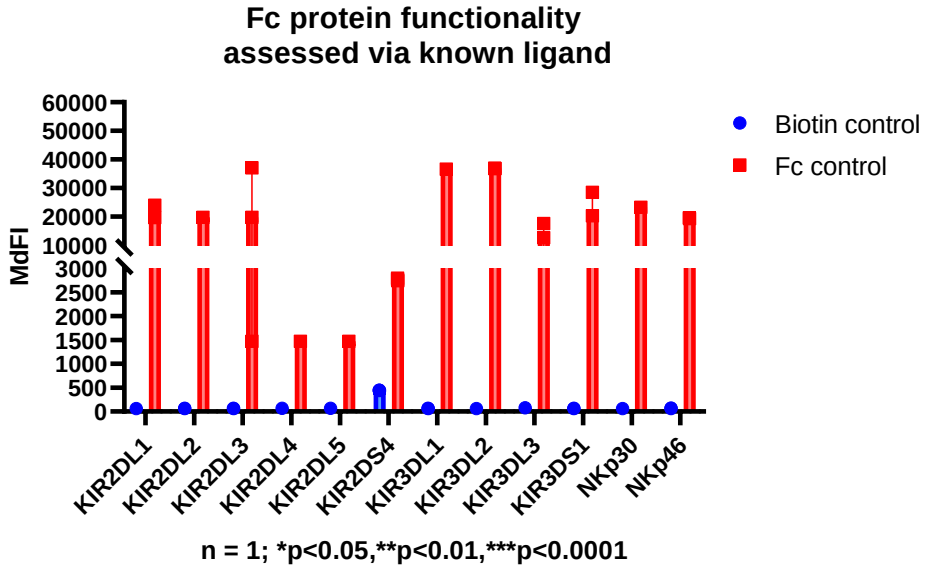

FIGURE 3.8: Results of KIR-Fc fusion construct proteins incubated with known ligands and stained for respective Fc tail shown for all biological replicates (n = 1). None of the KIR-Fc fusion construct proteins did show a statistically significant binding signal for their known interaction partners: KIR2DL1-Fc 23965.00 ± 354.00 $p>0.05$, KIR2DL2-Fc 19811.00 ± 48.00 $p>0.05$, KIR2DL3-Fc 19811.00 ± 17262.00 $p>0.05$, KIR2DL4-Fc 1472.00 ± 4.00 $p>0.05$, KIR2DL5-Fc 1475.00 ± 3.00 $p>0.05$, KIR2DS4-Fc 2769.00 ± 26.00 $p>0.05$, KIR3DL1-Fc 36620.00 ± 30.00 $p>0.05$, KIR3DL2-Fc 36891.00 ± 5.30 $p>0.05$, KIR3DL3-Fc 12656.00 ± 4952.00 $p>0.05$, KIR3DS1-Fc 20399.00 ± 100.00 $p>0.05$, NKp30-Fc 23293.00 ± 24.50 $p>0.05$, NKp46-Fc 19523.00 ± 48.00 $p>0.05$. Analysed with a Wilcoxon test corrected for multiple testing with Benjamini & Hochberg method [294].

3.1.2 Protein screen confirms KIR3DL3 & B7-H7 and NKp30 & B7-H6 interaction and hints towards KIR3DL2 & B7-H1 (PD-L1) interaction

After all controls confirmed their functionality the B7 proteins were incubated with the KIR-Fc fusion construct proteins. Interestingly, a binding signal for KIR3DL2-Fc fusion construct protein and the B7-H1 (PD-L1) protein was obtained, which had not been described before with a median MdFI of 842.00 ± 725.80 $p<0.05$ (Table 3.5). It was further investigated in a cellular context (section 3.2). An example of the primary data of the KIR3DL2-Fc screen is shown in Figure 3.13 and the overall results in Figure 3.9. Furthermore, a binding signal was obtained for the KIR3DL3-Fc fusion construct protein and B7-H7 as well as between NKp30-Fc fusion construct protein and B7-H6 with a median MdFI of 3972.00 ± 3816.00 $p<0.05$ and 2206.00 ± 659.00 $p<0.05$ respectively (Table 3.5). The two latter results were previously reported by Bhatt *et al.* and Brandt *et al.* [11, 16]. While the B7-H6 & NKp30 axis is well established and understood the cellular context and meaning of the B7-H7 & KIR3DL3 axis remains

elusive and therefore shall be investigated within this doctoral thesis. An example of the primary data of the KIR3DL3-Fc fusion construct protein and the NKp30-Fc fusion construct protein interaction are shown in Figure 3.14 and Figure 3.15 as well as the overall results in Figure 3.10 and Figure 3.11. For all other B7 proteins and KIR-Fc fusion construct proteins no binding was obtained and henceforth no follow up experiments conducted. The overall results are depicted in Figure 3.12.

TABLE 3.5: Median and MAD of the MdFIs obtained from the KIR-Fc fusion construct proteins incubated with the B7 proteins (n = 2).

KIR-Fc protein	Median MdFI	MAD MdFI	p-value compared to 2ndary control
KIR3DL2-Fc	842.00	725.80	<0.05
KIR3DL3-Fc	3972.00	3816.50	<0.05
NKp30-Fc	2206.00	659.00	<0.05

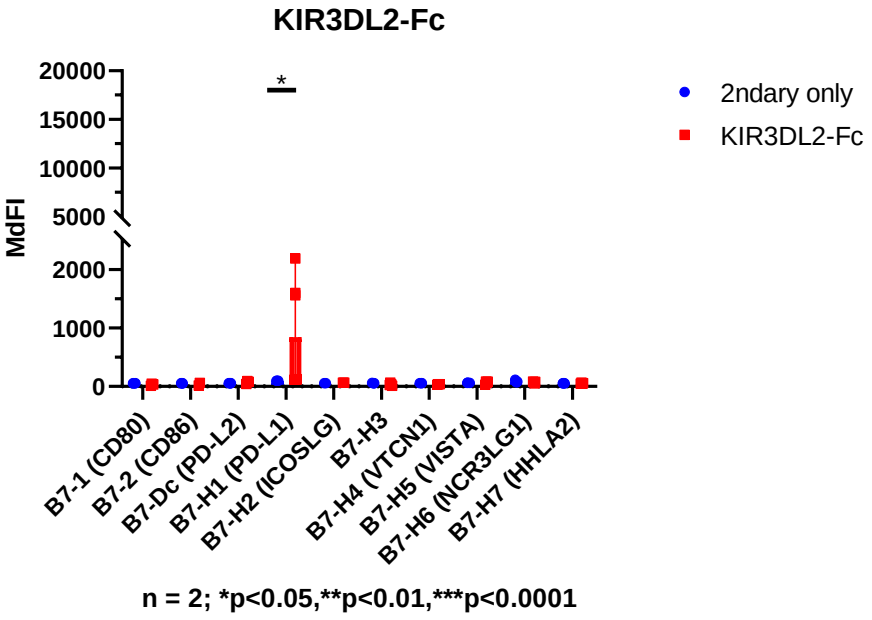

FIGURE 3.9: Results of KIR3DL2-Fc fusion construct proteins incubated with B7 proteins and stained for respective Fc tail shown for all biological replicates (n = 2). A statistically significant binding signal was obtained for the interaction of KIR3DL2-Fc and B7-H1 (PD-L1) (MdFI 842.00 ± 725.80) p<0.05 in comparison to its 2ndary only control (MdFI 98.00 ± 1.00). Analysed with a Wilcoxon-paired test.

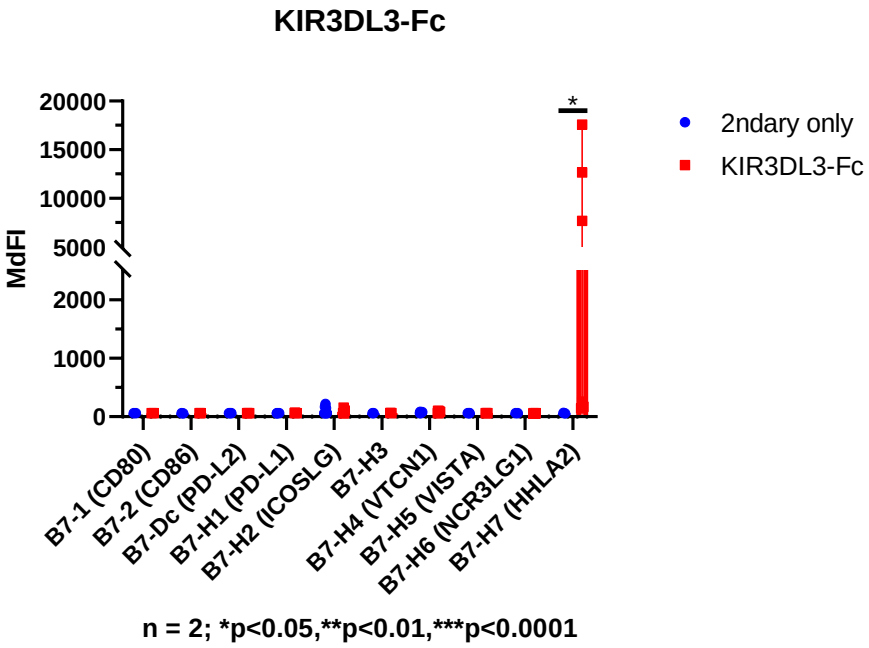

FIGURE 3.10: Results of KIR3DL3-Fc fusion construct proteins incubated with B7 proteins and stained for respective Fc tail shown for all biological replicates (n = 2). A statistically significant binding signal was obtained for the interaction of KIR3DL3-Fc and B7-H7 (HHLA2) (MdFI 3972.00 ± 3816.50) $p<0.05$ in comparison to its 2ndary only control (MdFI 61.40 ± 1.20). Analysed with a Wilcoxon-paired test.

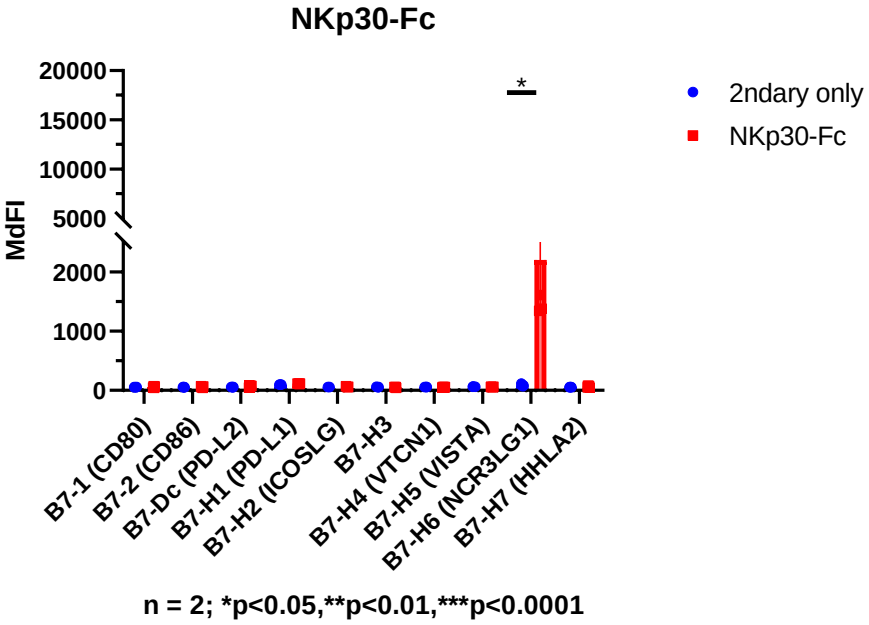

FIGURE 3.11: Results of NKp30-Fc fusion construct proteins incubated with B7 proteins and stained for respective Fc tail shown for all biological replicates (n = 2). A statistically significant binding signal was obtained for the interaction of NKp30-Fc and B7-H6 (NCR3LG1) (MdFI 2206.00 ± 659.00) $p<0.05$ in comparison to its 2ndary only control (MdFI 82.05 ± 6.85). Analysed with a Wilcoxon-paired test.

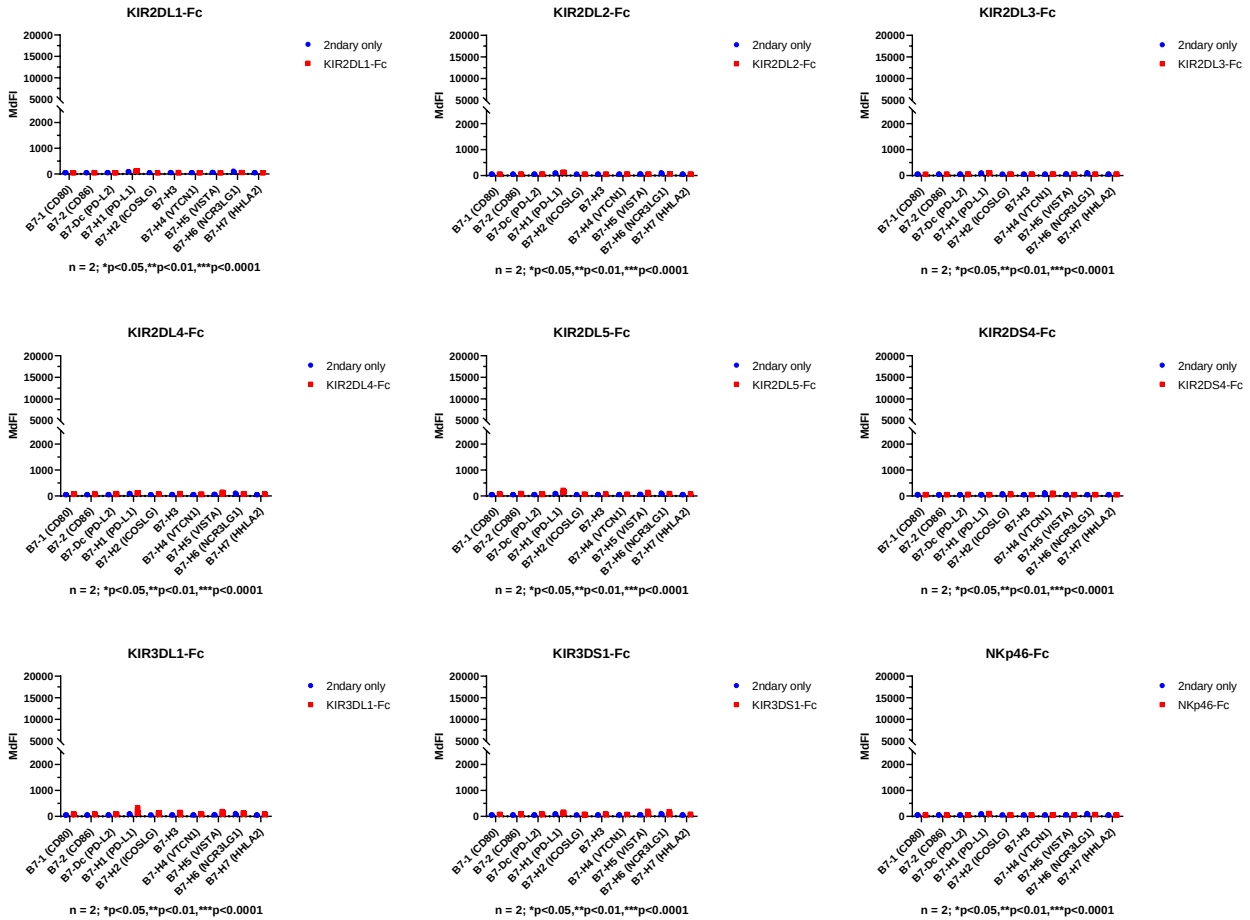

FIGURE 3.12: Results of all other Fc fusion construct proteins incubated with B7 proteins and stained for respective Fc tail shown for all biological replicates (n = 2). No binding could be observed between any B7 protein and KIR-Fc fusion construct protein.

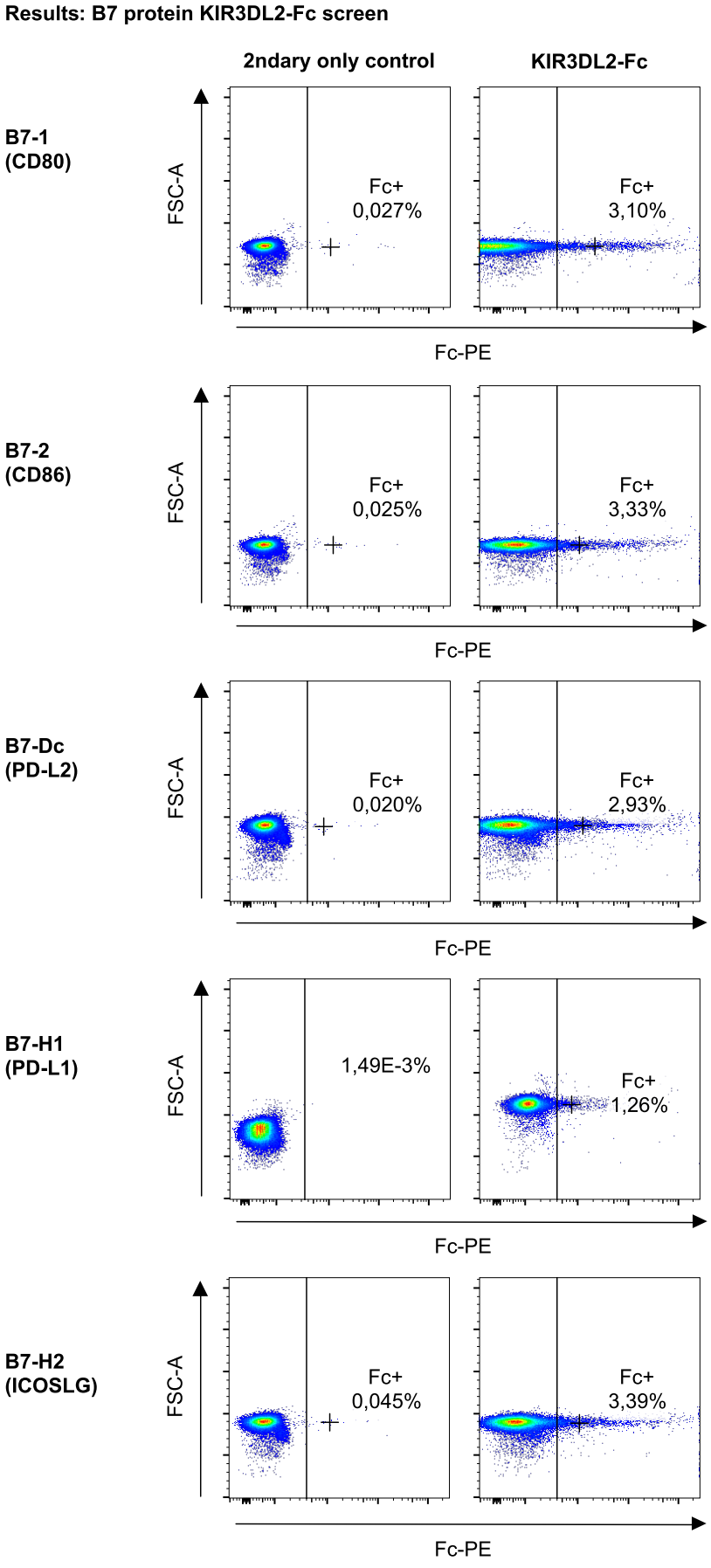
Results: B7 protein KIR3DL2-Fc screen
2ndary only control
KIR3DL2-Fc
B7-1
(CD80)
FSC-A
Fc+
0,027%
Fc+
3,10%
Fc-PE
B7-2
(CD86)
FSC-A
Fc+
0,025%
Fc+
3,33%
Fc-PE
B7-Dc
(PD-L2)
FSC-A
Fc+
0,020%
Fc+
2,93%
Fc-PE
B7-H1
(PD-L1)
FSC-A
1,49E-3%
Fc+
1,26%
Fc-PE
B7-H2
(ICOSLG)
FSC-A
Fc+
0,045%
Fc+
3,39%
Fc-PE

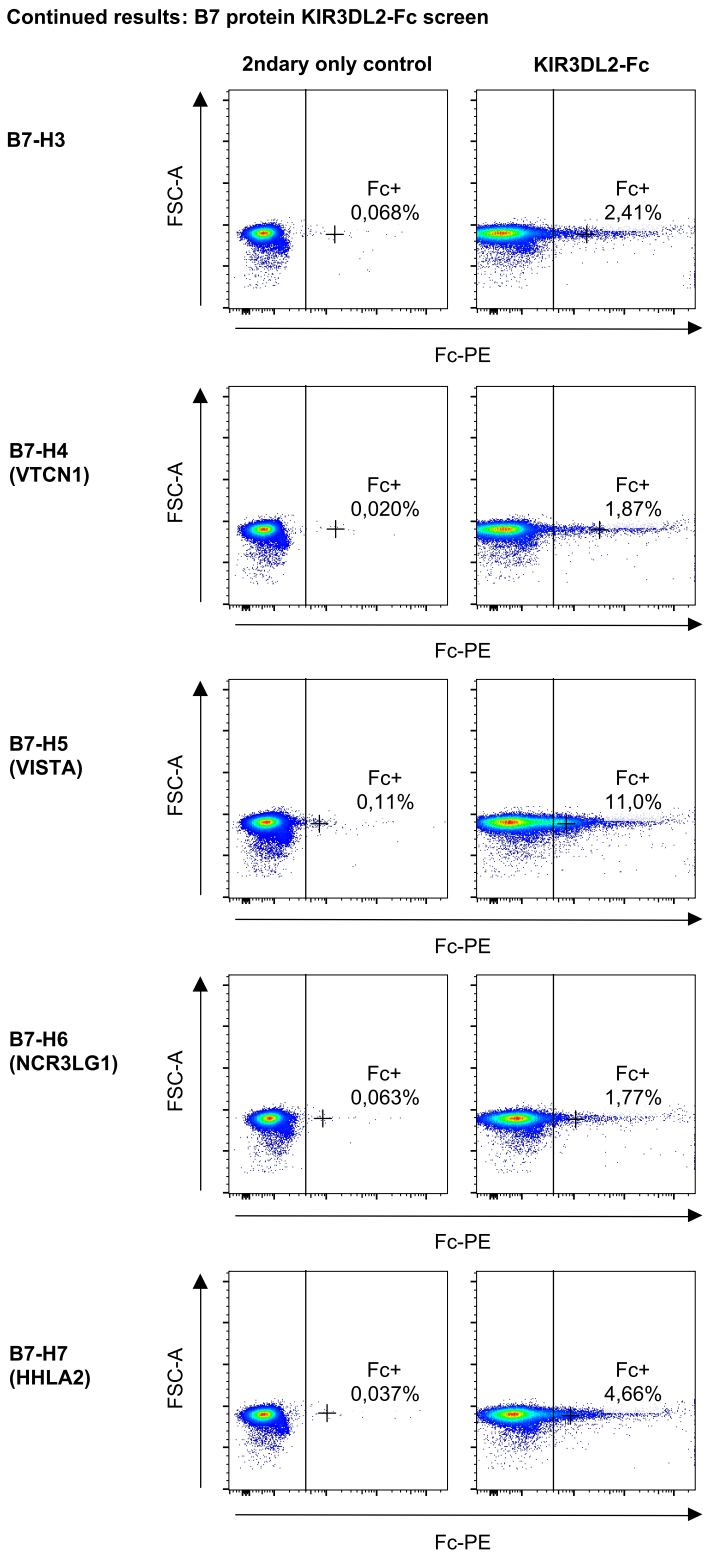

FIGURE 3.13: Primary data of KIR3DL2-Fc fusion construct proteins incubated with B7 proteins and stained for respective Fc tail shown for one technical triplicate (n = 1). A statistically significant signal was seen for the B7-H1 (PD-L1) KIR3DL2-Fc fusion construct protein interaction.

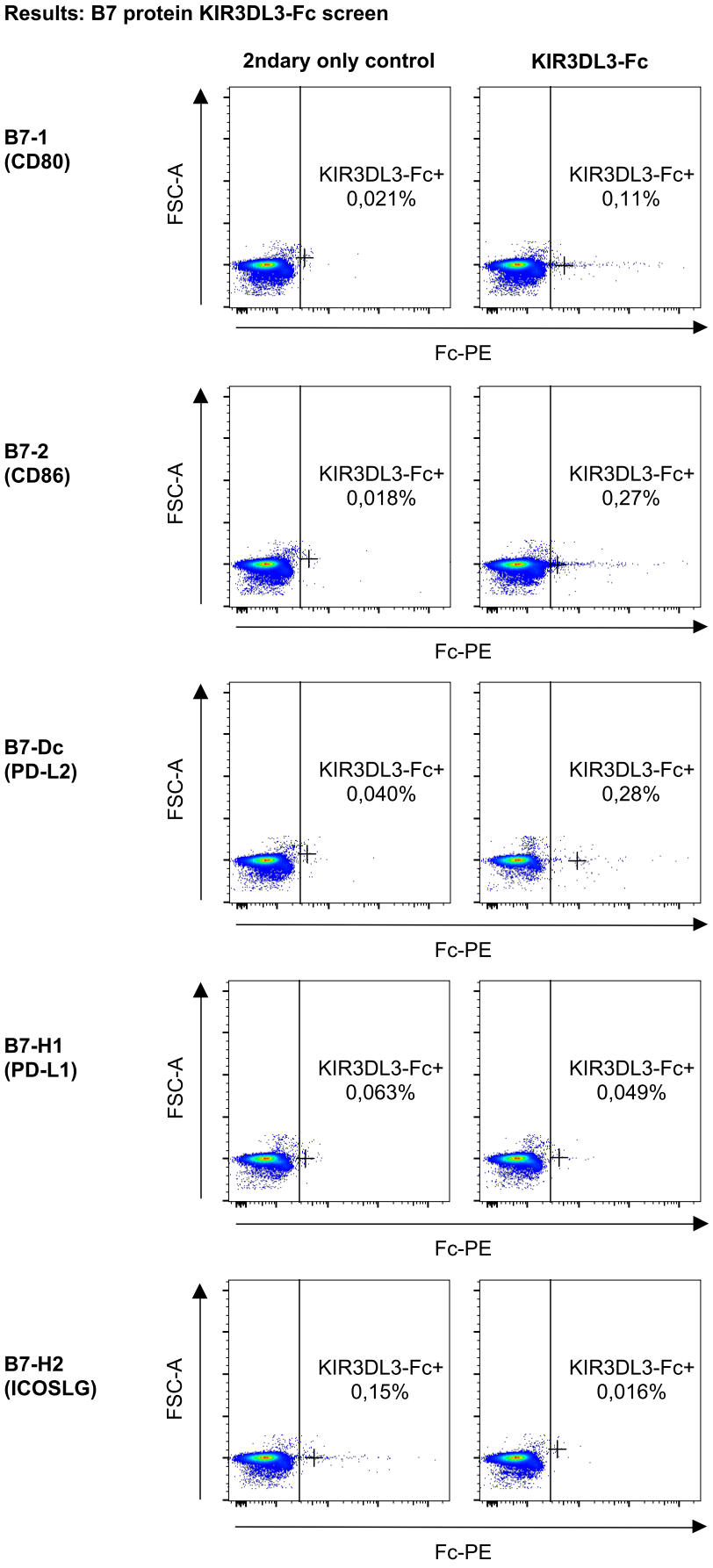
Results: B7 protein KIR3DL3-Fc screen
2ndary only control
KIR3DL3-Fc
B7-1
(CD80)
KIR3DL3-Fc+
0,021%
KIR3DL3-Fc+
0,11%
B7-2
(CD86)
KIR3DL3-Fc+
0,018%
KIR3DL3-Fc+
0,27%
B7-Dc
(PD-L2)
KIR3DL3-Fc+
0,040%
KIR3DL3-Fc+
0,28%
B7-H1
(PD-L1)
KIR3DL3-Fc+
0,063%
KIR3DL3-Fc+
0,049%
B7-H2
(ICOSLG)
KIR3DL3-Fc+
0,15%
KIR3DL3-Fc+
0,016%
FSC-A
Fc-PE

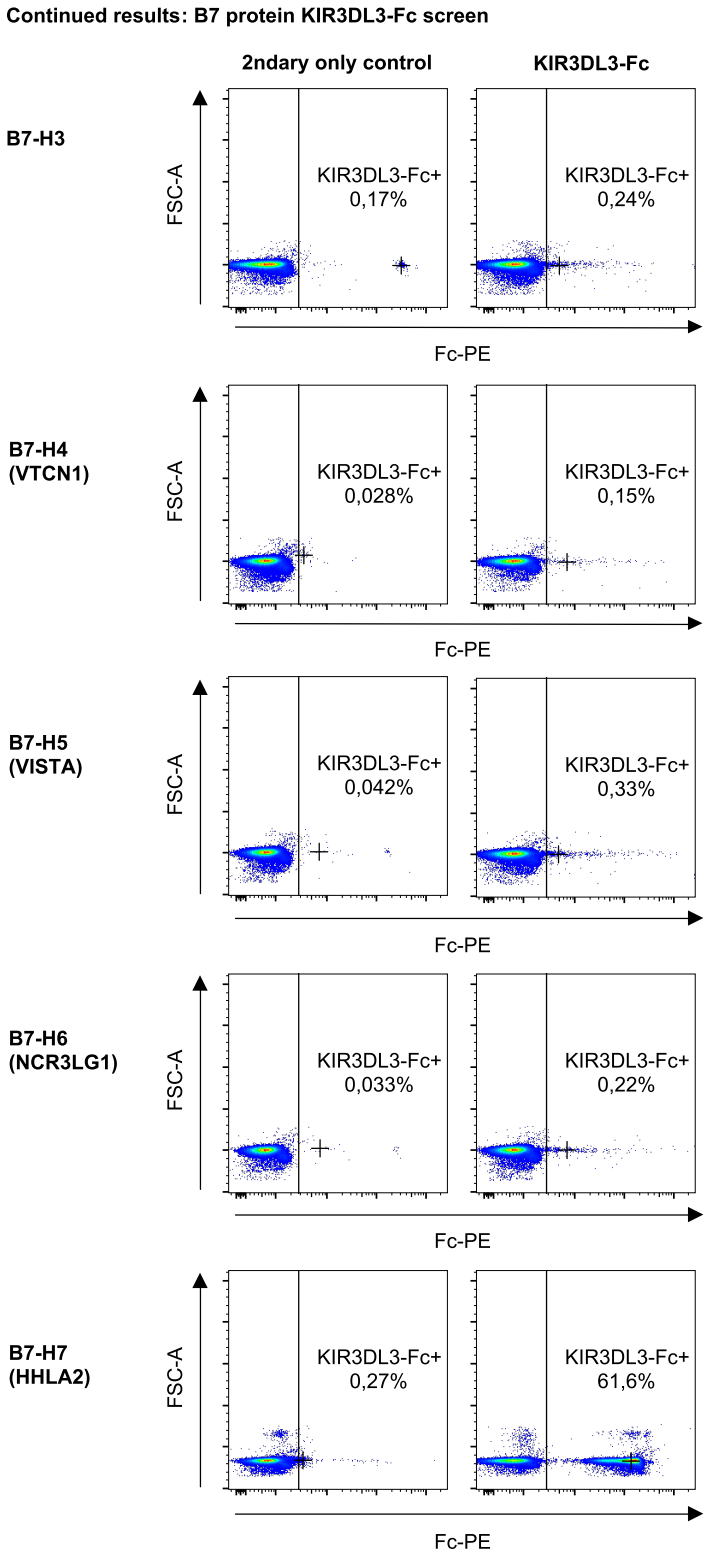

FIGURE 3.14: Primary data of KIR3DL3-Fc fusion construct proteins incubated with B7 proteins and stained for respective Fc tail shown for one technical triplicate (n = 1). A statistically significant signal was seen for the B7-H7 (HHLA2) KIR3DL3-Fc fusion construct protein interaction.

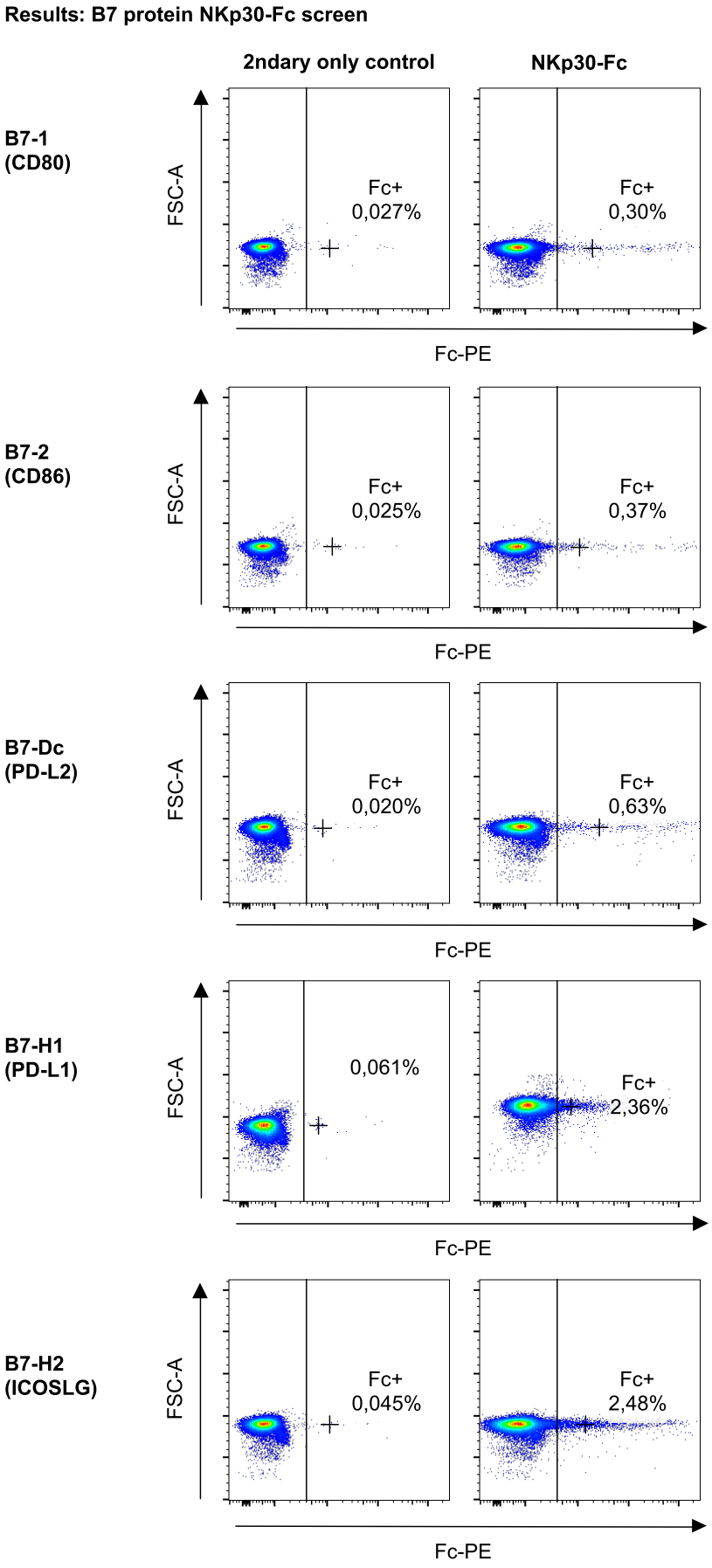
Results: B7 protein NKp30-Fc screen
2ndary only control
NKp30-Fc
B7-1
(CD80)
FSC-A
Fc+
0,027%
Fc+
0,30%
Fc-PE
B7-2
(CD86)
FSC-A
Fc+
0,025%
Fc+
0,37%
Fc-PE
B7-Dc
(PD-L2)
FSC-A
Fc+
0,020%
Fc+
0,63%
Fc-PE
B7-H1
(PD-L1)
FSC-A
0,061%
Fc+
2,36%
Fc-PE
B7-H2
(ICOSLG)
FSC-A
Fc+
0,045%
Fc+
2,48%
Fc-PE

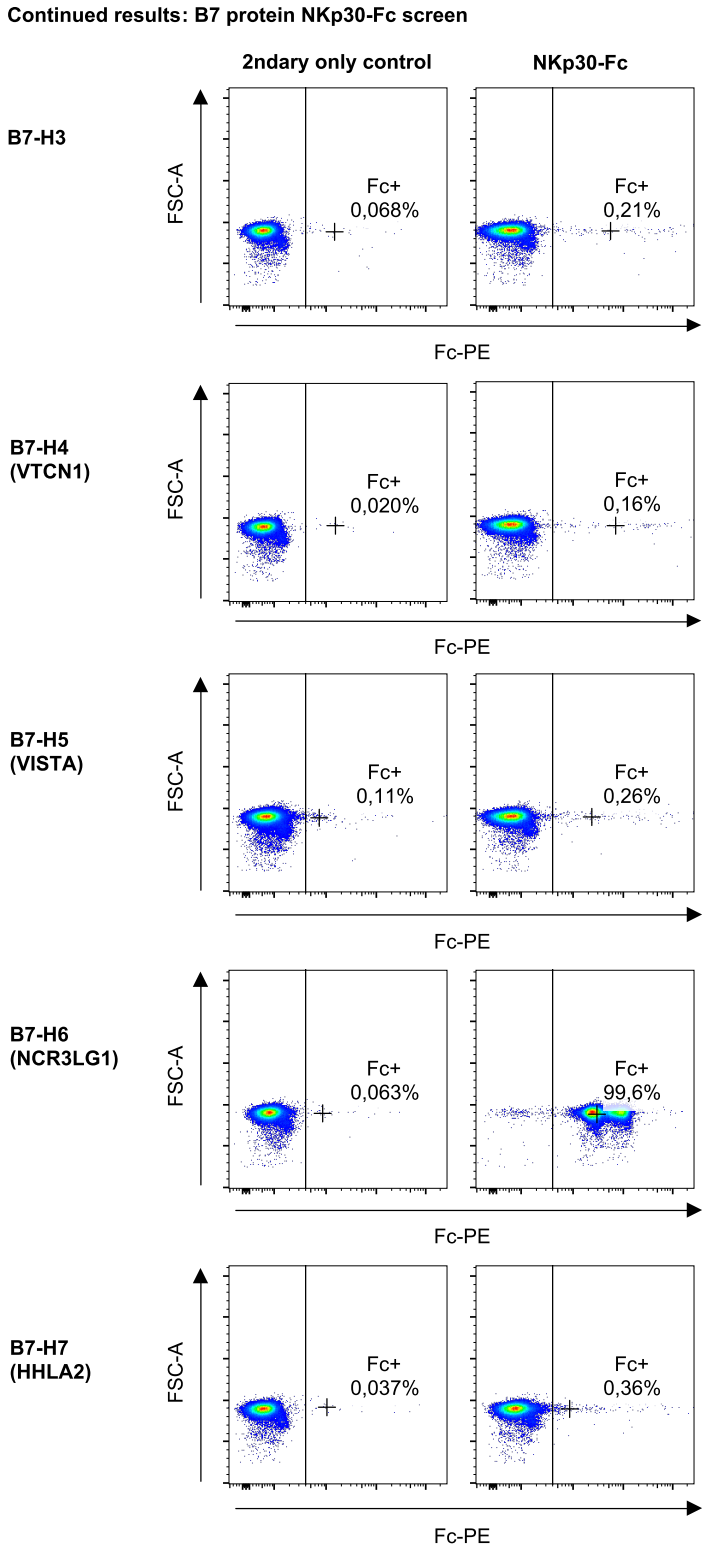

FIGURE 3.15: Primary data of NKp30-Fc fusion construct proteins incubated with B7 proteins and stained for respective Fc tail shown for one technical triplicate (n = 1). A statistically significant signal was seen for the B7-H6 (NCR3LG1) NKp30-Fc fusion construct protein interaction.

3.2 Cellular interaction between β2m-KO-Jurkat KIR3DL2 and B7-H1 (PD-L1)-Fc fusion construct protein cannot be confirmed

A KIR3DL1 transduced β2m-KO-Jurkat and a KIR2DS4 transduced β2m-KO-Jurkat cell line was previously designed by Dr. Wilfredo Garcia-Beltran and kindly provided for the experiment [205]. The β2m-KO-Jurkat KIR3DL2 and β2m-KO-Jurkat KIR2DS4 cell lines were, together with the plain β2m-KO-Jurkat cells, incubated with B7-H1 (PD-L1)-Fc fusion construct protein as previously described by our laboratory [90, 205]. The median fluorescence intensity (MdFI) was used as a read-out to determine the binding of the B7-H1 (PD-L1)-Fc fusion construct protein and the respective cell line (section 7.9, page 147). The median and the median absolute deviation (MAD) of all obtained MdFI values were then used for statistical testing (section 7.10, page 158).

The controls of the β2m-KO-Jurkat, β2m-KO-Jurkat KIR2DS4 and β2m-KO-Jurkat KIR3DL2 cells incubated with plain B7-H1 (PD-L1)-Fc fusion construct protein or plain secondary antibody did not show any background noise (Figure 3.16). The β2m-KO-Jurkat KIR2DS4 and β2m-KO-Jurkat KIR3DL2 cell line did express the respective KIR across all three biological triplicates with frequencies of parents of 92.00 % ± 4.00 % p>0.25 and 34.50 % ± 7.00 % p>0.25 (Figure 3.17).

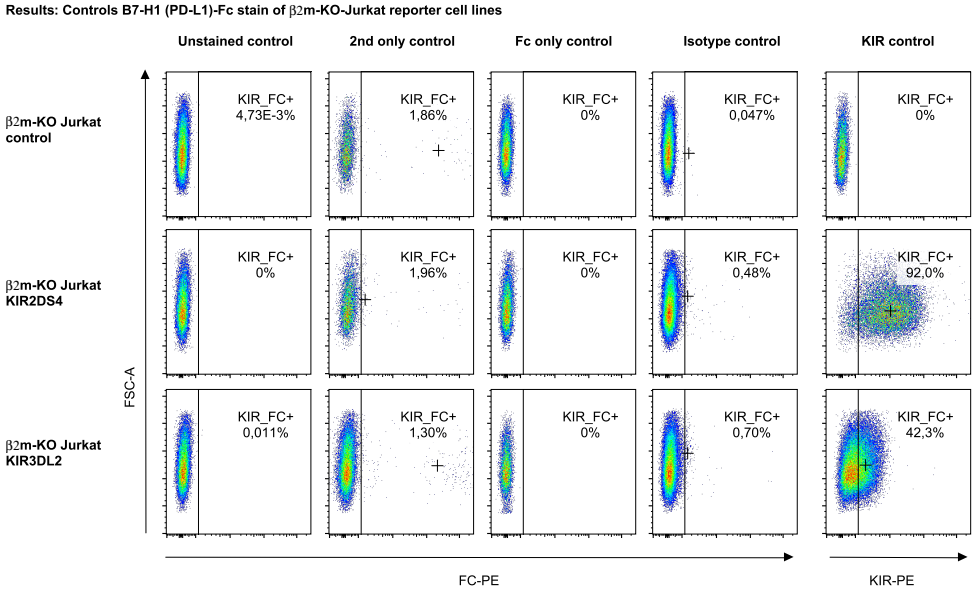

FIGURE 3.16: Controls of β2m-KO-Jurkat, β2m-KO-Jurkat KIR2DS4 and β2m-KO-Jurkat KIR3DL2 cell lines incubated with B7-H1 (PD-L1)-Fc fusion construct protein shown for one technical triplicate of three biological replications (n = 1). No background noise was seen for the 2ndary antibody nor the plain B7-H1 (PD-L1)-Fc fusion construct protein. The β2m-KO-Jurkat KIR2DS4 and β2m-KO-Jurkat KIR3DL2 cell line did express the respective KIR.

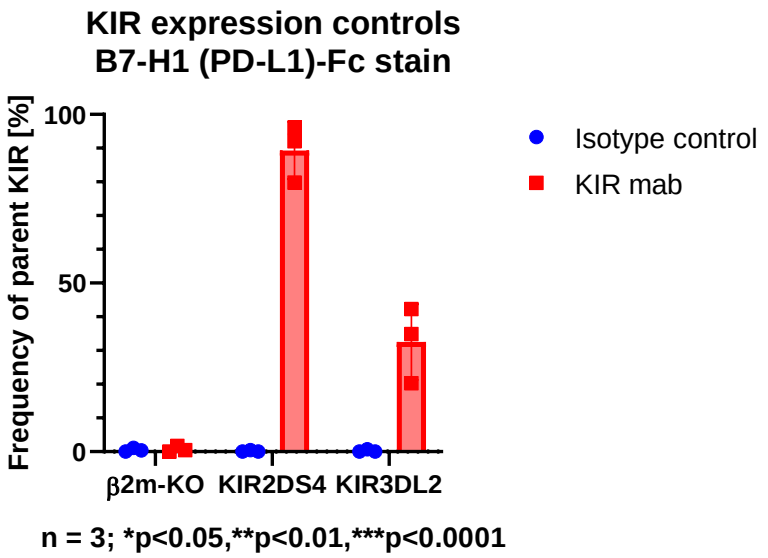

FIGURE 3.17: Results of β2m-KO-Jurkat, β2m-KO-Jurkat KIR2DS4 and β2m-KO-Jurkat KIR3DL2 cells incubated with KIR mab shown for all biological replicates (n = 3). The β2m-KO-Jurkat KIR2DS4 and β2m-KO-Jurkat KIR3DL2 cell line did express the respective KIR across all three biological replicates (n = 3) with frequencies of parents of 92.00 % ± 4.00 % p>0.25 and 34.50 % ± 7.00 % p>0.25. Analysed with a Wilcoxon-paired test.

No statistically significant binding of the B7-H1 (PD-L1)-Fc fusion construct protein could be obtained for the β2m-KO-Jurkat KIR3DL2 cell line (MdFI 25.60 ± 5.10 p>0.05). The median MdFIs of the other cell lines showed similar results (β2m-KO-Jurkat 20.50 ± 2.00, KIR2DS4 MdFI 30.70 ± 10.20) (Table 3.6). However, the MdFI difference between the β2m-KO-Jurkat KIR2DS4 cell line incubated with the B7-H1 (PD-L1)-Fc fusion construct protein in comparison to the untransduced β2m-KO-Jurkat cell line and the β2m-KO-Jurkat KIR3DL2 cell line incubated with the B7-H1 (PD-L1)-Fc fusion construct protein was reported as statistical significant by the post-hoc analysis after the Friedman test with Wilcoxon tests p<0.05. An example of the binding is shown in Figure 3.18 and the overall results in Figure 3.19.

TABLE 3.6: Median and MAD of the MdFIs obtained from the binding assay of the B7-H1 (PD-L1)-Fc fusion construct protein and the KIR expressing β2m-KO-Jurkat cell lines (n = 3).

Cell line	**Median MdFI**	**MAD MdFI**	**adjusted p-value compared to KIR3DL2**
β2m-KO-Jurkat	20.50	2.00	>0.05
β2m-KO-Jurkat KIR2DS4	30.70	10.20	<0.05
β2m-KO-Jurkat KIR3DL2	25.60	5.10	-

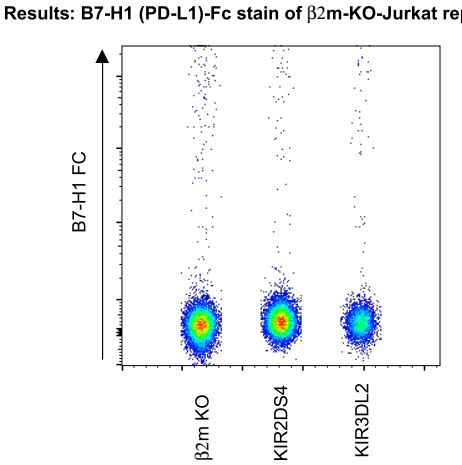

FIGURE 3.18: Primary data of β2m-KO-Jurkat, β2m-KO-Jurkat KIR3DL2, β2m-KO-Jurkat KIR2DS4 cells incubated with B7-H1 (PD-L1)-Fc fusion construct protein shown for one technical triplicate of three biological replicates (n = 1). None of the cell lines did show a positive binding signal for the B7-H1 (PD-L1)-Fc fusion construct protein binding.

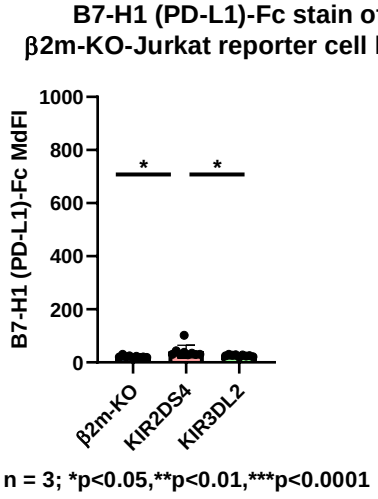

FIGURE 3.19: Results of β2m-KO-Jurkat, β2m-KO-Jurkat KIR2DS4 and β2m-KO-Jurkat KIR3DL2 cells incubated with B7-H1 (PD-L1)-Fc fusion construct protein for all biological replicates (n = 3). No statistically significant binding signal was seen between the β2m-KO-Jurkat KIR3DL2 cell line and the B7-H1 (PD-L1)-Fc fusion construct protein (MdFI 25.60 $\pm$ 5.10 $p>0.05$) in comparison to the β2m-KO-Jurkat cell line (MdFI 20.50 $\pm$ 2.00). However, a statistical difference in the binding signal between the β2m-KO-Jurkat KIR2DS4 cell line incubated with the B7-H1 (PD-L1)-Fc fusion construct protein and the untransduced β2m-KO-Jurkat cell line as well as the β2m-KO-Jurkat KIR3DL2 incubated with the B7-H1 (PD-L1)-Fc fusion construct protein was detected (MdFI 30.70 $\pm$ 10.20 $p<0.05$). Analysed with Wilcoxon-paired tests corrected for multiple testing with Benjamini & Hochberg method [294].

3.3 Cellular interaction between β2m-KO-Jurkat KIR3DL3 and B7-H7-Fc fusion construct protein can be confirmed

3.3.1 Generation of KIR3DL3 expressing β2m-KO-Jurkat cell lines

Naturally, β2m-KO-Jurkat cells derived from the human acute T cell leukaemia cell line JurkatE6.1 consisting of T lymphoblasts do not express KIRs and HLA receptors, due to a CRISPR-Cas9 knock out previously described by our laboratory [32, 205]. Therefore, they could be transduced using lentiviruses to express a single chimeric KIR of interest. The KIR is thereby fused to a CD3ζ chain which upon activation leads to the upregulation of CD69, the key read out of the reporter cell assay (section 3.4). The missing of HLA receptors on the cell surface is crucial as they are well known interaction partners of KIRs which would trigger an immediate activation of the transformed β2m-KO-Jurkat cells leading to exhaustion and cell death [206, 295, 296].

The KIR3DL3 expressing β2m-KO-Jurkat cell line was generated using the KIR3DL3 *001 allotype which together with the KIR3DL3*003 and KIR3DL3*009 allotype is the most abundant KIR3DL3 allotype within Caucasians [32, 194, 297]. A UniProt blast revealed that the *001 allotype does not differ in its extracellular domain from the other two allotypes (section A.1, page 205). The KIR3DL3 expression of the generated β2m-KO-Jurkat cell line was compared to unstained as well as untransduced cell lines using flow cytometry exporting the frequency of CD3 positive β2m-KO-Jurkat parent cells displaying the KIR3DL3 receptor (Figure 3.20). Next, the mean of the frequency of parent expression for KIR3DL3 and the standard deviation was calculated for the β2m-KO-Jurkat and β2m-KO-Jurkat KIR3DL3 cell lines.

The KIR3DL3 transduced β2m-KO-Jurkat cell line showed a positive signal expressing KIR3DL3 with a frequency of 41.87 % ± 8.02 % while the untransduced β2m-KO-Jurkat cell line did show a staining signal with a frequency of parent of 0.04 % ± 0.03 % (Figure 3.21). The β2m-KO-Jurkat KIR3DL3 cell line was used for the B7-H7-Fc fusion protein binding assay, the Jurkat reporter cell assay and as positive controls in other experiments.

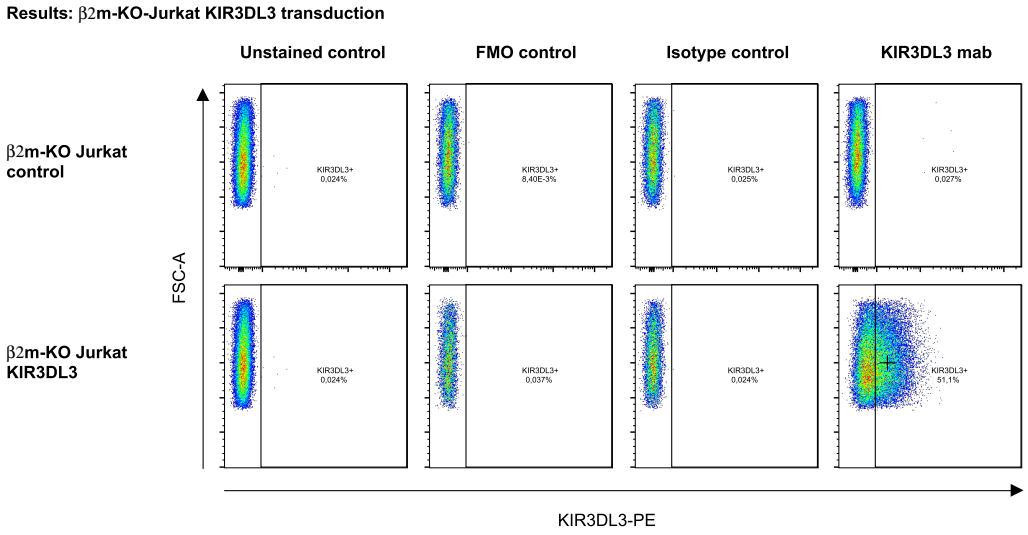

FIGURE 3.20: Primary data of β2m-KO-Jurkat cells transduced with KIR3DL3 stained for KIR3DL3 expression shown for one technical triplicate (n = 1). KIR3DL3 transduced β2m-KO-Jurkat cell line showed a positive signal expressing KIR3DL3 while the untransduced β2m-KO-Jurkat cell line did not show any staining signal. The β2m-KO-Jurkat KIR3DL3 cell line was used for the B7-H7-Fc fusion protein binding assay, the Jurkat reporter cell assay and as positive controls in other experiments.

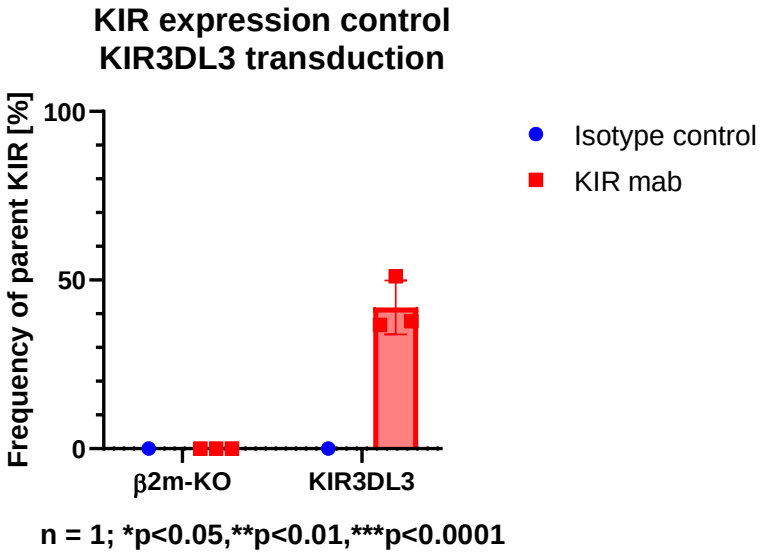

FIGURE 3.21: Results of β2m-KO-Jurkat cells transduced with KIR3DL3 stained for KIR3DL3 expression shown for all biological replicates (n = 1). KIR3DL3 transduced β2m-KO-Jurkat cell line showed a positive signal expressing KIR3DL3 41.87 % $\pm$ 8.02 % p=1.0 while the untransduced β2m-KO-Jurkat cell line did not show any staining signal 0.04 % $\pm$ 0.03 % p=1.0. The β2m-KO-Jurkat KIR3DL3 cell line was used for the B7-H7-Fc fusion construct protein binding assay, the Jurkat reporter cell assay and as positive controls in other experiments. Analysed with Wilcoxon-paired test.

3.3.2 B7-H7-Fc fusion construct protein exclusively binds β2m-KO-Jurkat KIR3DL3 cells

The successfully transduced β2m-KO-Jurkat KIR3DL3 cell line, together with transduced β2m-KO-Jurkat KIR2DL5 and β2m-KO-Jurkat KIR3DL1 cell line, both already available in our lab, were together with the plain β2m-KO-Jurkat cells incubated with B7-H7-Fc fusion construct protein [90, 205]. As described the median fluorescence intensity (MdFI) was used as a read-out to determine the binding of the B7-H7-Fc fusion construct protein and the respective cell line (section 7.9, page 147). The median and the median absolute deviation (MAD) of all obtained MdFI values were then used for statistical testing (section 7.10, page 158).

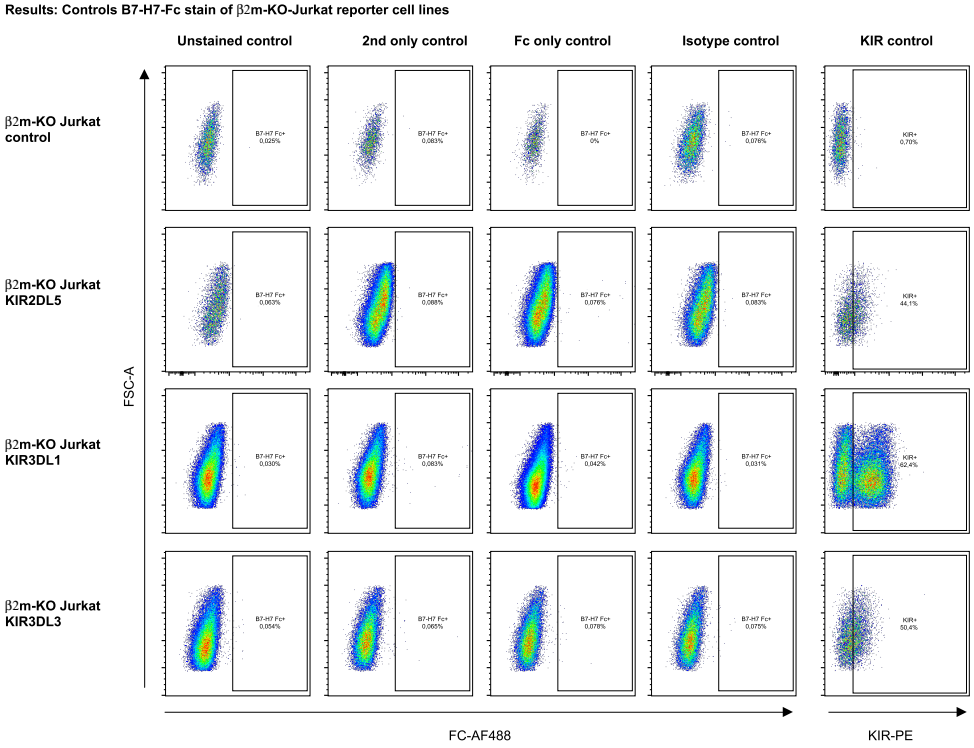

FIGURE 3.22: Controls of β2m-KO-Jurkat, β2m-KO-Jurkat KIR2DL5, β2m-KO-Jurkat KIR3DL1 and β2m-KO-Jurkat KIR3DL3 incubated with B7-H7-Fc fusion construct protein shown for one technical triplicate of three biological replications (n = 1). No background noise was seen for the 2ndary antibody nor the plain B7-H7 Fc fusion construct protein. The β2m-KO-Jurkat KIR2DL5, KIR3DL1, KIR3DL3 cell line did express the respective KIR.

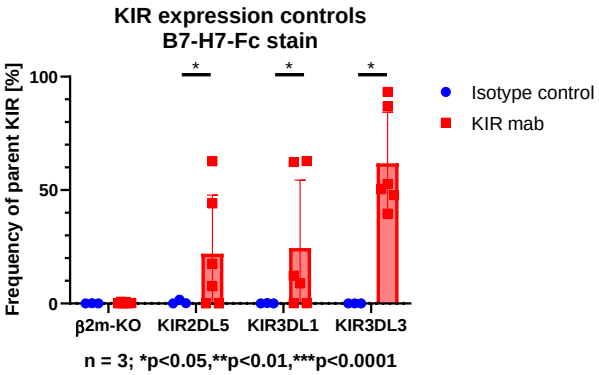

FIGURE 3.23: Results of β2m-KO-Jurkat, β2m-KO-Jurkat KIR2DL5, and β2m-KO-Jurkat KIR3DL1 and β2m-KO-Jurkat KIR3DL3 cells incubated with KIR mab shown for all biological replicates (n = 3). All β2m-KO-Jurkat cell lines did express the respective KIR across all three biological replicates (n = 3) with frequencies of parents of 20.54 % ± 22.20 % $p<0.05$, 24.94 % ± 33.00 % $p<0.05$ and 65.47 % ± 24.13 % $p<0.05$. Analysed with Wilcoxon-paired tests.

The controls of the β2m-KO-Jurkat, β2m-KO-Jurkat KIR2DL5 and β2m-KO-Jurkat KIR3DL1, β2m-KO-Jurkat KIR3DL3, cells incubated with plain B7-H7-Fc fusion construct protein or plain 2ndary antibody did not show any background noise (Figure 3.22). The β2m-KO-Jurkat KIR2DL5, KIR3DL1, KIR3DL3 cell lines did express the respective KIR across all three biological triplicates with respectively 20.54 % ± 22.20 % $p<0.05$, 24.94 % ± 33.00 % $p<0.05$ and 65.47 % ± 24.13 % $p<0.05$ (Figure 3.23).

A statistically significant binding of the B7-H7-Fc fusion construct protein could only be obtained for the β2m-KO-Jurkat KIR3DL3 cell line (MdFI 1068.00 ± 266.00 $p<0.01$) towards the untransduced β2m-KO-Jurkat cell line, while less binding was seen for the β2m-KO-Jurkat (MdFI 255.00 ± 40.00), β2m-KO-Jurkat KIR2DL5 (MdFI 418.00 ± 99.50) and β2m-KO-Jurkat KIR3DL1 (MdFI 314.00 ± 46.00) cell lines (Table 3.7). An example is shown in Figure 3.24 and the overall results in Figure 3.25.

TABLE 3.7: Median and MAD of the MdFIs obtained from the binding assay of the B7-H7-Fc fusion construct protein and the KIR expressing β2m-KO-Jurkat cell lines (n = 3).

Cell line	**Median MdFI**	**MAD MdFI**	**adjusted p-value compared to KIR3DL3**
β2m-KO-Jurkat	255.00	40.00	<0.01
β2m-KO-Jurkat KIR2DL5	418.00	99.50	<0.01
β2m-KO-Jurkat KIR3DL1	314.00	46.00	<0.01
β2m-KO-Jurkat KIR3DL3	1068.00	266.00	-

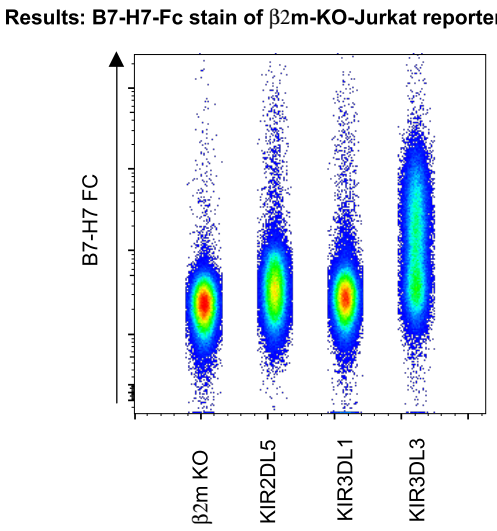

FIGURE 3.24: Primary data of β2m-KO-Jurkat, β2m-KO-Jurkat KIR2DL5, β2m-KO-Jurkat KIR3DL1 and β2m-KO-Jurkat KIR3DL3 cells incubated with B7-H7-Fc fusion construct protein shown for one technical triplicate of three biological replicates (n = 1). β2m-KO-Jurkat KIR3DL3 showed a positive binding signal for the B7-H7-Fc fusion protein binding, while the other cell lines did only show little binding of the Fc fusion construct protein.

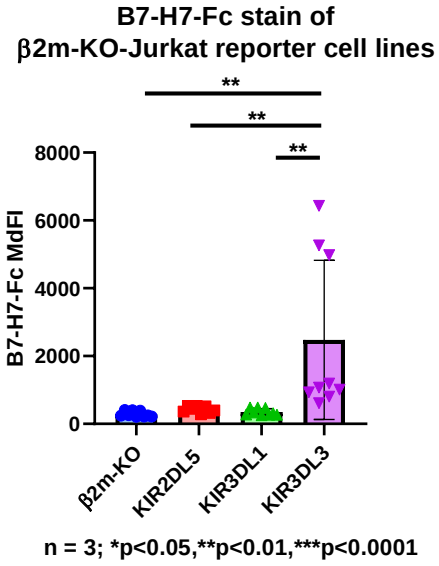

FIGURE 3.25: Results of β2m-KO-Jurkat, β2m-KO-Jurkat KIR2DL5, β2m-KO-Jurkat KIR3DL1 and β2m-KO-Jurkat KIR3DL3 cells incubated with B7-H7-Fc fusion construct protein for all biological replicates (n = 3). β2m-KO-Jurkat KIR3DL3 cells showed a statistically significant positive binding signal for B7-H7-Fc fusion construct protein (MdFI 1068.00 ± 266.00 $p<0.01$) in comparison to the untransduced β2m-KO-Jurkat cell line, while the other cell lines did only show little binding (KIR2DL5 MdFI 418.00 ± 99.50, KIR3DL1 MdFI 314.00 ± 46.00, β2m-KO-Jurkat 255.00 ± 40.00) of the B7-H7-Fc fusion construct protein. Analysed with Wilcoxon-paired tests corrected for multiple testing with Benjamini & Hochberg method [294].

3.4 B7-H7 protein exclusively activates KIR3DL3 receptor

As described the genetically modified β2m-KO-Jurkat KIR cell lines contain a CD3ζ domain which, upon KIR activation, allows them to recruit the CD69 receptor to the cell surface (subsection 7.8.3, page 141). To demonstrate a biological activation and interaction of the KIR3DL3 receptor upon B7-H7 binding, B7-H7 protein was coated on an untreated 96-well plate and incubated with the respective β2m-KO-Jurkat, β2m-KO-Jurkat KIR2DL5, β2m-KO-Jurkat KIR3DL1 and β2m-KO-Jurkat KIR3DL3 cell lines. The cells were then stained for CD69 expression.

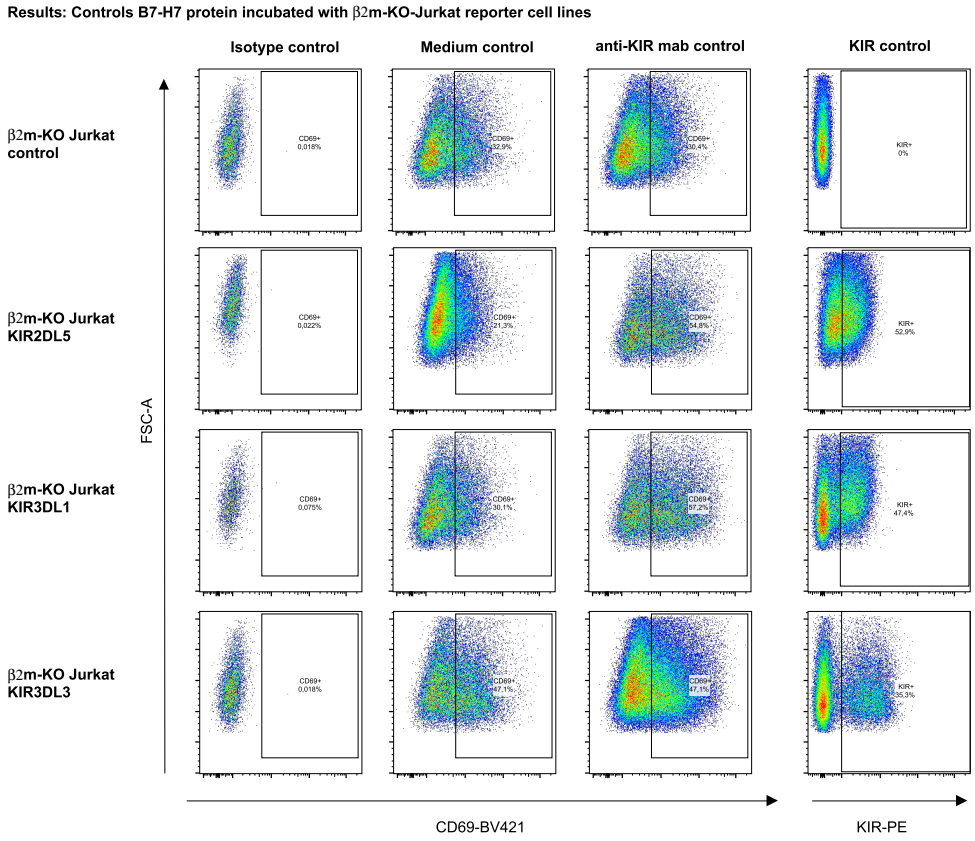

FIGURE 3.26: Controls of β2m-KO-Jurkat, β2m-KO-Jurkat KIR2DL5, β2m-KO-Jurkat KIR3DL1 and β2m-KO-Jurkat KIR3DL3 cell lines incubated with B7-H7 protein shown for one technical triplicate of three biological replications (n = 1). No background noise was seen for the isotype control. However, the cell lines did show a background CD69 expression in the medium control. The β2m-KO-Jurkat KIR3DL3, KIR2Dl5, KIR3DL1 cell line did express the respective KIR of interest and could be activated to upregulate CD69 expression with mab targeted against the respective KIR.

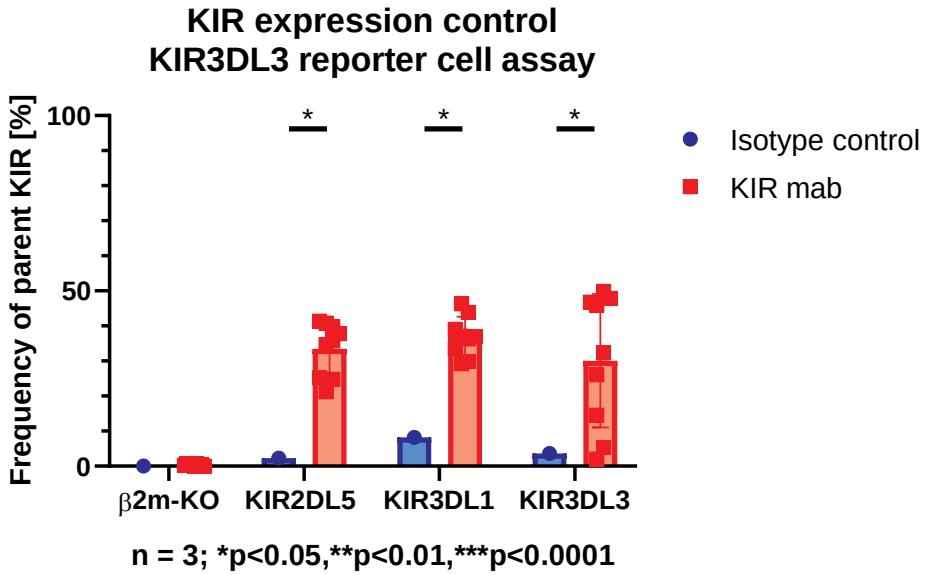

FIGURE 3.27: Results of β2m-KO-Jurkat, β2m-KO-Jurkat KIR2DL5, and β2m-KO-Jurkat KIR3DL1 and β2m-KO-Jurkat KIR3DL3 cells incubated with KIR mab shown for all biological replicates (n = 3). All β2m-KO-Jurkat cell lines did express the respective KIR across all three biological replicates (n = 3) with frequencies of parents of 33.49 % ± 7.71 % $p<0.05$, 30.07 % ± 19.06 % $p<0.05$ and 36.91 % ± 5.72 % $p<0.05$. Analysed with Wilcoxon-paired tests.

The controls of the β2m-KO-Jurkat, β2m-KO-Jurkat KIR2DL5, β2m-KO-Jurkat KIR3DL1 and β2m-KO-Jurkat KIR3DL3 cell lines incubated with B7-H7 protein did not show any background noise for the CD69 isotype control (Figure 3.26). However, the cell lines did show a background CD69 expression in the medium control with the CD69 antibody. The β2m-KO-Jurkat KIR3DL3, KIR2DL5, KIR3DL1 cell line did express the respective KIR of interest (Figure 3.27) and could be activated to upregulate CD69 expression with mab targeted against the respective KIR.

In terms of Jurkat reporter cell binding and activation a statistically significant signal for CD69 upregulation could only be obtained for the β2m-KO-Jurkat KIR3DL3 cell line incubated with the B7-H7 protein (MdFI 1067.00 ± 437.00 $p<0.01$) in comparison to its media control (MdFI 292.00 ± 20.00) and the β2m-KO-Jurkat (MdFI 295.00 ± 8.00), β2m-KO-Jurkat KIR2DL5 (MdFI 288.00 ± 34.00) and β2m-KO-Jurkat KIR3DL1 (MdFI 280.00 ± 2.00) cell lines incubated with the B7-H7 protein (all $p<0.001$) (Table 3.8). An example of the binding and activation for one technical triplicate of one biological replicate is shown in Figure 3.28 and the overall results for all biological replicates in Figure 3.29.

TABLE 3.8: Median and MAD of the MdFIs obtained from the Jurkat reporter cell assay of the KIR expressing β2m-KO-Jurkat cell lines (n = 3).

Cell line	**Median MdFI**	**MAD MdFI**	**adjusted p-value compared to KIR3DL3 with B7-H7 protein**
β2m-KO-Jurkat	295.00	8.00	<0.001
β2m-KO-Jurkat KIR2DL5	288.00	34.00	<0.001
β2m-KO-Jurkat KIR3DL1	280.00	2.00	<0.001
β2m-KO-Jurkat KIR3DL3	1067.00	437.00	-
β2m-KO-Jurkat KIR3DL3 medium control	292.00	20.00	<0.01

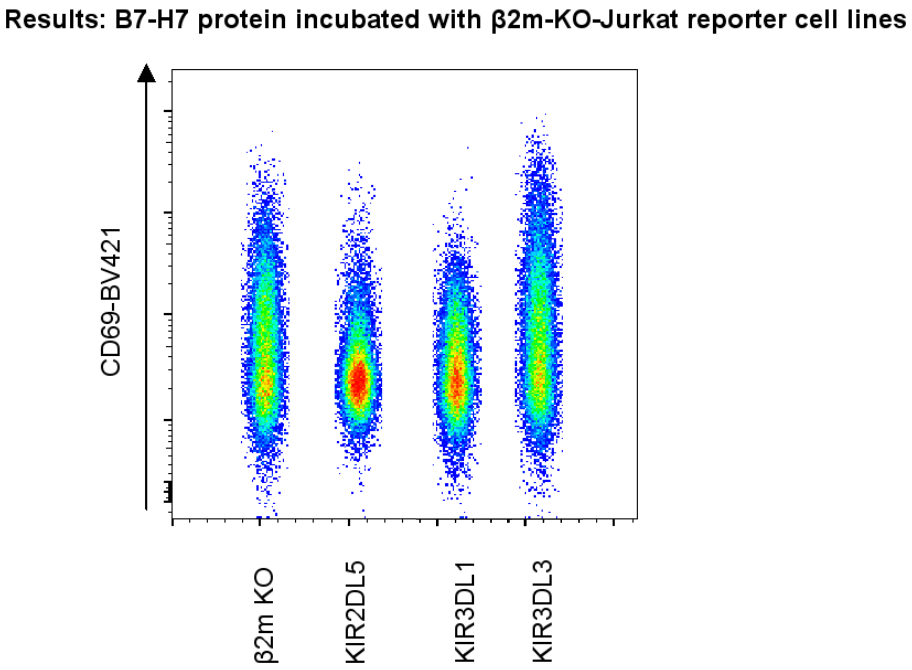

FIGURE 3.28: Primary data of β2m-KO-Jurkat, β2m-KO-Jurkat KIR2DL5, β2m-KO-Jurkat KIR3DL1 and β2m-KO-Jurkat KIR3DL3 cell lines incubated with B7-H7 protein shown for one technical triplicate of three biological replicates (n = 1). β2m-KO-Jurkat KIR3DL3 cells showed a statistically significant upregulation of CD69 upon protein binding, while the other Jurkat reporter cell lines showed little to no upregulation of CD69.

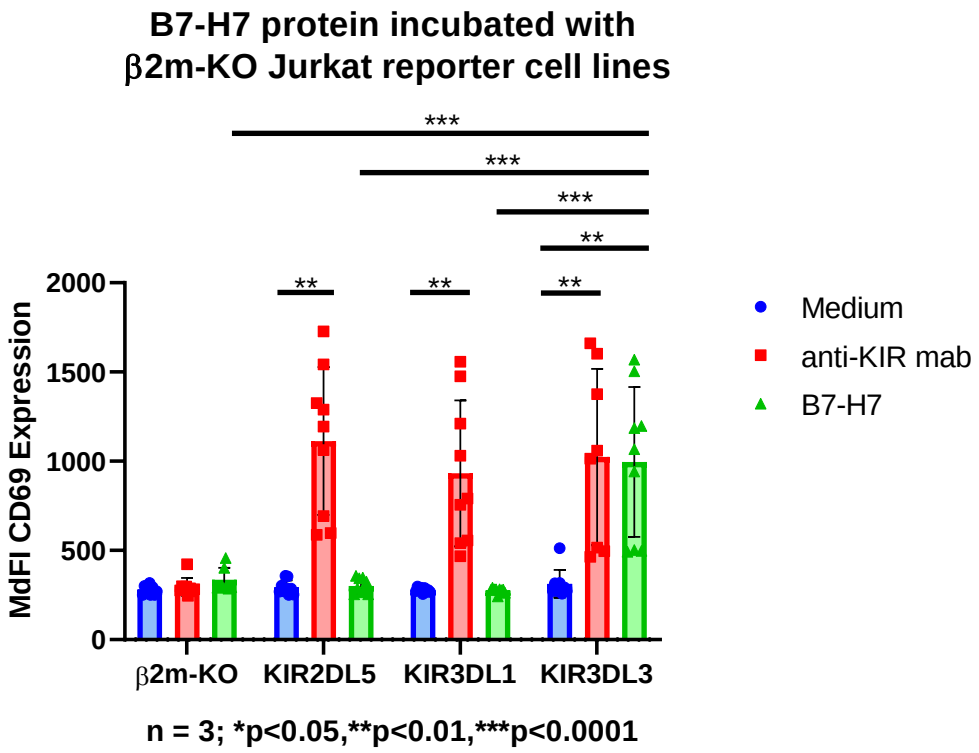

FIGURE 3.29: Results of β2m-KO-Jurkat, β2m-KO-Jurkat KIR2DL5, β2m-KO-Jurkat KIR3DL1 and β2m-KO-Jurkat KIR3DL3 cell lines incubated with B7-H7 protein for all three biological replications (n = 3). β2m-KO-Jurkat KIR3DL3 cells showed a statistically significant upregulation of CD69 (MdFI 1067.00 ± 437.00 $p<0.01$) in comparison to its media control (MdFI 292.00 ± 20.00) and the β2m-KO-Jurkat (MdFI 295.00 ± 8.00), β2m-KO-Jurkat KIR2DL5 (MdFI 288.00 ± 34.00) and β2m-KO-Jurkat KIR3DL1 (MdFI 280.00 ± 2.00) cell lines incubated with the B7-H7 protein (all $p<0.001$). Analysed with Wilcoxon-paired tests corrected for multiple testing with Benjamini & Hochberg method [294].

3.5 NK cell killing assay and its inhibition

3.5.1 Generation of B7-H7 expressing K562 cell line

Naturally, the human chronic myelogenous lymphoma derived cell line K562 does not express HLA class-I and class-II receptors on its cell surface, which makes it a suitable cell line to be used in NK cell killing experiments [32, 298, 299]. NK cells are constantly screening their surrounding for HLA expression and protein presentation and can get triggered upon missing HLA receptor presence on the cell surface [99, 100]. Upon activation NK cells can start to degranulate and kill the surrounding cells via granzyme B pathways which integrate perforin into the cell membrane [105, 106]. Additionally, my screenings with commercially available B7-H7 antibody did not show any intrinsic B7-H7 expression on K562 cells (Figure 3.30), although otherwise reported by Janakiram *et al.* [21].

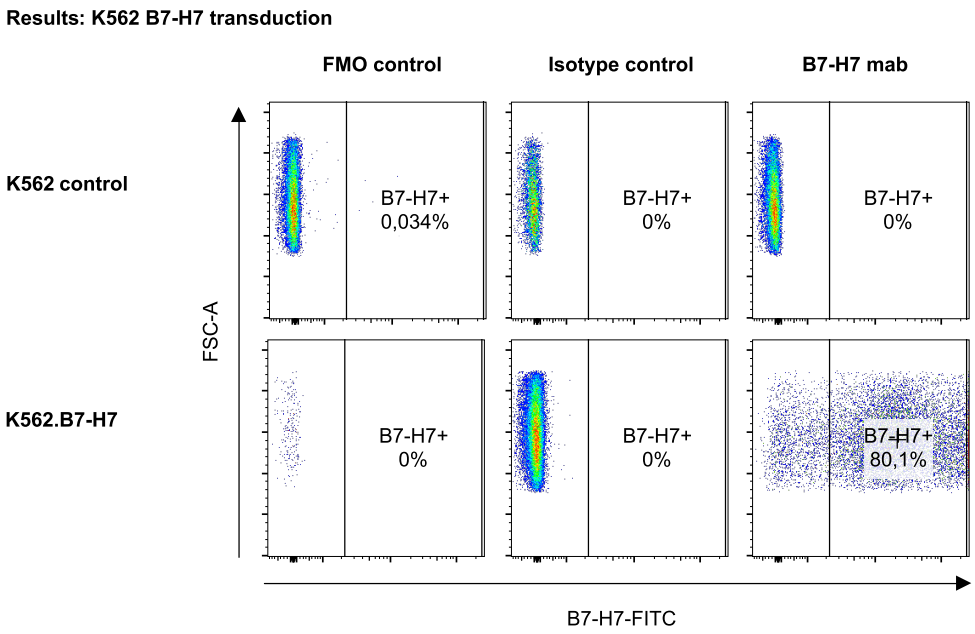

FIGURE 3.30: Primary data of K562 cells transduced with B7-H7 stained for B7-H7 expression shown for one technical triplicate (n = 1). B7-H7 transduced K562 cell line showed a positive signal expressing B7-H7 while the untransduced K562 cell line did not show any staining signal. The K562.B7-H7 cell line was used for the NK cell killing assay and as positive control in the compartment screen.

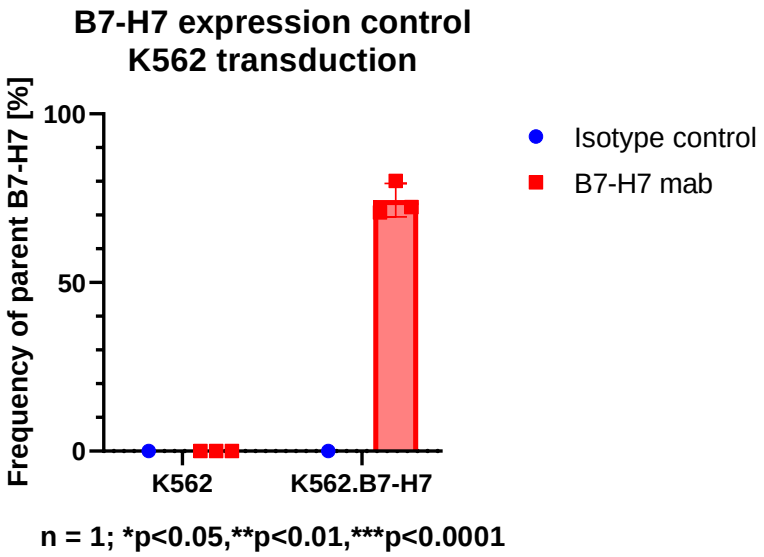

FIGURE 3.31: Results of K562 cells transduced with B7-H7 stained for B7-H7 expression shown for all biological replicates (n = 1). A B7-H7 transduced K562 cell line showed a positive signal expressing B7-H7 74.43 % ± 4.97 % p=1.0 while the untransduced K562 cell line did not show any staining signal 0.01 % ± 0.02 % p=1.0. The K562.B7-H7 cell line was used for the NK cell killing assay and as positive controls in other experiments. Analysed with Wilcoxon-paired tests.

Due to the given characteristics, K562 cells can be transduced using lentiviruses to express a full length B7-H7 receptor of interest [32]. The B7-H7 expressing K562 cell line was generated using the B7-H7*001 allotype (subsection A.1.8, page 213) after a NCBI protein blast revealed that the *001 allotype does not differ in its extracellular domain from the *002 allotype (Figure A.3, page 213). The B7-H7 expression of the generated K562.B7-H7 cell line was compared to unstained as well as untransduced K562 cells using flow cytometry exporting the frequency of CD3 negative K562 parent cells displaying the B7-H7 receptor (Figure 3.30). Next, the mean of the frequency of parent expression for B7-H7 and the standard deviation was calculated for the K562 and K562.B7-H7 cell lines.

The B7-H7 transduced K562 cell line showed a positive signal expressing B7-H7 with a mean frequency of parent of 74.43 % ± 4.97 % p=1.0 while the untransduced K562 cell line did show a staining signal with a frequency of parent of 0.01 % ± 0.02 % p=1.0 (Figure 3.31). The K562.B7-H7 cell line was used for the NK cell killing assay and as positive control in the compartment screen.

3.5.2 KIR3DL3 & B7-H7 interaction prevents killing and can be selectively blocked

After the results of the Jurkat reporter cell assay proved a binding and biological interaction of the B7-H7 protein and the KIR3DL3 receptor the next step was to show a biological relevance of the interaction. As previously shown by our laboratory, NK cell killing assays and the inhibition via mabs or induction of killing via antibody dependent cellular cytotoxicity (ADCC) are one way of many options to establish a biological link [90, 205].

As described, a mixture of K562 and K562.B7-H7 cells labelled with different LIVE/DEAD markers were incubated with the NK-92MI cell line purchased from ATCC [300]. Afterwards the killing rate of the NK-92MI : K562 & K562.B7-H7 mixture was compared with a 1:1 mixture of K562 and K562.B7-H7 cells (subsection 7.8.4, page 143). In parallel the experiment was conducted again by adding an unconjugated mab targeted against the B7-H7 protein to the cell mixture.

The controls of the K562 and K562.B7-H7 cells incubated with NK-92MI cells did not show any background noise for the isotype control of the KIR3DL3, B7-H7 antibody and the respective LIVE/DEAD dyes used for labelling the K562 and K562.B7-H7 cell lines (Figure 3.32). The respective K562 and K562.B7-H7 cell lines were distinguishable upon LIVE/DEAD labelling and did express B7-H7 across all runs (Figure 3.33).

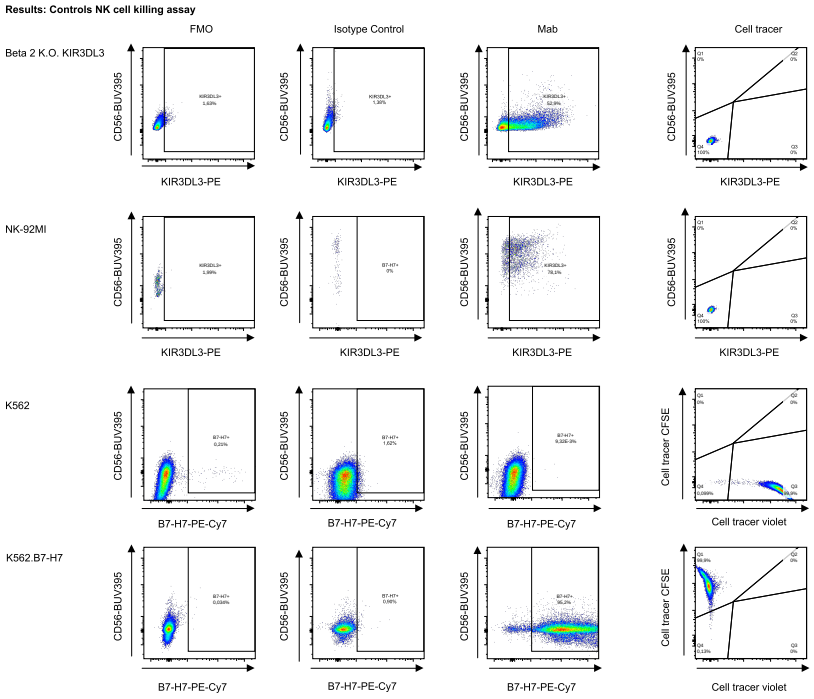

FIGURE 3.32: Controls of K562 and K562.B7-H7 cells incubated with NK-92MI cells shown for one technical triplicate of three biological replications (n = 1). No background noise was seen for the isotype control of the KIR3DL3, B7-H7 antibody and the respective LIVE/DEAD dyes used for labelling the K562 and K562.B7-H7 cell lines. The respective K562 and K562.B7-H7 cell lines can be distinguished upon LIVE/DEAD labelling.

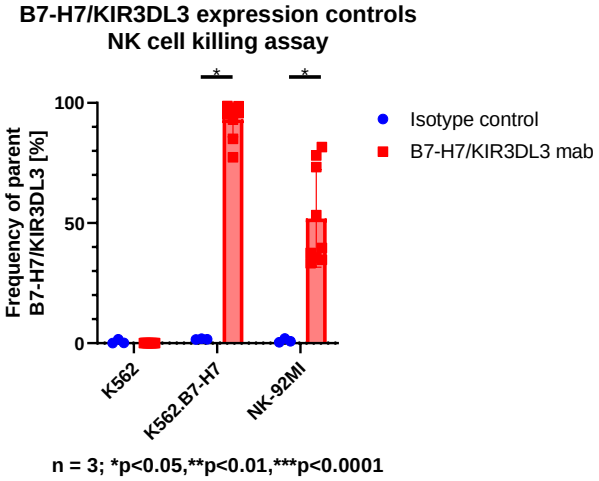

FIGURE 3.33: Results of K562, K562.B7-H7 and NK-92MI cells incubated with B7-H7 and KIR3DL3 mab shown for all biological replicates (n = 3). The K562.B7-H7 cell line showed a positive signal expressing B7-H7 93.16 % ± 7.26 % $p<0.05$ while the untransduced K562 cell line did not show any staining signal 0.02 % ± 0.91 % $p>0.05$. The NK-92MI cell line showed a positive signal expressing KIR3DL3 51.89 % ± 20.29 % $p<0.05$. Analysed with Wilcoxon-paired tests.

As depicted in the primary data in Figure 3.34 and the combined results in Figure 3.36, the killing activity of NK-92MI cells were statistically significant reduced towards K562.B7-H7 cells in the E:T ratios of 3:1 (0.72 ± 0.31 $p<0.05$), 1:1 (0.63 ± 0.25 $p<0.01$), 1:3 (0.58 ± 0.22 $p<0.01$) and 1:5 (0.57 ± 0.22 $p<0.01$) (Table 3.9). However, this trend was reversed in the experimental setup using anti-B7-H7 blocking antibody. The primary data in Figure 3.35 and the combined results in Figure 3.37 showed an increased killing towards K562.B7-H7 cells in the E:T ratios of 1:1 (2.12 ± 1.10 $p<0.01$), 1:3 (2.42 ± 1.11 $p<0.01$) and 1:5 (2.75 ± 1.22 $p<0.01$). The increased killing activity of NK-92MI cells towards the K562.B7-H7 cells pointed out that the K562.B7-H7 cells possessed the properties to be killed by NK cells in the first place.

Table 3.9: Mean and SD of the Frequency of parent obtained from the NK cell killing assay without anti-B7-H7 blocking antibody (n = 3).

NK-92MI : K562 & K562.B7-H7 ratio	**Mean Frequency of parent ratio**	**SD Frequency of parent ratio**	**adjusted p-value compared to only K562 : K562.B7-H7**
K562 : K562.B7-H7 only	1.00	0.09	-
5:1	0.80	0.24	>0.05
3:1	0.72	0.31	<0.05
1:1	0.62	0.25	<0.01
1:3	0.58	0.22	<0.01
1:5	0.57	0.22	<0.01

Table 3.10: Mean and SD of the Frequency of parent obtained from the NK cell killing assay with anti-B7-H7 blocking antibody (n = 3).

NK-92MI : K562 & K562.B7-H7 ratio	**Mean Frequency of parent ratio**	**SD Frequency of parent ratio**	**adjusted p-value compared to only K562 : K562.B7-H7**
K562 : K562.B7-H7 only	1.00	0.09	-
5:1	1.50	0.98	>0.90
3:1	1.71	1.26	>0.90
1:1	2.12	1.10	<0.01
1:3	2.42	1.11	<0.01
1:5	2.75	1.22	<0.01

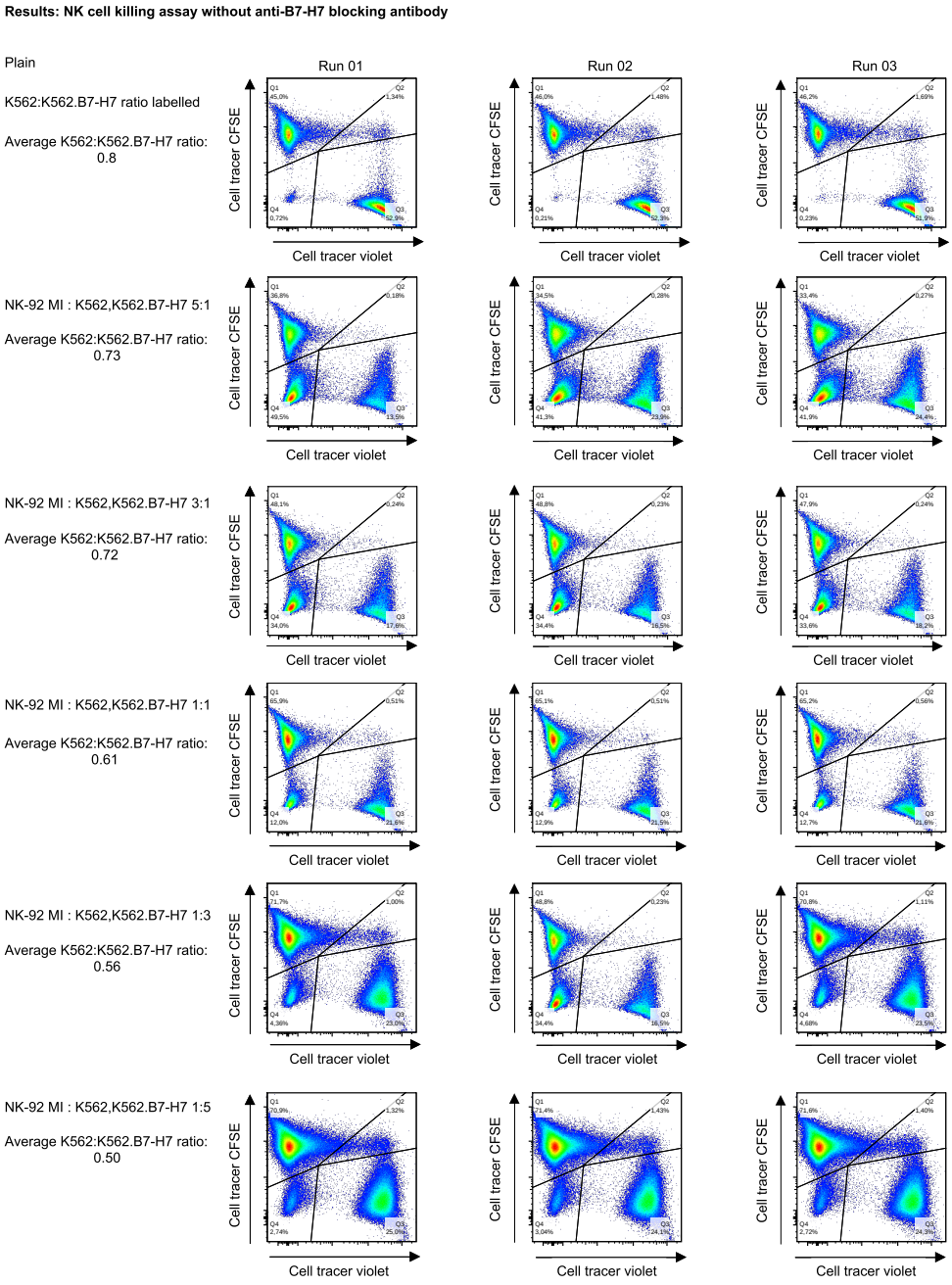

FIGURE 3.34: Primary data of K562 and K562.B7-H7 cells incubated with NK-92MI cells shown for one technical triplicate of three biological replications (n = 1). Calculated are the ratios of K562/K562.B7-H7 cells to determine NK-92MI cells killing activity. NK-92MI cells showed a statistically significant decreased killing activity towards B7-H7 transduced K562.B7-H7 cells in comparison to the untransduced K562 cells in NK-92MI to K562/K562.B7-H7 ratios of 3:1, 1:1, 1:3 and 1:5.

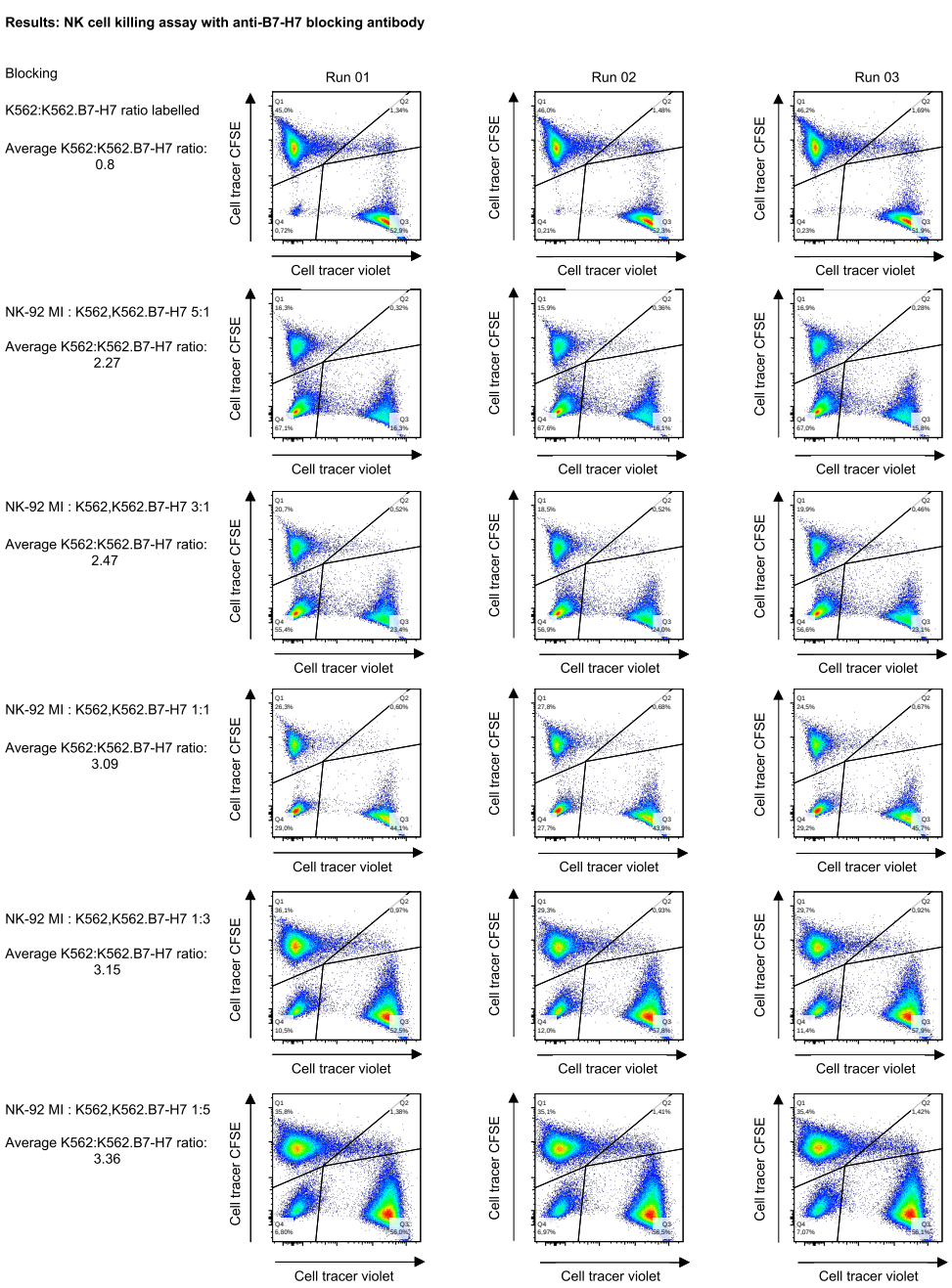

FIGURE 3.35: Primary data of K562 and K562.B7-H7 cells incubated with NK-92MI cells and anti-B7-H7 blocking antibody shown for one technical triplicate of three biological replications (n = 1). NK-92MI cells showed a statistically significant increased killing activity towards B7-H7 transduced K562.B7-H7 cells in comparison to the untransduced K562 cells in NK-92MI to K562/K562.B7-H7 ratios of 1:1, 1:3 and 1:5, thereby reversing the inhibitory function of the KIR3DL3 B7-H7 axis.

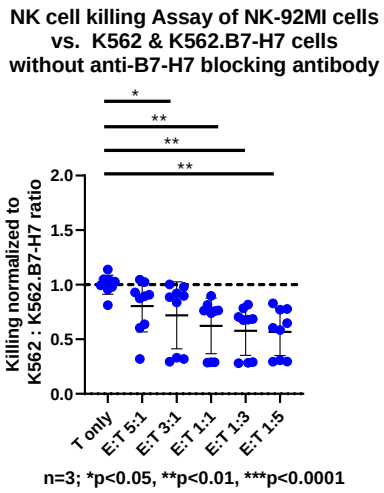

FIGURE 3.36: Results of K562 and K562.B7-H7 cells incubated with NK-92MI cells for all three biological replications (n = 3). A statistically significant decreased killing activity towards K562.B7-H7 cells in comparison to the untransduced K562 cells were seen for the E:T ratios of 3:1 (0.72 ± 0.31 $p<0.05$), 1:1 (0.63 ± 0.25 $p<0.01$), 1:3 (0.58 ± 0.22 $p<0.01$) and 1:5 (0.57 ± 0.22 $p<0.01$). Analysed with Wilcoxon-paired tests corrected for multiple testing with Benjamini & Hochberg method [294].

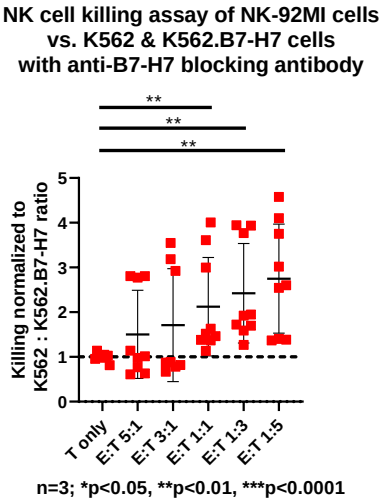

FIGURE 3.37: Results of K562 and K562.B7-H7 cells incubated with anti-B7-H7 blocking antibody and NK-92MI cells for all three biological replications (n = 3). A previously detected inhibition of K562.B7-H7 cells was reversed and a statistically significant increased killing activity towards K562.B7-H7 cells in comparison to the untransduced K562 cells were seen for the E:T ratios of 1:1 (2.12 ± 1.10 $p<0.01$), 1:3 (2.42 ± 1.11 $p<0.01$) and 1:5 (2.75 ± 1.22 $p<0.01$). Analysed with Wilcoxon-paired tests corrected for multiple testing with Benjamini & Hochberg method [294].

3.6 KIR3DL3 receptor and B7-H7 protein are found in peripheral blood

3.6.1 KIR3DL3 is expressed on NK cells isolated from peripheral blood but does not define specific sub-populations

As described (subsection 7.8.5, page 146), NK cells isolated from peripheral blood of six healthy cohort donors were stained for KIR3DL3 and other well-known NK cell receptors such as NKG2A, NKG2C, NKG2D, NKp30, NKp44 and NKp46 to define potential sub-populations of NK cells on day 0, 3 and 7 after the isolation. The KIR3DL3 expression of the PBMCs was compared among CD3 negative, CD16 positive and CD56$^{bright/dim}$ NK cells using flow cytometry. KIR3DL3 mab functionality was shown by staining a β2m-KO-Jurkat KIR3DL3 cell line using flow cytometry on day 0, 3 and 7 and exporting the frequency of parent expressing KIR3DL3. An example of one time point for one technical triplicate of one biological replicate (n = 1) is shown in Figure 3.38.

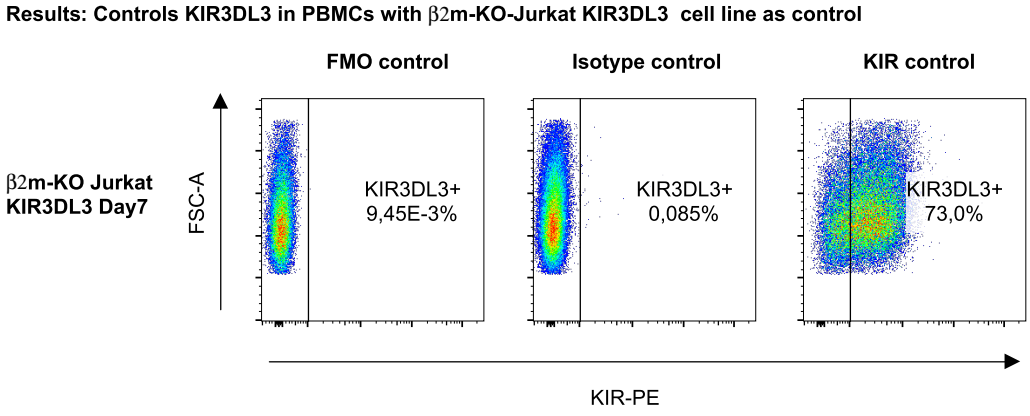

FIGURE 3.38: Primary data of β2m-KO-Jurkat KIR3DL3 cells stained for KIR3DL3 expression on day 0, 3 and 7 here shown for one technical triplicate (n = 1) on day 7. β2m-KO-Jurkat KIR3DL3 cell line showed a positive signal expressing KIR3DL3 while the isotype control did not show any staining signal.

The β2m-KO-Jurkat KIR3DL3 cell line showed a positive signal expressing KIR3DL3 at all time points with a mean frequency of parent of 51.13 % ± 24.64 % p>0.2 (day 0), 18.33 % ± 21,84.00 % p>0.5 (day 3) and 62.90 % ± 14,28 % p>0.2 (day 7) respectively while the isotype controls did not show a staining signal with a frequency of parent of 0.17 % ± 0.22 % (Figure 3.39).

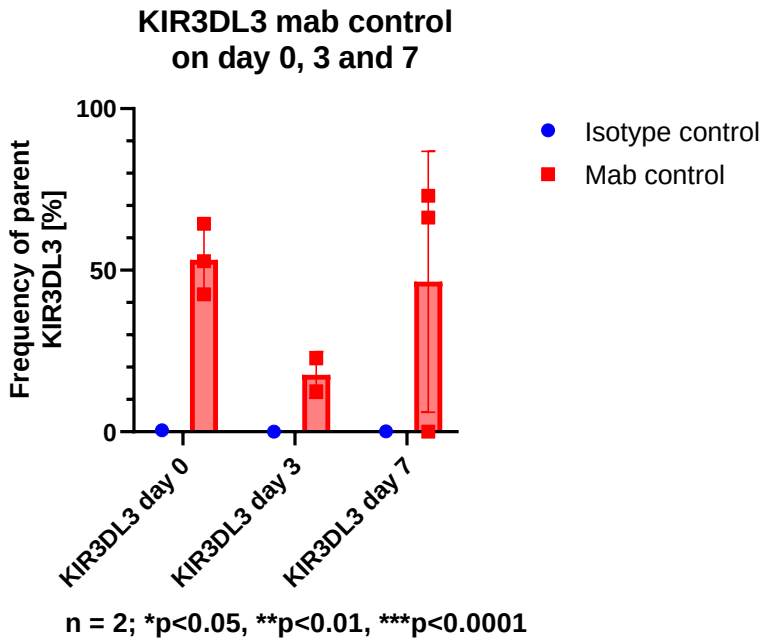

FIGURE 3.39: Results of β2m-KO-Jurkat KIR3DL3 cells incubated with KIR mab on day 0, 3 and 7 shown for all biological replicates (n = 3). The KIR3DL3 mab did work at all times by staining 51.13 % ± 24.64 % p>0.2 (day 0), 18.33 % ± 21.84 % p>0.5 (day 3) and 62.90 % ± 14.28 % p>0.2 (day 7) of the β2m-KO-Jurkat KIR3DL3 cell line respectively while the isotype control did show a signal for 0.17 % ± 0.22 % of cells. Analysed with Wilcoxon-paired tests.

The isolated NK cells did express KIR3DL3 in the following frequencies of parents on the day of isolation: KIR3DL3 only 1.17 % ± 0.91 %, KIR3DL3/NKG2A 5.86 % ± 4.71 % p<0.01, KIR3DL3/NKG2C 3.63 % ± 2.98 % p<0.05, KIR3DL3/NKG2D 4.30 % ± 3.08 p<0.01, KIR3DL3/NKp30 5.77 % ± 3.72 % p<0.01, KIR3DL3/NKp44 1.93 % ± 0.79 % p<0.01, KIR3DL3/NKp46 6.52 % ± 4.31 % p<0.01 (Table 3.11). Three days later the cultivated cells showed the following values: KIR3DL3 only 1.05 % ± 0.99 %, KIR3DL3/NKG2A 5.73 % ± 2.54 % p<0.01, KIR3DL3/NKG2C 3.79 % ± 1.50 % p>0.50, KIR3DL3/NKG2D 3.73 % ± 2.31 % p<0.01, KIR3DL3/NKp30 2.21 % ± 0.85 % p<0.0001, KIR3DL3/NKp44 1.28 % ± 0.37 % p<0.01, KIR3DL3/NKp46 4.16 % ± 2.28 % p<0.01 (Table 3.12). After 7 days the following frequencies of parents could be obtained: KIR3DL3 only 0.39 % ± 0.32 %, KIR3DL3/NKG2A 1.49 % ± 1.22 % p<0.05, KIR3DL3/NKG2C 2.97 % ± 2.23 % p>0.40, KIR3DL3/NKG2D 1.62 % ± 1.32 % p<0.05, KIR3DL3/NKp30 1.16 % ± 0.93 % p<0.05, KIR3DL3/NKp44 0.29 % ± 0.28 % p<0.05, KIR3DL3/NKp46 2.26 % ± 1.83 % p<0.05 (Table 3.13). Henceforth, there were no specific sub-populations defined by the KIR3DL3 expression. An example of the NK cell receptors for one technical triplicate of one biological replicate (n = 1) is shown in Figure 3.38 and the overall results for all biological replicates (n = 6) in Figure 3.39.

TABLE 3.11: Mean and SD of the Frequency of parent obtained from the KIR3DL3 screen on NK cells on day 0 (n = 6).

NK cell receptor	**Mean Frequency of parent [%]**	**SD Frequency of parent [%]**	**adjusted p-value compared to KIR3DL3**
KIR3DL3 only	1.17	0.91	-
KIR3DL3/NKG2A	5.86	4.71	<0.01
KIR3DL3/NKG2C	3.63	2.98	<0.05
KIR3DL3/NKG2D	4.30	3.08	<0.01
KIR3DL3/NKp30	5.77	3.72	<0.01
KIR3DL3/NKp44	1.93	0.79	<0.01
KIR3DL3/NKp46	6.52	4.31	<0.01

TABLE 3.12: Mean and SD of the Frequency of parent obtained from the KIR3DL3 screen on NK cells on day 3 (n = 6).

NK cell receptor	**Mean Frequency of parent [%]**	**SD Frequency of parent [%]**	**adjusted p-value compared to KIR3DL3**
KIR3DL3 only	1.05	0.99	-
KIR3DL3/NKG2A	5.73	2.54	<0.01
KIR3DL3/NKG2C	3.79	1.50	>0.50
KIR3DL3/NKG2D	3.73	2.31	<0.01
KIR3DL3/NKp30	2.21	0.85	<0.0001
KIR3DL3/NKp44	1.28	0.37	<0.01
KIR3DL3/NKp46	4.16	2.28	<0.01

TABLE 3.13: Mean and SD of the Frequency of parent obtained from the KIR3DL3 screen on NK cells on day 7 (n = 6).

NK cell receptor	**Mean Frequency of parent [%]**	**SD Frequency of parent [%]**	**adjusted p-value compared to KIR3DL3**
KIR3DL3 only	0.39	0.32	-
KIR3DL3/NKG2A	1.49	1.22	<0.05
KIR3DL3/NKG2C	2.97	2.23	>0.40
KIR3DL3/NKG2D	1.62	1.32	<0.05

TABLE 3.13: Continued mean and SD of the Frequency of parent obtained from the KIR3DL3 screen on NK cells on day 7 (n = 6).

NK cell receptor	**Mean Frequency of parent [%]**	**SD Frequency of parent [%]**	**adjusted p-value compared to KIR3DL3**
KIR3DL3/NKp30	1.16	0.93	<0.05
KIR3DL3/NKp44	0.29	0.28	<0.05
KIR3DL3/NKp46	2.26	1.83	<0.05

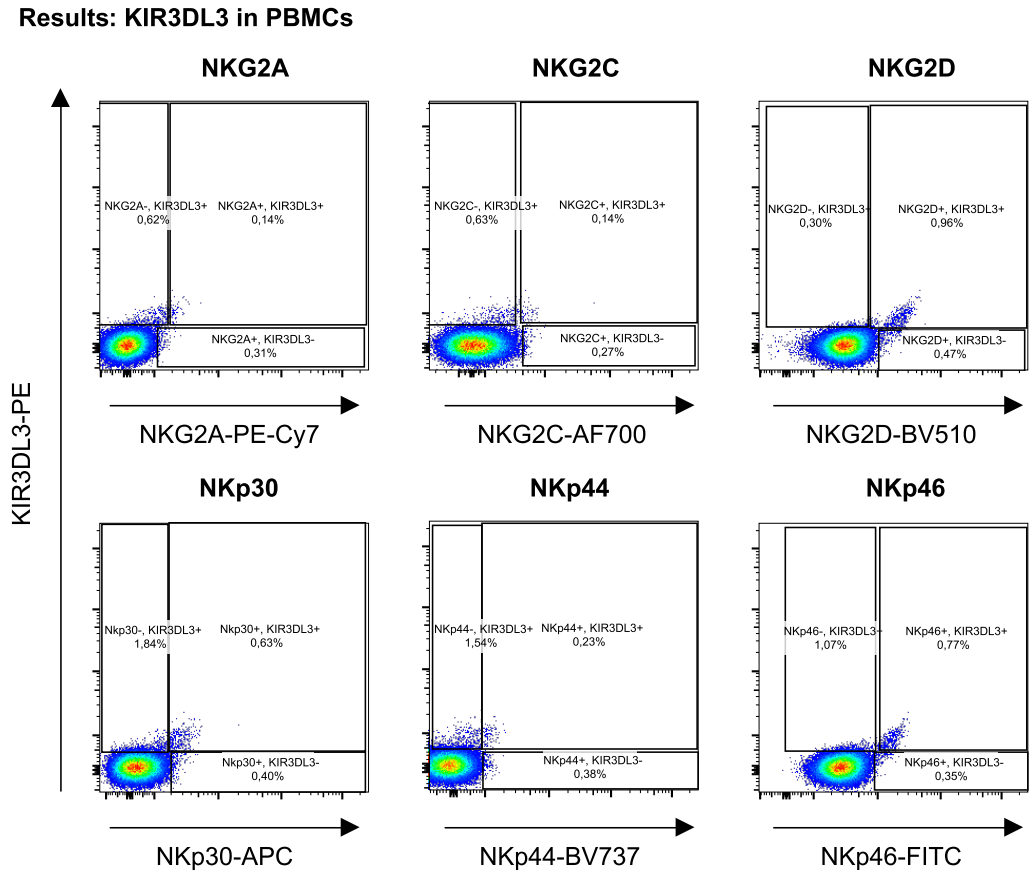

FIGURE 3.40: Primary data of NK cells isolated from peripheral blood stained for KIR3DL3 expression on day 0, 3 and 7 here shown for one technical triplicate (n = 1) on day 7. NK cells showed a positive signal expressing KIR3DL3 in combination with multiple other important NK cell receptors.

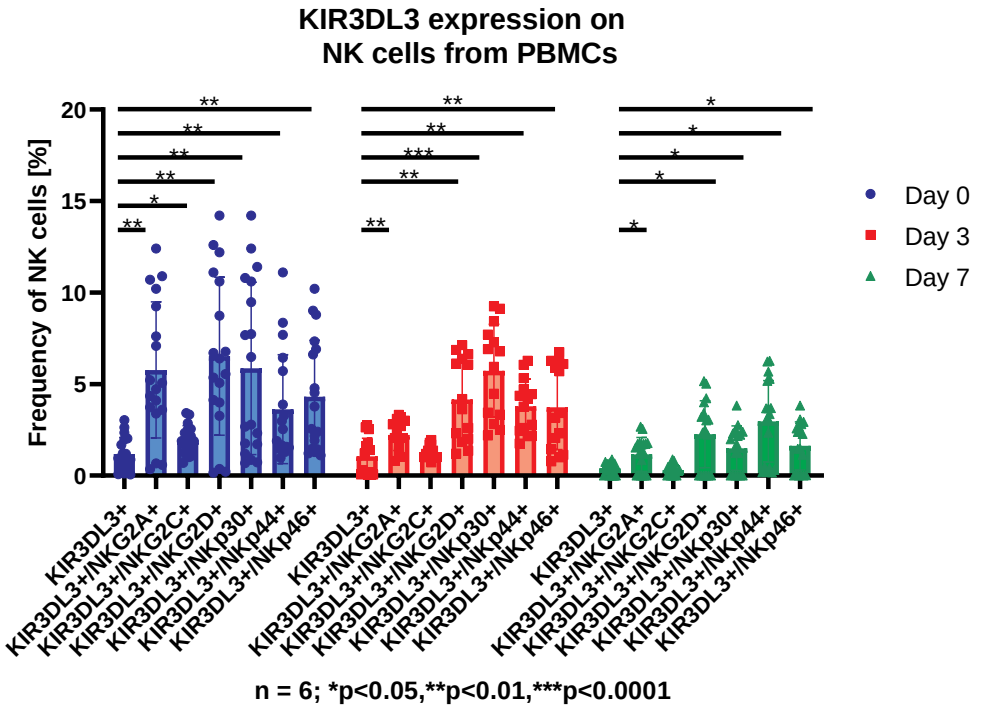

FIGURE 3.41: Results of NK cells isolated from peripheral blood stained for KIR3DL3 expression on day 0, 3 and 7 shown for all biological replicates from different donors (n = 6). On day 3 the folowing values were obtained: KIR3DL3 only 1.17 % ± 0.91 %, KIR3DL3/NKG2A 5.86 % ± 4.71 % $p<0.01$, KIR3DL3/NKG2C 3.63 % ± 2.98 % $p<0.05$, KIR3DL3/NKG2D 4.30 % ± 3.08 $p<0.01$, KIR3DL3/NKp30 5.77 % ± 3.72 % $p<0.01$, KIR3DL3/NKp44 1.93 % ± 0.79 % $p<0.01$, KIR3DL3/NKp46 6.52 % ± 4.31 % $p<0.01$. On day 3: KIR3DL3 only 1.05 % ± 0.99 %, KIR3DL3/NKG2A 5.73 % ± 2.54 % $p<0.01$, KIR3DL3/NKG2C 3.79 % ± 1.50 % $p>0.50$, KIR3DL3/NKG2D 3.73 % ± 2.31 % $p<0.01$, KIR3DL3/NKp30 2.21 % ± 0.85 % $p<0.0001$, KIR3DL3/NKp44 1.28 % ± 0.37 % $p<0.01$, KIR3DL3/NKp46 4.16 % ± 2.28 % $p<0.01$. After 7 days the following values were measured: KIR3DL3 only 0.39 % ± 0.32 %, KIR3DL3/NKG2A 1.49 % ± 1.22 % $p<0.05$, KIR3DL3/NKG2C 2.97 % ± 2.23 % $p>0.40$, KIR3DL3/NKG2D 1.62 % ± 1.32 % $p<0.05$, KIR3DL3/NKp30 1.16 % ± 0.93 % $p<0.05$, KIR3DL3/NKp44 0.29 % ± 0.28 % $p<0.05$, KIR3DL3/NKp46 2.26 % ± 1.83 % $p<0.05$. Analysed with Wilcoxon-paired tests corrected for multiple testing with Benjamini & Hochberg method [294].

In general NK cells isolated from peripheral blood did tend to downregulate KIR3DL3 expression in all receptor combinations investigated starting from the day of isolation (Figure 3.42). After 7 days almost no signal was detectable (Table 3.13).

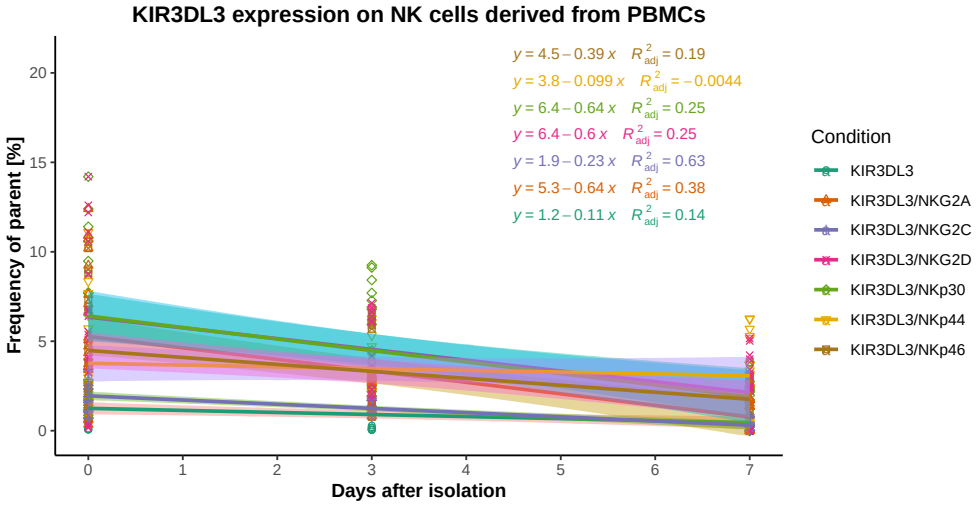

FIGURE 3.42: Regression analysis of NK cells isolated from peripheral blood stained for KIR3DL3 expression on day 0, 3 and 7 here shown for all donors (n = 6). NK cells showed a positive signal expressing KIR3DL3 across all days. However, the expression decreased over time for all sub-populations combinations for the measured frequency of parent, besides the one from KIR3DL3/NKp44 (KIR3DL3 -0.11 % / day, $r^2 = 0.14$; KIR3DL3/NKG2A -0.64 % / day, $r^2 = 0.38$; KIR3DL3/NKG2C -0.23 % / day, $r^2 = 0.63$; KIR3DL3/NKG2D -0.60 % / day, $r^2 = 0.25$; KIR3DL3/NKp30 -0.64 % / day, $r^2 = 0.25$; KIR3DL3/NKp44 -0.1 % / day, $r^2 = 0.00$; KIR3DL3/NKp46 -0.39 % / day, $r^2 = 0.19$).

3.6.2 KIR3DL3 shows scattered signal on $\gamma\delta$ cells but does not define a distinct population

As described (subsection 7.8.5, page 146), T cell sub-populations isolated from peripheral blood of nine healthy cohort donors were stained for KIR3DL3. The KIR3DL3 expression of the PBMCs was compared among CD3 positive, CD4 or CD8 or $\gamma\delta$ T cells using flow cytometry. KIR3DL3 mab functionality was shown by staining a β2m-KO-Jurkat KIR3DL3 cell line using flow cytometry and exporting the frequency of parent expressing KIR3DL3. An example for one technical triplicate of one biological replicate (n = 1) for the KIR3DL3 mab control and the T cell sub-populations are shown in Figure 3.43 and Figure 3.45. The KIR3DL3 mab did work in all three runs for nine different donors staining 17.61 % ± 26.86 % p=0.5 (Figure 3.44).

The isolated CD4 and CD8 T cells did show a low signal of KIR3DL3 expression of 1.01 % ± 0.91 % p>0.18 and 1.83 % ± 1.79 % p>0.20 for CD4 and CD8 sub-populations (Table 3.14). The $\gamma\delta$ T cell population did show some more pronounced KIR3DL3 expression with a mean frequency of parent of 25.10 % ± 29.57 % p>0.58 which was not statistically significant to the isotype control during the screen (13.69 % ± 14.48 %). The summary of the nine healthy cohort individuals investigated are shown in Figure 3.46.

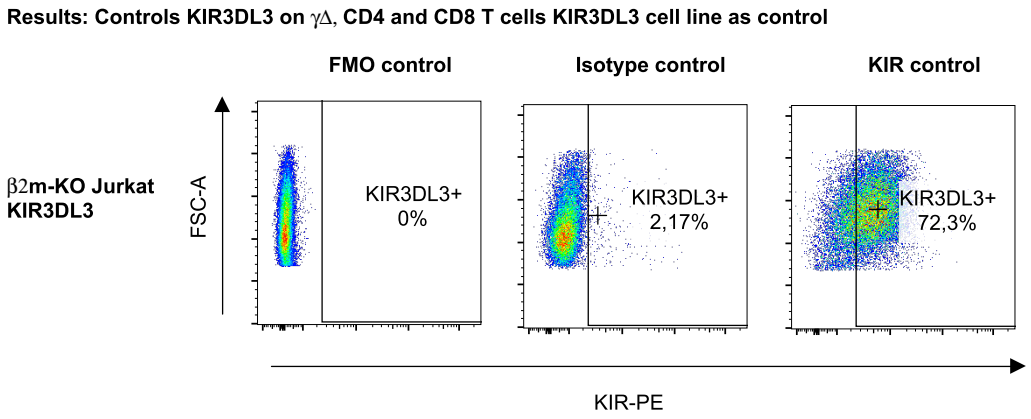

FIGURE 3.43: Primary data of β2m-KO-Jurkat KIR3DL3 cells stained for KIR3DL3 expression during T cell screen here shown for one technical triplicate (n = 1). β2m-KO-Jurkat KIR3DL3 cell line showed a positive signal expressing KIR3DL3 while the isotype control did show low background staining signal.

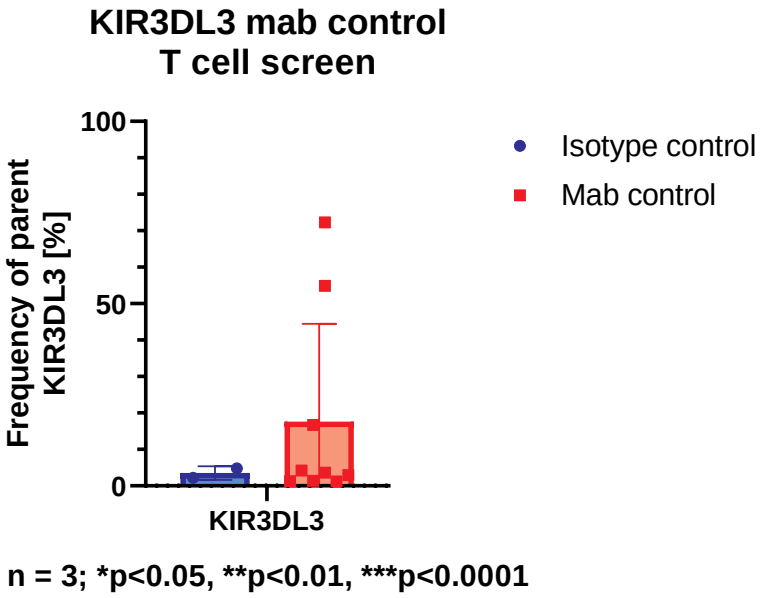

FIGURE 3.44: Results of β2m-KO-Jurkat KIR3DL3 cells incubated with KIR3DL3 mab during T cell screen shown for all biological replicates (n = 3). The KIR3DL3 mab did work at all times by staining 17.61 % ± 30.32 % p=0.5 of the β2m-KO-Jurkat KIR3DL3 cell line respectively while the isotype control did show a signal for 3.50 % ± 1.88 % of cells. Analysed with Wilcoxon-paired tests.

TABLE 3.14: Mean and SD of the Frequency of parent obtained from the KIR3DL3 screen on T cells isolated from peripheral blood (n = 9).

T cell population	**Mean Frequency of parent [%]**	**SD Frequency of parent [%]**	**p-value compared to isotype control**
CD4 isotype	0.78	1.15	-
CD4	1.01	0.91	>0.18
CD8 isotype	1.29	1.74	-
CD8	1.83	1.79	>0.20
$\gamma\delta$ isotype	13.69	14.48	-
$\gamma\delta$	25.10	29.57	>0.58

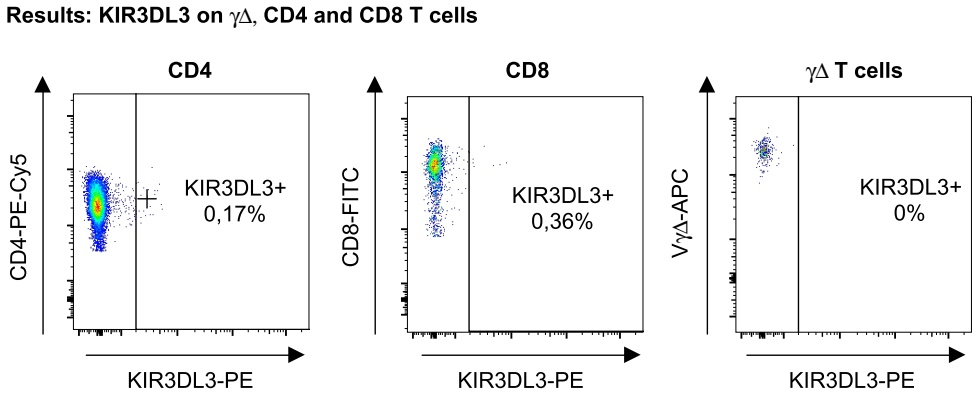

FIGURE 3.45: Primary data of $\gamma\delta$, CD4, CD8 T cells isolated from peripheral blood stained for KIR3DL3 expression here shown for one technical triplicate (n = 1). No distinguishable signal for any subpopulation was detected.

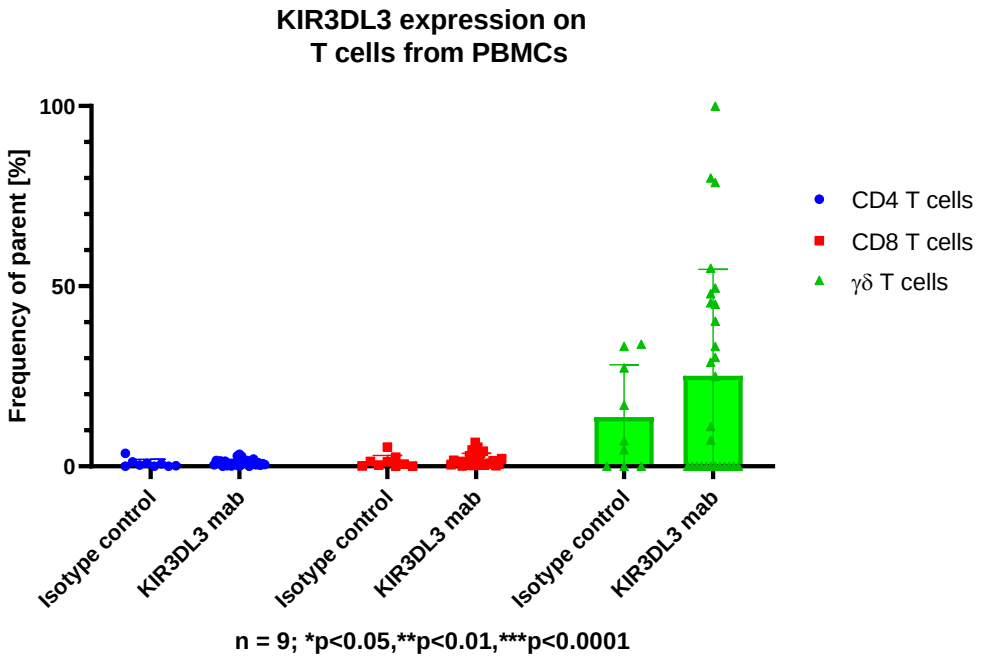

FIGURE 3.46: Results of $\gamma\delta$, CD4, CD8 T cells isolated from peripheral blood stained for KIR3DL3 expression shown for all biological replicates (n = 9). CD4 and CD8 T cells showed low KIR3DL3 expression with 1.01 % ± 0.91 % p>0.18 and 1.83 % ± 1.79 % p>0.20 respectively. The $\gamma\delta$ T cell population did show some more KIR3DL3 expression with a mean frequency of parent of 25.10 % ± 29.57 % p>0.58, which was not statistically significant to its isotype control. Analysed with unpaired Wilcoxon tests.

3.6.3 B7-H7 is expressed on monocytes/macrophages isolated from peripheral blood and form a distinct sub-group

As described (subsection 7.8.5, page 146), monocyte/macrophage and B cell populations isolated from peripheral blood of four healthy cohort donors were stained for B7-H7. The B7-H7 expression of the PBMCs was compared among monocytes/ macrophages and B cells using flow cytometry. An example for one technical triplicate of one biological replicate (n = 1) for the monocyte and B cell populations are shown in Figure 3.47. The isolated monocytes/macrophages did show a statistically significant low signal of B7-H7 expression of 21.78 % ± 10.43 % p<0.01 while the isolated B cells did not 0.86 % ± 1.05 % p>0.75 (Table 3.14). The summary of the four healthy cohort individuals investigated are shown in Figure 3.48.

TABLE 3.15: Mean and SD of the Frequency of parent obtained from the B7-H7 screen on monocytes/macrophages and B cells isolated from peripheral blood (n = 4).

Cell population	**Mean Frequency of parent [%]**	**SD Frequency of parent [%]**	**p-value compared to isotype control**
Monocyte isotype	3.21	3.12	-
Monocyte	21.78	10.43	<0.01
B cell isotype	32.0	55.77	-
B cell	0.86	1.05	>0.75

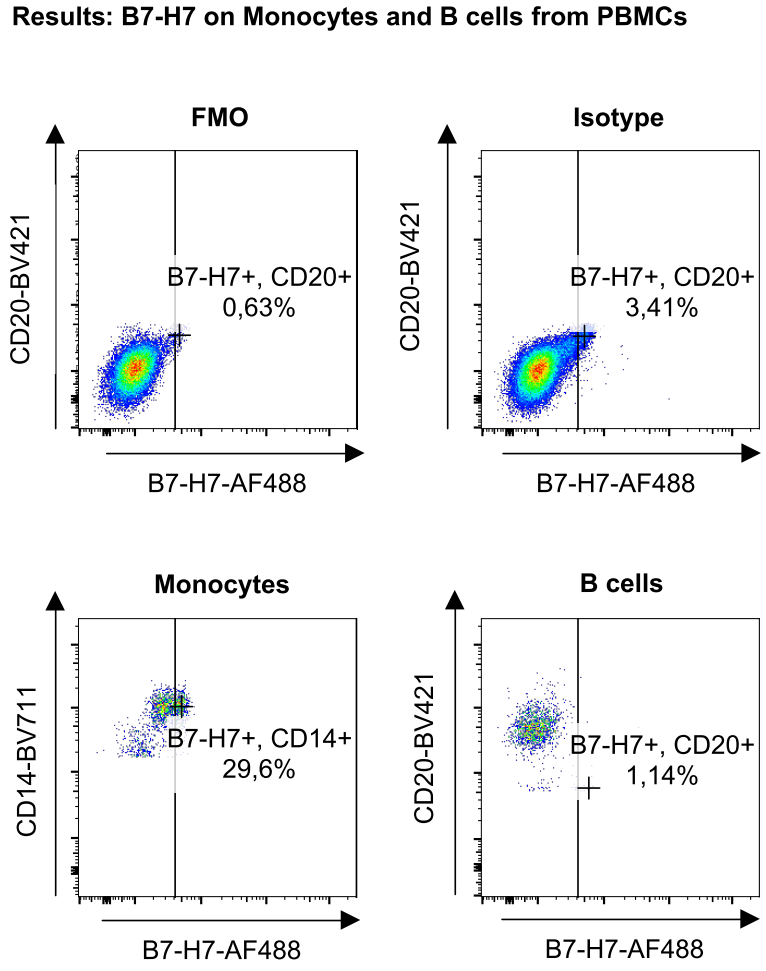

FIGURE 3.47: Primary data of monocytes/macrophages and B cells stained for B7-H7 expression isolated from peripheral blood here shown for one technical triplicate (n = 1). Monocytes/macrophages showed a positive signal expressing B7-H7 while B cells did not. The isotype control did show a low background staining signal.

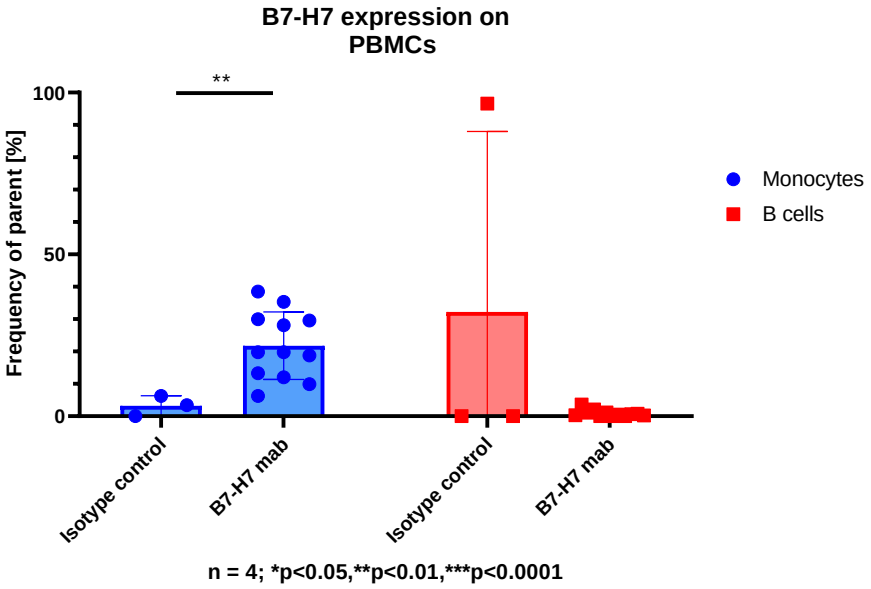

FIGURE 3.48: Results of monocytes/macrophages and B cells stained for B7-H7 expression isolated from peripheral blood shown for all biological replicates (n = 4). The isolated monocytes/macrophages did show a statistically significant low signal of B7-H7 expression of 21.78 % ± 10.43 % p<0.01 while the isolated B cells did not 0.86 % ± 1.05 % p>0.75. Analysed with Wilcoxon-paired tests.

3.6.4 B7-H7 and KIR3DL3 are expressed on different cell types in the small intestine of adults and point towards a biological interaction

As described (subsection 7.8.5, page 146), T cells, NK cells and epithelial cells derived from adult IEL gut samples isolated from seven healthy anatomical reconstruction samples were stained for KIR3DL3 and B7-H7. KIR3DL3 and B7-H7 mab functionality was shown by staining a β2m-KO-Jurkat KIR3DL3 cell line and a K562.B7-H7 cell line using flow cytometry and exporting the frequency of parent of KIR3DL3 and B7-H7 expressing cells. An example for one technical triplicate of one biological replicate (n = 1) for the KIR3DL3 mab and B7-H7 mab control is shown in Figure 3.49. The KIR3DL3 mab did stain β2m-KO-Jurkat KIR3DL3 cells in all three runs for seven different donors staining 21.60 % ± 12.42 % p=0.5 of cells similar to the B7-H7 mab which stained 79.91 % ± 18.39 % p=0.25 of K562.B7-H7 cells (Figure 3.50).

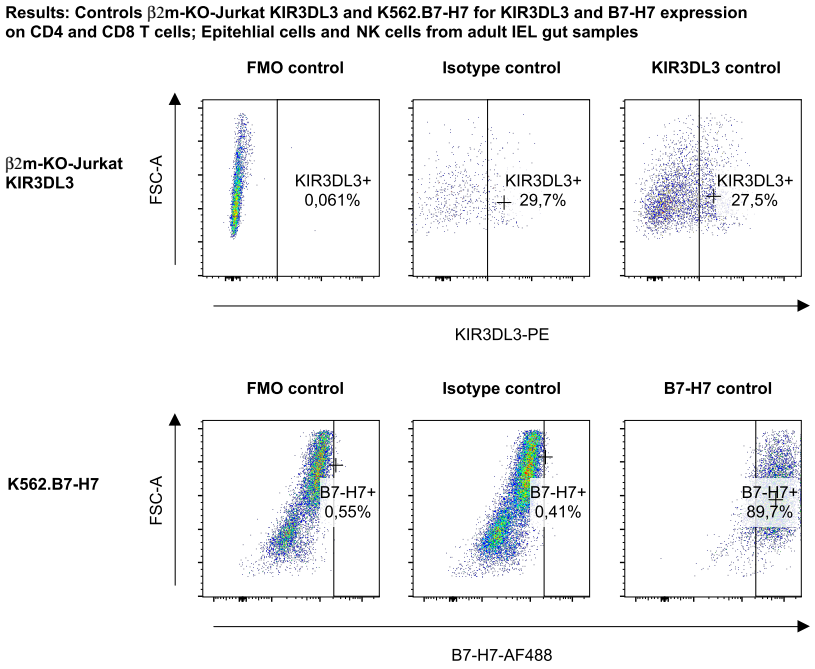

FIGURE 3.49: Primary data of β2m-KO-Jurkat KIR3DL3 cells stained for KIR3DL3 expression and K562.B7-H7 stained for B7-H7 expression during IEL gut sample screen here shown for one technical triplicate (n = 1). Both the β2m-KO-Jurkat KIR3DL3 cell line and the K562.B7-H7 cell line showed a positive signal expressing KIR3DL3 and B7-H7 while the isotype control did show low background staining signal.

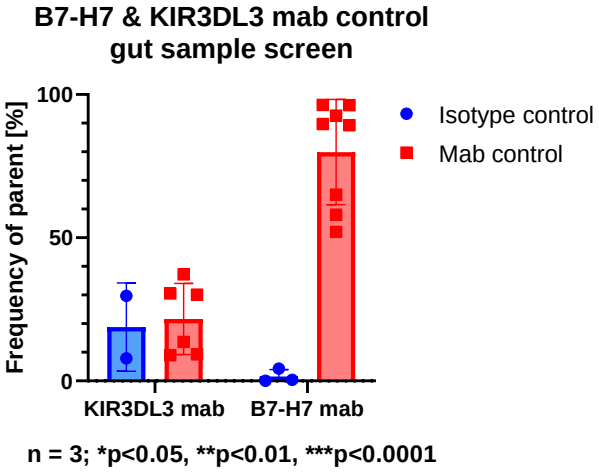

FIGURE 3.50: Results of β2m-KO-Jurkat KIR3DL3 mab and K562.B7-H7 stained with B7-H7 mab during IEL gut sample screen shown for all biological replicates (n = 3). The KIR3DL3 mab did work at all times by staining 21.60 % ± 12.42 % of the β2m-KO-Jurkat KIR3DL3 cell line respectively while the isotype control did show a signal for 18.74 % ± 15.37 % p=0.5 of cells. The B7-H7 mab did work at all times by staining 79.91 % ± 18.39 % p=0.25 of the K562.B7-H7 cell line respectively while the isotype control did show a signal for 1.56 % ± 2.36 % of cells. Analysed with Wilcoxon-paired tests.

The isolated CD4 and CD8 T cells showed the lowest KIR3DL3 expressions with 11.92 % ± 11.69 % p>0.62 and 13.10 % ± 12.30 % p<0.05, while the epithelial and NK cell sub-populations did show higher KIR3DL3 expressions of 21.59 % ± 11.93 % p>0.14 and 29.74 % ± 18.03 % p>0.22 (Table 3.16). With the CD8 population being the only sub-population with statistical significance in comparison to its isotype control. In terms of B7-H7 expression CD4 and CD8 T cells showed again the lowest B7-H7 expressions with 14.64 % ± 30.04 % p>0.97 and 8.21 % ± 18.84 % p>0.33 respectively, which were not statistically significant to their isotype controls. The epithelial and NK cell populations did show some more B7-H7 expression with a mean frequency of parent of 20.39 % ± 23.15 % p>0.22 and 20.79 % ± 18.66 % p>0.31 respectively, which were not statistically significant to their isotype controls either (Table 3.17).

Table 3.16: Mean and SD of the Frequency of parent obtained from the KIR3DL3 screen on adult IEL gut samples (n = 7).

Cell population	**Mean Frequency of parent [%]**	**SD Frequency of parent [%]**	**p-value compared to isotype control**
CD4 T cell isotype	12.25	20.92	-
CD4 T cell	11.92	11.69	>0.62
CD8 T cell isotype	4.22	5.09	-
CD8 T cell	13.10	12.30	<0.05
Epithelial cell isotype	14.32	14.17	-
Epithelial cell	21.59	11.93	>0.14
NK cell isotype	20.55	17.50	-
NK cell	29.74	18.03	>0.22

Table 3.17: Mean and SD of the Frequency of parent obtained from the B7-H7 screen on adult IEL gut samples (n = 7).

Cell population	**Mean Frequency of parent [%]**	**SD Frequency of parent [%]**	**p-value compared to isotype control**
CD4 T cell isotype	8.81	14.33	-
CD4 T cell	14.64	30.04	>0.97
CD8 T cell isotype	2.67	5.27	-
CD8 T cell	8.21	18.84	>0.33
Epithelial cell isotype	11.57	14.38	-

TABLE 3.17: Continued mean and SD of the Frequency of parent obtained from the B7-H7 screen on gut samples (n = 7).

Cell population	**Mean Frequency of parent [%]**	**SD Frequency of parent [%]**	**p-value compared to isotype control**
Epithelial cell	20.39	23.15	>0.22
NK cell isotype	16.19	21.06	-
NK cell	20.79	18.66	>0.31

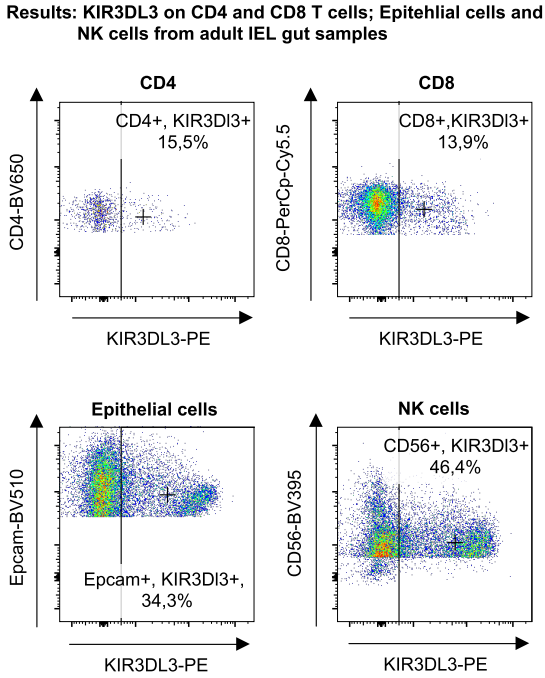

FIGURE 3.51: Primary data of adult IEL gut samples stained for KIR3DL3 expression here shown for one technical triplicate (n = 1). Epithelial cells and NK cells showed separate KIR3DL3 positive populations which were not statistically significant different from the isotype controls.

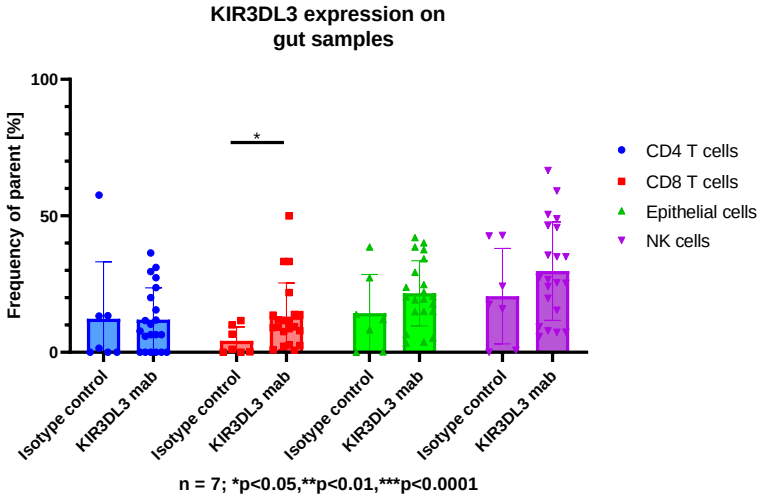

FIGURE 3.52: Results of adult IEL gut samples stained for KIR3DL3 expression shown for all biological replicates (n = 7). CD4 and CD8 T cells showed the lowest KIR3DL3 expressions with 11.92 % ± 11.69 % p>0.62 and 13.10 % ± 12.30 % p<0.05 respectively, with the CD8 population being statistically significant to its isotype control. The epithelial and NK cell populations did show some more KIR3DL3 expression with a mean frequency of parent of 21.59 % ± 11.93 % p>0.14 and 29.74 % ± 18.03 % p>0.22 respectively, which were not statistically significant to their isotype controls. Analysed with unpaired Wilcoxon tests.

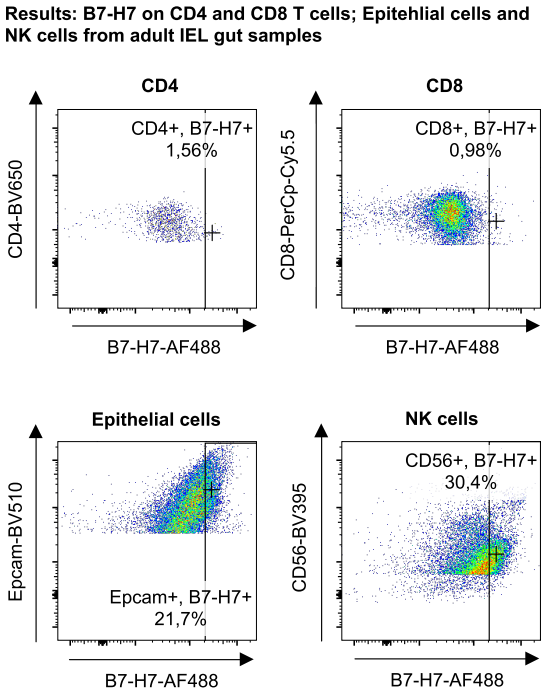

FIGURE 3.53: Primary data of adult IEL gut samples stained for B7-H7 expression here shown for one technical triplicate (n = 1). No distinguishable signal for any sub-population was detected.

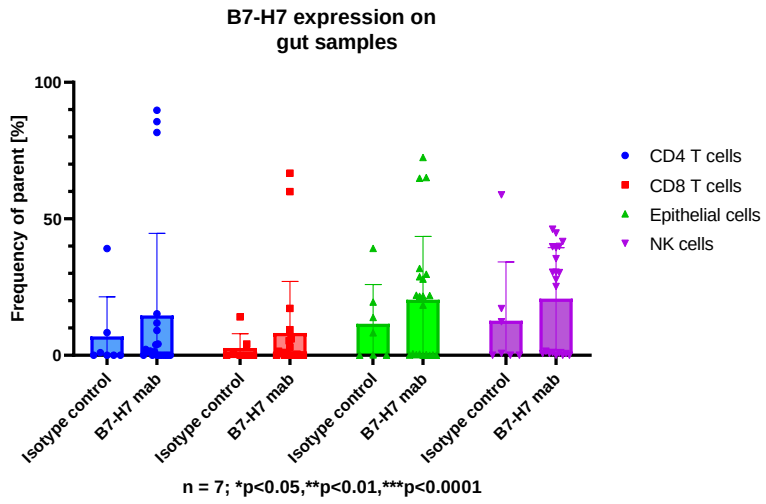

FIGURE 3.54: Results of adult IEL gut samples stained for B7-H7 expression shown for all biological replicates (n = 7). CD4 and CD8 T cells showed the lowest B7-H7 expressions with 14.64 % ± 30.04 % p>0.97 and 8.82 % ± 18.84 % p>0.33 respectively, which were not statistically significant to their isotype controls. The epithelial and NK cell populations did show some more B7-H7 expression with a mean frequency of parent of 20.39 % ± 23.15 % p>0.22 and 20.79 % ± 18.66 % p>0.31 respectively, which were not statistically significant to their isotype controls. Analysed with unpaired Wilcoxon tests.

4 Discussion

The human immune system helped the species to survive despite constant selection pressure from a plethora of pathogens [29]. Its capability of both reacting fast and unspecific to any infection and specialised but slower to long-term or reoccurring infections make it an interesting target for scientists, who for decades, tried to understand involved cells as well as receptors and signalling cascades [30]. Given this backdrop the presented dissertation focused on the identification of ligands for so-called killer cell immunoglobulin-like receptors (KIRs). These receptors were first described in the late 1980's and 1990's as new surface markers for NK cells but were later also found on CD8 T cells [1–5].

As of today, 15 different *KIR* genes are known and encoded in the *MHC* region [6–9]. Defects in these genes which lead to a lack of KIR expression are associated with multiple abnormalities which range from susceptibilities to autoimmune diseases over cancer and infectious diseases to reproduction problems [301–304]. Interestingly, the lack of specific KIR expression can also have beneficial consequences for the host as KIR3DS1, for example allows for slower Human-Immunodeficiency-Virus (HIV) infection progression or KIR2DL3 allows for a quicker Hepatitis-C-Virus (HCV) clearance [304–306]. Henceforth, the individual set of KIRs in patients has attracted attention of researchers and clinicians alike to provide best care. While many of the *KIRs* can be present or absent in human individuals or differ in their gene copy numbers, every human has exactly two copies of *KIR3DL3* which sets it aside from its peers [146, 219–221]. Furthermore, it also differs in its domains as it only shows one intracellular ITIM and a truncated TMD which led to speculations that it is a dysfunctional pseudogene [10, 219, 235]. Another hint in this direction was that for a long time no KIR3DL3 protein was detectable on cell surfaces nor intracellularly [10, 17]. Recent investigations have shown that this is mainly due to a hyper-methylation of the *KIR3DL3* promoter and therefore a poorly transcription and a post-transcriptional regulation via miRNAs [230–232]. The receptor was finally described on decidual NK cells, NK cells, CD8 T cells and $\gamma\delta$ T cells [5, 10, 11, 17, 18, 179, 180].

NK cells on which many KIRs can be found, form part of the innate immune response and were first described in 1975 [87, 124, 307]. They are characterised by the absence of CD3, CD14, CD19 and CD34 receptors and the presence of CD7, CD45 receptors and the relative presence or absence of CD56 ($CD56^{bright/dim}$) and CD16 [48, 93]. In general, NK cells constantly patrol the human body and take over the important task to screen their surrounding for so-called "missing-self" and can engage in killing

activity if no HLA class I molecule with human "self" peptides are presented [98–100]. Due to the severe consequences of an NK cell activation and cell killing, NK cells are tightly regulated via inhibiting and activating receptors. Both receptors thereby add another layer of complexity to the NK cell regulation as some activating receptors can bind both activating and inhibiting ligands same as some intrinsically inhibiting receptors [96, 125]. These receptors are thereby germline encoded and allow for a broad and rather unspecific response [33–35, 38–40, 213]. Henceforth, NK cells are counted to the innate immune system although studies of the early 2000's have hinted towards NK cells which do show memory-like features and persistence which are components of the adaptive immunity [156–165].

NK cells essential role to the host defence is highlighted by the outcomes of NK cell deficiencies in humans. In general, NK cell immunodeficiencies (NKDs) can be broadly classified into classical NKDs in which patients lack NK cells and functional NKDs in which patients do have NK cells but due to some genetic defects they are not functional. So far, no acquired NKDs are known [308]. Other human immunodeficiencies like severe combined immunodeficiency (SCID) exist which additionally impair NK cells, but they do not preliminary focus on or derive from NK cells [309]. Interestingly, the classical NKDs are not per se lethal during fetal development and more or less healthy individuals do exist [308]. These individuals usually suffer from severe reoccurring bacterial infections like Mycobacterium tuberculosis infections and viral infections such as Herpesvirus infections, mainly from Varizella-Zoster-Virus, Herpes-Simplex-Virus and Cyto-Megalo-Virus as well as Humanpapillomavirus infections [308]. Functional NKDs show similar infections patterns of Herpesviruses and Papillomaviruses and do not seem to differ in terms of severity [308, 310]. Henceforth, both patient groups require additional and constant medical treatment to prevent death from viral infections which could be easily cleared or controlled by the human immune system in healthy individuals [308].

CD8 T cells and $\gamma\delta$ T cells on the other hand which are also known to express some KIRs, are part of the adaptive immunity, which is characterised by a slow but targeted response through hyper-mutated receptors [55–58]. CD8 T cells are thereby the counterpart to $CD56^{dim}$ NK cells from the innate immune system, which do not recognize the absence of HLA class I molecules with "self" peptides, but foreign peptides presented on HLA class I molecules and initiate a killing of the infected host cell [32, 71, 72]. $\gamma\delta$ T cells are the most recently discovered T cells which exhibit the ability to detect antigens in an HLA independent manner and can rapidly produce large quantities of cytokines similar to $CD56^{bright}$ NK cells of the innate immune system [76–78]. Furthermore, $\gamma\delta$ T cells exhibit both innate and adaptive immunity characteristics such as phagocytosis as well as memory phenotypes which suggest a bridge function between the two arms of the immune system [78, 79].

T cell deficiencies on the other hand, are more broadly studied and can be divided into inherited (primary) and acquired (secondary) immunodeficiencies which both can be

sub-classified into the complete absence of T cells or a decreased or lack of functionality [311]. While arguably most primary defects are lethal during fetal development the ones which do survive show, like NKDs, high susceptibilities to a broad variety of fungi, bacterial and viral infections which are atypical including mycobacterial, pneumococcus and rhinoviruses, because these infections usually do not pose a threat to healthy individuals [312–314]. Recent studies additionally suggest that the absence of some T cell classes, due to primary immunodeficiencies, are the cause for autoimmune diseases as natural regulators for homeostasis are missing [315]. Furthermore, secondary immunodeficiencies might develop from minor undetected primary immunodeficiencies as additional fighters of the immune system are missing making the individuals prone to acquire additional immunodeficiencies on top like HIV or haematological malignancies [316]. Taken together these deficiencies point out why it is important to understand the role of the immune cells and the respective receptors presented on the cell surface to allow for best medical care.

Up until recently KIR3DL3 has been considered an orphan receptor with no ligands known. The previous description of B7-H7 as ligand of KIR3DL3 by Bhatt *et al.*, Wei *et al.* and Palmer *et al.* in late 2020 and 2021 added another piece to the KIR puzzle of the human immune system and caught immunologists' attention [11, 17, 18]. The B7 protein family itself, first described as receptors of B cells, contains a collection of important immunological molecules such as B7-1 (CD80), B7-2 (CD86) and B7-H1 (PD-L1) which are known regulators of T cell reactions of the adaptive immune response [12–15]. Furthermore, it contains NK cell regulators such as B7-H6 for the activating receptor NKp30 [16]. Interestingly, the B7 protein family does not share as much sequence or protein homology as the family name might suggest. In fact, only 17 % - 20 % of gene sequence similarity and 18 % - 20 % amino acid sequence similarity can be found among the members of the family which are scattered across multiple chromosomes [12, 15, 237]. The family is rather a loose association of historically discovered B cell receptors which were numbered due to the time of their discovery. *B7-H7* nevertheless, is unique of its kind as it does not have any homologous gene in mice although being conserved in primates [19]. B7-H7 is the largest B7 protein with a length of 414 amino acids and three extracellular Ig domains [19, 282]. It can be over expressed in multiple cancers such as renal cell carcinoma, acute lymphoblastic laeukemia, non-small lung cancer, gallbladder and stomach cancer and is also considered a marker of T cell exhaustion [11, 17–25].

Given the structural variety of B7 proteins and their importance in the human immune system, the presented study therefore hypothesised that additional KIRs bind to B7 proteins and form a complex network for NK cell and T cell regulation [16].

This hypothesis was tested with a high throughput screen (HTS) on the protein level with all known members of the B7 protein family and all commercially available KIR receptors as KIR-Fc fusion construct proteins. Fusion construct proteins consist of a normal KIR extracellular domain, while the intracellular part is replaced with the

constant region of an antibody which can be detected via a secondary monoclonal antibody targeted against the constant region. For the assay the B7 proteins were immobilised on a 96-well plate and the KIR-Fc proteins added. After a short incubation time the KIR-Fc fusion construct proteins were washed off and the secondary antibody targeted against the constant region added. After a short incubation time the secondary antibody was washed off and the samples analysed on a flow cytometer, which allows for a quantitative analysis of protein samples. The conducted KIR-Fc screening assay versus all members of the B7 protein family revealed the already known interaction partners of KIR3DL3 & B7-H7 and NKp30 & B7-H6 as well as a novel interaction pair between KIR3DL2 & B7-H1 (PD-L1). The latter interaction was of particular interest as B7-H1 (PD-L1) checkpoint inhibitors are already widely used in clinical settings and are considered a *game changer* in the treatment of multiple cancers [256]. The interaction between KIR3DL2 & B7-H1 (PD-L1) had not been described in literature before. Besides the identified hits the results of B7-H4 and B7-H5 (VISTA) remain elusive as the coating itself was successful but the extracellular functional domain could not be checked for B7-H4 and seemed to be impaired for B7-H5 making it likely that some potential hits were missed.

In a follow up experiment β2m-KO-Jurkat cells stably transduced with KIR3DL2 receptor and β2m-KO-Jurkat as well as β2m-KO-Jurkat KIR2DS4 cells were incubated with B7-H1 (PD-L1)-Fc fusion construct protein to determine potential binding between KIR3DL2 and B7-Ha (PD-L1) on a cellular level. The assay conducted did not show any binding signal between the two receptors in any of the biological replicates although all KIRs were properly expressed between 50 % to 95 %. One reason for the non-binding between the two receptors might be a false positive hit from the protein HTS. This is quite likely as the results from the different runs did show signal differences of two to three log scales. Furthermore, the false discovery rate (FDR) of 5 % was used for target identification and correction for multiple testing within the HTS and not the family-wise error rate (FWER). The reason for this decision was that FWER is a highly conservative approach and only controls for false positive results (type I errors), while the power of the statistical test (1-type II errors), to find true positives, is greatly diminished [317–319]. Henceforth, many potential hits will go unnoticed under the FWER approach as they are labelled statistically not significant. FDR on the other hand sufficiently controls for type I errors and keeps a high statistical power of the test statistic but allows 5 % of all hits to be false positive instead of 5 % of all presented results [318]. In conclusion this means that FDR slightly overestimates the amount of positive hits, while FWER greatly underestimates the real number of hits.

As the KIR3DL2 & B7-H1 (PD-L1) interaction could not be reproduced on a cellular level the dissertation focused on the interaction of KIR3DL3 & B7-H7 (HHLA2) and investigated the cellular mechanisms and outcomes of the signalling pathway. In the first step a stably KIR3DL3 expressing β2m-KO-Jurkat cell line was created via lentiviral transduction. The β2m-KO-Jurkat cells were thereby JurkatE6.1 cells

derived from a human acute T cell leukaemia cell line consisting of T lymphoblasts derived from a male patient which, through CRISPR-Cas9 knockout previously conducted by Dr. Wilfredo Garcia-Beltran from our lab, were missing the β2m chain required for HLA expression [205]. This was important as otherwise the HLA receptors would constantly interact with other KIRs present on the cell surface leading to constant activation of the cell line and ultimate exhaustion. The KIR3DL3 receptor used for transduction was additionally modified by replacing the intracellular domain with the CD3ζ domain. The CD3ζ domain allows for the recruitment of ZAP-70 or Fyn which activate the RAS-RAF-ERK pathway or PIP2-PKC-NF-κB pathway which lead to an upregulation of CD69 expression on the cell surface which can be detected via antibodies upon KIR activation [48, 188].

The successfully transduced β2m-KO-Jurkat KIR3DL3 cells as well as β2m-KO- Jurkat, β2m-KO-Jurkat KIR2DL5, β2m-KO-Jurkat KIR3DL1 were incubated with B7-H7-Fc to determine a potential binding between KIR3DL3 & B7-H7 on a cellular level. A statistically significant binding between KIR3DL3 & B7-H7 could be obtained with two log scale higher signals in comparison to other β2m-KO-Jurkat cell lines, which did not yield any positive signals although the KIRs were expressed on 40 % to 70 % of all cells. This finding confirmed that the B7-H7 protein does not generally recognise KIRs with a 3D or 2D Ig-like extracellular domain, but specifically binds to B7-H7 as its natural ligand. The results are in line with Bhatt *et al.*'s experiments who used a library of transfected mouse cells to determine KIR3DL3-Fc binding on a cellular level and did also only obtain a binding signal for B7-H7 [11].

Further investigation of the KIR3DL3 & B7-H7 axis featured a β2m-KO-Jurkat reporter cell assay. For the assay B7-H7 full length protein was immobilised on a 96-well plate and incubated with β2m-KO-Jurkat KIR3DL3 as well as β2m-KO-Jurkat, β2m-KO-Jurkat KIR2DL5 and β2m-KO-Jurkat KIR3DL1 cells. After 5 h of incubation time the cells were stained for CD69 and respective KIR expression before being fixed and analysed on a flow cytometer. Here the B7-H7 protein only triggered a statistically significant response in KIR3DL3 expressing β2m-KO-Jurkat cell lines while plain β2m-KO-Jurkat cells, β2m-KO-Jurkat KIR2DL5 cells and β2m-KO-Jurkat KIR3DL1 cells did not show an activation via CD69 although KIRs were present on 30 % to 40 % of all cells. This result further indicates that the B7-H7 protein does not only exclusively bind to KIR3DL3, but also does not bind off-target to other receptors on β2m-KO-Jurkat cells. Additionally, B7-H7 protein does not trigger a response in cells expressing any 3D or 2D extracellular KIR domain but only triggers a response in KIR3DL3 expressing cells. Monoclonal antibodies targeted against the KIRs furthermore showed that in theory the other β2m-KO-Jurkat cell lines were able to get activated and express CD69. The findings are in line with similar results from Bhatt *et al.* and Palmer *et al.* who report increased gene expression of a luciferase assay upon KIR3DL3 & B7-H7 interaction [11, 18]. These upregulations were not seen in other KIR-luciferase constructs pointing towards a unique KIR3DL3 & B7-H7 interaction

[11, 18].

To establish a physiological relevance of the KIR3DL3 & B7-H7 interaction full-length B7-H7 transfected K562 cells and plain K562 cells were incubated for 2 h with NK-92MI cells in the effector to target ratios of 5:1, 3:1, 1:1, 1:3, 1:5 and the killing capabilities compared. A reduced killing activity could be observed for the K562.B7-H7 cells in the E:T ratios of 1:1, 1:3 and 1:5. These results could be reversed via the blockage of the B7-H7 protein via monoclonal antibodies targeted versus the B7-H7 protein on the cell surface. The blockage was thereby so successful that it outperformed the killing seen in the plain K562 control. As this effect is specifically due to the blockage of the KIR3DL3 & B7-H7 axis interaction and not via an induced ADCC as the human natural killer cell NK-92MI cell line does not express the required CD16 (FcγRIII) receptor, the question arises whether the overcompensation is the result of an interaction of KIR3DL3 with yet another receptor or whether more inhibitory pathways are blocked via the KIR3DL3 & B7-H7 axis [300]. In the land-marking papers by Bhatt *et al.* and Palmer *et al.* similar results were found for B cell derived Raji cells. Janakiram *et al.* previously reported the intrinsic expression of B7-H7 on K562 cells which might pose an answer to the question of overcompensation but during the three years of experimental work no B7-H7 expression on naïve K562 cells with any commercially available monoclonal antibody was seen [21]. On the other hand, full-length B7-H7 lentivirus transduced K562 cells did express the receptor of interest stably at 80 %.

After the functional assessment of the KIR3DL3 & B7-H7 axis the thesis tried to identify different compartments in which both the KIR3DL3 receptor and the B7-H7 receptor are present and might form a crucial signalling axis for NK cell inhibition and homeostasis. Therefore NK cells were isolated from peripheral blood and stained for KIR3DL3 expression. Interestingly, 1 - 15 % of NK cells from different donors tended to express KIR3DL3. The low expression frequencies of the peripheral blood derived NK cells fit the general profile of KIR3DL3 as low expressed receptor and highly methylated gene which was barely detected as protein on cell surfaces in the first place [10, 146, 219–223, 230]. Similar results for blood NK cells were also reported by Palmer *et al.* [17]. However, much higher frequencies without stimulation were reported by Wei *et al.* with more than 30 % of isolated NK cells from PBMCs [18]. Yet all results still raise the question why the receptor is evolutionary highly conserved as it is apparently only expressed in low frequencies on different PBMC derived NK cells.

KIR3DL3 did only seldom occur as single receptor on NK cells but most of the time was co-expressed with activating receptors such as NKG2A, C, D and NKp30, 44, 46. The expression pattern with other NK cell receptors were not systematically approached before. This result points towards an important inhibitory function of the receptor in terms of immune response termination. This hypothesis is also supported by the fact, that KIR3DL3 was reported by Bhatt *et al.* on CD4 and CD8 T cells also positive for

NKG2A, posing a unique subset, after an extensive stimulation of the CD3 and CD28 receptor known for their important role in the immune system activation via TCRs [11]. The co-expression with activating receptors resembles a previously described common pattern of NK cells which always show activating and inhibiting receptors on the cell surface which make a proper signal integration necessary [96]. Furthermore, inhibitory signals always overrule activating signals on NK cells.

During the cultivation of the isolated NK cells from PBMCs with IL-2 and IL-15 the amount of KIR3DL3 expression for all donors and all receptor combinations with NKG2A, C, D, NKp30, 44 and 46 decreased rapidly within 3 to 7 days to values between 0 - 5 %. These results point towards the fact that NK cells which express KIR3DL3 need to have a specific stimulus which allows them or potentially forces them to express KIR3DL3 on the cell surface. With the isolation of the PBMCs this stimulus is eradicated and the KIR3DL3 expression slowly decreases. As the used R10 cultivation media was spiked with the activating cytokines IL-2 and IL-15 their absence cannot be the cause for the downregulation.

Next, different T cell sub-populations isolated from peripheral blood were reported to express KIR3DL3 during the work on the dissertation. On CD8 T cells in small amounts freshly after isolation and more pronounced after the previously mentioned CD3 and CD28 stimulation for 28 days [11]. Interestingly, very low expression levels of KIR3DL3 of 1 - 2 % for CD4 and CD8 T cells like Bhatt *et al.* and Wei *et al.* were obtained and higher expression levels of 25 % for $\gamma\delta$ T cells which were statistically not significant but comparable to the findings of Palmer *et al.* [11, 17, 18].

B7-H7 on the other hand, is well known to be expressed on monocytes/macrophages and B cells. The respective expression was investigated on freshly isolated peripheral blood, but only an expression on monocytes/macrophages could be detected [11, 17–26]. Given that monocytes/macrophages are an essential bridge between the adaptive and innate immunity the B7-H7 expression on one side and the KIR3DL3 expression on NK cells and T cell subsets on the other side poses the question whether the axis mediates a stop to the immunological response due to its inhibitory nature.

B7-H7 is furthermore well known to be expressed on intestinal tissue [21, 22]. Henceforth, the next step was to check whether previous findings of B7-H7 expression could be reproduced and whether KIR3DL3 expressing cells could also be found within the same tissue. Therefore cells from intraepithelial layers (IELs) from healthy human intestinal gut samples were isolated with the help of EDTA/DTT buffers and hybridisation incubators [320]. The obtained cells were stained for CD4 cells, CD8 cells, NK cells and epithelial cells and analysed on a flow cytometer for their KIR3DL3 and B7-H7 expression [320]. Interestingly, CD8 T cells derived from IEL tissue did statistically significantly express KIR3DL3 on their cell surface while no statistically

significant signal was found for CD4 T cells, NK cells nor epithelial cells. For B7-H7 no statistically significant signals were found for any investigated sub-population. These results stand in sharp contrast to the results reported by Janakiram *et al.* and Luu *et al.* as B7-H7 should have been present on epithelial cells of the intraepithelial layer as well as on T cell sub-populations [21, 25]. Reason for the missing B7-H7 expression can be manifold. On one side, the receptor might have been lost during the IEL tissue processing or the samples were not fresh enough. Additionally, the samples originated from the anatomical reconstruction or inflammation samples of the small intestine, which as a disease setting, might have also impaired the B7-H7 expression in the overall intestine.

Taken together the presented results derive from a successful conducted B7 protein KIR-Fc fusion construct screening assay which yielded between the already known interactions of KIR3DL3 & B7-H7 and NKp30 & B7-H6 as well as one new interaction between the KIR3DL2 & B7-H1 protein. However, the latter interaction could not be confirmed in cellular based follow up experiments. All the investigations of the KIR3DL3 & B7-H7 axis including a KIR3DL3 & B7-H7-Fc binding assay, a KIR3DL3 & B7-H7 reporter cell assay, a KIR3DL3 & B7-H7 killing assay and a KIR3DL3 compartment analysis did yield similar results in terms of physiological function and compartmentalisation as recently published by Palmer *et al.*, Bhatt *et al.* and Wei *et al.*, which lead the field of KIR3DL3 investigations. B7-H7 compartment studies on the other hand greatly differed from literature presented by Janakiram *et al.* and Luu *et al.* as no expression in the small intestine was statistically significant and no sub-population of T cells or epithelial cells of the IEL, were positive for B7-H7. Monocytes/macrophages which were positive for B7-H7 expression in accordance with Zhao *et al.* could be obtained [11, 17–26].

In terms of limitations of the thesis it is important to mention that it does not introduce a disease model of relevance for infectious diseases which include the upregulation of KIR3DL3 or up/downregulation of its counterpart B7-H7 and a model of such, still does not exist. Up until today only a cancer disease model is described [11]. Given the key role KIRs play in the immunological response to pathogens an investigation of expression patterns in different infectious diseases is of crucial interest. Through the identification of a disease pattern in which the KIR3DL3 & B7-H7 axis is deregulated the evolutionary importance of KIR3DL3 could be further understood. Additional studies should also focus on decidual NK cells and surrounding tissue in which KIR3DL3 was first described and explore regulations and interactions with B7-H7. If both receptors are present within the decidual tissue it might help to understand mechanisms in stillbirth, miscarriage, and eclampsia. The data presented here and in literature are furthermore based on tumour derived NK-92MI cells in terms of physiological functionality assessments. It is therefore of crucial interest to repeat multiple functional assays with human derived KIR3DL3 positive NK or T cells or respective clones of them as they resemble the physiological condition of KIR3DL3 expressing

cells. Interestingly, both receptors are present on different subsets of PBMCs, namely monocytes/macrophages and NK cells and T cells. Henceforth, the KIR3DL3 & B7-H7 axis might play a crucial role in bridging the innate and adaptive immune response and might help to end an immunological response. Finally, the presented results of the dissertation are limited to KIRs as ligands for B7 proteins which vastly differ both in amino acid sequence and structure as well as expression patterns. Henceforth, more yet unknown ligands might exist but were not identified during the here presented screening assays. A broader screen with more immunological relevant proteins might yield additional insights into the complex KIR and B7 protein biology.

5 Outlook and conclusion

In summary, the presented dissertation points out that KIR3DL3 expressing cells remain poorly understood and characterised. Besides contradicting expression data and similarities depending on the tissue they are derived from, the key role within the human immune system is not solved. Future work will have to focus on potential effects of KIR3DL3 knock outs to shed light on the question why the gene is evolutionary conserved, yet only scarcely expressed on different tissues and cell systems in different individuals. If these questions are answered it might pose as a novel checkpoint antigen in multiple cancers and virus infections. Furthermore, the question will need to be answered whether the different T cells and NK cells expressing KIR3DL3 engage in similar functions in different compartments or also vary by their immunological tasks. B7 proteins on the other hand, are better characterised although B7-H4 still remains an orphan receptor. Future work might focus on a B7-H4 ligand identification and involved pathways for its regulation. Besides having established signalling pathways and interaction partners, B7 proteins are vastly different in their sequence, expression pattern and protein structure and might have more interaction partners than currently anticipated. These new and old ligands might be interesting targets to develop novel cancer and viral therapies targeting B7 proteins as they are key mediators in the human immune system and widely modulated in different disease contexts. Especially, B7-H7 which has been described as therapeutic marker in a plethora of cancers is of crucial interest as it signals independent of the B7-H1 (PD-L1) axis. Ongoing clinical trials phase I of the monoclonal antibodies NPX267 and HBM1020 targeting the KIR3DL3 & B7-H7 axis may help to shed light on the significance of the interaction.

6 Materials

6.1 Antibodies

Table 6.1: List of antibodies used for experiments.

Epitope	**Fluorochrome**	**Clone**	**Species**	**Channel BD LSR Fortessa**	**Dilution**	**Manufacturer**	**Catalogue number**
Anti-Biotin	PE	1D4-C5	Mouse	YG4	1:100	BioLegend	409004
Anti-human B7-Dc	PE	24F.10C12	Mouse	YG4	1:100	BioLegend	329606
Anti-human B7-H1	APC	29E.2A3	Mouse	R3	1:100	BioLegend	329708
Anti-human B7-H2	PE	2D3	Mouse	YG4	1:100	BioLegend	309404
Anti-human B7-H3	APC	MIH42	Mouse	R3	1:100	BioLegend	351006
Anti-human B7-H4	PE	MIH43	Mouse	YG4	1:100	BioLegend	358104
Anti-human B7-H5	PE	MIH65.rMAb	Mouse	YG4	1:100	BD Biosciences	566669
Anti-human B7-H6	PE	875001	Mouse	YG4	1:100	R&D Systems	FAB7144P

Table 6.1: Continued list of antibodies used for experiments.

Epitope	**Fluorochrome**	**Clone**	**Species**	**Channel BD LSR Fortessa**	**Dilution**	**Manufacturer**	**Catalogue number**
Anti-human B7-H7	AF488	907812	Mouse	B2	1:100 – 1:5	R&D Systems	FAB80841G
Anti-human B7-H7	PE-Cy7	MA57YW	Mouse	YG1	1:25	Invitrogen / Thermo Fisher Scientific	25-6537-42
Anti-human B7-H7	Unconjugated	MAB80841	Mouse	-	10 µg/mL	R&D Systems	MAB80841
Anti-human CD3	BUV395	UCHT1	Mouse	UV2	1:100	BD Biosciences	563546
Anti-human CD3	BUV737	SK7	Mouse	UV1	1:100	BD Biosciences	612752
Anti-human CD4	APC	RPA-T4	Mouse	R3	1:100	BioLegend	300537
Anti-human CD4	BV650	RPA-T4	Mouse	V3	1:100	BioLegend	300536
Anti-human CD4	FITC	RPA-T4	Mouse	B2	1:100	BioLegend	300538
Anti-human CD4	PE-Cy5	RPA-T4	Mouse	YG2	1:100	BioLegend	300510
Anti-human CD8	FITC	SK1	Mouse	B2	1:100	BioLegend	980908
Anti-human CD8	PE	SK1	Mouse	YG4	1:100	BioLegend	980902
Anti-human CD8	Per-Cp-5.5	SK1	Mouse	B1	1:100	BD Biosciences	565310
Anti-human CD14	APC-Cy7	HCD14	Mouse	R1	1:100	BioLegend	325620
Anti-human CD14	PE-Cy7	HCD14	Mouse	YG1	1:100	BioLegend	325618
Anti-human CD14	BV711	M5E2	Mouse	V2	1:100	BioLegend	301838

Table 6.1: Continued list of antibodies used for experiments.

Epitope	**Fluorochrome**	**Clone**	**Species**	**Channel BD LSR Fortessa**	**Dilution**	**Manufacturer**	**Catalogue number**
Anti-human CD16	BV785	B73.1	Mouse	V1	1:100	BioLegend	360734
Anti-human CD19	APC-Cy7	HIB19	Mouse	R1	1:100	BioLegend	302218
Anti-human CD20	APC-Cy7	2H7	Mouse	R1	1:100	BioLegend	302314
Anti-human CD20	BV421	2H7	Mouse	V7	1:100	BioLegend	302330
Anti-human CD56	BUV395	NCAM16.2	Mouse	UV2	1:100	BD Biosciences	563554
Anti-human CD56	BV421	5.1H11	Mouse	V7	1:100	BioLegend	362552
Anti-human CD56	BV510	5.1H11	Mouse	V6	1:100	BioLegend	362534
Anti-human CD56	BV650	HCD56	Mouse	V3	1:100	BioLegend	318344
Anti-human CD56	BV786	NCAM16.2	Mouse	V1	1:100	BD Biosciences	564058
Anti-human CD69	BV421	FN50	Mouse	V7	1:200	BioLegend	310930
Anti-human CD80	BV421	2D10	Mouse	V7	1:100	BioLegend	305222
Anti-human CD86	BV421	BU63	Mouse	V7	1:100	BioLegend	374212
Anti-human Epcam	BV510	9C4	Mouse	V6	1:100	BioLegend	324236
Anti-human KIR2DL3	PE	DX27	Mouse	YG4	1:100	BioLegend	312606
Anti-human KIR2DL5	PE	UP-R1	Mouse	YG4	1:100	BioLegend	341304
Anti-human KIR2DL5	Unconjugated	UP-R1	Mouse	-	1:10	Miltenyi Biotec	130-096-200

Table 6.1: Continued list of antibodies used for experiments.

Epitope	**Fluorochrome**	**Clone**	**Species**	**Channel BD LSR Fortessa**	**Dilution**	**Manufacturer**	**Catalogue number**
Anti-human KIR3DL1	PE	5.133	Mouse	YG4	1:25	Miltenyi Biotec	130-124-439
Anti-human KIR3DL1	Unconjugated	DX9	Mouse	-	1:10	BD Biosciences	555964
Anti-human KIR3DL3	PE	1136B	Rabbit	YG4	1:25	R&D Systems	FAB8919P
Anti-human KIR3DL3	Unconjugated	1136B	Rabbit	-	10 µg/mL	R&D Systems	MAB8919
Anti-human NKG2A	PE-Cy7	S19004C	Mouse	YG1	1:100	BioLegend	375114
Anti-human NKG2C	AF700	134522	Mouse	R2	1:25	R&D Systems	FAB1381N-100UG
Anti-human NKG2D	BV510	1D11	Mouse	V6	1:100	BioLegend	320816
Anti-human NKp30	APC	P30-15	Mouse	R3	1:100	BioLegend	325226
Anti-human NKp44	BUV737	p44-8	Mouse	UV1	1:100	BD Biosciences	749172
Anti-human NKp46	FITC	9E2	Mouse	B2	1:100	BioLegend	331922
Isotype control IgG1,κ mouse	APC	MOPC-21	Mouse	R3	1:100	BioLegend	400120
Isotype control IgG1,κ mouse	BV421	MOPC-21	Mouse	V7	1:100	BioLegend	400158
Isotype control IgG1,κ mouse	FITC	MOPC-21	Mouse	B2	1:100	BioLegend	981802

Table 6.1: Continued list of antibodies used for experiments.

Epitope	**Fluorochrome**	**Clone**	**Species**	**Channel BD LSR Fortessa**	**Dilution**	**Manufacturer**	**Catalogue number**
Isotype control IgG1,κ mouse	PE	MOPC-21	Mouse	YG4	1:100	BioLegend	400112
Isotype control IgG1,κ mouse	PE-Cy7	MOPC-21	Mouse	YG1	1:100	BioLegend	981816
Isotype control IgG1,κ rabbit	PE	60024B	Rabbit	YG4	1:100	R&D Systems	IC1051P
F(ab')2-Goat anti-Human IgG Fc Secondary Antibody	FITC	-	Goat	B2	1:200	Invitrogen / Thermo Fisher Scientific	H10101C
F(ab')2-Goat anti-Human IgG Fc Secondary Antibody	PE	-	Goat	YG4	1:200	Invitrogen / Thermo Fisher Scientific	H10104
Secondary mab anti-mouse	AF488	-	Donkey	B2	1:200	Invitrogen / Thermo Fisher Scientific	A32790
Secondary mab anti-rabbit	AF546	-	Donkey	YG4	1:200	Invitrogen / Thermo Fisher Scientific	A10040

6.2 Biological samples and ethics

As previously stated by Dr. Pia Fittje, peripheral blood mononuclear cells (PBMCs) isolated from peripheral blood and used for the different experiments were obtained from the Hamburg Healthy Cohort (HCHH) supervised by the University Medical Center Hamburg-Eppendorf, Hamburg, Germany [31, 90]. The cohort donors provided written informed consent and the study was approved by the ethics committee of the Ärztekammer Hamburg (PV4780) [31, 90].

As previously stated by Dr. Johannes Jung, intestinal tissues used for intraepithelial layer isolation were obtained with written informed consent from adult donors or the legal guardians of paediatric donors with approval by the ethics committee of the Medical Association of the Freie Hansestadt Hamburg (Ärztekammer Hamburg) at Altona Children's Hospital and University Medical Center Hamburg-Eppendorf (PV4898, PV4081) [321]. Samples without signs of inflammation were collected during anatomical reconstruction [321].

6.3 Cell lines

Table 6.2: List of cell lines used for experiments derived from Vollmers *et al.* [32].

Cell line	**Characterization**	**Source and Research Resource Identifier (RRID)**	**Application**
β2m-KO-Jurkat KIR2DL5*001	β2m-KO-Jurkat cell line transduced with KIR2DL5*001 and CD3ζ	Leibniz institute of Virology, Hamburg Germany; Dr. Pia Fittje [90]	Reporter cell assays, Fc screens
β2m-KO-Jurkat KIR2DS4*001	β2m-KO-Jurkat cell line transduced with KIR2DS4*001 and CD3ζ	Ragon Institute of MGH, MIT and Harvard, Cambridge, MA, USA; Dr. Wilfredo Garcia-Beltran [205, 322]	Reporter cell assays, Fc screens

TABLE 6.2: Continued list of cell lines used for experiments derived from Vollmers *et al.* [32].

Cell line	**Characterization**	**Source and Research Resource Identifier (RRID)**	**Application**
β2m-KO-Jurkat KIR3DL1*001	β2m-KO-Jurkat cell line transduced with KIR3DL1*001 and CD3ζ	Ragon Institute of MGH, MIT and Harvard, Cambridge, MA, USA; Dr. Wilfredo Garcia-Beltran [205, 322]	Reporter cell assays, Fc screens
β2m-KO-Jurkat KIR3DL2*001	β2m-KO-Jurkat cell line transduced with KIR3DL2*001 and CD3ζ	Ragon Institute of MGH, MIT and Harvard, Cambridge, MA, USA; Dr. Wilfredo Garcia-Beltran [205, 322]	Reporter cell assays, Fc screens
β2m-KO-Jurkat KIR3DL3*001[1]	β2m-KO-Jurkat cell line transduced with KIR3DL3*001 and CD3ζ	This thesis	Reporter cell assays, Fc screens
JurkatE6.1-$\Delta\beta$m (β2m-KO-Jurkat)	Human acute T cell leukaemia cell line consisting of T lymphoblasts derived from male patient, Clone E6-1, stable β2m knockout (KO)	Ragon Institute of MGH, MIT and Harvard, Cambridge, MA, USA; CVCL_0367	Production of stable KIR3DL3/ 2DL5/3DL1-CD3ζ expressing cell lines, control cell lines

[1]The plasmid constructs to generate β2m-KO-Jurkat KIR3DL3-CD3ζ cell line contain the signal peptide, extracellular and transmembrane domain of the respective KIR allotype and the cytoplasmic domain of CD3ζ [32]. All cloned sequences of KIR are provided in the appendix (see A.1 on page 205).

Table 6.2: Continued list of cell lines used for experiments derived from Vollmers *et al.* [32].

Cell line	Characterization	Source and Research Resource Identifier (RRID)	Application
K562	Chronic myelogenous leukemilymphoma, isolated from the bone marrow of a 53-year-old female	ATCC, No. CCL-243; CVCL_0004	Production of B7-H7 control cell line, negative control for *in vivo* models
K562.B7-H7	K562 transduced with B7-H7 full length receptor	This thesis	Positive control for *in vivo* models
NK-92MI	Non-Hodgkin's lymphoma, derived from peripheral blood mononuclear cells from a 50-year-old white male	ATCC, No. CRL-2408; CVCL_3755	Killing assay

6.4 Cell culture reagents

6.4.1 Cell culture media

Table 6.3: List of cell culture media used for respective cell lines derived from Vollmers *et al.* [32].

Cell line / Cell type	Media	Supplements
β2m-KO-Jurkat, K562	RPMI - 1640	10 % (v/v) fetal bovine serum, 100 U/mL penicillin, 100 µg/mL streptomycin[2]

[2]RPMI – 1640 with 10 % (v/v) fetal bovine serum, 100 U/mL penicillin, 100 µg/mL streptomycin is referred to as R10.

Table 6.3: Continued list of cell culture media used for respective cell lines derived from Vollmers *et al.* [32].

Cell line / Cell type	Media	Supplements
PBMC	RPMI - 1640	10 % (v/v) fetal bovine serum, 100 U/mL penicillin, 100 µg/mL streptomycin, 50 U/mL Interleukin-2, 5 ng/mL Interleukin-15
HEK-293T	DMEM	10 % (v/v) fetal bovine serum, 100 U/mL penicillin, 100 µg/mL streptomycin
NK-92MI	RPMI - 1640	10 % (v/v) fetal bovine serum, 10 % (v/v) fetal horse serum, 100 U/mL penicillin, 100 µg/mL streptomycin, 5 ng/mL Interleukin-15
Transduced β2m-KO Jurkat, Transduced K562	RPMI - 1640	10 % (v/v) fetal bovine serum, 1 µg/mL puromycin, 100 U/mL penicillin, 100 µg/mL streptomycin

6.4.2 Cell culture raw materials

Table 6.4: List of manufacturers for used cell culture media and supplements.

Media / Supplement	Manufacturer	Catalogue number
Cell culture flask, T-25	Sarstedt	83.3910.002
Cell culture flask, T-75	Sarstedt	83.3911.002
Cell culture plate, 6 well	Sarstedt	83.3920.500
Cell culture plate, 24 well	Sarstedt	83.3922.005
Cell culture plate, 96 well	Sarstedt	83.3926

Table 6.4: Continued list of manufacturers for used cell culture media and supplements.

Media / Supplement	**Manufacturer**	**Catalogue number**
Cell culture plate, 96 well, non-cell culture treated	Corning	351172
Cluster Tube 8-Cap Strips, 12 Strips per Bag, Sterile	Corning	4418
CryoPure tubes	Sarstedt	72.377
Dulbecco's Modified Eagle's Medium (DMEM)	Gibco / Thermo Fisher Scientific	31966047
Fetal bovine serum (FBS)	Capricorn Scientific	FBS-11A
Conical tubes, 15 mL	Thermo Fisher Scientific	AM12500
Conical tubes, 50 mL	Thermo Fisher Scientific	AM12502
Interleukin-2 (IL-2), recombinant human	PeproTech	200-02-500
Interleukin-15 (IL-15), recombinant human	PeproTech	200-15-100
Iscove's Modified Dulbecco's Medium (IMDM)	Gibco / Thermo Fisher Scientific	21980032
L-Glutamine	MERCK / Sigma- Aldrich	G7513
Penicillin-Streptomycin	MERCK / Sigma- Aldrich	P4333
Puromycin	InvivoGen	ANT-PR-1
Roswell Park Memorial Institute (RPMI)-1640	Gibco / Thermo Fisher Scientific	21875091
StrataCooler Cryo Presevation Module -80 °C	Agilent Technologies	400005

6.5 Buffer, media and solutions

6.5.1 Self-prepared buffer, media and solutions

TABLE 6.5: List of self-prepared buffer, media and solutions derived from Vollmers *et al.* [32].

Buffer / Media / Solution	**Composition**
Biotin solution	12.5 mg dissolved in 50 mL Phosphate buffered saline (PBS) [90]
Cell freezing medium (cell lines and primary cells)	Fetal bovine serum (FBS) supplemented with 10 % (v/v) dimethyl sulfoxide (DMSO) [32]
EDTA/DTT buffer	94 % (v/v) IMDM supplemented with: 5 % (v/v) Fetal bovine serum (FBS), 100 U/mL penicillin, 100 µg/mL streptomycin, 5 mM (final) EDTA (1:100), 2 mM (final) DTT (1:500) [320]
Enrichment buffer	Phosphate buffered saline (PBS) supplemented with 2 % (v/v) fetal bovine serum (FBS) and 1 mM ethylenediaminetetraacetic acid (EDTA) [320]
Fixation buffer	Deionized water supplemented with 4 % (v/v) paraformaldehyde (PFA) [32]
Glycine buffer, 100 mM, pH 2.7	7.5 g glycine (75 g/M) in 1 L distilled water [320]
LB agar	32 g LB Agar in 1 L water; autoclaved [32]
LB medium	20 g LB Broth Base in 1 L water; autoclaved [32]
Staining buffer	Phosphate buffered saline (PBS) supplemented with 2 % (v/v) fetal bovine serum (FBS) [32]
Tris Acetate EDTA (TAE) 50x buffer	242 g Tris Base (Tris-(hydroxymethyl)-aminomethane), 57.1 mL Glacial Acetic Acid, 7.4 g Disodium EDTA dihydrate [32]
Tris-(hydroxymethyl)-aminomethane (Tris) buffer, 1 M, pH 9.0	121.1 g Tris (121,14 g/M) in 1 L distilled water [32]

TABLE 6.5: Continued list of self-prepared buffer, media and solutions derived from Vollmers *et al.* [32].

Buffer / Media / Solution	**Composition**
Washing medium	97 % (v/v) IMDM supplemented with, 2 % (v/v) fetal bovine serum (FBS) and 100 U/mL penicillin, 100 µg/mL streptomycin [320]

6.5.2 Purchased buffer, media and solutions

TABLE 6.6: List of purchased buffer, media and solutions.

Buffer / Media / Solution	**Manufacturer**	**Catalogue number**
autoMACS Running Buffer	Miltenyi Biotec	130-091-221
Dulbecco's Phosphate Buffered saline (PBS)	MERCK / Sigma-Aldrich	D8537
Hanks' Balanced Salt solution (Hanks)	MERCK / Sigma-Aldrich	H9394
Opti-MEM	Gibco / Thermo Fisher Scientific	31985047
S.O.C. medium	Thermo Fisher Scientific	15544034

6.6 NK cell Fc fusion construct proteins

TABLE 6.7: List of commercially available KIR-Fc and NK cell receptor-Fc fusion construct proteins used for B7 protein KIR-Fc screen derived from Vollmers *et al.* [32].

KIR-Fc fusion construct protein	**Manufacturer**	**Catalogue number**	**Characterisation**
KIR2DL1-Fc	R&D Systems	1844-KR-050	D1, D2 and stem domains of KIR2DL1 and the Fc region of a human IgG1 antibody [32]

TABLE 6.7: Continued list of commercially available KIR-Fc and NK cell receptor-Fc fusion construct proteins used for B7 protein KIR-Fc screen derived from Vollmers *et al.* [32].

KIR-Fc fusion construct protein	**Manufacturer**	**Catalogue number**	**Characterisation**
KIR2DL2-Fc	R&D Systems	3015-KR-050	D1, D2 and stem domains of KIR2DL2 and the Fc region of a human IgG1 antibody [32]
KIR2DL3-Fc	R&D Systems	2014-KR-050	D1, D2 and stem domains of KIR2DL3 and the Fc region of a human IgG1 antibody [32]
KIR2DL4-Fc	R&D Systems	2238-KR-050	D1, D2 and stem domains of KIR2DL4 and the Fc region of a human IgG1 antibody [32]
KIR2DL5-Fc	R&D Systems	6634-KR-050	D1, D2 and stem domains of KIR2DL5 and the Fc region of a human IgG1 antibody [32]
KIR2DS4-Fc	R&D Systems	1847-KR-050	D1, D2 and stem domains of KIR2DS4 and the Fc region of a human IgG1 antibody [32]

Table 6.7: Continued list of commercially available KIR-Fc and NK cell receptor-Fc fusion construct proteins used for B7 protein KIR-Fc screen derived from Vollmers *et al.* [32].

KIR-Fc fusion construct protein	**Manufacturer**	**Catalogue number**	**Characterisation**
KIR3DL1-Fc	R&D Systems	1225-KR-050	D0, D1, D2 and stem domains of KIR3DL1 and the Fc region of a human IgG1 antibody [32]
KIR3DL2-Fc	R&D Systems	2878-KR-050	D0, D1, D2 and stem domains of KIR3DL2 and the Fc region of a human IgG1 antibody [32]
KIR3DL3-Fc	R&D Systems	10104-KR-050	D0, D1, D2 and stem domains of KIR3DL3 and the Fc region of a human IgG1 antibody [32]
KIR3DS1-Fc	R&D Systems	4136-KR-050	D0, D1, D2 and stem domains of KIR3DS1 and the Fc region of a human IgG1 antibody [32]
NKp30-Fc	R&D Systems	1849-NK-025	Extracellular domains of NKp30 and the Fc region of a human IgG1 antibody [32]
NKp46-Fc	R&D Systems	1850-NK-025	Extracellular domains of NKp46 and the Fc region of a human IgG1 antibody [32]

6.7 B7 biotinylated proteins

TABLE 6.8: List of commercially available B7 proteins used for Fc-B7 protein screen.

B7 protein	**Manufacturer**	**Catalogue number**	**Characterisation by manufacturer**
B7-1 (CD80)	Sino Biological Inc.	10698-H08H-B	"DNA sequence encoding the extracellular domain (Met1-Asn242) of human B7-1 (NP_005182.1) precursor was fused with a polyhistidine tag at the C-terminus. The purified protein was biotinylated *in vitro*." [323]
B7-2 (CD86)	Sino Biological Inc.	10699-H08H-B	"DNA sequence encoding the extracellular domain (Met1-His239) of human B7-2 (NP_008820.2) was fused with a polyhistidine tag at the C-terminus. The purified protein was biotinylated *in vitro*." [324]
B7-Dc (PD-L2)	Sino Biological Inc.	10292-H08H-B	"DNA sequence encoding the extracellular domain (Met1-Pro219) of human PD-L2 (NP_079515.2) was expressed with a C-terminal polyhistidine tag. The purified protein was biotinylated *in vitro*." [325]

Table 6.8: Continued list of commercially available B7 proteins used for Fc-B7 protein screen.

B7 protein	**Manufacturer**	**Catalogue number**	**Characterisation by manufacturer**
B7-H1 (PD-L1)	Sino Biological Inc.	10084-H08H-B	"DNA sequence encoding the N-terminal segment (Met1-Thr239) of the extracellular domain of human B7-H1 (NP_054862.1) was expressed with a C-terminal polyhistidine tag. The purified protein was biotinylated *in vitro*." [326]
B7-H2 (ICOSLG)	Sino Biological Inc.	11559-H08H-B	"DNA sequence encoding the human ICOSLG (NP_056074.1) (Met1-Ser258) was expressed with a C-terminal polyhistidine tag. The purified protein was biotinylated *in vitro*." [327]
B7-H3	Sino Biological Inc.	11188-H08H-B	"DNA sequence encoding the human CD276 (Q5ZPR3-1) extracellular domain (Met1-Thr461) was expressed, with a polyhistidine tag at the C-terminus. The purified protein was biotinylated *in vitro*." [328]

Table 6.8: Continued list of commercially available B7 proteins used for Fc-B7 protein screen.

B7 protein	**Manufacturer**	**Catalogue number**	**Characterisation by manufacturer**
B7-H4 (VTCN1)	Sino Biological Inc.	10738-H08H-B	"DNA sequence encoding the human VTCN1(Q7Z7D3-1) (Phe29-Ala258) with a C-terminal polyhistidine tag was expressed. The purified protein was biotinylated *in vitro*." [329]
B7-H5 (VISTA)	Sino Biological Inc.	13482-H08H-B	"DNA sequence encoding the human VSIR / VISTA (AAH20568.1) (Met1-Ala194) was expressed with a C-terminal polyhistidine tag. The purified protein was biotinylated *in vitro*." [330]
B7-H6 (NCR3LG1)	Sino Biological Inc.	16140-H08H-B	"DNA sequence encoding the human NCR3LG1 (NP_001189368.1) (Met1-Ser262) was expressed with a polyhistidine tag at the C-terminus. The purified protein was biotinylated *in vitro*." [331]
B7-H7 (HHLA2)	Sino Biological Inc.	16139-H08H-B	"DNA sequence encoding the human HHLA2 (NP_009003.1) (Met1-Asn344) was expressed with a polyhistidine tag at the C-terminus. The purified protein was biotinylated *in vitro*." [332]

6.8 Peptide loaded HLA receptors and KIR-Fc fusion construct protein controls

Table 6.9: List of peptide loaded HLA receptors used as positive controls for Fc fusion construct proteins.

HLA receptor / Control protein	**Peptide sequence**	**Manufacturer**	**KIR binding partner**
B7-H6 (NCR3LG1) biotinylated	NA	Sino Biological Inc., Cat. No. 16140-H08H-B	NKp30-Fc [16]
B7-H7 (HHLA2) biotinylated	NA	Sino Biological Inc., Cat. No. 16139-H08H-B	KIR3DL3-Fc [11]
Complement Factor P	NA	TECOmedical-Quidel, Cat. No. A412	NKp46-Fc [333]
CD155 (PVR) biotinylated	-	AcroBiosystems, Cat. No. CD5-H82E3	KIR2DL5-Fc [90]
HLA-A*11 biotinylated	RLRAEAQVK	NIH Tetramer Core Facility at Emory University, Emory University Vaccine Center 954 Gatewood Road Atlanta, GA 30329	KIR2DS4-Fc [334], KIR3DL2-Fc [335]
HLA-B*13 (with Bw4 motif) biotinylated	RQDILDLWI	NIH Tetramer Core Facility at Emory University, Emory University Vaccine Center 954 Gatewood Road Atlanta, GA 30329	KIR2DL3-Fc [336], KIR3DL1-Fc [337]

Table 6.9: Continued list of peptide loaded HLA receptors used as positive controls for Fc fusion construct proteins.

HLA receptor / Control protein	**Peptide sequence**	**Manufacturer**	**KIR binding partner**
HLA-C*01 biotinylated	FSPEPGFSL	NIH Tetramer Core Facility at Emory University, Emory University Vaccine Center 954 Gatewood Road Atlanta, GA 30329	KIR2DL1-Fc [322], KIR2DL2-Fc [338]
HLA-F biotinylated	NA	Fred Hutchinson cancer research centre	KIR3DS1-Fc [321]
HLA-G*01 biotinylated	KGPPAALTL	NIH Tetramer Core Facility at Emory University, Emory University Vaccine Center 954 Gatewood Road Atlanta, GA 30329	KIR2DL4-Fc [339]

6.9 B7 protein functionality controls

No functionality control for B7-H4 was included as the receptor is considered an orphan receptor [340].

Table 6.10: List of Fc fusion construct receptors used as positive functionality controls for B7 proteins.

Control protein	**Manufacturer**	**Catalogue number**	**B7 binding partner**
CTLA4-Fc	R&D Systems	325-CT-200	B7-1 (CD80) [341], B7-2 (CD86) [342, 343]
ICOS-Fc	R&D Systems	169-CS-050	B7-H2 (ICOSLG) [344]
IL20RA-Fc	R&D Systems	1176-IR-050	B7-H3 [345]

Table 6.10: Continued list of Fc fusion construct receptors used as positive functionality controls for B7 proteins.

Control protein	**Manufacturer**	**Catalogue number**	**B7 binding partner**
NKp30-Fc	R&D Systems	1849-NK-025	B7-H6 [16]
PD-1-Fc	R&D Systems	1086-PD-01M	B7-Dc [346], B7-H1 (PD-L1) [347, 348]
PSGL-1-Fc	R&D Systems	3345-PS-050	B7-H5 (VISTA) [349]
TMIGD2 (CD28H)	R&D Systems	8316-TR-050	B7-H7 [279]

6.10 Chemicals and reagents

Table 6.11: List of additionally used chemicals and reagents.

Chemical / Reagent	**Manufacturer**	**Catalogue number**
ACK lysing buffer	Gibco / Thermo Fisher Scientific	A1049201
Agarose	MERCK / Sigma-Aldrich	A2790
Anti-PE Microbeads	Miltenyi Biotec	130-048-801
Ampicillin	MERCK / Sigma-Aldrich	A5354-10ML
B7-H7-Fc	R&D	8084-B7
BD FACSuite CS&T Research Beads	BD Biosciences	650622
Biotin	MERCK / Sigma-Aldrich	B4501
Cell Counting Slides for TC10 / TC20	Bio Rad	1450015
Cellfectin II	Thermo Fisher Scientific	10362100
Cell Strainer, 70 µm, White, Sterile, Individually Packaged, 50/Case	Corning	352350
Dimethyl sulfoxide (DMSO)	MERCK / Sigma-Aldrich	D2650

TABLE 6.11: Continued list of additionally used chemicals and reagents.

Chemical / Reagent	**Manufacturer**	**Catalogue number**
Dynabeads M-280 Streptavidin	Thermo Fisher Scientific	11205D
DTT, Molecular Grade (DL-Dithiothreitol)	Promega	P1171
Ethylenediamine-tetraacetic acid (EDTA), 0.5 M	Promega	V4231
Ethanol absolute	Th. Geyer	2273-5L
Human TruStain Fc (Fc Receptor Blocking Solution)	BioLegend	422302
ImmunoCult Human CD3/CD28 T-Cell Activator	Stemcell Technologies	10991
LB Agar, powder (Lennox L agar)	Thermo Fisher Scientific	22700025
LB Broth Base	Thermo Fisher Scientific	12780052
Lenti-X concentrator	Clontech Labs 3P	631232
Lipofectamine 3000	Thermo Fisher Scientific	L3000001
Lymphocytes Separation Medium	Capricorn Scientific	LSM-A
MassRuler High Range DNA Ladder, ready-to-use	Thermo Fisher Scientific	SM0393
MassRuler Low Range DNA Ladder, ready-to-use	Thermo Fisher Scientific	SM0383
One Shot Stbl3 Chemically Competent *E. coli*	Thermo Fisher Scientific	C737303
Puromycin	Thermo Fisher Scientific	J67236.XF
RNase AWAY	Thermo Fisher Scientific	7000TS1

Table 6.11: Continued list of additionally used chemicals and reagents.

Chemical / Reagent	Manufacturer	Catalogue number
SYBR® Safe DNA Gel Stain	Thermo Fisher Scientific	S33102
Steriflip-HV, 0.45 µm, PVDF, γ-sterilisiert	Milipore / MERCK	SE1M003M00
Tris-(hydroxy-methyl)-amino methane (Tris)	Carl Roth	A411.3
Trypan blue solution, 0.4 %	MERCK / Sigma-Aldrich	T8154
Trypsin-EDTA solution	MERCK / Sigma-Aldrich	T3924

6.11 Microbiological reagents

6.11.1 Primer and constructs

Table 6.12: List of primers and constructs derived from Vollmers *et al.* [32].

Primer / Construct	Sequence (5' -> 3')	Manufacturer
B7-H7 sequence	See subsection A.1.8, page 213	Thermo Fisher Scientific Gene Art
KIR3DL3 sequence	See subsection A.1.2, page 206	Thermo Fisher Scientific Gene Art
KIR sequencing forward	TTT ACT GTT TTC GTA CAC GTT TTG	IDT integrated data technologies
KIR sequencing reverse	GGA AGC TGT CTT CCA TGA GCG	IDT integrated data technologies
pLVX-SIP sequencing forward	GCG CCT TAT TTG AAT TAA CC	IDT integrated data technologies
pLVX-SIP sequencing reverse	ACA CCG GCC TTA TTC CAA GC	IDT integrated data technologies

Table 6.12: Continued list of primers and constructs derived from Vollmers *et al.* [32].

Primer / Construct	**Sequence (5' -> 3')**	**Manufacturer**
Stopp codon KIR3DL3-CD3ζ sequence	AGG CCC TGC CAC CTA GAT AGG CCG CGG A	IDT integrated data technologies

6.11.2 Restriction enzymes

Table 6.13: List of restriction enzymes derived from Vollmers *et al.* [32].

Restriction enzyme	**Sequence (5' -> 3')**	**Manufacturer**	**Catalogue number**
EcoRI	G'AATTC	New England BioLabs GmbH	R0101L
NotI-HF	GC'GGCCGC	New England BioLabs GmbH	R3189L

6.11.3 Plasmids

Table 6.14: List of plasmids derived from Vollmers *et al.* [32].

Name	**Manufacturer / Source**	**Application**
pCMV-VSVG	Addgene, 8454	VSV-G expression plasmid for lentiviral production
pLVX-SIP	Ragon Institute of MGH, MIT and Harvard, Charlestown, MA, USA; Dr. Thomas Pertel	Lentiviral transfer vector for B7-H7 and KIR3DL3 cell line
psPAX2	NIH Aids Research Program, ARP-11348	HIV-1 gag-pol packaging plasmid for lentiviral production

6.12 Kits

Table 6.15: List of kits derived from Vollmers *et al.* [32].

Kit Name	**Manufacturer**	**Catalogue number**
Advantage HF 2 PCR Kit	Takara Bio Group	639123
ArC Amine Reactive Compensation Bead Kit	Invitrogen / Thermo Fisher Scientific	A10346
CellTrace CFSE Cell Proliferation Kit	Invitrogen / Thermo Fisher Scientific	C34554
CellTrace cell proliferation kit violet	Invitrogen / Thermo Fisher Scientific	C34557
CompBeads Anti-mouse Ig, / negative control compensation particles set	BD Bioscience	552843
Compensation Beads	BioLegend	424602
Cytofix/Cytoperm Fixation/Permeabilisation Solution Kit	BD Bioscience	554714
EasyEight EasySep Magnet	Stemcell	18103
EasySep Magnet	Stemcell	18000
HiSpeed Plasmid Maxi Kit	Qiagen	12663
LIVE/DEAD Fixable Near-IR Dead Cell Stain Kit	Invitrogen / Thermo Fisher Scientific	L34976
LIVE/DEAD Fixable Aqua Dead Cell Stain Kit	Invitrogen / Thermo Fisher Scientific	L34957
NEBuilder HiFi DNA Assembly Master Mix Kit	New England BioLabs GmbH	E2621L
Platinum SuperFi DNA Polymerase	Invitrogen / Thermo Fisher Scientific	12351010
QIAquick Gel Extraction Kit	Qiagen	28706
QIAprep Spin Minipep Kit	Qiagen	27106
QuickChange II XL Site-Directed Mutagenesis Kit	Agilent Technologies	200521

Table 6.15: Continued list of kits derived from Vollmers *et al.* [32].

Kit Name	Manufacturer	Catalogue number
SuperScript III One-Step RT-PCR System with Platinum Taq DNA Polymerase	Invitrogen / Thermo Fisher Scientific	12574026

6.13 Analytic devices and software

6.13.1 Analytic and experimental devices

Table 6.16: List of analytic devices derived from Vollmers *et al.* [32].

Device Name	Manufacturer	Serial number
Biological safety cabinet Herasafe 2030i 1.8	Thermo Fisher Scientific	51032676
BD LSR Fortessa	Becton Dickinson (BD) Biosciences	63478
BD FACS Aria Fusion	Becton Dickinson (BD) Biosciences	60050
Centrifuge 5415 R	Eppendorf	5426
Eclipse Ti2	Nikon	-
Flex cycler	Analytik Jena	180978642
HB-1000 Hybridizer	UVP Laboratory products	582858
Heraeus Megafuge 16R Cetrifuge	Thermo Fisher Scientific	75004270
Heracel VIOS 160i CO2 Incubator, 165 L	Thermo Fisher Scientific	51033559
Microscope Leica DM IL	Leica	582910
Nanodrop 1000 Spectrophotometer	Peqlab	ND-3300
Rotation Shaker	Heidolph	101141
Rotor H-Flex 1 Megafuge	Thermo Fisher Scientific	75003300
TC20 Automated Cell Counter	Bio-Rad	1450102

Table 6.16: Continued list of analytic devices derived from Vollmers *et al.* [32].

Device Name	Manufacturer	Serial number
Test tube shakers Genie® Vortex Mixer Model: Vortex-Genie® 2T with integrated timer	VWR distributed by Carl Roth	X561.1

6.13.2 Software

Table 6.17: List of software derived from Vollmers *et al.* [32].

Software	Manufacturer	Version
BD FACS Diva Software	BD Biosciences	7.0
BioRender	BioRender	NA
Excel	Microsoft Corporation	2302
FlowJo	Becton Dickinson Biosciences	10.8.2
GraphPad Prism	GraphPad software	9.5.1
LaTex	Overleaf	-
NIS AR Analytic	Nikon Instruments Inc.	5.21.02
R	r-project.org	R-4.3.2
R Studio	Posit PBC Inc.	2023.06.02+561
SnapGene Viewer	SnapGene	5.2.4
Word	Microsoft Corporation	2302
Zotero Desktop	Corporation for Digital Scholarship	6.0.26.

7 Methods

7.1 Experimental acknowledgement

Multiple methods and protocols used in this dissertation were established and standardised in our laboratory by previous doctoral researchers and post-docs. I therefore want to thank these researchers and want to specifically point out that my methods, materials, and experiments build on the work conducted previously. Some methods can therefore be found in publications by Dr. Sébastien Brias, Dr. Pia Fittje and Dr. Sarah Vollmers [31, 32, 124]. Protocol steps and volumes from doctoral researchers and manufacturer protocols are cited to my best knowledge.

7.2 Experimental setup

As previously described in the dissertation of Dr. Sarah Vollmers, experiments involving cell lines were conducted under S2 biosafety conditions in a biological safety cabinet with laminar airflow [32]. Microbiological work was done in a semi-sterile setting of a work bench with a burning Bunsen burner within 5 cm reach of the respective sample [32]. All cultivation media and buffers were used at room temperature (RT) if not otherwise stated [32]. Their respective components are summarised in chapter 6.4 and 6.5 (page 104 - 107) [32]. In general, experiments were conducted in a way to achieve equal conditions for all samples [32]. Work with B7 proteins and KIR-Fc fusion constructs were performed on ice or at 4 °C [32]. All centrifuges were used with maximum acceleration and deceleration settings, except the density gradient centrifugation for peripheral blood mononuclear cells (PBMCs) isolation [32].

7.3 Cell biology

7.3.1 Isolation of peripheral blood mononuclear cells (PBMCs)

As previously described in the dissertation of Dr. Sarah Vollmers, peripheral blood mononuclear cells (PBMCs) were isolated from donated EDTA whole blood tubes from the healthy cohort (HHCH) of the UKE [31, 32]. In accordance with the original publication by Ulmer *et al.* (1984) PBMCs were isolated by density gradient centrifugation (Figure 7.1) [32, 350]. The method allows to separate blood cells from each other based on their different density and size [32]. In short, 20 mL of blood drawn in EDTA tubes were mixed with 10 mL of Hank's solution prewarmed to 37 °C in 50 mL

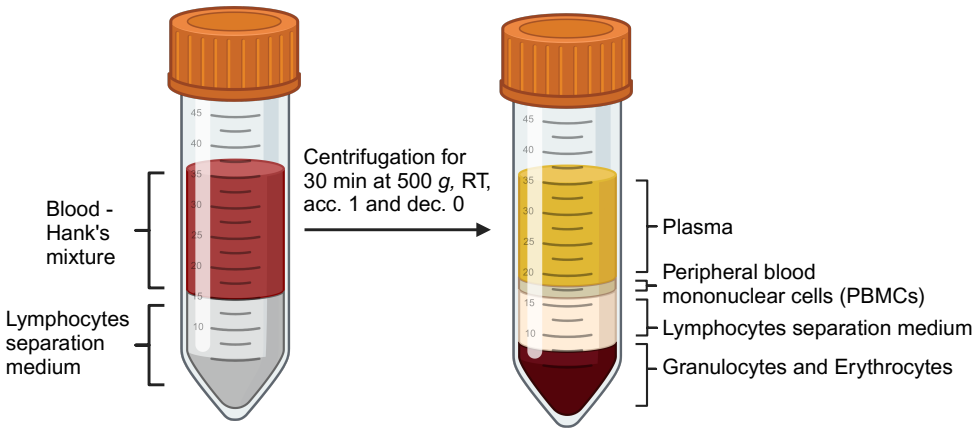

FIGURE 7.1: PBMCs isolation process and layers. First the EDTA blood was mixed with Hank's solution prewarmed and carefully layered on top of a lymphocyte separation medium with a density of 1.077 g/mL. After a centrifugation for 30 min at 500 g with acceleration of 1 g and a deceleration of 0 g at room temperature the layers of plasma, peripheral blood mononuclear cells (PBMCs) and granulocytes and erythrocytes were visible. The PBMCs were harvested using a serological pipette at the interface of lymphocyte separation medium and plasma. The figure was adapted from Ulrich *et al.* and Vollmers *et al.* and created with BioRender.com [32, 350].

conical tubes [32]. Next, the 30 mL of blood solution were carefully layered on top of 15 mL lymphocytes separation medium and centrifuged for 30 min at 500 g at RT with acceleration of 1 g and deceleration of 0 g [32]. As a result, the tubes displayed the different blood layers depicted in Figure 7.1 with the PBMCs being present as a white layer just below the yellow plasma [32]. The PBMCs were harvested using a 5 mL serological pipette and transferred into a new 50 mL conical tube [32]. The cells were washed once by filling up the tube to 30 mL with Hank's solution prewarmed to 37 °C and spun down 5 min at 500 g at RT [32]. The supernatant was removed with a 10 mL serological pipette and then 3 mL of ACK lysis buffer added [32]. After pipetting up and down the cells were incubated for 3 min before the tube was filled up again with Hank's solution prewarmed to 37 °C to 40 mL and centrifuged for 5 min at 500 g at RT [32]. After the centrifugation, the supernatant was removed and the PBMCs pellet was resuspended in 10 mL cultivation medium and counted on the Bio-Rad T20 [32]. PBMCs were then used for further experiments, cryopreserved, cultivated overnight, or used for NK cell or CD4 T cell enrichment [32].

7.3.2 Cell cultivation

As previously described in the dissertation of Dr. Sarah Vollmers, isolated PBMCs were cultivated in T-25 cell culture flasks at a density of 2×10^6 cells/mL in RPMI - 1640 and supplements described in Table 6.3 (page 104) at 37 °C and 5 % ppm CO_2 [32]. The other suspension cell lines described in Table 6.3 were cultured in T-25 cell culture flasks, T-75 cell culture flasks or 24-well plates with their respective media at

37 °C and 5 % ppm CO_2 at a density of $0.5 - 1.0 \times 10^6$ cells/mL and passaged every 2-3 days depending on the cell density and viability [32].

Adherent HEK-293T cells were cultured as monolayer at 90 % confluency before being used for lentivirus production [32]. To passage HEK-293T cells, old medium was carefully removed, and cells were washed under gentle shaking once with PBS to remove dead and non-adherent cells, respectively [32]. After removal of PBS the HEK293-T cells were incubated for 5 min at 37 °C and 5 % ppm CO_2 with 0.05 % (v/v) trypsin-EDTA solution [32]. After the incubation, cells were washed off with cultivation medium twice the volume of trypsin-EDTA solution used and centrifuged for 5 min at 500 *g* to inactivate and remove the trypsin-EDTA solution [32]. The supernatant was discarded and 1:5 of the cells was seeded in new DMEM [32].

The K562 cell line naturally lacking HLA class I receptors and B7-H7[1] expression was stably transduced with the B7-H7 receptor and used for the killing assays as well as a positive control in other experiments. β2m-KO-Jurkat cells were used for Fc staining's and during reporter cell assays and were therefore stably transduced with KIR3DL3-CD3ζ gene constructs. Further β2m-KO-Jurkat cell lines transduced with KIR2DL5-CD3ζ, KIR3DL2-CD3ζ, KIR2DS4-CD3ζ and KIR3DL1-CD3ζ were generated in our laboratory before by Dr. Wilfredo Garcia-Beltran and Dr. Pia Fittje [90, 205, 322].

7.3.3 Cell thawing

As previously described in the dissertation of Dr. Sarah Vollmers, cells frozen in liquid nitrogen were moved on dry ice to the laboratory and thawed in a water bath warmed to 37 °C until a small frozen pellet remained in the cryotube [32]. The cells and the small remaining pellet were resuspended in 9 mL of the respective cell culture media warmed to RT and transferred into a 15 mL falcon tube [32]. Cells were centrifuged for 5 min at 500 *g* at RT and supernatant discarded [32]. Cells were resuspended in 10 mL of fresh cultivation medium used for the cell line, counted once with Bio Rad analyser, and adjusted to the desired density in a respective cell culture flask [32]. Cells were then cultivated at 37 °C and 5 % ppm CO_2 until further usage [32].

7.3.4 Cell storage

As previously described in the dissertation of Dr. Sarah Vollmers, long-term storage in liquid nitrogen was facilitated by aliquoting 1×10^7 cells from the different cell lines [32]. To do so, cells for storage were counted using the Bio-Rad T20 cell counter (Bio-Rad) and respective volume spun down in 50 mL conical tube for 5 min at 500 *g* at RT [32]. The supernatant was discarded, and cells resuspended in 1 mL of cell freezing medium before being transferred into a CryoPure tube [32]. The tubes were

[1] Janakiram *et al.* reported K562 as B7-H7 expressing cell line but multiple tests in our laboratory with commercially available B7-H7 antibodies did not confirm the presented results (Figure 3.30, page 62) [21].

placed in a 4 °C cold StrataCooler and stored at – 80 °C overnight [32]. The next day cells were transferred on dry ice into liquid nitrogen tanks [32].

7.3.5 Cell density and viability assessment

As previously described in the dissertation of Dr. Sarah Vollmers, specific cell concentrations were obtained by counting cell samples with the Bio-Rad T20 cell counter (Bio-Rad) according to the manufacturers protocol [32, 351]. The device detects trypan blue stained cells through light emission and can exclude them from other objects counted upon changing the light wavelength [351]. Henceforth the concentration and viability of a sample can be determined as trypan blue is a dye that is only absorbed by dead cells through a disrupted cell membrane [32]. The optimal concentration range for cell counting is $0.1 - 5.0 \times 10^6$ cells/mL [32, 351]. Before testing 10 µL of cells in media were mixed with 10 µL of trypan blue and then 10 µL of the mixture were transferred into a Bio-Rad counting slide [32]. Isolated PBMCs were prediluted 1:10 (v/v) in RPMI – 1640 before being mixed as described before with trypan blue and analysed [32]. For PBMCs, cells with a diameter from 6 – 17 µm were counted by selecting a gate within the Bio-Rad device [32].

7.3.6 Stimulation of NK cells

As previously described in the dissertation of Dr. Sarah Vollmers, NK cells in PBMCs were cultured at 2.5×10^6 cells/mL in cultivation medium with 50 U/mL IL-2 and 5 ng/mL IL-15 overnight at 37 °C and 5 % ppm CO_2 [32].

7.3.7 Isolation of intraepithelial layer samples from gut donors

As previously described by members of our laboratory, the intraepithelial layer samples (IEL) were isolated from fresh anatomical reconstruction or inflammation samples of the small intestine [320]. In short, the intestine was cut open and washed with ice-cold sterile PBS to remove blood before the fat tissue and muscle layer were removed [320]. For further processing the sample was cut into 0.5 cm^2 large pieces and put in 10 mL EDTA/DTT buffer in a 50 mL conical tube [320]. Next, the sample was incubated for 20 min in a hybridization incubator at 37 °C under constant rotation of 6 rpm [320]. After 20 min the sample was vortexed thoroughly for 2 min at the highest speed before being incubated for 20 min in a hybridization incubator at 37 °C under constant rotation of 6 rpm again [320]. The sample was vortexed again for 2 min at the highest speed before tissue pieces were placed into a 6-well plate for mincing [320]. After the mincing the IEL fraction was filtered through 70 µm filter and washed with additional 35 mL of IEL washing medium [320]. Next the IEL cells were pelleted for 5 min at 500 *g* at 4 °C and the supernatant carefully discarded [320]. Cells were then two times in 5 mL of IEL washing media for 5 min at 500 *g* at 4 °C [320]. IEL cells were then resuspended in 10 mL of Hank's buffer and carefully layered on 4 mL of Lymphocytes Separation Medium in a 15 mL conical flask [320]. The flask was

centrifuged for 22 min at 1000 *g* at 4 °C with an acceleration of 1 and a deceleration of 0. Finally, IEL cells were collected with a Pasteur pipette two times with washing medium for 5 min at 500 *g* at 4 °C [320]. Cells were used for cell staining or frozen for long term storage [32].

7.4 Microbiology

7.4.1 Cloning and cell line generation

As previously noted in the dissertation of Dr. Sarah Vollmers, microbiological cloning is used to amplify DNA fragments of interest [32]. Depending on the length of the DNA fragment it can either be amplified by PCR (usually 1 - 3 kBp) or by ligating it into a plasmid which gets transformed into bacteria and then expanded via bacterial growth (everything $>$ 4 kBp). The reason for this is that longer DNA fragments amplified by PCRs become more error prone unless smaller segments are replicated and then fused together [352, 353]. In this dissertation the former method was used for the DNA inserts used and the latter method via bacterial growth was used for DNA fragment amplification of fused receptors.

Plasmids used for DNA fragment amplification carry antibiotic resistance genes [32]. As previously described by Bergmann *et al.* plasmids with antibiotic resistance and DNA fragments are cleaved via the same restriction enzymes with complementary base pairs at the 3' and 5' prime end [354]. Upon ligation of the gene and plasmid, the plasmid is fused together and transformed into competent cells via heat shock or Ca-stress [355, 356]. The bacteria cells are then grown in broth or agar mixed with the antibiotic of their resistance to positively select only the bacteria cells which did take up the required plasmid [356]. After successful growth of the bacteria clones, plasmid DNA from bacteria is isolated via lysation of the bacteria cells, centrifugation and bind-wash-elute procedures using commercial miniprep kits from Qiagen [32, 357, 358]. During the process plasmid DNA binds to a silica membrane while contaminating reagents are washed out with buffer solution [32, 357]. Finally, the pure plasmid DNA is eluted in water [32, 357]. To verify the integrity of the DNA sequence plasmids were sequenced at the Microsynth SEQLAB facility with specific sequencing primer (Table 6.12, page 118) [32].

For the dissertation plasmid DNA was generated for the KIR3DL3-CD3ζ Jurkat reporter cell line and the K562.B7-H7 cell line (Figure 7.2) [32]. For the B7-H7 cell line the sequence was synthesized by GeneArt GeneSynthesis (Thermo Fisher Scientific), cloned into a lentiviral transfer vector (pLVX-SIP) and used to generate full length B7-H7 expressing K562 cells [31, 32, 363]. For the KIR3DL3-CD3ζ Jurkat reporter cell line a plasmid containing the transmembrane domain of KIR3DL3*001 and the cytoplasmic domain of the CD3ζ chain were synthesized by GeneArt GeneSynthesis (Thermo Fisher Scentific), cloned into a lentiviral transfer vector (pLVX-SIP) and used to generate KIR3DL3-CD3ζ expressing Jurkat reporter cells [32, 363].

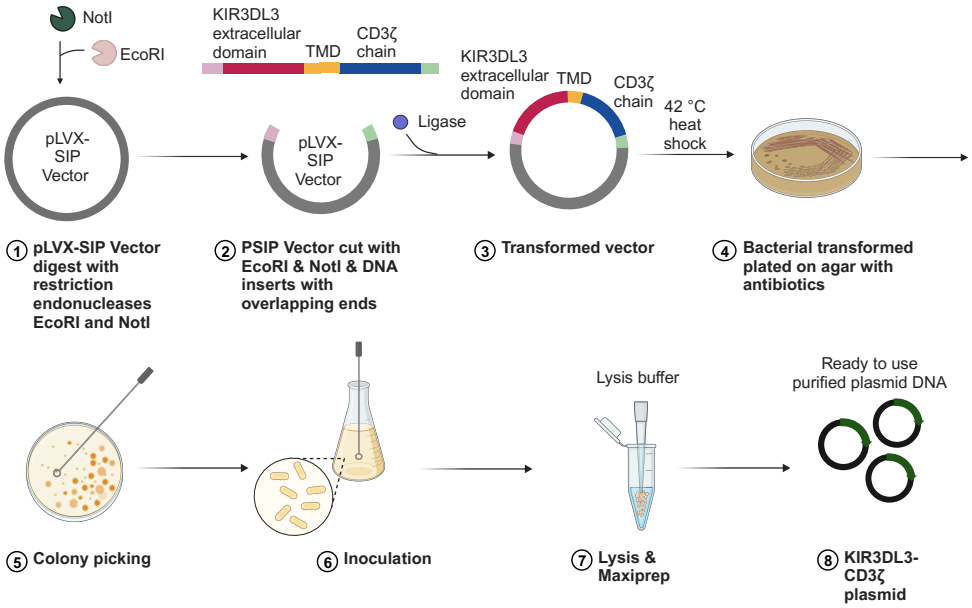

FIGURE 7.2: Vector plasmid generation and amplification. Here shown as an example for the KIR3DL3-CD3ζ construct used to generate β2m-KO-Jurkat KIR3DL3 reporter cells. The B7-H7 cell line con-structs were created analogously but without CD3ζ domain. First the transfer vector pLVX-SIP was cut with restriction enzymes NotI and EcoRI before the KIR3DL3-CD3ζ construct with corresponding overlapping gene ends was ligated into the transfer vector [32, 359, 360]. After a heat shock into StbI competent *E. Coli* cells they were plated on an agar mixed with antibiotic of the antibiotic resistance of the transfer vector to positively select for bacteria which were successfully transformed [32, 361]. Next colonies were picked and inoculated in LB broth overnight before being lysed and purified with a Qiagen Maxi prep Kit [32, 357]. The figure was adapted from Thomas *et al.* and created with BioRender.com [362].

7.4.2 Plasmid and DNA fragment amplification

Before the pLVX-SIP plasmid and the B7-H7, KIR3DL3-CD3ζ constructs could be used for further molecular biological experiments they were amplified in a PCR. This was done using 50 ng of the respective plasmid and constructs and the Advantage HF 2 PCR Kit (Takara Bio Group) adding 5 µL of 10x Advantage-HF 2 PCR Buffer, 5 µL of 10x Advantage-HF dNTP Mix, 10 µM of the respective forward and reverse primer and deionized water to a total volume of 50 µL in a PCR tube [364]. The tube was placed in a Flex Thermo Cycler (Analytik Jena) with the following program: 94 °C 2 min; 40 cycles of 94 °C 20 sec, 55 °C 20 sec, 72 °C 4 min; 72 °C 6 min. After the PCR the tubes were stored at 4 °C until further usage.

7.4.3 Plasmid preparation and DNA fragment insertion

As previously described in the dissertation of Dr. Sarah Vollmers, KIR3DL3-CD3ζ and B7-H7 sequences were ordered from GeneArt GeneSynthesis (Thermo Fisher Scientific) with an EcoRI recognition site (G'AATTC) at the 5' end and a NotI recognition site (GC'GGCCGC) at the 3' end for the assembly with the lentiviral transfer vector pLVX-SIP [32, 363]. Before insertion the 2 µg of vector was digested with EcoRI and NotI restriction enzyme for 3 h at 37 °C (Figure 7.2) [32, 359]. Afterwards, the cut vector was run on a 1 % agarose gel stained with SYBR Safe DNA Gel stain (Thermo Fisher Scientific) and 1 kBp ready to use ladder. The fragment of ~8 kBp size was cut and extracted from the gel using QIAquick Gel Extraction Kit (Qiagen) [358]. The concentration was measured on a nanodrop device (Peqlab) before insert and cut vector were incubated according to the manufacturer protocol at a molar ratio of Insert:Vector of 5:1 with NEBuilder HiFi DNA assembly master mix (NEB) for 1 h at 50 °C [32, 360]. Reaction product was sent for sequencing to Microsynth Seqlab using the KIR sequencing forward and reverse primer (Table 6.12, page 118) [32]. The rest of the reaction was diluted 1:10 (v/v) and stored at 4 °C until bacterial transformation [32].

7.4.4 Site-directed mutagenesis

As the sequencing results did show a missing stop codon in the KIR3DL3-CD3ζ construct it was artificially inserted using mutagenesis primers (Table 6.12, page 118) designed with the QuickChange Primer Design (Agilent Technologies) and ordered at Integrated DNA Technologies (IDT) [365]. As previously described in the dissertation by Dr. Sarah Vollmers, the mutant strand synthesis reaction was prepared and amplified in a flex thermo cycler (Analytik Jena) using the primers in combination with the Quick-Change II XL Site-Directed Mutagenesis Kit (Agilent Tehnologies) following Agilents protocol [32, 366]. Afterwards the product was digested in Cutsmart buffer (NEB) for 1 h at 37 °C with DpnI to remove non-mutated plasmids [32, 359]. Plasmids were sequenced again via Microsynth Seqlab using the KIR primers and showed a functional KIR3DL3-CD3ζ sequence [32]. The plasmids were stored at 4 °C until bacterial transformation [32].

7.4.5 Bacterial transformation and resistance selection

As previously described in the dissertation of Dr. Sarah Vollmers, B7-H7 plasmids were transformed into chemically competent one shot StbI3 *E. coli* (Thermo Fisher Scientific) for expansion [32, 361]. Following Thermo Fisher Scientific's protocol, plasmid DNA was incubated with the competent cells on ice and then heated to 42 °C for 20 sec, which allows the uptake of plasmid DNA into the cell through cell membrane disruption (Figure 7.2) [32, 361].

For the mutated KIR3DL3-CD3ζ plasmids XL10-Gold ultracompetent cells from Agilent Technologies were used provided with the mutagenesis kit [32, 366]. The protocol

from the manufacturer was followed and the cells and plasmids incubated at 50 °C for 45 sec [32, 366].

50 µL of the component cells were plated on LB agar plates pre-warmed to 37 °C containing 100 µg/mL ampicillin and were incubated overnight at 37 °C [32]. The following day, 2-5 colonies were picked and transferred into 250 mL of LB medium with 100 µg/mL ampicillin and incubated over night at 37 °C and shaking at 250 rpm overnight [32].

7.4.6 Plasmid purification

As previously described in the dissertation of Dr. Sarah Vollmers, purification of up to 750 µg plasmid DNA for the KIR3DL3-CD3ζ and B7-H7 construct was performed using the HiSpeed Plasmid Maxi Kit (Qiagen) according to Qiagen's protocol [32, 357]. Isolated plasmid DNA was sequenced by Microsynth Seqlab using the using the KIR primers and stored at - 20 °C until usage (Figure 7.2) [32]. Sequencing results were checked for correct results using SnapGene Viewer (SnapGene).

7.5 Virology

7.5.1 Lentivirus production

As previously pointed out in the dissertation of Dr. Sarah Vollmers, lentiviral particles containing the plasmids of interest were produced with a 2nd generation lentivirus packaging system described previously by Kalidasan [32, 367]. As depicted in Figure 7.3 the following three components were used: 1) the lentiviral transfer vector (pLVX-SIP) with the inserted sequence of B7-H7 and KIR3DL3-CD3ζ chain, 2) the packaging plasmid (psPAX2) which contains the HIV-1 proteins Gag and Pol and 3) the envelope plasmid (pCMV-VSVG) expressing vesicular stomatitis virus glycoprotein (VSVG) [32].

As described by our laboratory earlier, HEK293-T cells were cultured in a 6-well plate and 1 mL of cultivation medium without antibiotics until a 90 % confluence was observed [32, 205]. Adapted from the Thermo Fisher Scientific protocol for one well, 6 µL Lipofectamine 3000 was mixed with 250 µL Opti-MEM and incubated for 5 min [32, 368]. Next, 2 µg of transfer vector pLVX-SIP with the respective construct, 1 µg of packaging plasmid psPAX2 and 0.5 µg of envelope plasmid pCMV-VSVG were diluted in 250 µL Opti-MEM with 7 µL P3000 reagent [32, 368]. Lipofectamine 3000 was slowly dropped into the plasmid mixture and incubated for 20 min at RT [32, 368]. During the incubation time, the cultivation medium was removed from the HEK-293T cells and cells were carefully washed with 2 mL PBS [32, 368]. 2 mL Opti-MEM was added to the cells, as well as the plasmid/Lipofectamine mix and incubated at 37 °C and 5 % ppm CO_2 [32]. 48 h later, the supernatant was collected using a 1000 mL pipette, centrifuged for 5 min at 500 *g* at RT and filtered through a 0.45 µm Steriflip

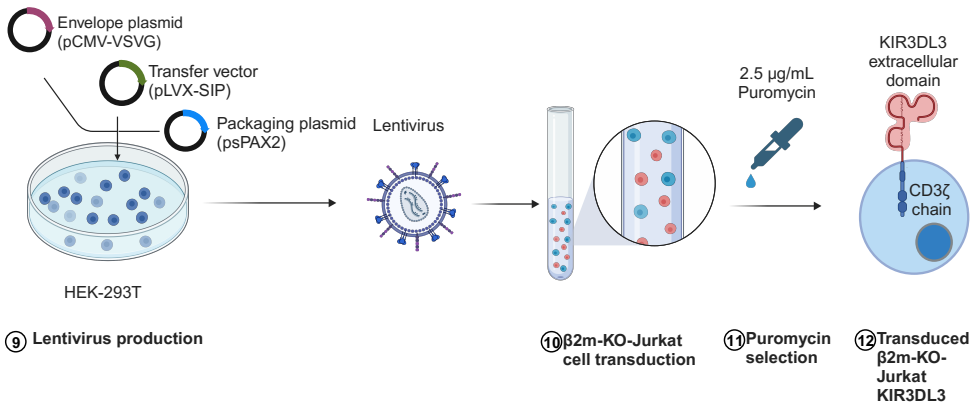

FIGURE 7.3: Lentiviral production and transduction of cell line. Here shown as an example for the KIR3DL3-CD3ζ construct used to generate β2m-KO-Jurkat KIR3DL3 reporter cells. The B7-H7 cell line was created analogously. First, HEK-293T cells were grown to 90 % confluency before Lipofectamine 3000 was mixed with Opti-MEM, transfer vector pLVX-SIP, packaging vector psPAX2 and envelope vector pCMV-VSVG [32, 205, 368]. The Opti-MEM mixture was added to the cells and incubated at 37 °C for 3 days before supernatant was harvested, sterile filtered and added to β2m-KO-Jurkat cells for transduction [32]. β2m-KO-Jurkat were carefully monitored and selected via addition of puromycin [32]. The figure was adapted from Kalidasan *et al.* and created with BioRender.com [367].

into a 50 mL falcon [32]. 2 mL aliquots were stored at - 80 °C until further usage for lentiviral transduction [32].

7.5.2 Lentiviral transduction

As previously described by our laboratory, K562 and β2m-KO-Jurkat cells were cultured in a 6-well plate at a concentration of 0.25×10^6 cells/mL [32, 205]. 2 mL aliquot of - 80 °C frozen lentivirus or 2 mL cultivation medium for the untransduced control were added and incubated at 37 °C and 5 % ppm CO_2 (Figure 7.3) [32, 205]. After three days, 2.5 µg/mL puromycin was added for a positive selection and the viability observed throughout the next week [32, 205]. The viability decreased in the beginning from 98 % to 75 % killing off all untransduced cells which were lacking the puromycin resistance from the pLVX-SIP vector and then slowly recovering to 90 %. Cell lines were then stained for receptor expression via flow cytometry and sorted for high expressing cells using a fluorescence-activated cell sorting (FACS) Aria Fusion flow cytometer from BD Bioscience [32]. Sorted cells were constantly cultured in RPMI – 1640 with 10 % (v/v) fetal bovine serum, 100 U/mL penicillin, 100 µg/mL streptomycin with 1 µg/mL of puromycin to keep selection pressure.

7.6 Protein biochemistry

7.6.1 Biotin & Streptavidin interaction

The biotin-streptavidin interaction is the strongest known non-covalent biological bond with a dissociation constant of 4×10^{-14} M [369]. Henceforth, it is used in many biological settings to link two molecules together without triggering immunological adverse effects. In this thesis the interaction was used to couple biotinylated B7 or HLA receptors of interest to streptavidin metallic beads which can be detected via flow cytometry.

7.6.2 Protein solvation and streptavidin bead coating

As previously described in our laboratory, biotinylated B7 proteins (Sino Biological Inc.) and biotin (MERCK) were dissolved on ice in PBS at a concentration of 0.25 µg/µL [90]. Dynabeads M-280 Streptavidin (Thermo Fisher Scientific) were vortexed for 30 sec and then 20 µL per B7 protein transferred into a 1.5 mL Eppendorf cup (eppi) [90]. Beads were washed once with 1 mL of cold PBS and placed in a Stemcell magnet (Stemcell) to remove the supernatant [90]. Dissolved biotin and B7 proteins were diluted to a final concentration of 0.05 µg/µL using PBS and 200 µL added on top of the streptavidin beads [90]. The eppis were placed in a shaker (Heidolph) flipping the samples every 5 sec at 4 °C overnight [90]. The next day the beads were washed two times with 1 mL with cold PBS using the magnet to retain the beads [90]. Finally, the coated beads were dissolved in 200 µL of PBS. Beads were stored at 4 °C until further usage [90].

7.6.3 Tetramerization of HLA receptors

HLA receptors were tetramerized so that they can be used as positive controls for the KIR-Fc fusion construct proteins according to the protocol of the NIH Tetramer core facility [370]. In short 10 µL of Dynabeads M-280 Streptavidin (Thermo Fisher Scientific) were added into an 1.5 mL eppi and washed once with 1 mL PBS [370]. Next, the biotinylated HLA receptors were diluted to 0.25 µg/µL and 4 µL were transferred into the streptavidin eppi [370]. After 10 min another 4 µL of biotinylated HLA receptor was added to the streptavidin beads and the process repeated for a total of 10 times [370]. After final incubation the tetramerized HLA receptors were frozen in aliquots of 10 µL at - 80 °C until further usage [370].

7.7 Flow cytometry

7.7.1 Basics of flow cytometry

As previously pointed out in the dissertation of Dr. Sarah Vollmers, flow cytometry allows for rapid analysis of the physical and chemical attributes of biological samples by light scattering [32, 371]. As described by Adan *et al.* cytometer consist of

three main components: a fluidic chamber, an optical unit, and an electronic system (Figure 7.4) [32, 372].

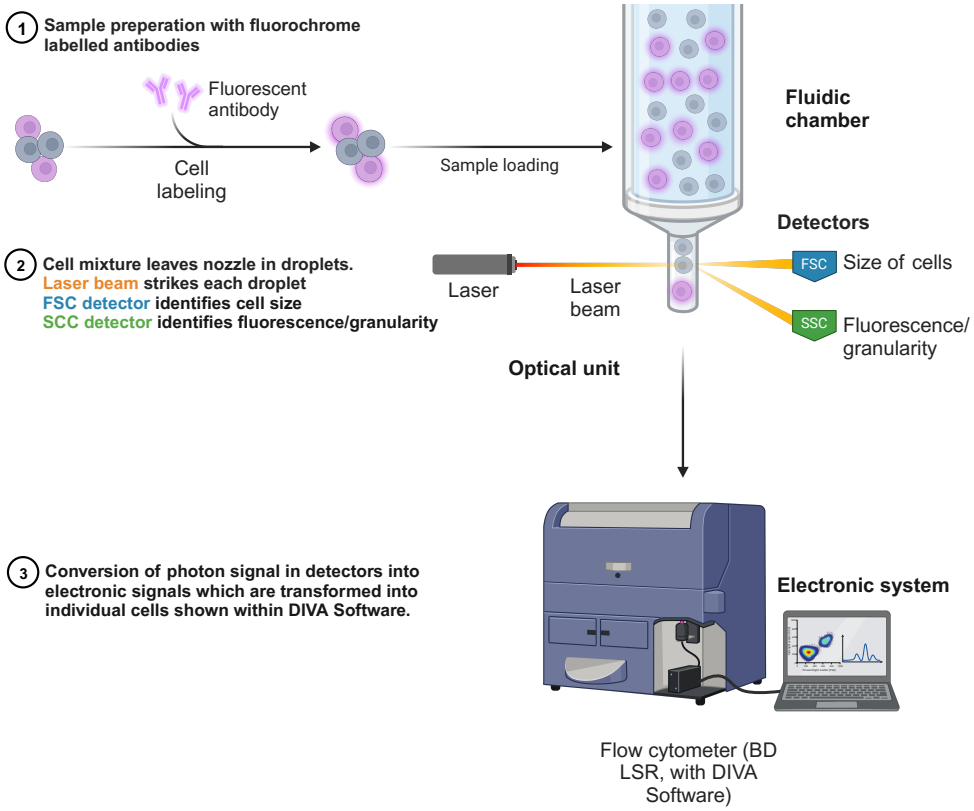

FIGURE 7.4: Overview of flow cytometer components. In the beginning samples are labelled with an antibody coupled with a fluorochrome before they are acquired in the fluidic chamber [32, 372]. The samples pass through the optical unit containing a laser and multiple filters, mirrors, and detectors. The detectors recognize photons and convert it into an electric current which gets transformed via the DIVA Software into a data point on the screen [32, 373, 374]. The figure was adapted from Austin Suthanthiraraj *et al.* and created with BioRender.com [375].

In the beginning of a measurement the biological sample be it a cell suspension or proteins or lipids coupled to metallic beads are injected into the fluidic chamber through a needle inlet [32]. A sheath fluid constantly running at the same pace through the flow cytometer focuses the sample hydrodynamically and dissects the cell and protein molecules from each other so that one molecule at a time moves through a laser beam [32, 376]. Typical sheath fluid speeds are 12 µL/min (low), 72 µL/min (medium) or 144 µL/min (high) [377]. For the experiments described the highest flow rate was used.

The optical unit consisting of multiple lasers, lenses, filters, and mirrors detect the light scattered by each molecule passing through the laser beam [32]. Thereby the laser beam gets scattered into a forward and a sidewards direction [32]. The forward scatter light (FSC) is proportional to the size of the object and the sideward scatter

light (SSC) is proportional to the object granularity or density passing through the laser beam [32, 378]. If the object passing through the laser beam is additionally labelled with a fluorochrome the electrons of the fluorochrome absorb energy at a specific wavelength and are therefore elevated to another energy level [32, 373]. Shortly after the electrons undergo relaxation into their original energy level emitting light at another wavelength which can be detected by the photodetectors after the emission light has gone through multiple filters and mirrors [32, 373].

After the photon detection the signal is converted into an electronic current which is then transformed by the electronic system through various algorithms into a visual dot in the flow cytometry software [32, 374]. Each dot thereby represents one event or object passing the laser beam. Due to delocalized electrons in aromatic systems every fluorochrome absorbs and emits light at an optimal excitation and emission wavelength but can also be excited at other wave lengths [32]. As a result, fluorochromes can emit light over the whole spectrum overlapping with each other and making a compensation with positive controls for each fluorochrome used in each experiment necessary [32, 373, 379].

7.7.2 Sample and compensation control preparation for flow cytometry

To allow for the data collection via flow cytometry the respective biological samples and structures of interest (antigens) need to be labelled with fluorescent dyes (fluorochromes). Within the field of immunology antibodies have emerged as particularly suitable tools to label biological samples as they are by default created to bind specifically to antigens and allow for the identification and localisation of surface or intracellular target structures [32, 373, 380]. Furthermore, antibodies are large enough to get tagged with fluorescent dyes without altering their chemical and biological proportions. Although antibodies attached to the target of interest might alter its biological properties [32, 381].

Target structures in a cellular context are often proteins and are referred to by an international catalogue the so-called cluster of differentiation (CD), with each protein having one unique identifier number: the CD number [382]. The usage of antibodies conjugated with a fluorochrome can therefore also be used to characterise cellular subsets phenotypically as well as functionally [32].

Biological samples can be labelled by using primary monoclonal antibodies (mabs) labelled with a fluorochrome directed against the CD structure of interest [32, 383]. If nonprimary antibody with fitting fluorochrome is available, it is also possible to use an unconjugated primary antibody targeted against the structure of interest [32, 384]. As the unlabelled primary antibody was created in another species than human e.g., mouse or rabbit a secondary antibody labelled with a fluorescent dye which is reactive against the species of the primary unlabelled antibody can be used to stain

the cells indirectly. The secondary mab must be created in another species than the primary mab e.g., in goat or donkey. As described by our laboratory before, the same approach was used for Fc fusion construct proteins used in this thesis as no primary labelled Fc of KIRs exist [207]. If target structures within a cell shall be stained the cells need to be fixed and permeabilised after the cell surface staining [32]. Usually, cells are fixed in paraformaldehyde (PFA) before being acquired on a flow cytometer [32].

In general, the biologicals samples are washed with PBS between staining steps to remove leftover antibodies and to prevent off-target signals [32, 385, 386]. However, background noise can still occur as some cell lines present Fc-gamma receptors (FcγRs) including CD16, CD32 and CD64 on the cell surface which in a cellular context bind to IgG covered particles for phagocytosis, but during experiments unspecifically bind the added primary or secondary antibodies [387]. Therefore, these receptors should be pre-blocked for 20 min using solutions like the Human TruStain FcX Fc blocking solution from BioLegend before initiating the staining protocol [388].

Another vital part of the staining procedure is to distinguish between cells which are dead or alive [32]. Usually this is done by adding a LIVE/DEAD marker e.g., LIVE/ DEAD Fixable Near-IR Dead Cell Kit or LIVE/DEAD Fixable Aqua Dead Cell Stain Kit (Thermo Fisher Scientific) into the master mix in a dilution of 1:1000 used for staining the biological sample [32, 389]. The kits use amine-reactive dyes with an excitation maximum of ~633 nm and ~405 nm [32, 389]. Dead cells with a disrupted cell membrane absorb the dye where it reacts with intracellular free amines coming from the break down and destruction of the DNA and on the cell surface, resulting in a bright fluorescent staining [32]. Viable cells do not take up the dye which then only reacts with cell surface amines with a low fluorescence [32].

Finally, compensation controls in the respective fluorochromes used within the experiments need to be prepared before the measurement [32, 373]. As mentioned before (subsection 7.7.1, page 132) fluorochromes do absorb and emit light at a broader range of wavelengths. These can be filtered with multiple pass filters but not all overlap can be removed. Henceforth, by just measuring the emission spectra and their overlap of the different fluorochromes an algorithm can calculate and reduce the background noise of a sample. For the compensation controls compensation beads are used which are species specific beads that bind fluorochrome conjugated antibodies [32, 390]. For preparation, a drop of beads was gently mixed with 0.5 - 1 µL of anti-body in a FACS tube and stored at 4 °C. Directly before usage, the bead/ antibody mixture was filled-up with 300 µL PBS [32].

7.7.3 Data collection and gating strategies

As previously described in the dissertation of Dr. Sarah Vollmers, samples labelled with fluorochromes allow the identification and comparison of homogeneous populations across samples [32, 391]. This is achieved by hierarchical gating strategies implemented in FACS DIVA software or FlowJo software [32]. Fluorescence minus one (FMO), unstained controls and positive controls for respective surface markers were used to define gates [32].

For all experiments, samples were acquired on a BD LSR Fortessa flow cytometer with five lasers for up to 18 different parameters (fluorochromes) in the core facility Fluorescence Cytometry at the Leibniz Institute of Virology (LIV) [32, 377]. An overview of the different fluorochrome acquirable at the flow cytometer and its different short and long pass filters are listed in Table 7.1 and core facility Fluorescence Cytometry at the Leibniz Institute of Virology (LIV) [377]. Long pass filters thereby reject wavelengths with a length lower than the selected cutoff frequency and let waves with longer wavelengths than the cutoff length pass while as low band pass filters reject wavelengths with a length higher than the selected cutoff frequency and let waves with shorter wavelengths than the cutoff length pass. The acquired samples were hierarchically gated to isolate and define homogeneous populations which were later analysed for their characteristics using the BD FlowJo software [32].

TABLE 7.1: Fluorochrome and laser overview of BD LSR Fortessa flow cytometer adapted from the core facility Fluorescence Cytometry at the Leibniz Institute of Virology (LIV) and Vollmers *et al.* [32, 377].

Detector Array	**Laser**	**Parameter**	**LP Filter**	**BP-Filter & Designated Channel**	**Fluorochrome**
Trigon	Ultraviolet 355 nm	1	690 LP	UV1 740/35	BUV563
		2		UV2 380/14	BUV395
Octagon	Violet 405 nm	3	750 LP	V1 780/60	BV785
		4	670 LP	V2 710/40	BV711
		5	635 LP	V3 675/50	BV650
		6	600 LP	V4 610/20	BV605
		7	570 LP	V5 586/15	-
		8	505 LP	V6 525/50	BV510, LD Aqua
		9		V7 450/50	BV421, Pacific-Blue

Table 7.1: Continued Fluorochrome and laser overview of BD LSR Fortessa flow cytometer adapted from the core facility Fluorescence Cytometry at the Leibniz Institute of Virology (LIV) and Vollmers *et al.* [32, 377].

Detector Array	**Laser**	**Parameter**	**LP Filter**	**BP-Filter & Designated Channel**	**Fluorochrome**
Octagon	Blue 488 nm	10	685 LP	B1 710/50	PerCP-Cy5.5
		11	505 LP	B2 530/30	AF488, FITC
		SSC		SSC	-
Octagon	Yellow-Green 561 nm	12	750 LP	YG1 780/60	PE-Vio770, PE-Cy7
		13	630 LP	YG2 670/30	PE-Cy5
		14	600 LP	YG3 610/20	PE-Vio615
		15		YG4 586/15	PE
Trigon	Red 633 nm	16	750 LP	R1 780/60	APC-Cy7, LD Near IR
		17	690 LP	R2 730/45	AF700
		18		R3 670/14	APC, AF647

7.8 Functional sssays

7.8.1 Implementation of the B7 protein KIR-Fc fusion construct protein screening

As previously described by our laboratory and the dissertation of Dr. Pia Fittje, the coated B7/HLA protein beads (subsection 7.6.2, page 132) were incubated with commercially available KIR-Fc fusion construct proteins as well as Fc fusion construct protein controls dissolved in PBS [90, 207]. A Fc fusion construct protein consists of the extracellular domains of the KIR receptor or desired control receptor fused to the Fc region of an IgG antibody [32, 90]. The IgG part can then be detected with a secondary anti-human IgG-FITC antibody, which binds to the Fc part of the fusion construct protein (Figure 7.5) [32, 90].

For the assay, the successful coating of the Dynabeads M-280 Streptavidin beads (Thermo Fisher Scientific) with the respective B7 proteins was proven by transferring

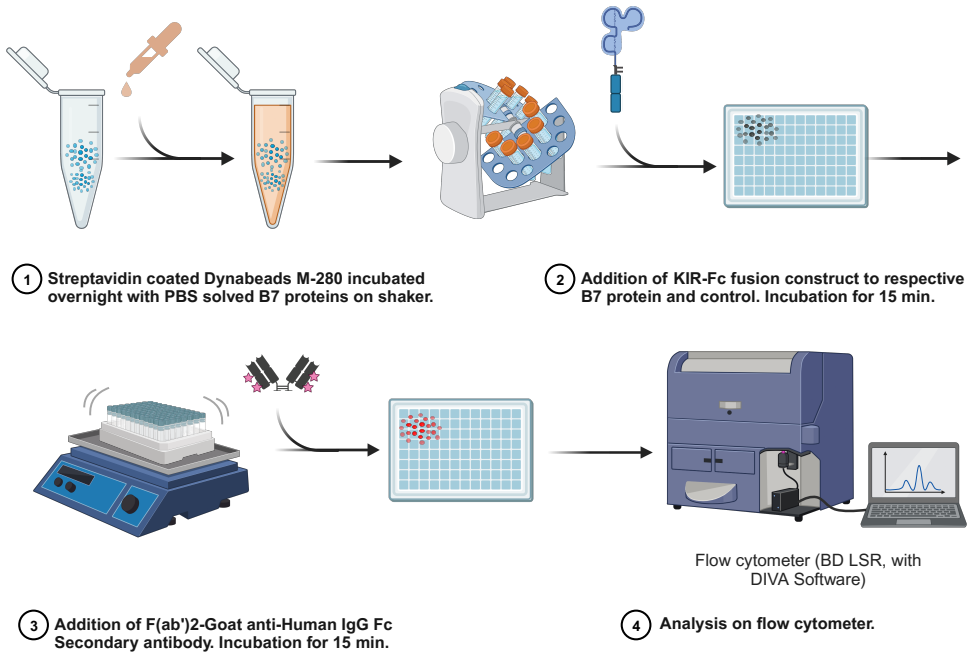

FIGURE 7.5: Bead Fc screening assay. As previously described, streptavidin coated Dynabeads were incubated with B7 proteins dissolved in PBS overnight at 4 °C under constant flipping [31, 90, 207]. The next day the beads were washed two times with 1 mL of cold PBS and placed in a Stemcell magnet to remove the supernatant [31, 90, 207]. KIR-Fc fusion construct protein and Fc fusion construct protein controls at a concentration of 31.25 µg/mL were added and incubated for 15 min under constant shaking of 150 rpm at 4 °C in the dark [31, 32, 90, 207]. After the incubation the beads were washed two times with autoMACS buffer before being incubated with F(ab')2-Goat anti-Human IgG Fc secondary antibody for 15 min under constant shaking of 150 rpm at 4 °C in the dark [31, 32, 90, 207]. After the incubation the beads were washed two times with autoMACS buffer before being resuspended and analysed on a BD LSR Fortessa flow cytometer [31, 32, 90, 207]. The figure was created with BioRender.com.

3 µL of beads coated with one of the B7 proteins into a 96-well plate and then incubating the beads with 1 µL of the mab targeted against the respective B7 protein for 30 min at 4 °C in the dark. As a negative control, beads coated only with biotin were incubated with the same monoclonal antibodies for 30 min at 4 °C in the dark [90, 207]. Next all beads were washed two times with autoMACS buffer for 3 min at 2000 g at 4 °C before being resuspended in 100 µL autoMACS buffer [90, 207].

Furthermore, the functionality of the Dynabeads M-280 Streptavidin beads (Thermo Fisher Scientific) coated with the respective B7 proteins was proven by transferring 10 µL of beads coated with one of the B7 proteins into a 96-well plate and then incubating the beads with 40 µL of a known binder Fc fusion construct protein (Table 6.10, page 115) at a concentration of 31.25 µg/mL for 15 min under constant shaking of 150 rpm at 4 °C in the dark [90, 207]. As a negative control, beads coated only with biotin were incubated with the same B7 binder Fc fusion construct protein for 15 min

under constant shaking of 150 rpm at 4 °C in the dark [90, 207]. After the incubation the beads were washed two times with autoMACS buffer for 3 min at 2000 *g* at 4 °C before being incubated with 50 µL of F(ab')2-Goat anti-Human IgG Fc secondary antibody PE (1:200) for 15 min under constant shaking of 150 rpm at 4 °C in the dark [31, 90, 207]. After the incubation the beads were washed two times with autoMACS buffer for 3 min at 2000 *g* at 4 °C before being resuspended in 100 µL autoMACS buffer [90, 207]. Finally, samples were transferred into cluster tubes and analysed at a BD LSR Fortessa flow cytometer [32].

To proof KIR-Fc fusion construct functionality and to screen for potential B7 protein interactions 40 µL of KIR-Fc fusion construct protein at a concentration of 31.25 µg/mL was incubated with 10 µL of tetramerized HLA receptors or 10 µL of B7 protein coated beads transferred into a 96-well plate for 15 min under constant shaking of 150 rpm at 4 °C in the dark [90, 207]. After the incubation the beads were washed two times with autoMACS buffer for 3 min at 2000 *g* at 4 °C before being incubated with 50 µL of F(ab')2-Goat anti-Human IgG Fc secondary antibody FITC (1:200) for 15 min under constant shaking of 150 rpm at 4 °C in the dark [31, 90, 207]. After the incubation the beads were washed two times with autoMACS buffer for 3 min at 2000 *g* at 4 °C before being resuspended in 100 µL autoMACS buffer [90, 207]. Finally, samples were transferred into cluster tubes and analysed at a BD LSR Fortessa flow cytometer [32].

7.8.2 Implementation of the *β*2m-KO-Jurkat KIR3DL2 & B7-H1 (PD-L1)-Fc and *β*2m-KO-Jurkat KIR3DL3 & B7-H7-Fc fusion construct protein binding assay

As previously described in the Dissertation by Dr. Sarah Vollmers, a cellular binding can be proved between B7-H1 (PD-L1) & KIR3DL2 and B7-H7 & KIR3DL3 via a B7-H1 (PD-L1)-Fc and B7-H7-Fc fusion construct protein binding assay [32, 207]. KIR3DL2 and KIR2DS4 transduced β2m-KO-Jurkat cell lines as well as plain β2m-KO-Jurkat cells were incubated with the B7-H1 (PD-L1)-Fc fusion construct protein. Separately, KIR3DL3, KIR3DL1 and KIR2DL5 transduced β2m-KO-Jurkat cell lines as well as plain β2m-KO-Jurkat cells were incubated with the B7-H7-Fc fusion construct protein (Figure 7.6).

The B7-H1 (PD-L1)-Fc and B7-H7-Fc fusion construct protein consist of the extracellular part of the B7-H1 (PD-L1) and B7-H7 receptor which binds to the KIR outer domain and the Fc region of an IgG antibody [32]. The IgG part can then be detected with a secondary anti-human IgG antibody, which binds to the Fc part of the fusion construct protein [32]. For the assay, cell lines were counted and washed with PBS staining buffer and for each condition 100,000 cells were transferred into a 96-well plate [32]. The plate was centrifuged for 5 min at 500 *g* at 4 °C and the supernatant was carefully discarded. Next, each condition was blocked following the manufactures protocol [388]. Briefly, the BioLegend TruStain FcX kit was added to the cells

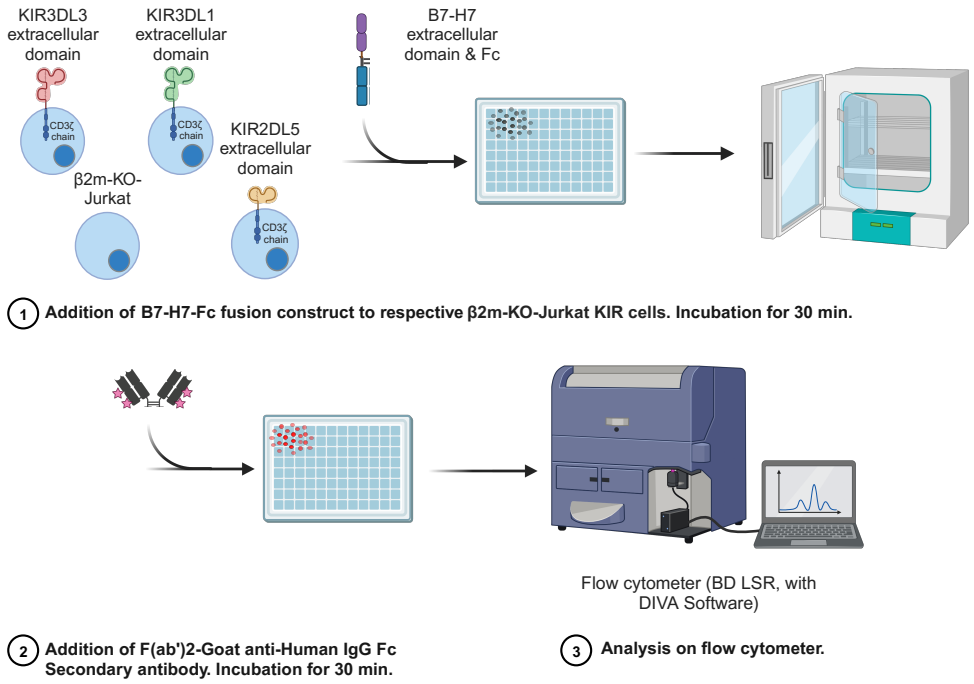

FIGURE 7.6: Fc fusion construct protein binding assay. Here shown for the KIR3DL3, KIR3DL1 and KIR2DL5 transduced β2m-KO-Jurkat cell lines as well as plain β2m-KO-Jurkat cells incubated with the B7-H7-Fc fusion construct protein consisting of the extracellular part of the B7-H7 receptor and the Fc region of an IgG antibody. The IgG part was detected with a secondary anti-human IgG antibody, which binds to the Fc part of the fusion construct protein [32]. After the incubation the cells were washed two times and fixed, before being resuspended and analysed on a BD LSR Fortessa flow cytometer [32]. The assay was performed analogously for the KIR3DL2 and KIR2DS4 transduced β2m-KO-Jurkat cell lines as well as plain β2m-KO-Jurkat cells incubated with the B7-H1 (PD-L1)-Fc fusion construct protein [32]. The figure was created with BioRender.com.

in a 1:25 dilution for 30 min at 4 °C before being two times with cold PBS staining buffer for 5 min at 500 g at 4 °C. Cells were resuspended in 25 µL B7-H1 (PD-L1)-Fc or B7-H7-Fc fusion construct protein in 25 µg/mL dissolved in PBS and incubated for 30 min at 4 °C [32]. After the incubation, the cells were washed two times with cold staining buffer for 5 min at 500 g at 4 °C and then stained for 30 min at 4 °C in the dark with 50 µL LIVE/DEAD Near-IR viably dye (1:1000), F(ab')2-Goat anti-human IgG Fc secondary antibody PE (1:200) for B7-H1 (PD-L1)-Fc fusion construct protein and F(ab')2-Goat anti-human IgG Fc secondary antibody FITC (1:200) for B7-H7-Fc fusion construct protein and the respective KIR antibodies in PE (1:25 - 1:100) or the FITC and PE isotype controls [31, 32, 90, 389]. After the incubation the conditions were washed two times with PBS staining buffer for 5 min at 500 g at 4 °C and the supernatant discarded. Finally, all cell lines were resuspended in 100 µL 4 % PFA and transferred into cluster tubes and analysed at a BD LSR Fortessa flow cytometer [32].

Besides the B7-H7-Fc fusion construct protein incubation, all cell lines were stained

only with the F(ab')2-Goat anti-human IgG Fc secondary antibody FITC, without previous fusion construct protein labelling. In the B7-H1 (PD-L1)-Fc fusion construct protein incubation, all cell lines were stained only with the F(ab')2-Goat anti-human IgG Fc secondary antibody PE, without previous fusion construct protein labelling. The samples incubated with plain F(ab')2-Goat anti-human IgG were used to determine unspecific binding of the antibody [31, 32, 90]. Furthermore, all cell lines were incubated only with the B7-H1 (PD-L1)-Fc and B7-H7-Fc fusion construct without a secondary mab to prove no background noise was present from the Fc fusion construct protein alone. As described before, all cells were also stained for their respective KIR receptor to prove the KIR expression on the transduced cell lines [32].

7.8.3 Implementation of the β2m-KO-Jurkat KIR3DL3 B7-H7 protein reporter cell assay

As pointed out by Dr. Sarah Vollmers dissertation, a physiological binding can be shown via the incubation of KIR and its ligand [32]. Here done with the KIR3DL3 receptor and the B7-H7 protein, whose binding affinity was assessed in an assay, previously described by our laboratory [90]. The B7-H7 protein was coated to a 96-well plate and the β2m-KO-Jurkat cells untransduced and transduced with KIR3DL3-CD3ζ, KIR3DL1-CD3ζ and KIR2DL5-CD3ζ constructs as reporter cells (effector cells) added [32, 207]. As depicted in Figure 7.7, binding and activation of the respective KIR receptor fused to the CD3ζ chain triggers the recruitment of adapter proteins like ZAP-70 or Fyn which activate the RAS-RAF-ERK pathway or PIP2-PKC-NF-κB pathway which lead to an upregulation of CD69 expression on the cell surface [32, 188].

One day before the incubation of the cells and proteins a sterile non-tissue culture-treated flat-bottom 96-well plate was coated with plain PBS as negative control and purified unlabelled mab targeted against the respective KIR epitope of each reporter cell line in a concentration 5 µg/mL as a positive control (Figure 7.8). Additionally, wells for each reporter cell lines / condition were coated with the biotinylated B7-H7 protein provided by Sino Biological Inc. at a concentration of 10 µg/mL.

The plate was placed on a shaker at 100 rpm at 4 °C and incubated overnight. The next day the plate was two times with cold PBS staining buffer for 5 min at 500 g at 4 °C and the supernatant discarded. Next the β2m-KO-Jurkat reporter cells were counted with the T20 Cell counter (Bio-Rad), washed with PBS staining buffer, and resuspended at a concentration of 2.5×10^6 cells/mL in cultivation medium [32]. For the assay, 100 µL of Jurkat reporter cells (250,000 cells/well) were added to the pre-coated 96-well plate and incubated for 5 h at 37 °C and 5 % ppm CO_2 [32]. After the incubation time the cells were transferred into a conical shaped 96-well plate spun for 5 min at 500 g at 4 °C and the supernatant discarded [32]. Next each condition was blocked using the BioLegend TruStain kit with 1:25 dilution for 30 min at 4 °C before being two times with cold PBS staining buffer for 500 g at 4 °C. The cells were

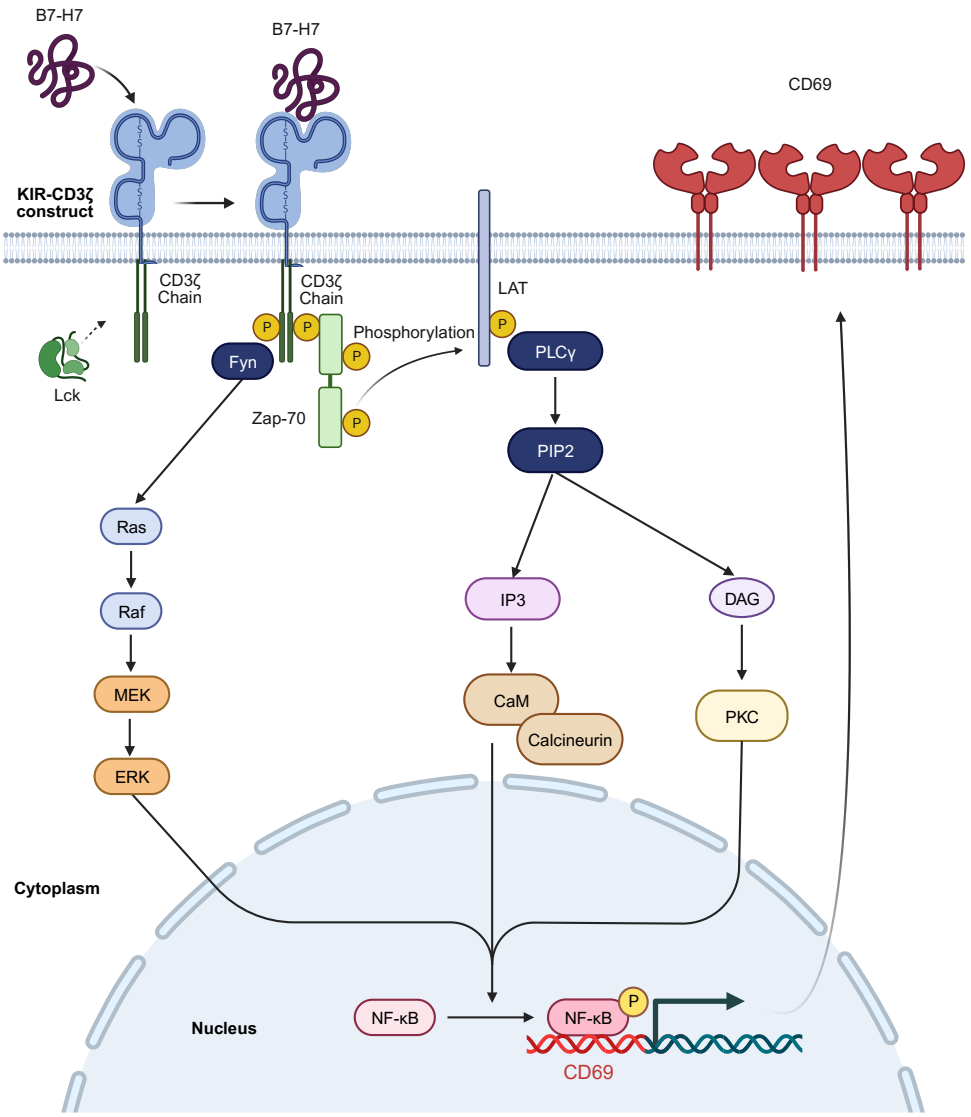

FIGURE 7.7: CD3ζ-CD69 pathway. Upon binding of the ligand to KIR fused to the CD3ζ chain LcK gets recruited and phosphorylates the CD3ζ chain. Afterwards adapter proteins like ZAP-70 or Fyn are recruited which activate the RAS-RAF-ERK pathway or PIP2-PKC-NF-κB pathway which lead to an upregulation of CD69 expression on the cell surface. The figure was adapted from Janeway *et al.*, Paulsen *et al.* and created with BioRender.com [48, 188].

then resuspended in 50 µL antibody mix with CD3-BUV395 (1:100), CD69-BV421 (1:100) or BV421 isotype control, KIR-PE (1:25 – 1:100) and LIVE/DEAD Near-IR viability dye (1:1000) in PBS staining buffer and incubated for 30 min at 4 °C in the dark [32]. Cells were then two times with staining buffer for 5 min at 500 *g* at 4 °C before they were resuspended in 100 µL of 4 % PFA and transferred to cluster tubes for further flow cytometry analysis on a BD LSR Fortessa [32]. Similar as before the following controls were used: KIR receptor staining to determin the KIR expression of the transduced cell lines, isotype controls for CD69 read out and an untransduced β2m-KO-Jurkat cell line [32].

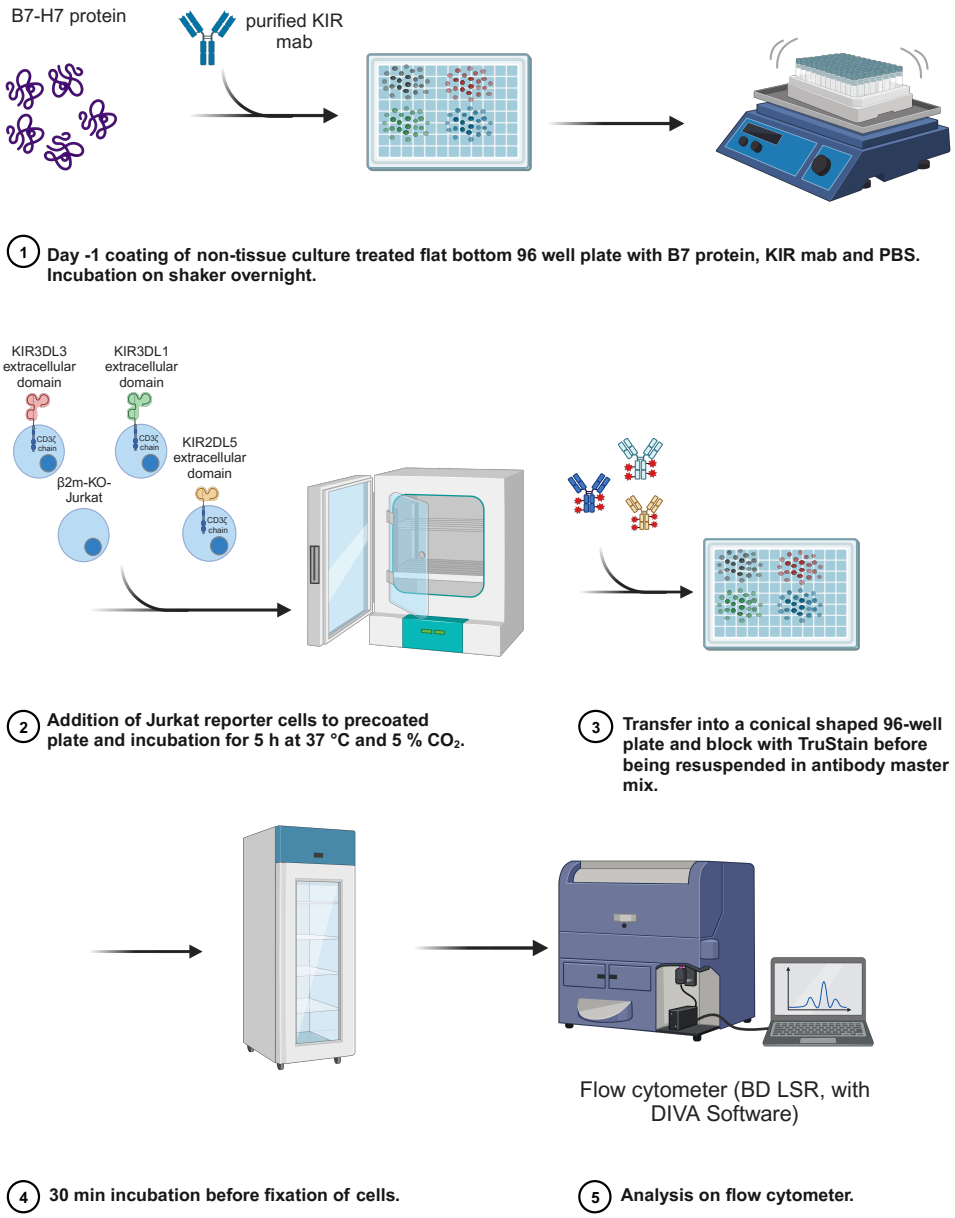

FIGURE 7.8: Jurkat reporter cell assay. One day before experimenting non-tissue culture-treated flat-bottom 96-well plate was coated with plain PBS, purified unlabelled mab and B7-H7 protein overnight [90, 207]. The next day β2m-KO-Jurkat reporter cells were counted, washed, and added to the pre-coated plate before being incubated for 5 h at 37 °C and 5 % ppm CO_2 [32, 90]. After the incubation time the cells were transferred into a conical shaped 96-well plate pre-blocked using the BioLegend TruStain FcX kit [388]. Next, cells were washed two times and stained in antibody master mix [32, 90]. After the incubation the cells were washed two times and fixed, before being resuspended and analysed on a BD LSR Fortessa flow cytometer [32, 90]. The figure was created with BioRender.com.

7.8.4 Implementation of the NK cell killing assay and its inhibition

In the next step, the physiological relevance of the KIR3DL3 & B7-H7 interaction was demonstrated with an NK cell killing assay as previously described [392]. In short

NK cells constantly screen their surrounding for foreign or human receptors and can get activated when they notice the missing of human receptors ("missing-self") or recognize a foreign receptor which might pose a threat [99, 100]. Upon activation they can degranulate and kill the surrounding cells via granzyme B pathways which integrate perforin into the cell membrane [105, 106]. Here the KIR3DL3 expressing cell line NK-92MI (effector cells) were co-incubated with K562 cells and B7-H7 transduced K562.B7-H7 cells (target cells) in the effector to target ratios (E:T) of 5:1, 3:1, 1:1, 1:3 and 1:5 with one unit representing 100,000 cells (Figure 7.9).

The K562, K562.B7-H7 and NK-92MI cells were counted, washed with PBS staining buffer for 5 min at 500 *g* at RT and resuspended at 2.5×10^6 cells/mL. Next, the cells from the NK-92MI cell line and some cells of the K562 and K562.B7-H7 cell line were set aside as an unstained control for later measurements. The remaining K562 and K562.B7-H7 cells were labelled with 1 µL/mL CellTrace dyes (K562 violet, K562.B7-H7 CFSE) (Thermo Fisher Scientific) 20 min at 37 °C in the dark according to protocol [393]. Afterwards, the cells were washed two times with R10 for 5 min at 500 *g* at RT and all cells resuspended in R10 concentration of at 1.5×10^7 cells/mL. Next, the cells were counted twice with the TC20 cell counter (Bio-Rad) before being diluted to a final concentration of 1.0×10^7 cells/mL. The labelled K562, K562.B7-H7 and unlabelled NK-92MI cells were mixed in a 96-well plate (plate 1) according to the E:T ratios of 5:1, 3:1, 1:1, 1:3 and 1:5. Additionally, one 1:1 mixture of K562 and K562.B7-H7 cells was prepared and plated without any NK-92MI cells. This mixture is used as a killing reference to see how the ratio of K562 and K562.B7-H7 cells look like after 2 h of incubation. In a separate 96-well plate (plate 2) unstained controls were distributed and both plates were briefly spun down for 2 min at 300 *g* at RT. The plates were then incubated for 2 h at 37 °C and 5 % ppm CO_2. Afterwards cells from both plates were fixed for 30 min with 4 % PFA at 4 °C without washing to not loose cells.

Next, cells pipetted in a separate plate (plate 2) for control purposes were washed two times with PBS staining buffer for 5 min at 500 *g* at 4 °C before being resuspended in 50 µL of KIR3DL3-unconjugated (10 µg/mL) antibody. Cells were incubated for 30 min at 4 °C in the dark before being washed two times with PBS staining buffer for 5 min at 500 *g* at 4 °C. Next, cells were resuspended in 50 µL of anti-rabbit AF546 (1:500) and incubated for 30 min at 4 °C in the dark, before being two times with PBS staining buffer for 5 min at 500 *g* at 4 °C. In the next step, wells in both plates got 50 µL of antibody mix added with CD3-BUV737 (1:100), CD56-BUV395 (1:100), B7-H7-Pe-Cy7 (1:25), CD16-BV785 (1:100) and LIVE/DEAD Near-IR viability dye (1:1000) in PBS and incubated for 30 min at 4 °C in the dark. Afterwards, cells in both plates were washed once with PBS staining buffer for 5 min at 500 *g* at 4 °C and the cells resuspended in 100 µL before being measured at the BD LSR Fortessa flow cytometer. The following controls were measured with the samples: unlabelled K562 and K562.B7-H7 cells, K562 and K562.B7-H7 cells stained for B7-H7 to determine

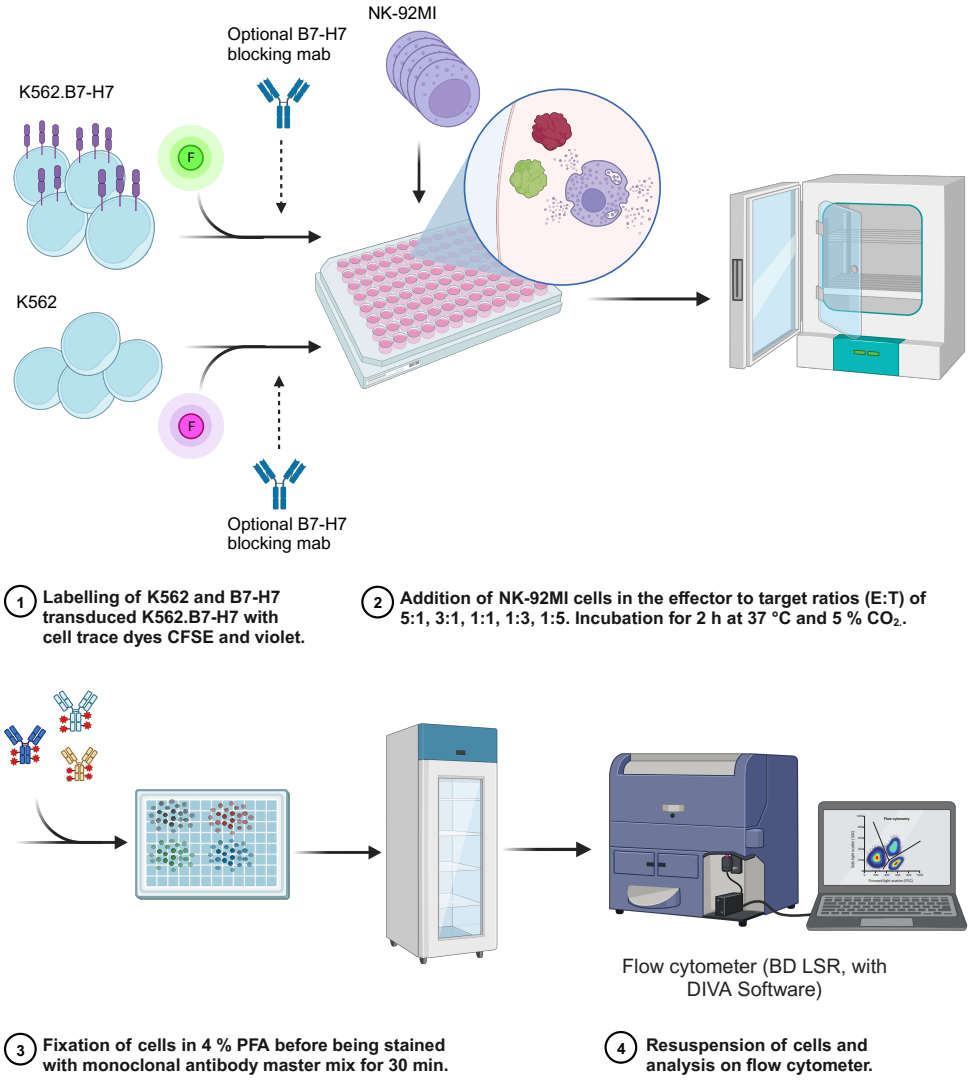

FIGURE 7.9: Workflow of killing assay and its inhibition. As previously described, K562 and K562.B7-H7 cells (target cells) were labelled with CellTrace dyes and co-incubated for 2 h at 37 °C and 5 % ppm CO_2 with KIR3DL3 expressing cell line NK-92MI (effector cells) in the effector to target ratios (E:T) of 5:1, 3:1, 1:1, 1:3 and 1:5 [392]. Afterwards cells from both plates were fixed for 30 min with 4 % PFA at 4 °C without washing to not loose cells. Next, cells were stained with an antibody master mix before being and measured at the BD LSR Fortessa flow cytometer. To proof specificity of the KIR3DL3 B7-H7 interaction the experiment was repeated with both K562 and K562.B7-H7 cells being incubated with B7-H7 blocking antibody during the labelling and incubation process. The figure was created with BioRender.com.

the expression level as well as NK-92MI cells for the KIR3DL3 expression, AF546 only controls for the NK-92MI cells as secondary antibody control and the respective isotype controls of PE-Cy7, AF546, FITC and BV421.

To proof specificity of the KIR3DL3 B7-H7 interaction and that the K562 cells were susceptible to killing the experiment was prepared in parallel in the same setup with

both K562 and K562.B7-H7 cells being incubated with B7-H7 blocking antibody (50 µg/mL) during the labelling and incubation process. In theory the blocking should reverse the reduced killing activity of NK-92MI cells towards K562.B7-H7 through the KIR3DL3 B7-H7 axis, thereby also proving killing susceptibility of the K562 and K562.B7-H7 cells.

7.8.5 Implementation of the KIR3DL3 and B7-H7 screen in cell systems

After a physiological functionality of the KIR3DL3 B7-H7 interaction was demonstrated, the next step was to search the human system for physiological compartments, in which cell types presenting KIR3DL3 or B7-H7 or both were present. Given that Bhatt *et al.* reported the expression of KIR3DL3 on NK cells and Palmer *et al.* on $\gamma\delta$ T cells, CD4 and CD8 T cells specifically also within small intestine the first approach was to screen PBMCs isolated from whole blood of the healthy cohort and within intraepithelial layer (IEL) derived from small intestine [11, 17]. Furthermore, the expression pattern of KIR3DL3 on NK cells isolated from PBMCs were checked for co-expression of other well-known NK cell receptors such as NKp30 to 46 and diverse NKG2A-D receptors. For B7-H7, PBMCs from whole blood were screened as well as IEL cells derived from small intestine as Zhao *et al.*, Wei *et al.* and Li *et al.* did report overexpression of B7-H7 in intestinal cancers and on B cells and monocytes/macrophages [18, 19, 394].

In short, PBMCs and IEL were isolated as described before (subsection 7.3.1, page 123 and subsection 7.3.7, page 126). Next, the PBMCs, IELs cells as well as the control cell lines of K562.B7-H7 and β2m-KO-Jurkat KIR3DL3 were counted, washed with PBS staining buffer, and resuspended at a concentration of 1×10^7 cells/mL in PBS staining buffer [32]. For the staining, 100 µL of cells (1×10^6 cells/well) were distributed over a 96-well plate. The 96-well plate was spun for 5 min at 500 *g* at 4 °C and the supernatant discarded. Next each well was blocked using the BioLegend TruStain FcX kit with 1:25 dilution for 30 min at 4 °C before being two times with cold PBS staining buffer for 500 *g* at 4 °C [388]. The cells were then resuspended in 50 µL antibody mix with the following panels: For $\gamma\delta$, CD4, and CD8 T cells from PBMCs 1) CD3-BUV395 (1:100), CD4-PE-Cy5 (1:100), CD8-FITC (1:100), CD16-BV785 (1:100), CD56-BV510 (1:100), KIR3DL3-PE (1:25) and LIVE/DEAD Near-IR viability dye (1:1000); for monocytes/macrophages and B cells from PBMCs 2) CD3-BUV395 (1:100), CD14-BV711 (1:100), CD20-BV421, B7-H7-FITC (1:100), LIVE/DEAD Near-IR viability dye (1:1000); for NK cells from PBMCs 3) CD3-BUV395 (1:100), CD16-BV785 (1:100), CD19-APC-Cy7 (1:100), CD20-APC-Cy7 (1:100), CD56-BV421 (1:100), NKG2A-PE-Cy7 (1:100), NKG2C-AF700 (1:100), NKG2D-BV510 (1:100), KIR3DL3-PE (1:25), NKp30- APC (1:100), NKp44-BUV737 (1:100), NKp46-FITC (1:100), and LIVE/DEAD Near-IR viability dye (1:1000); and for IELs

4) CD3-BUV737 (1:100), CD4-BV650 (1:200), CD8-PerCP-Cy5.5 (1:100), CD14-PE-Cy7 (1:100), Epcam-BV510 (1:100), CD16- BUV785 (1:100), CD19-APC-Cy7 (1:100), CD20-APC-Cy7 (1:100), CD56-BUV395 (1:100), B7-H7-AF488 (1:25), KIR3DL3-PE (1:25) and LIVE /DEAD Near-IR viability dye (1:1000). Additionally, the respective isotype controls of PE, PE-Cy7, AF488 and APC were incubated for 30 min at 4 °C in the dark. Cells were then two times with staining buffer for 5 min at 500 *g* at 4 °C before being fixed in 100 µL of 4 % PFA and being analysed on a BD LSR Fortessa.

NK cells from PBMCs were cultured for 7 days and were stained for KIR3DL3 and NK cell receptor expression on day 0 (day of isolation), day 3 and day 7.

7.9 Data analysis

7.9.1 General procedures

Data generated by flow cytometry were analysed with the software FlowJo 10.8.2 from BD Biosciences. As described before (subsection 7.7.1, page 132), biological samples labelled with fluorochromes allow for identification and comparison of homogeneous populations across samples through hierarchical gating strategies [32]. Fluorescence minus one (FMO), isotype controls, positive controls and unstained controls were used as gating controls [32]. In the following sub-chapters, the different read-outs and gating strategies of the different functional assays will be presented.

7.9.2 Read-out B7 protein KIR-Fc fusion construct protein screening

The Dynabeads M-280 Streptavidin (Thermo Fisher Scientific) coated with the respective B7 proteins (Sino Biological Inc.) and HLA receptors (NIH Tetramer core facility) incubated with the KIR-Fc fusion construct proteins (R&D Systems), Fc fusion construct protein controls (R&D Systems) and respective B7 antibodies were gated according to the scheme presented in Figure 7.10. The median fluorescence intensity (MdFI) for the read-out gates was exported using the FlowJo software. The raw data were then statistically analysed using R Studio and visualised using GraphPad Prism (subsection 7.10.3, page 159).

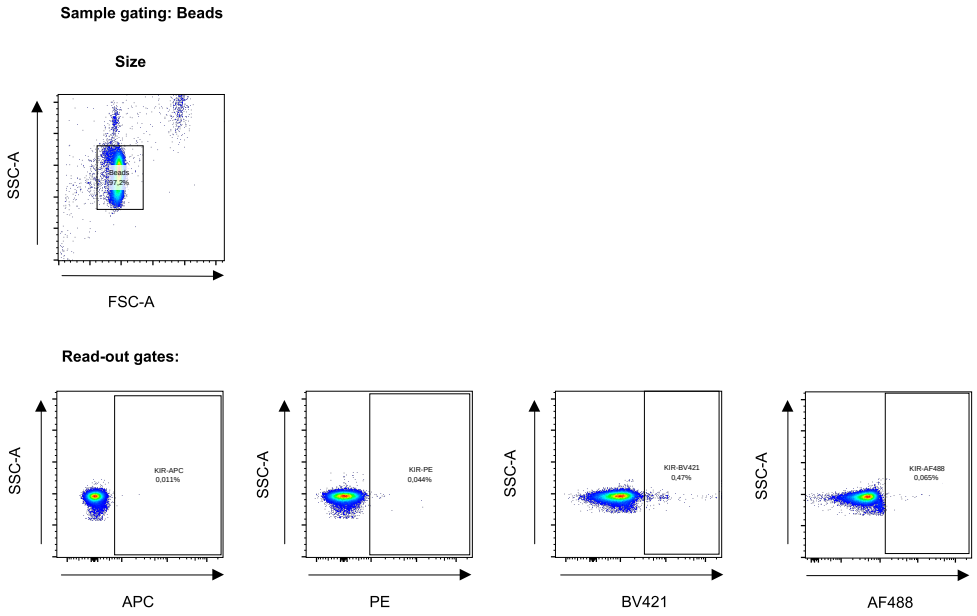

FIGURE 7.10: Gating strategy for Dynabeads M-280 Streptavidin (Thermo Fisher Scientific) coated with the respective B7 proteins (Sino Biological Inc.) and HLA receptors (NIH Tetramer core facility) incubated with the KIR-Fc fusion construct proteins (R&D Systems), Fc fusion construct protein controls (R&D Systems) and respective B7 antibodies. First, beads were gated to their size before gates for respective proteins and Fc fusion construct proteins were set with the FMO controls.

7.9.3 Read-out β2m-KO-Jurkat KIR3DL2 and B7-H1-Fc fusion construct protein binding assay

The β2m-KO-Jurkat reporter cells expressing KIR3DL2, KIR2DS4 or the untransduced version stained for KIR expression or stained with B7-H1 (PD-L1)-Fc fusion construct protein were gated according to the scheme presented in Figure 7.11. The median fluorescence intensity (MdFI) for the read-out gates was exported using the FlowJo software. The raw data were then statistically analysed using R Studio and visualised using GraphPad Prism (subsection 7.10.4, page 160).

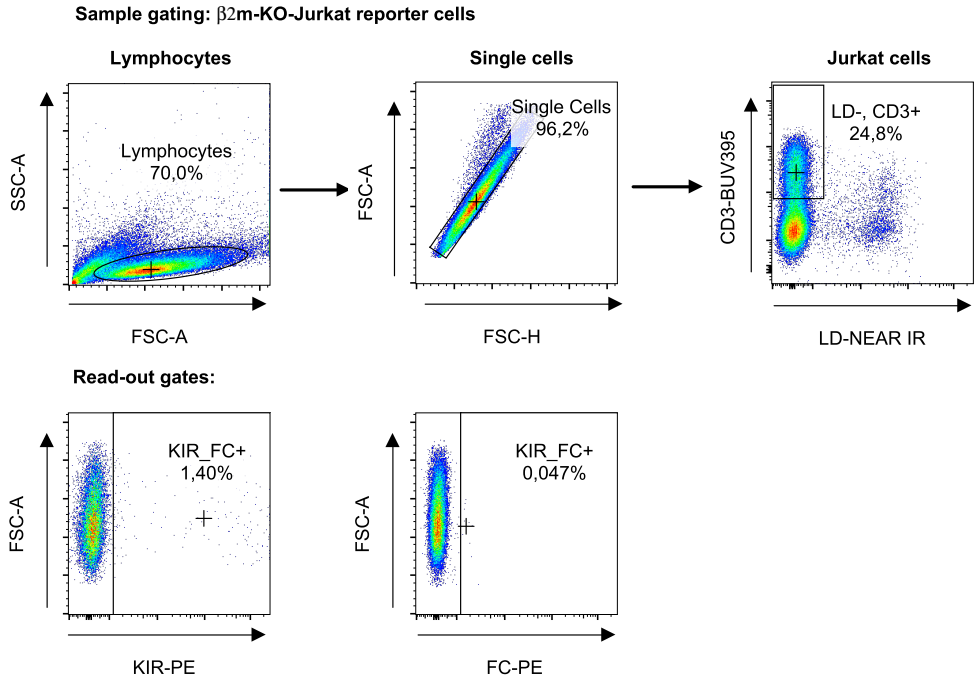

FIGURE 7.11: Gating strategy for β2m-KO-Jurkat reporter cells KIR3DL2, KIR2DS4 or the untransduced version stained stained for KIR expression or with B7-H1 (PD-L1)-Fc fusion construct protein. Here shown as an example for the untransduced β2m-KO-Jurkat reporter cells. First, cells were gated to their size, then duplets were removed, before only living cells were considered and gated for CD3 expression. Next, gates for B7-H1 (PD-L1)-Fc fusion construct proteins and KIR expression were set with the FMO controls.

7.9.4 Read-out β2m-KO-Jurkat KIR3DL3 and B7-H7-Fc fusion construct protein binding assay

The KIR3DL3 transduced β2m-KO-Jurkat reporter cell was assessed for their expression of KIR3DL3 according to the gating strategy presented in Figure 7.12. The frequency of parents expressing the KIR3DL3 receptor was exported from the read-out gates using the FlowJo software.

The β2m-KO-Jurkat reporter cells expressing KIR3DL3, KIR3DL1, KIR2DL5 or the untransduced version stained with B7-H7-Fc fusion construct protein were gated according to the scheme presented in Figure 7.13. The median fluorescence intensity (MdFI) for the read-out gates was exported using the FlowJo software. The raw data were then statistically analysed using R Studio and visualised using GraphPad Prism (subsection 7.10.5, page 161).

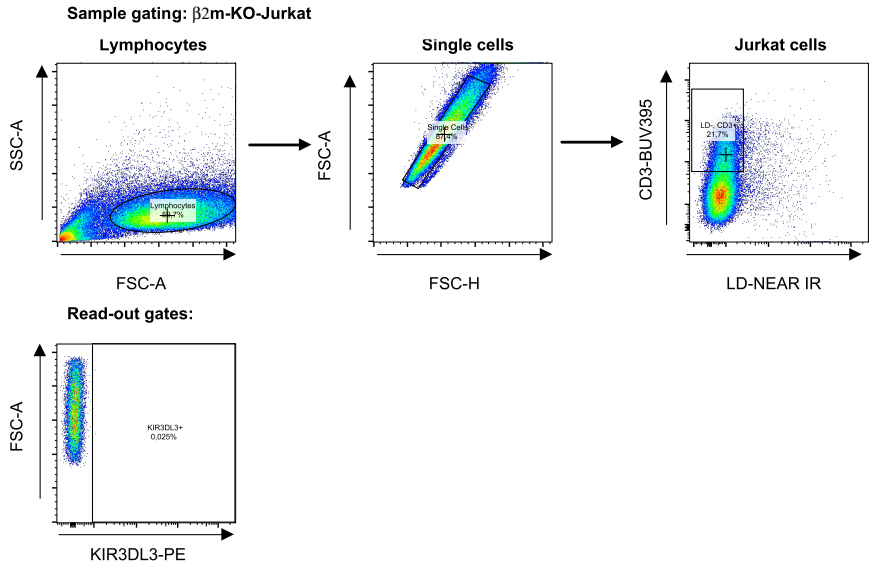

FIGURE 7.12: Gating strategy KIR3DL3 expression β2m-KO-Jurkat reporter cell line. Here shown as an example for the untransduced β2m-KO-Jurkat reporter cells. First, cells were gated to their size, then duplets were removed, before only living cells were considered and gated for CD3 expression. Next, gates for KIR3DL3 expression were set with the FMO control.

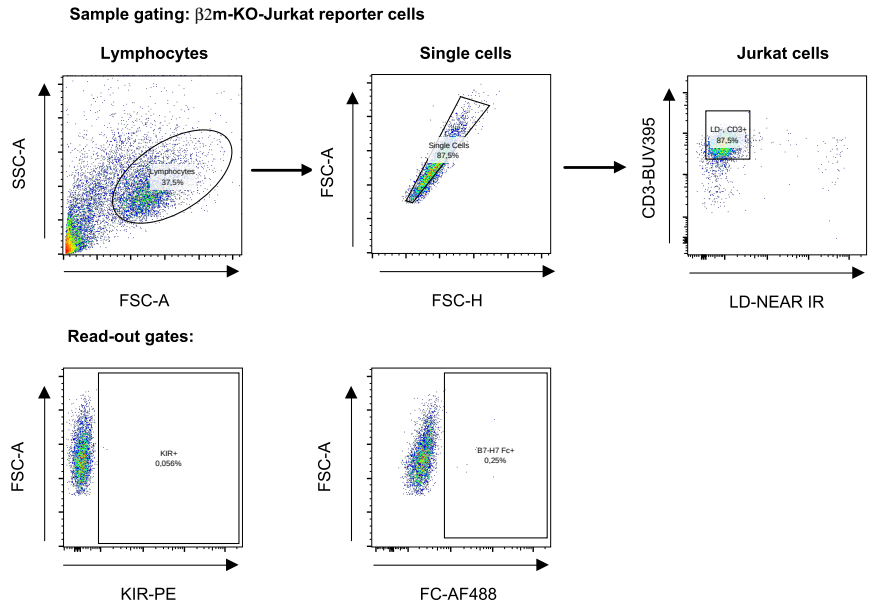

FIGURE 7.13: Gating strategy for β2m-KO-Jurkat reporter cells expressing KIR3DL3, KIR3DL1, KIR2DL5 or the untransduced version stained with B7-H7-Fc fusion construct protein. Here shown as an example for the untransduced β2m-KO-Jurkat reporter cells. First, cells were gated to their size, then duplets were removed, before only living cells were considered and gated for CD3 expression. Next, gates for KIR-Fc fusion construct proteins and KIR3DL3 expression were set with the FMO controls.

7.9.5 Read-out β2m-KO-Jurkat KIR3DL3 B7-H7 protein reporter cell assay

The β2m-KO-Jurkat reporter cells expressing KIR3DL3, KIR3DL1, KIR2DL5 or the untransduced version stimulated with B7-H7 protein were gated according to the scheme presented in Figure 7.14. The median fluorescence intensity (MdFI) for the read-out gates was exported using the FlowJo software. The raw data were then statistically analysed using R Studio and visualised using GraphPad Prism (subsection 7.10.6, page 162).

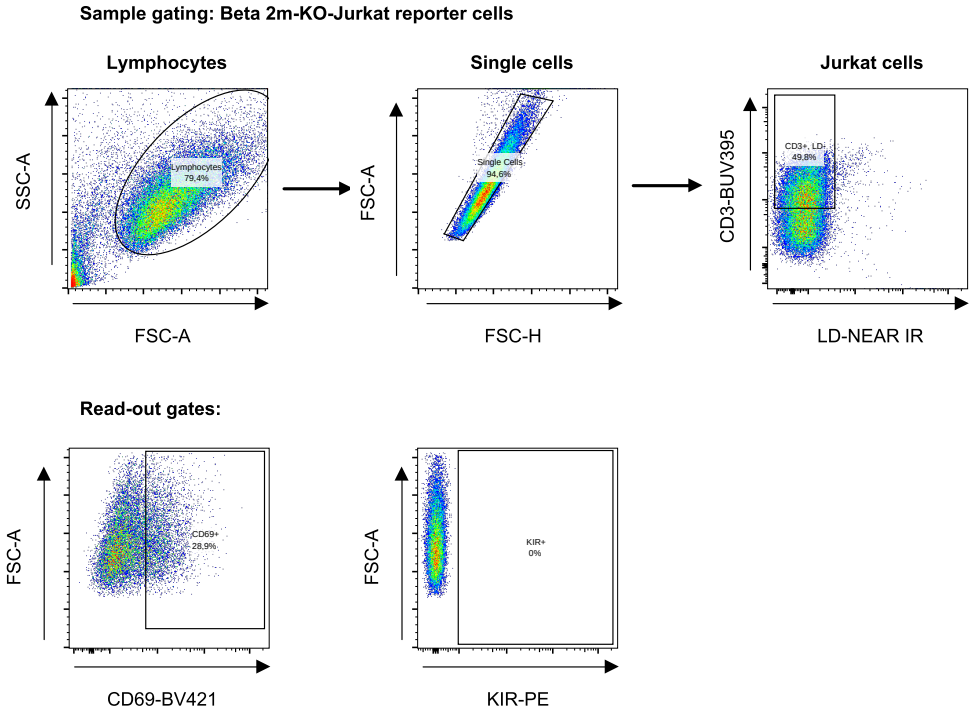

FIGURE 7.14: Gating strategy for β2m-KO-Jurkat reporter cells expressing KIR3DL3, KIR3DL1, KIR2DL5 or the untransduced version stimulated with B7-H7 protein. Here shown as an example for the untransduced β2m-KO-Jurkat reporter cells. First, cells were gated to their size, then duplets removed, before only living cells were considered and gated for CD3 expression. Next, gates for CD69 and KIR expression were set with the isotype controls.

7.9.6 Read-out NK cell killing assay and its inhibition

Untransduced labelled K562 and B7-H7 transduced labelled K562.B7-H7 cells incubated with NK-92MI were gated according to the scheme presented in Figure 7.15. The frequencies of NK-92MI, K562 and K562.B7-H7 from the whole population of living cells were exported using FlowJo software.

In the next step the ratio of K562 to K562.B7-H7 for all conditions and replicates was calculated in Excel according to Equation 7.1.

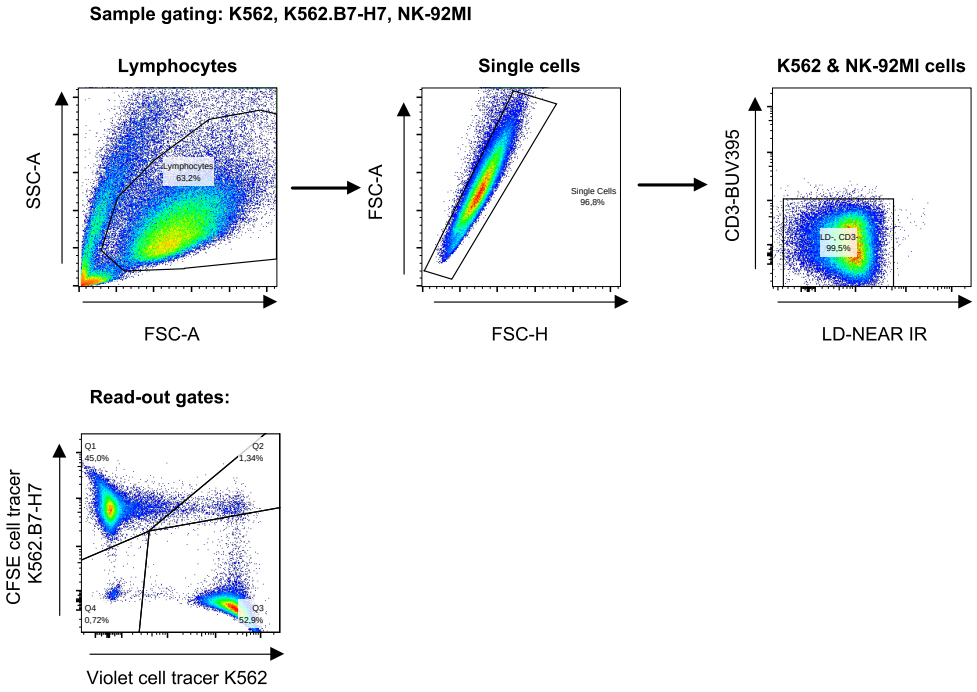

FIGURE 7.15: Gating strategy for K562, K562.B7-H7 and NK-92MI cells. Here shown as an example for the 1:1 mixture of labelled K562 and K562.B7-H7 without NK-92MI. First, cells were gated to their size, then duplets were removed, before only living cells were considered and gated for missing CD3 expression. Next, gates for K562 cells positive for the violet cell tracer, K562.B7-H7 cells positive for the CFSE cell tracer and the NK-92MI cells negative for both tracers were set with the respective labelled controls.

$$Ratio\ K562/K562.B7-H7 = \frac{Frequency\ of\ Parent\ from\ living\ cells_{K562}}{Frequency\ of\ Parent\ from\ living\ cells_{K562.B7-H7}} \tag{7.1}$$

After the ratio K562/K562.B7-H7 calculation the arithmetic mean of the ratios K562/ K562.B7-H7 for the cells which were labelled and incubated in a 1:1 mixture without NK-92MI cells was calculated (Equation 7.2). This mean calculated for each biological triplicate was used for normalisation purposes (Equation 7.3) as growth dynamics differed between the biological replications.

$$\bar{x} = \frac{1}{n}\sum_{i=1}^{n} x_i \tag{7.2}$$

With $\bar{x}$ as the mean, x_i as the ith observation and n as total of observations made.

$$Ratio\ K562/K562.B7-H7_{normalised} = \frac{Ratio\ K562/K562.B7-H7_{with\ NK-92MI}}{Mean\ Ratio\ K562/K562.B7-H7_{1:1\ mixture\ without\ NK-92MI}} \tag{7.3}$$

The normalised data were then statistically analysed using R Studio and visualised using GraphPad Prism (subsection 7.10.7, page 163).

7.9.7 Read-out KIR3DL3 and B7-H7 screen in cell systems

PBMCs stained for B7-H7 on monocytes/macrophages and B cells were gated according to the scheme presented in Figure 7.16. NK cells from PBMCs stained for KIR3DL3 and other NK cell receptors were gated according to the scheme presented in Figure 7.17. PBMCs stained for KIR3DL3 on $\gamma\delta$-, CD4 and CD8 T cells were gated according to the scheme presented in Figure 7.18. IEL samples stained for KIR3DL3, B7-H7 were gated according to the scheme presented in Figure 7.19.

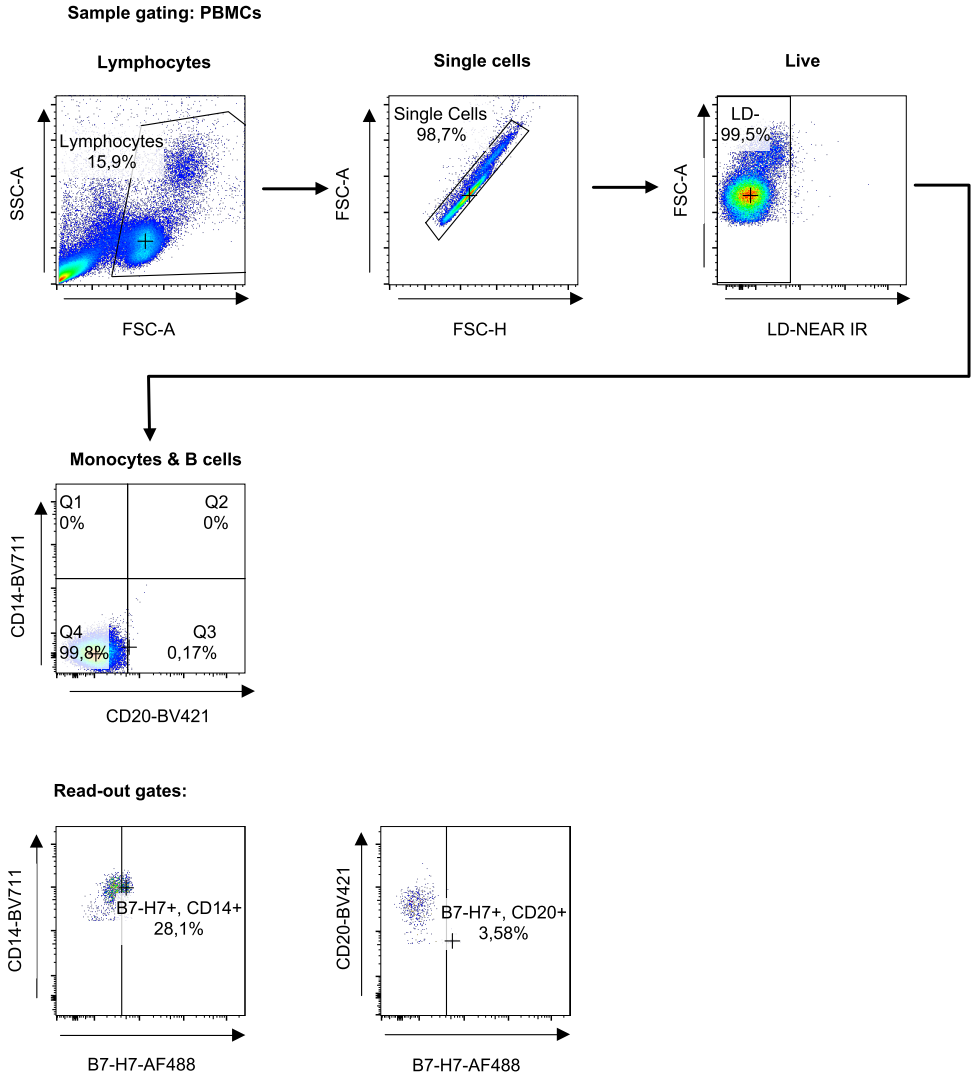

FIGURE 7.16: Gating scheme for B7-H7 on monocytes/macrophages and B cells from PBMCs. Here shown as an example for one triplicate of one donor. First, cells were gated to their size, then duplets were removed, before only living cells were considered and gated for CD14 and CD20 expression. Next, gate for B7-H7 was set with the respective FMO controls.

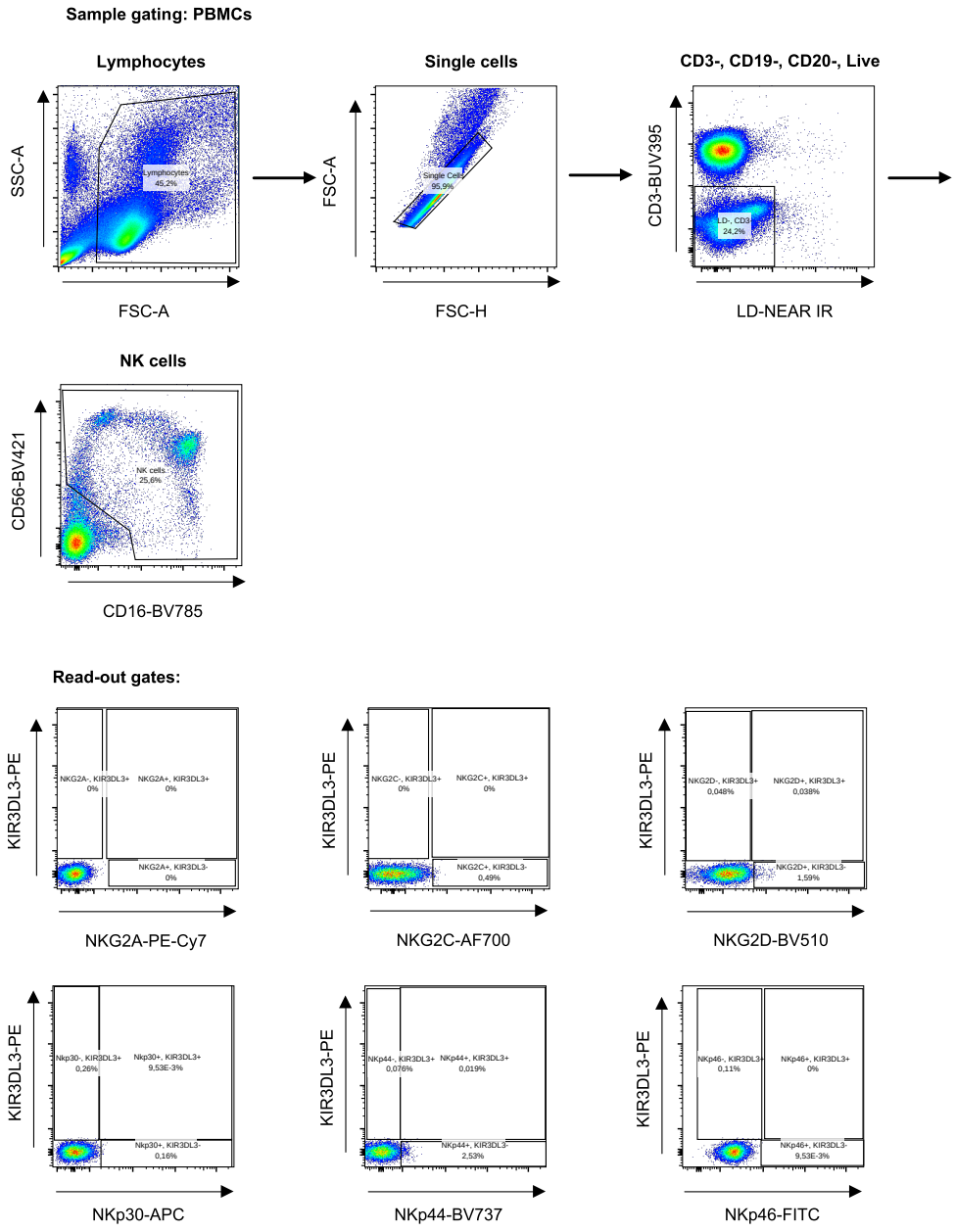

FIGURE 7.17: Gating scheme for KIR3DL3 on NK cells from PBMCs. Here shown as an example for one triplicate of one donor on day 0. First, cells were gated to their size, then duplets were removed, before only living cells, negative for CD19 and CD20 were considered and gated for missing CD3 expression. NK cells were defined via CD16 and CD56 expression. Next, gates for KIR3DL3 and the respective KIR receptors NKG2A, -C, -D and NKp30, -44, -46 were set with the respective FMO controls.

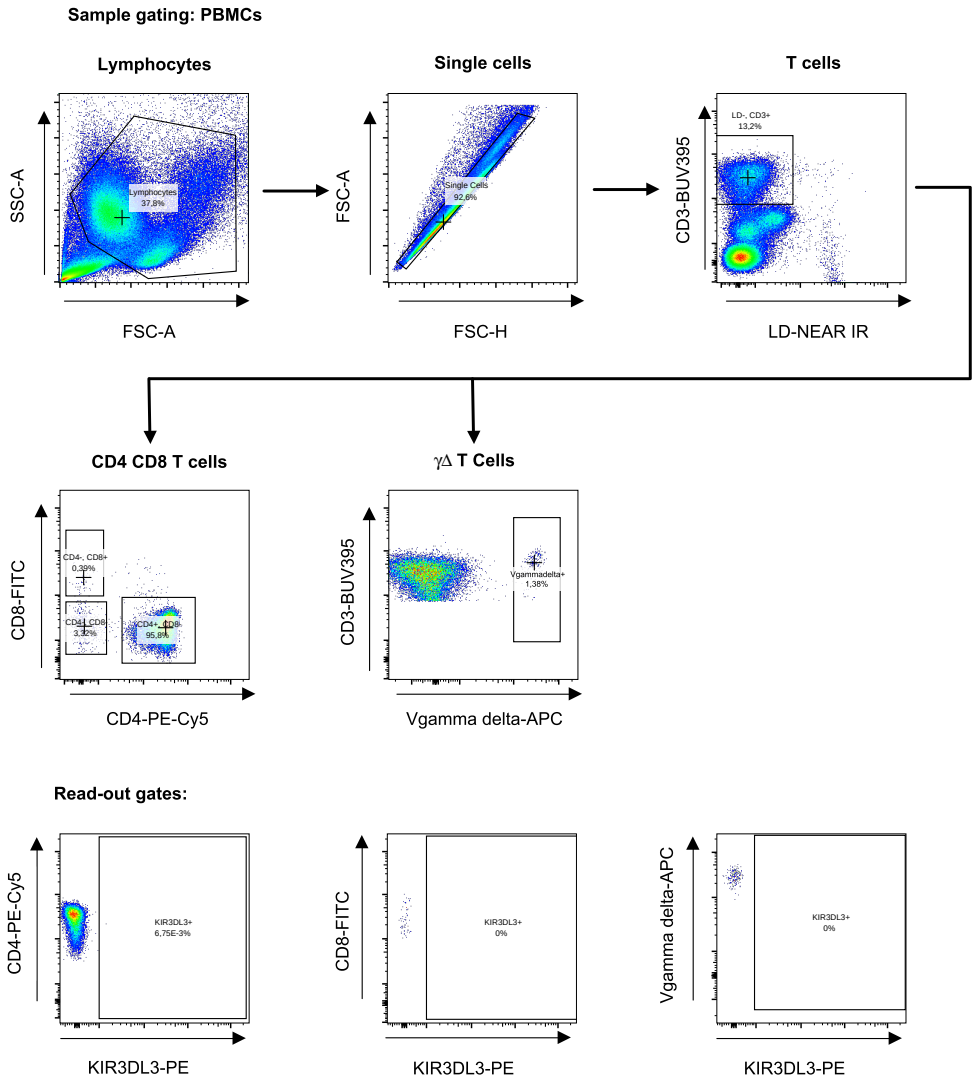

FIGURE 7.18: Gating scheme for KIR3DL3 on $\gamma\delta$-, CD4 and CD8 T cells from PBMCs. Here shown as an example for one triplicate of one donor. First, cells were gated to their size, then duplets were removed, before only living cells were considered and gated for CD3 expression. Next, gates for CD4, CD8 and $\gamma\delta$-T cells were set before KIR3DL3 gates were set with the respective FMO controls.

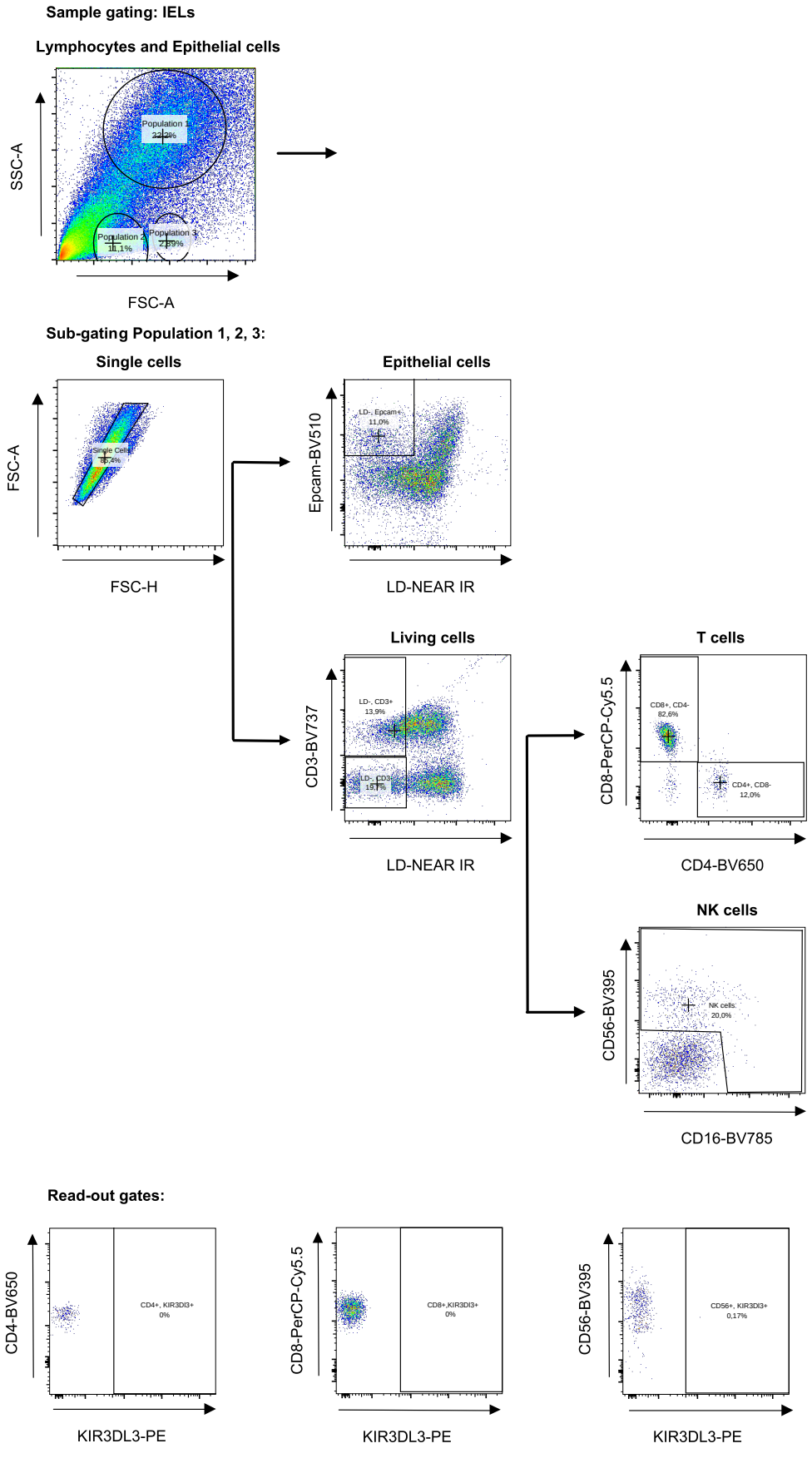
Sample gating: IELs
Lymphocytes and Epithelial cells
SSC-A
FSC-A
Population 1
Population 2
Population 3
Sub-gating Population 1, 2, 3:
Single cells
Epithelial cells
FSC-A
FSC-H
Single Cells
Epcam-BV510
LD-NEAR IR
LD-, Epcam+
11,0%
Living cells
T cells
CD3-BV737
LD-NEAR IR
LD-, CD3+
13,9%
CD8-PerCP-Cy5.5
CD4-BV650
CD8+, CD4-
82,6%
CD4+, CD8-
12,0%
NK cells
CD56-BV395
CD16-BV785
NK cells
20,0%
Read-out gates:
CD4-BV650
KIR3DL3-PE
CD4+, KIR3DI3+
0%
CD8-PerCP-Cy5.5
KIR3DL3-PE
CD8+,KIR3DI3+
0%
CD56-BV395
KIR3DL3-PE
CD56+, KIR3DI3+
0,17%

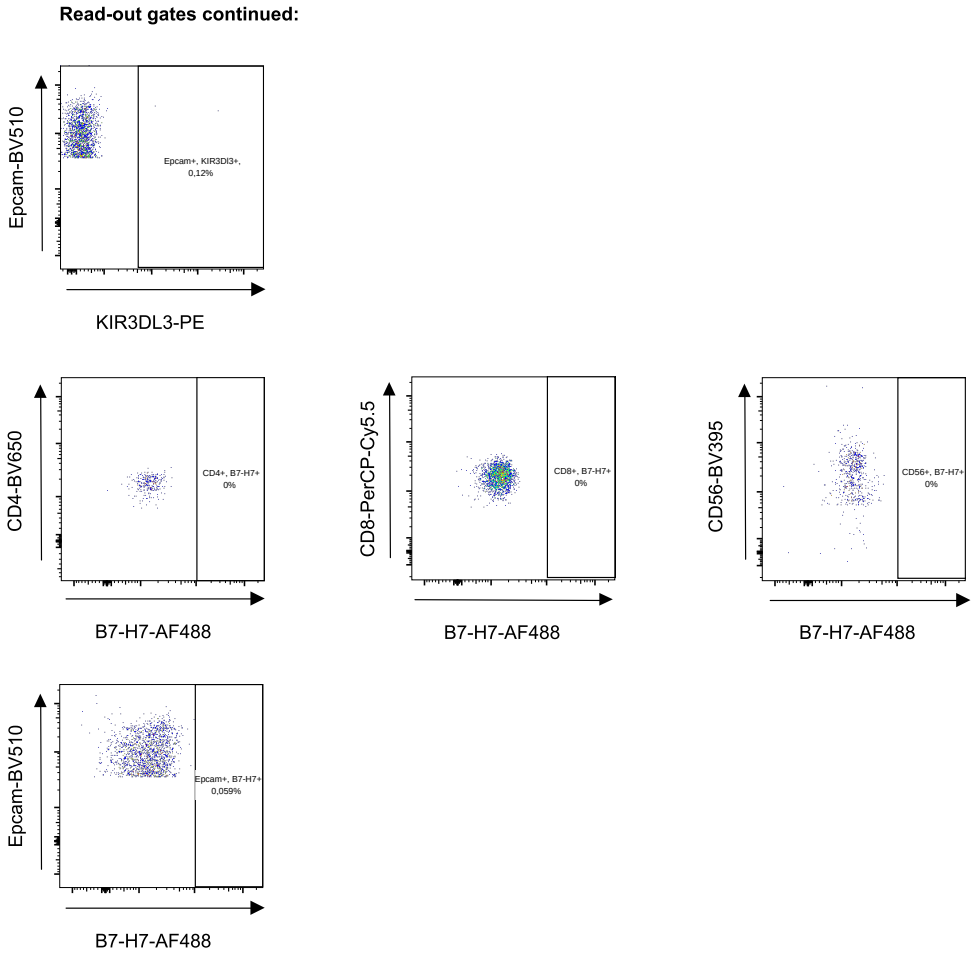

FIGURE 7.19: Gating scheme for KIR3DL3 and B7-H7 on IEL gut samples. Here shown as an example for one triplicate of one donor. First, cells were gated to their size, then duplets were removed, before only living cells were considered and gated for CD3 or Epcam expression. Next, gates for CD4 or CD8 T cells within the CD3 positive cells were set or CD56, CD16 positive and CD19, CD20 negative for NK cells before KIR3DL3 and B7-H7 were set with the respective FMO controls.

Next, gates for KIR3DL3 and B7-H7 in the different samples were assessed whether a distinct cell population was present. If a population was present, the frequency of parents was exported to an Excel file from FlowJo and statistically analysed using R Studio and visualised using GraphPad Prism (subsection 7.10.8, page 164).

7.10 Statistical analysis and testing

7.10.1 Median and MAD

By design the median (Equation 7.4) is less prone to outliers than its more commonly used counterpart mean (Equation 7.2) [395, 396]. Henceforth, the median was used for evaluating signal changes across the different experiments and was exported to Excel via the FlowJo software. As the calculation of a mean and standard deviation (Equation 7.5) from medians would violate its original purpose of being less prone to outliers medians of the exported medians were calculated and their deviation accessed by calculating the median absolute deviation (MAD) (Equation 7.6).

$$\tilde{x} = \begin{cases} x_{\frac{n+1}{2}} & \text{for } n \text{ odd} \\ \frac{1}{2}\left(x_{\frac{n}{2}} + x_{\frac{n}{2}+1}\right) & \text{for } n \text{ even} \end{cases} \tag{7.4}$$

With $\tilde{x}$ representing the median, x as observation and n as total of observations made.

$$s_x = \sqrt{\frac{\sum (x - \bar{x})^2}{n-1}} \tag{7.5}$$

With s_x representing the standard deviation, x as observation, $\bar{x}$ as mean and n as total of observations made.

$$m_x = \begin{cases} (x_i - \tilde{x})_{\frac{n+1}{2}} & \text{for } n \text{ odd} \\ \frac{1}{2}\left((x_i - \tilde{x})_{\frac{n}{2}} + (x_i - \tilde{x})_{\frac{n}{2}+1}\right) & \text{for } n \text{ even} \end{cases} \tag{7.6}$$

With m_x representing the median absolute deviation (MAD), $\tilde{x}$ as the median, x_i as ith observation and n as total of observations made.

7.10.2 Correction for multiple testing and False Discovery Rate

High throughput screens (HTSs) and subgroup analysis allow to test for multiple hypothesis and the identification of many potential biological targets. However, with the number of statistical tests conducted, the number of false positive results increases and call for a correction of multiple testing [397]. An easy way to do this is via the Bonferroni correction which belongs to the family-wise error rate (FWER) methods and simply divides the p-value threshold, e.g. 0.05, by the number of tests conducted [317]. Each individual p-value from the tests must then be below the value of p/n to be considered statistically significant. However, this approach is highly conservative and only controls for false positive (type I errors) while the power of the statistical test (1-type II errors), to find true positives, is greatly diminished [317–319]. This is specifically a problem for HTSs in which multiple hundreds to thousands of tests are conducted. The power can then be as low as 2 % (n = 1,000), but also a moderate

amount of ten tests (n = 10) already lowers the power from a general setting of 80 % to 33 % [318].

In recent years, the False Discovery Rate (FDR) which describes the expected proportion of discoveries which are falsely rejected, was proposed as an alternative method to correct for multiple testing [317, 398]. The idea is that in many times, it is already sufficient, to know that with a chance of 95 % or higher a group of values is not drawn to the null hypothesis and not every single value of a test statistic [319]. To elaborate, it is sufficient to know that none of the reported "hits" of a screen are false positive with a probability of 95 % or higher but one does not necessarily need to know that every value, even the negative test results, are correct with a probability of 95 % or higher. By this trade-off, the amount of hits increases and with it partially the false positive events, but the type I error is sufficiently controlled, and the statistical power of the respective test stays at roughly 56 % (n = 1,000) [318]. Analogous to the p-value as an outcome of the normal test statistic the FDR correction estimates a q-value which in simple terms means: with a q*100 % probability the seen "hit" is a false positive event [399].

To control for q-values, as they set the limit of how many false positive results are acceptable, multiple additional correction methods have been proposed with the first one from Benjamini & Hochberg and its later review from Benjamini, Krieger and Yekutieli [294, 400]. Since their proposal they have developed into the standard for FDR control and have been implemented in multiple static programs such as R, GraphPad Prism and SPSS. While recent publications propose new algorithms for biological and medical samples, which have not yet been implemented in statistical programs and are tailored for specific data sets like genome-wide association studies (GWAS), the data obtained during this dissertation will use the broadly available and reviewed Benjamini & Hochberg method at a FDR of 5 % for the following analyses [401–406]. The outcomes of these analysis and corrections will be reported as FDR adjusted p-values as originally intended by Benjamini & Hochberg and not as q-value [294].

7.10.3 Analysis of the B7 protein KIR-Fc fusion construct protein screening

The MdFIs of all read-out fluorophores from all biological replicates from all controls and the B7 protein KIR-Fc screen exported from FlowJo were imported into Excel, R and GraphPad Prism. In Excel the median and MAD of the MdFIs were calculated according to Equation 7.4 and Equation 7.6 and presented in Table 3.1, Table 3.2, Table 3.3, Table 3.4 and Table 3.5.

In R the statistical testing of MdFI differences between the control groups and the B7 proteins, KIR-Fc fusion construct proteins and respective mabs was calculated using paired Wilcoxon tests for $n \geq 2$ while normal Wilcoxon tests were used for $n = 1$, as

data sets with three and six individual values cannot assume normal distribution and the data originated from one and two biological replicates from the same beads and fusion constructs. The results were adjusted for multiple testing according to Benjamini & Hochberg with an FDR of 5 % using the FDR estimation package (subsection 7.10.2) and presented as FDR adjusted p-values in Table 3.1, Table 3.2, Table 3.3, Table 3.4 and Table 3.5 [294, 407].

As all results for the KIR-Fc fusion construct functionality assessment ($n = 1$) were not statistically significant, albeit their big difference of 3 to 4 logarithmic units from their biotin controls, a simulation for more runs with dummy variables which are normally distributed around the median MdFIs and have the same standard deviation of MAD like the first measurement was created. The simulation showed that already a biological replicate number of $n = 2$ would yield statistically significant results for all Fc fusion construct proteins besides the KIR2DL3-Fc fusion construct protein. The R code used for the statistical analysis is provided in subsection A.2.1.

In GraphPad Prism the MdFIs and MAD obtained from the three biological replicates of the controls and the B7 proteins, KIR-Fc fusion construct proteins and respective mabs were visualised as single values. Statistically significant bars were added according to the findings from the statistical analysis in R with the following scale *$p<0.05$, **$p<0.01$, ***$p<0.0001$. The results are depicted in Figure 3.2, Figure 3.4, Figure 3.6, Figure 3.8, Figure 3.9, Figure 3.10, Figure 3.11 and Figure 3.12.

7.10.4 Analysis of the β2m-KO-Jurkat KIR3DL2 and B7-H1-Fc fusion construct protein binding assay

The MdFIs of all Fc measurements and the frequencies of parents from all KIR measurements from all biological replicates from all controls and the B7-H1-Fc fusion construct protein binding assay, exported from FlowJo, were imported into Excel, R and GraphPad Prism. In Excel the median and MAD of the MdFIs were calculated according to Equation 7.4 and Equation 7.6 and presented in Table 3.6. Additionally, the means and standard deviation for the frequencies of parents were calculated according to Equation 7.2 and Equation 7.5.

In R the statistical testing of MdFI differences between the untransduced β2m-KO-Jurkat controls and the β2m-KO-Jurkat KIR2DS4 and β2m-KO-Jurkat KIR3DL2 cell lines were performed using non-parametric Friedman test and Wilcoxon tests for the post-hoc analysis of groups. The Friedman test, resembles an ANOVA test structure, discriminating between different groups or conditions, but does not require the prerequisite of normal distribution [408]. Henceforth, fewer requirements must be met. Expression levels of KIR on the respective β2m-KO-Jurkat cell lines via frequency of parents were assessed using Wilcoxon paired tests. All non-parametric tests were chosen because data sets with nine individual values cannot assume normal distribution and the data originated from three biological replicates from the same

cell lines and fusion constructs making them technically paired measurements. The results of the post-hoc analysis from the Friedman test and multiple Wilcoxon tests were adjusted for multiple testing according to Benjamini & Hochberg using an FDR of 5 % with the p.adjust function of the R stat package and presented as FDR adjusted p-values in Table 3.6 [294, 407]. The R code used for the statistical analysis is provided in subsection A.2.2.

In GraphPad Prism the MdFIs and MAD obtained from the three biological replicates of the controls and the B7-H1-Fc fusion construct protein stain as well as the mean and standard deviation of the frequencies of parents were visualised as single values. Statistically significant bars were added according to the findings from the statistical analysis in R with the following scale *p<0.05, **p<0.01, ***p<0.0001. The results are depicted in Figure 3.17 and Figure 3.19.

7.10.5 Analysis of the β2m-KO-Jurkat KIR3DL3 and B7-H7-Fc fusion construct protein binding assay

The MdFIs of all Fc measurements and the frequencies of parents from all KIR measurements from all biological replicates from all controls and the B7-H7-Fc fusion construct protein binding assay, exported from FlowJo, were imported into Excel, R and GraphPad Prism. In Excel the median and MAD of the MdFIs were calculated according to Equation 7.4 and Equation 7.6 and presented in Table 3.7. Additionally, the means and standard deviation for the frequencies of parents were calculated according to Equation 7.2 and Equation 7.5.

In R the statistical testing of MdFI differences between the untransduced β2m-KO-Jurkat controls and the β2m-KO-Jurkat KIR2DL5, β2m-KO-Jurkat KIR3DL1 and β2m-KO-Jurkat KIR3DL3 cell lines were performed using non-parametric Friedman test and Wilcoxon tests for the post-hoc analysis of groups. The Friedman test, resembles an ANOVA test structure, discriminating between different groups or conditions, but does not require the prerequisite of normal distribution [408]. Henceforth, fewer requirements must be met. Expression levels of KIR on the respective β2m-KO-Jurkat cell lines via frequency of parents were assessed using Wilcoxon paired tests. All non-parametric tests were chosen because data sets with nine individual values cannot assume normal distribution and the data originated from three biological replicates from the same cell lines and fusion constructs making them technically paired measurements. The results of the post-hoc analysis from the Friedman test and multiple Wilcoxon tests were adjusted for multiple testing according to Benjamini & Hochberg using an FDR of 5 % with the p.adjust function of the R stat package and presented as FDR adjusted p-values in Table 3.7 [294, 407]. The R code used for the statistical analysis is provided in subsection A.2.3.

In GraphPad Prism the MdFIs and MAD obtained from the three biological replicates of the controls and the B7-H7-Fc fusion construct protein stain as well as the mean

and standard deviation of the frequencies of parents were visualised as single values. Statistically significant bars were added according to the findings from the statistical analysis in R with the following scale *p<0.05, **p<0.01, ***p<0.0001. The results are depicted in Figure 3.22 and Figure 3.23.

7.10.6 Analysis of the β2m-KO-Jurkat KIR3DL3 B7-H7 protein reporter cell assay

The CD69 MdFIs of all measurements and the frequencies of parents from all KIR measurements from all biological replicates, exported from FlowJo, were imported into Excel, R and GraphPad Prism. In Excel the median and MAD of the MdFIs were calculated according to Equation 7.4 and Equation 7.6 and presented in Table 3.8. Additionally, the means and standard deviation for the frequencies of parents were calculated according to Equation 7.2 and Equation 7.5.

In R the statistical testing of CD69 MdFI differences between the untransduced β2m-KO-Jurkat controls and the β2m-KO-Jurkat KIR2DL5, β2m-KO-Jurkat KIR3DL1 and β2m-KO-Jurkat KIR3DL3 cell lines for the B7-H7 condition were performed using a non-parametric Friedman test and Wilcoxon tests for the post-hoc analysis of groups. Additionally, a non-parametric Friedman test and Wilcoxon tests for the post-hoc analysis of groups were used for the analysis of differences between the medium, mab and B7-H7 treated conditions of each cell line. The Friedman test, resembles an ANOVA test structure, discriminating between different groups or conditions, but does not require the prerequisite of normal distribution [408]. Henceforth, fewer requirements must be met. Expression levels of KIR on the respective β2m-KO-Jurkat cell lines via frequency of parents were assessed using Wilcoxon paired tests. All non-parametric tests were chosen because data sets with nine individual values cannot assume normal distribution and the data originated from three biological replicates from the same cell lines making them technically paired measurements. The results of the post-hoc analysis from the Friedman test and multiple Wilcoxon tests were adjusted for multiple testing according to Benjamini & Hochberg using an FDR of 5 % with the p.adjust function of the R stat package and presented as FDR adjusted p-values in Table 3.8 [294, 407]. The R code used for the statistical analysis is provided in subsection A.2.4.

In GraphPad Prism the MdFIs and MAD obtained from the three biological replicates of the controls and the reporter cell stains as well as the mean and standard deviation of the KIR frequencies of parents were visualised as single values. Statistically significant bars were added according to the findings from the statistical analysis in R with the following scale *p<0.05, **p<0.01, ***p<0.0001. The results are depicted in Figure 3.27 and Figure 3.29.

7.10.7 Analysis of the NK cell killing assay and its inhibition

The frequencies of parents of all four quadrants of CD3 and LIVE/DEAD negative cells (K562 violet+, CFSE-; K562.B7-H7 violet-; CFSE+, NK cells violet-, CFSE-; debris violet+, CFSE+) were exported from FlowJo for all biological replicates of the experiment with a B7-H7 blocking antibody and without a B7-H7 blocking antibody and imported into Excel. Next, the ratio of labelled K562 to labelled K562.B7-H7 cells was calculated according to Equation 7.1 (page 152) for all E:T ratios of both conditions (with B7-H7 blocking mab and without B7-H7 blocking mab). In the next step, the mean of the ratio of labelled K562 and labelled K562.B7-H7 only cells was calculated according to Equation 7.2. The calculated ratio of K562 and K562.B7-H7 only samples was then used for normalisation as described in Equation 7.3 for the two conditions. Afterwards the mean (Equation 7.2) and standard deviation (Equation 7.5) of the normalised ratios for all E:T ratios for both conditions were calculated and loaded into R and GraphPad Prism. Additionally, the frequencies of parents for B7-H7 and KIR3DL3 expression were exported from FlowJo for all biological replicates and imported into Excel. The means and standard deviation for the frequencies of parents for B7-H7 and KIR3DL3 were calculated according to Equation 7.2 and Equation 7.5 and imported into R and GraphPad Prism.

In R the statistical testing of ratio differences of the K562 to K56.B7-H7 cells between the different E:T ratios for both conditions (with B7-H7 blocking mab and without B7-H7 blocking mab) conditions were performed using a non-parametric Friedman test and Wilcoxon tests for the post-hoc analysis of groups. The Friedman test, resembles an ANOVA test structure, discriminating between different groups or conditions, but does not require the prerequisite of normal distribution [408]. Henceforth, fewer requirements must be met. Expression levels of B7-H7 and KIR3DL3 on the respective K562, K562.B7-H7 and NK-92MI cell lines were assessed using Wilcoxon paired tests for their frequencies of parents. All non-parametric tests were chosen because data sets with nine individual values cannot assume normal distribution and the data originated from three biological replicates from the same cell lines making them technically paired measurements. The results of the post-hoc analysis from the Friedman test and multiple Wilcoxon tests were adjusted for multiple testing according to Benjamini & Hochberg using an FDR of 5 % with the p.adjust function of the R stat package and presented as FDR adjusted p-values in Table 3.9 and Table 3.10 [294, 407]. The R code used for the statistical analysis is provided in subsection A.2.5.

In GraphPad Prism the ratios of labelled K562 to labelled K562.B7-H7 cells obtained from the three biological replicates were visualised as single values. In similar ways the frequencies of parents for the expression levels of B7-H7 and KIR3DL3 on the K562, K562.B7-H7 and NK-92MI cells were visualised. Statistically significant bars were added according to the findings from the statistical analysis in R with the following scale *$p<0.05$, **$p<0.01$, ***$p<0.0001$. The results are depicted in Figure 3.36 and Figure 3.37.

7.10.8 Analysis of the KIR3DL3 and B7-H7 screen in cell systems

7.10.8.1 Analysis of KIR3DL3 expression on NK cells isolated from peripheral blood

The frequencies of parents from all stained NK cell receptors from all healthy blood donors and all frequencies of parents for all KIR3DL3 control measurements from all biological replicates, exported from FlowJo, were imported into Excel. In Excel the means and standard deviation for the frequencies of parents were calculated according to Equation 7.2 and Equation 7.5. Values with more than ten times of the standard deviation were labelled as outliers and excluded from further analysis. The rest of the measurements were imported into R and GraphPad Prism. The results of the calculations are presented in Table 3.11, Table 3.12 and Table 3.13.

In R the statistical testing of KIR3DL3 expression differences between healthy cohort donors for all time points were performed using a non-parametric Friedman test and Wilcoxon tests for the post-hoc analysis of groups. The Friedman test, resembles an ANOVA test structure, discriminating between different groups or conditions, but does not require the prerequisite of normal distribution [408]. Henceforth, fewer requirements must be met. KIR3DL3 mab functionality in all runs was evaluated by using Wilcoxon paired tests for the KIR3DL3 frequency of parent on the β2m-KO-Jurkat KIR3DL3 cell line in comparison to its isotype control. All non-parametric tests were chosen because data sets from six different donors cannot assume normal distribution. Furthermore, the data originated from three different time points which make them paired measurements. The results of the post-hoc analysis from the Friedman test and multiple Wilcoxon tests were adjusted for multiple testing according to Benjamini & Hochberg using an FDR of 5 % with the p.adjust function of the R stat package and presented as FDR adjusted p-values in Table 3.11, Table 3.12 and Table 3.13 [294, 407]. The R code used for the statistical analysis is provided in subsubsection A.2.6.1.

In GraphPad Prism the frequencies of parents for KIR3DL3 and other NK cell receptors obtained from the six biological replicates were visualised as single values. In similar ways the frequencies of parents for the expression levels of KIR3DL3 on the β2m-KO-Jurkat KIR3DL3 were visualised. Statistically significant bars were added according to the findings from the statistical analysis in R with the following scale *p<0.05, **p<0.01, ***p<0.0001. The results are depicted in Figure 3.41 and Figure 3.42.

7.10.8.2 Analysis of KIR3DL3 expression on $\gamma\delta$, CD4 and CD8 T cells

The frequencies of parents for KIR3DL3 expression from the $\gamma\delta$, CD4 and CD8 T cell populations from all healthy blood donors and all frequencies of parents for all KIR3DL3 control measurements from all biological replicates, exported from FlowJo, were imported into Excel, R and GraphPad Prism. In Excel the means and standard

deviation for the frequencies of parents were calculated according to Equation 7.2 and Equation 7.5 and presented in Table 3.14.

In R the statistical testing of KIR3DL3 expression differences between isotype controls and antibody staining for all healthy cohort donors were performed using non-parametric unpaired Wilcoxon tests. The reason for this is, that the samples were not timely paired and originated from nine different individuals but could not claim normal distribution due to a small sample size. KIR3DL3 mab functionality in all runs was evaluated by using Wilcoxon paired tests for the KIR3DL3 frequency of parent on the β2m-KO-Jurkat KIR3DL3 cell line in comparison to its isotype control. Samples were not adjusted for multiple testing, because each population was independent, and the populations not compared among each other. The R code used for the statistical analysis is provided in subsubsection A.2.6.2.

In GraphPad Prism the frequencies of parents for KIR3DL3 obtained from the nine biological replicates were visualised as single values. In similar ways the frequencies of parents for the expression levels of KIR3DL3 on the β2m-KO-Jurkat KIR3DL3 were visualised. Statistically significant bars were added according to the findings from the statistical analysis in R with the following scale *p$<$0.05, **p$<$0.01, ***p$<$0.0001. The results are depicted in Figure 3.44 and Figure 3.46.

7.10.8.3 Analysis of B7-H7 expression on monocytes/macrophages and B cells

The frequencies of parents for B7-H7 expression from the monocytes/macrophages and B cell populations from all healthy blood donors and all frequencies of parents for all B7-H7 control measurements from all biological replicates, exported from FlowJo, were imported into Excel, R and GraphPad Prism. In Excel the means and standard deviation for the frequencies of parents were calculated according to Equation 7.2 and Equation 7.5 and presented in Table 3.15.

In R the statistical testing of B7-H7 expression differences between isotype controls and antibody staining for all healthy cohort donors were performed using non-parametric unpaired Wilcoxon tests. The reason for this is, that the samples were not timely paired and originated from four different individuals but could not claim normal distribution due to a small sample size. Samples were not adjusted for multiple testing, because each population was independent, and the populations not compared among each other. The R code used for the statistical analysis is provided in subsubsection A.2.6.3.

In GraphPad Prism the frequencies of parents for B7-H7 obtained from the four biological replicates were visualised as single values. Statistically significant bars were added according to the findings from the statistical analysis in R with the following scale *p$<$0.05, **p$<$0.01, ***p$<$0.0001. The results are depicted in Figure 3.47 and Figure 3.48.

7.10.8.4 Analysis of KIR3DL3 and B7-H7 expression on IELs

The frequencies of parents for KIR3DL3 and B7-H7 expression from CD4 and CD8 T cell populations as well as epithelial cells and NK cells from all healthy adult IEL gut samples and all frequencies of parents for all KIR3DL3 and B7-H7 control measurements from all biological replicates, exported from FlowJo, were imported into Excel, R and GraphPad Prism. In Excel the means and standard deviation for the frequencies of parents were calculated according to Equation 7.2 and Equation 7.5. The results of the calculations are presented in Table 3.16 and Table 3.17.

In R the statistical testing of KIR3DL3 and B7-H7 expression differences between isotype controls and antibody staining for all healthy adult IEL gut samples were performed using non-parametric unpaired Wilcoxon tests. The reason for this is, that the samples were not timely paired and originated from seven different individuals but could therefore not claim normal distribution due to a small sample size. KIR3DL3 and B7-H7 mab functionality in all runs was evaluated by using Wilcoxon paired tests for the KIR3DL3 and B7-H7 frequency of parent on the β2m-KO-Jurkat KIR3DL3 cell line and K562.B7-H7 cell line in comparison to its isotype control. Samples were not adjusted for multiple testing, because each population was independent and the populations not compared among each other. The R code used for the statistical analysis is provided in subsubsection A.2.6.4.

In GraphPad Prism the frequencies of parents for KIR3DL3 and B7-H7 obtained from the seven biological replicates were visualised as single values. In similar ways the frequencies of parents for the expression levels of KIR3DL3 on the β2m-KO-Jurkat KIR3DL3 and B7-H7 on K562.B7-H7 were visualised. Statistically significant bars were added according to the findings from the statistical analysis in R with the following scale *$p<0.05$, **$p<0.01$, ***$p<0.0001$. The results are depicted in Figure 3.50, Figure 3.52 and Figure 3.54.

8 Confirmation of English language authenticity

I, Sreejith Rajasekharan, born on 04.11.1986 in India, hereby declare that the thesis with the title “The B7 protein family as ligands for Killer Cell Immunoglobulin-like Receptors (KIRs)” written by Nils Dominik Lonken is written in grammatically correct English [32].

Hiermit erkläre ich, Sreejith Rajasekharan, geboren am 04.11.1986 in Indien, dass die Dissertation mit dem Titel “The B7 protein family as ligands for Killer Cell Immunoglobulin-like Receptors (KIRs)” geschrieben von Nils Dominik Lonken in einem korrekten Englisch verfasst wurde [32].

Signed:

Hamburg, Date: 16.02.2024

Bibliography

1. Harel-Bellan, A. *et al.* Natural Killer Susceptibility of Human Cells May Be Regulated by Genes in the HLA Region on Chromosome 6. *Proceedings of the National Academy of Sciences of the United States of America* **83,** 5688–5692. ISSN: 0027-8424. pmid: 2426704 (Aug. 1986).
2. Moretta, A. *et al.* A Novel Surface Antigen Expressed by a Subset of Human CD3- CD16+ Natural Killer Cells. Role in Cell Activation and Regulation of Cytolytic Function. *The Journal of Experimental Medicine* **171,** 695–714. ISSN: 0022-1007. pmid: 2137855 (Mar. 1, 1990).
3. Falk, C. S., Steinle, A. & Schendel, D. J. Expression of HLA-C Molecules Confers Target Cell Resistance to Some Non-Major Histocompatibility Complex-Restricted T Cells in a Manner Analogous to Allospecific Natural Killer Cells. *The Journal of Experimental Medicine* **182,** 1005–1018. ISSN: 0022-1007. pmid: 7561674 (Oct. 1, 1995).
4. Mingari, M. C. *et al.* HLA-class I-specific Inhibitory Receptors in Human Cytolytic T Lymphocytes: Molecular Characterization, Distribution in Lymphoid Tissues and Co-Expression by Individual T Cells. *International Immunology* **9,** 485–491. ISSN: 0953-8178. pmid: 9138008 (Apr. 1997).
5. Parham, P. Immunogenetics of Killer Cell Immunoglobulin-like Receptors. *Molecular Immunology* **42,** 459–462. ISSN: 0161-5890. pmid: 15607799 (Feb. 2005).
6. Valiante, N. M. *et al.* Functionally and Structurally Distinct NK Cell Receptor Repertoires in the Peripheral Blood of Two Human Donors. *Immunity* **7,** 739–751. ISSN: 1074-7613. pmid: 9430220 (Dec. 1997).
7. Bono, M. *et al.* Analysis of KIR3DP1 Polymorphism Provides Relevant Information on Centromeric KIR Gene Content. *Journal of Immunology (Baltimore, Md.: 1950)* **201,** 1460–1467. ISSN: 1550-6606. pmid: 30068594 (Sept. 1, 2018).
8. Velickovic, M., Velickovic, Z. & Dunckley, H. Diversity of Killer Cell Immunoglobulin-like Receptor Genes in Pacific Islands Populations. *Immunogenetics* **58,** 523–532. ISSN: 0093-7711. pmid: 16733717 (July 2006).
9. Murdoch, S., Seoud, M., Kircheisen, R., Mazhar, B. & Slim, R. Detailed Gene and Allele Content Analysis of Three Homozygous KIR Haplotypes. *Tissue Antigens* **68,** 72–77. ISSN: 0001-2815. pmid: 16774543 (July 2006).
10. Trundley, A. E. *et al.* Molecular Characterization of KIR3DL3. *Immunogenetics* **57,** 904–916. ISSN: 0093-7711. pmid: 16391939 (Jan. 2006).

11. Bhatt, R. S. *et al.* KIR3DL3 Is an Inhibitory Receptor for HHLA2 That Mediates an Alternative Immunoinhibitory Pathway to PD1. *Cancer immunology research* **9,** 156–169. ISSN: 2326-6074 2326-6066. pmid: 33229411 (Feb. 2021).
12. West, S. M. & Deng, X. A. Considering B7-CD28 as a Family through Sequence and Structure. *Experimental Biology and Medicine (Maywood, N.J.)* **244,** 1577–1583. ISSN: 1535-3699. pmid: 31208204 (Dec. 2019).
13. June, C. H., Ledbetter, J. A., Linsley, P. S. & Thompson, C. B. Role of the CD28 Receptor in T-cell Activation. *Immunology Today* **11,** 211–216. ISSN: 0167-5699. pmid: 2162180 (June 1990).
14. Cohen, J. New Protein Steals the Show as 'costimulator' of T Cells. *Science (New York, N.Y.)* **262,** 844–845. ISSN: 0036-8075. pmid: 7694360 (Nov. 5, 1993).
15. Zhao, Y., Zheng, Q. & Jin, L. The Role of B7 Family Molecules in Maternal-Fetal Immunity. *Frontiers in Immunology* **11,** 458. ISSN: 1664-3224. pmid: 32265918 (2020).
16. Brandt, C. S. *et al.* The B7 Family Member B7-H6 Is a Tumor Cell Ligand for the Activating Natural Killer Cell Receptor NKp30 in Humans. *The Journal of experimental medicine* **206,** 1495–1503. ISSN: 1540-9538 0022-1007. pmid: 19528259 (July 6, 2009).
17. Palmer, W. H. *et al.* Polymorphic KIR3DL3 Expression Modulates Tissue- Resident and Innate-like T Cells. *Science immunology* **8,** eade5343. ISSN: 2470-9468. pmid: 37390222 (June 30, 2023).
18. Wei, Y. *et al.* KIR3DL3-HHLA2 Is a Human Immunosuppressive Pathway and a Therapeutic Target. *Science immunology* **6.** ISSN: 2470-9468. pmid: 34244312 (July 9, 2021).
19. Zhao, R. *et al.* HHLA2 Is a Member of the B7 Family and Inhibits Human CD4 and CD8 T-cell Function. *Proceedings of the National Academy of Sciences of the United States of America* **110,** 9879–9884. ISSN: 1091-6490. pmid: 23716685 (June 11, 2013).
20. Cheng, H. *et al.* Wide Expression and Significance of Alternative Immune Checkpoint Molecules, B7x and HHLA2, in PD-L1-Negative Human Lung Cancers. *Clinical Cancer Research: An Official Journal of the American Association for Cancer Research* **24,** 1954–1964. ISSN: 1557-3265. pmid: 29374053 (Apr. 15, 2018).
21. Janakiram, M. *et al.* Expression, Clinical Significance, and Receptor Identification of the Newest B7 Family Member HHLA2 Protein. *Clinical cancer research : an official journal of the American Association for Cancer Research* **21,** 2359–2366. ISSN: 1557-3265 1078-0432. pmid: 25549724 (May 15, 2015).
22. Wang, D. *et al.* A Deep Proteome and Transcriptome Abundance Atlas of 29 Healthy Human Tissues. *Molecular Systems Biology* **15,** e8503. ISSN: 1744-4292. pmid: 30777892 (Feb. 18, 2019).
23. Jing, C.-Y. *et al.* HHLA2 in Intrahepatic Cholangiocarcinoma: An Immune Checkpoint with Prognostic Significance and Wider Expression Compared with

PD-L1. *Journal for Immunotherapy of Cancer* **7,** 77. ISSN: 2051-1426. pmid: 30885276 (Mar. 18, 2019).

24. Zhou, Q.-H. *et al.* HHLA2 and PD-L1 Co-Expression Predicts Poor Prognosis in Patients with Clear Cell Renal Cell Carcinoma. *Journal for Immunotherapy of Cancer* **8,** e000157. ISSN: 2051-1426. pmid: 31959726 (Jan. 2020).
25. Luu, K., Schwarz, H. & Lundqvist, A. B7-H7 Is Inducible on T Cells to Regulate Their Immune Response and Serves as a Marker for Exhaustion. *Frontiers in Immunology* **12,** 682627. ISSN: 1664-3224. pmid: 34140952 (2021).
26. Mortezaee, K. HHLA2 Immune-Regulatory Roles in Cancer. *Biomedicine & Pharmacotherapy = Biomedecine & Pharmacotherapie* **162,** 114639. ISSN: 1950-6007. pmid: 37011487 (June 2023).
27. Gunn, S. & Patel, S. *Template for a Masters or Doctoral Thesis* (ed Overleaf) 27.08.2017). https://www.overleaf.com/latex/templates/template-for-a-masters-slash-doctoral-thesis/mkzrzktcbzfl (2023).
28. LIV, UHH & Rieder, L. *Logo UHH, LIV* Aug. 1, 2023. https://www.overleaf.com/latex/templates/uni-hamburg-earth-system-sciences-bachelor-slash-master-thesis-template/kyvwthcnmsmh%20;%20https://www.leibniz-liv.de/.
29. Rodríguez, R. M., López-Vázquez, A. & López-Larrea, C. Immune Systems Evolution. *Advances in experimental medicine and biology* **739,** 237–251. ISSN: 0065-2598. pmid: 22399406 (2012).
30. Chaplin, D. D. Overview of the Immune Response. *The Journal of allergy and clinical immunology* **125,** S3–23. ISSN: 1097-6825 0091-6749. pmid: 20176265 (2 Suppl 2 Feb. 2010).
31. Fittje, P. *Impact of Interactions Between Killer Cell Immunoglobulin-like Receptors and Their Non-Classical Cellular Ligands on the Antiviral Activity of NK Cells* (UHH, Hamburg, July 2022). https://ediss.sub.uni-hamburg.de/handle/ediss/9966 (2023).
32. Vollmers, S. *Impact of KIR/HLA-C Interactions on the Anti-HIV-1 Activity of NK Cells* PhD thesis (UHH, Hamburg). 167 pp. https://ediss.sub.uni-hamburg.de/handle/ediss/9814 (2023).
33. Gonzalez, S. *et al.* Conceptual Aspects of Self and Nonself Discrimination. *Self-/nonself* **2,** 19–25. ISSN: 1938-2030 1938-2049. pmid: 21776331 (Jan. 2011).
34. Burnet, F. M. & Fenner, F. Production of Antibodies. *Nature* **166,** 204–205. ISSN: 1476-4687. https://doi.org/10.1038/166204a0 (Aug. 1, 1950).
35. Janeway, C. A. J. The Immune System Evolved to Discriminate Infectious Nonself from Noninfectious Self. *Immunology today* **13,** 11–16. ISSN: 0167-5699 . pmid: 1739426 (Jan. 1992).
36. Teague, H. *LUBAC Is Required for the RIG-I Mediated Antiviral Response* PhD thesis (University of Cambridge, Cambridge, Aug. 2021). 233 pp. https://www.repository.cam.ac.uk/bitstream/handle/1810/331213/Teague%20-%20Thesis.pdf?isAllowed=y&sequence=4 (2024).

37. Li, Z. *Evaluation of the Role of Innate Lymphoid Cells Following Viral Vector Vaccination* (The Australian National University, Australia, Mar. 2018). 278 pp. https://openresearch-repository.anu.edu.au/bitstream/1885/147596/1/PhD%20Thesis%20Li%202018.pdf (2024).
38. Riera Romo, M., Pérez-Martínez, D. & Castillo Ferrer, C. Innate Immunity in Vertebrates: An Overview. *Immunology* **148,** 125–139. ISSN: 1365-2567 0019-2805. pmid: 26878338 (June 2016).
39. Artis, D. & Spits, H. The Biology of Innate Lymphoid Cells. *Nature* **517,** 293–301. ISSN: 1476-4687. https://doi.org/10.1038/nature14189 (Jan. 1, 2015).
40. Kumar, V. & McNerney, M. E. A New Self: MHC-class-I-independent Natural-Killer-Cell Self-Tolerance. *Nature reviews. Immunology* **5,** 363–374. ISSN: 1474-1733. pmid: 15841099 (May 2005).
41. Murao, A., Aziz, M., Wang, H., Brenner, M. & Wang, P. Release Mechanisms of Major DAMPs. *Apoptosis : an international journal on programmed cell death* **26,** 152–162. ISSN: 1573-675X 1360-8185. pmid: 33713214 (Apr. 2021).
42. Helmy, K. Y. *et al.* CRIg: A Macrophage Complement Receptor Required for Phagocytosis of Circulating Pathogens. *Cell* **124,** 915–927. ISSN: 0092-8674. pmid: 16530040 (Mar. 10, 2006).
43. Köhl, J. Anaphylatoxins and Infectious and Non-Infectious Inflammatory Diseases. *Molecular immunology* **38,** 175–187. ISSN: 0161-5890 . pmid: 11532279 (Aug. 2001).
44. Schraufstatter, I. U., Trieu, K., Sikora, L., Sriramarao, P. & DiScipio, R. Complement C3a and C5a Induce Different Signal Transduction Cascades in Endothelial Cells. *Journal of immunology (Baltimore, Md. : 1950)* **169,** 2102–2110. ISSN: 0022-1767. pmid: 12165538 (Aug. 15, 2002).
45. Hadders, M. A., Beringer, D. X. & Gros, P. Structure of C8alpha-MACPF Reveals Mechanism of Membrane Attack in Complement Immune Defense. *Science (New York, N.Y.)* **317,** 1552–1554. ISSN: 1095-9203 0036-8075 . pmid: 17872444 (Sept. 14, 2007).
46. Scibek, J. J., Plumb, M. E. & Sodetz, J. M. Binding of Human Complement C8 to C9: Role of the N-terminal Modules in the C8 Alpha Subunit. *Biochemistry* **41,** 14546–14551. ISSN: 0006-2960. pmid: 12463754 (Dec. 10, 2002).
47. Gasque, P. Complement: A Unique Innate Immune Sensor for Danger Signals. *Molecular immunology* **41,** 1089–1098. ISSN: 0161-5890. pmid: 15476920 (Nov. 2004).
48. Janeway, M. K. *Janeway's Immunobiology* red. by Edition, 9. ISBN: 978-0-8153-4445-2 (Garland Science, Oxford UK, 2017).
49. Lim, J. J., Grinstein, S. & Roth, Z. Diversity and Versatility of Phagocytosis: Roles in Innate Immunity, Tissue Remodeling, and Homeostasis. *Frontiers in Cellular and Infection Microbiology* **7,** 191. ISSN: 2235-2988 . pmid: 28589095 (2017).

50. Rowley, D. The Role of Opsonins in Non-Specific Immunity. *The Journal of Experimental Medicine* **111,** 137–144. ISSN: 0022-1007. pmid: 14439720 (Jan. 1, 1960).
51. Check, J. H., O'Neill, E. A., O'Neill, K. E. & Fuscaldo, K. E. Effect of Anti-B Antiserum on the Phagocytosis of Escherichia Coli. *Infection and Immunity* **6,** 95–96. ISSN: 0019-9567. pmid: 4564154 (July 1972).
52. Cohn, M. The Common Sense of the Self-Nonself Discrimination. *Springer Seminars in Immunopathology* **27,** 3–17. ISSN: 0344-4325. pmid: 15711952 (June 2005).
53. Litman, G. W., Rast, J. P. & Fugmann, S. D. The Origins of Vertebrate Adaptive Immunity. *Nature Reviews. Immunology* **10,** 543–553. ISSN: 1474-1741. pmid: 20651744 (Aug. 2010).
54. Cooper, M. D. & Herrin, B. R. How Did Our Complex Immune System Evolve? *Nature Reviews. Immunology* **10,** 2–3. ISSN: 1474-1741. pmid: 20039476 (Jan. 2010).
55. Fugmann, S. D., Lee, A. I., Shockett, P. E., Villey, I. J. & Schatz, D. G. The RAG Proteins and V(D)J Recombination: Complexes, Ends, and Transposition. *Annual Review of Immunology* **18,** 495–527. ISSN: 0732-0582. pmid: 10837067 (2000).
56. Jung, D., Giallourakis, C., Mostoslavsky, R. & Alt, F. W. Mechanism and Control of V(D)J Recombination at the Immunoglobulin Heavy Chain Locus. *Annual Review of Immunology* **24,** 541–570. ISSN: 0732-0582. pmid: 16551259 (2006).
57. Schatz, D. G. V(D)J Recombination. *Immunological Reviews* **200,** 5–11. ISSN: 0105-2896. pmid: 15242391 (Aug. 2004).
58. Schatz, D. G. & Swanson, P. C. V(D)J Recombination: Mechanisms of Initiation. *Annual Review of Genetics* **45,** 167–202. ISSN: 1545-2948. pmid: 21854230 (2011).
59. Klein, L., Hinterberger, M., Wirnsberger, G. & Kyewski, B. Antigen Presentation in the Thymus for Positive Selection and Central Tolerance Induction. *Nature Reviews. Immunology* **9,** 833–844. ISSN: 1474-1741. pmid: 19935803 (Dec. 2009).
60. Melchers, F. *et al.* Repertoire Selection by Pre-B-cell Receptors and B-cell Receptors, and Genetic Control of B-cell Development from Immature to Mature B Cells. *Immunological Reviews* **175,** 33–46. ISSN: 0105-2896. pmid: 10933589 (June 2000).
61. Starr, T. K., Jameson, S. C. & Hogquist, K. A. Positive and Negative Selection of T Cells. *Annual Review of Immunology* **21,** 139–176. ISSN: 0732-0582. pmid: 12414722 (2003).
62. Hoffman, W., Lakkis, F. G. & Chalasani, G. B Cells, Antibodies, and More. *Clinical journal of the American Society of Nephrology: CJASN* **11,** 137–154. ISSN: 1555-905X. pmid: 26700440 (Jan. 7, 2016).

63. Allen, C. D., Okada, T. & Cyster, J. G. Germinal Center Organization and Cellular Dynamics. *Immunity* **27,** 190–202. ISSN: 1074-7613. pmid: 17723214. https://www.ncbi.nlm.nih.gov/pmc/articles/PMC2242846/ (2023) (Aug. 2007).
64. Malhotra, S., Kovats, S., Zhang, W. & Coggeshall, K. M. B Cell Antigen Receptor Endocytosis and Antigen Presentation to T Cells Require Vav and Dynamin. *The Journal of biological chemistry* **284,** 24088–24097. ISSN: 0021-9258 1083-351X. pmid: 19586920 (Sept. 4, 2009).
65. Garcillán, B. *et al.* T Lymphocytes in the Diagnosis of Human T Cell Receptor Immunodeficiencies. *Frontiers in Immunology* **6,** 20. ISSN: 1664-3224. pmid: 25688246. https://www.ncbi.nlm.nih.gov/pmc/articles/PMC4310324/ (2023) (Jan. 29, 2015).
66. Mellins, E. *et al.* Defective Processing and Presentation of Exogenous Antigens in Mutants with Normal HLA Class II Genes. *Nature* **343,** 71–74. ISSN: 0028-0836. pmid: 1967485 (Jan. 4, 1990).
67. Wang, R., Murphy, K. M., Loh, D. Y., Weaver, C. & Russell, J. H. Differential Activation of Antigen-Stimulated Suicide and Cytokine Production Pathways in CD4+ T Cells Is Regulated by the Antigen-Presenting Cell. *Journal of Immunology (Baltimore, Md.: 1950)* **150,** 3832–3842. ISSN: 0022-1767. pmid: 7682585 (May 1, 1993).
68. Cowdery, J. S. & Fleming, A. L. In Vivo Depletion of CD4 T Cells Increases B Cell Sensitivity to Polyclonal Activation: The Role of Interferon-Gamma. *Clinical Immunology and Immunopathology* **62,** 72–77. ISSN: 0090-1229. pmid: 1370259 (1 Pt 1 Jan. 1992).
69. Sander, B., Cardell, S. & Möller, E. Interleukin 4 and Interferon Gamma Production in Restimulated CD4+ and CD8+ Cells Indicates Memory Type Responsiveness. *Scandinavian Journal of Immunology* **33,** 287–296. ISSN: 0300-9475. pmid: 1826374 (Mar. 1991).
70. Kopp, W. C. *et al.* Immunomodulatory Effects of Interferon-Gamma in Patients with Metastatic Malignant Melanoma. *Journal of Immunotherapy with Emphasis on Tumor Immunology: Official Journal of the Society for Biological Therapy* **13,** 181–190. ISSN: 1067-5582. pmid: 8471592 (Apr. 1993).
71. Bertoletti, A. *et al.* HLA Class I-restricted Human Cytotoxic T Cells Recognize Endogenously Synthesized Hepatitis B Virus Nucleocapsid Antigen. *Proceedings of the National Academy of Sciences of the United States of America* **88,** 10445–10449. ISSN: 0027-8424. pmid: 1660137 (Dec. 1, 1991).
72. Lee, M. N. & Meyerson, M. Antigen Identification for HLA Class I- and HLA Class II-restricted T Cell Receptors Using Cytokine-Capturing Antigen- Presenting Cells. *Science Immunology* **6,** eabf4001. ISSN: 2470-9468. pmid: 33483338 (Jan. 22, 2021).

73. Andreasen, S. O., Christensen, J. E., Marker, O. & Thomsen, A. R. Role of CD40 Ligand and CD28 in Induction and Maintenance of Antiviral CD8+ Effector T Cell Responses. *Journal of Immunology (Baltimore, Md.: 1950)* **164,** 3689–3697. ISSN: 0022-1767. pmid: 10725727 (Apr. 1, 2000).
74. Blazevic, V., Trubey, C. M. & Shearer, G. M. Analysis of the Costimulatory Requirements for Generating Human Virus-Specific in Vitro T Helper and Effector Responses. *Journal of Clinical Immunology* **21,** 293–302. ISSN: 0271-9142. pmid: 11506200 (July 2001).
75. Weninger, W., Manjunath, N. & von Andrian, U. H. Migration and Differentiation of CD8+ T Cells. *Immunological Reviews* **186,** 221–233. ISSN: 0105-2896. pmid: 12234374 (Aug. 2002).
76. Sciammas, R., Tatsumi, Y., Sperling, A. I., Arunan, K. & Bluestone, J. A. TCR Gamma Delta Cells: Mysterious Cells of the Immune System. *Immunologic Research* **13,** 268–279. ISSN: 0257-277X. pmid: 7616054 (1994).
77. Sciammas, R. *et al.* Unique Antigen Recognition by a Herpesvirus-Specific TCR-gamma Delta Cell. *Journal of Immunology (Baltimore, Md.: 1950)* **152,** 5392–5397. ISSN: 0022-1767. pmid: 8189058 (June 1, 1994).
78. Ribot, J. C., Lopes, N. & Silva-Santos, B. T Cells in Tissue Physiology and Surveillance. *Nature Reviews Immunology* **21,** 221–232. ISSN: 1474-1741. https://www.nature.com/articles/s41577-020-00452-4 (2023) (4 Apr. 2021).
79. Romagnoli, P. A., Sheridan, B. S., Pham, Q.-M., Lefrançois, L. & Khanna, K. M. IL-17A-producing Resident Memory T Cells Orchestrate the Innate Immune Response to Secondary Oral Listeria Monocytogenes Infection. *Proceedings of the National Academy of Sciences of the United States of America* **113,** 8502–8507. ISSN: 1091-6490. pmid: 27402748 (July 26, 2016).
80. Gasteiger, G. & Rudensky, A. Y. Interactions between Innate and Adaptive Lymphocytes. *Nature Reviews. Immunology* **14,** 631–639. ISSN: 1474-1741. pmid: 25132095 (Sept. 2014).
81. Jost, S. & Altfeld, M. Control of Human Viral Infections by Natural Killer Cells. *Annual Review of Immunology* **31,** 163–194. ISSN: 1545-3278. pmid: 23298212 (2013).
82. Good-Jacobson, K. L. & Tarlinton, D. M. Multiple Routes to B-cell Memory. *International Immunology* **24,** 403–408. ISSN: 1460-2377. pmid: 22451529 (July 2012).
83. Hataye, J., Moon, J. J., Khoruts, A., Reilly, C. & Jenkins, M. K. Naive and Memory CD4+ T Cell Survival Controlled by Clonal Abundance. *Science (New York, N.Y.)* **312,** 114–116. ISSN: 1095-9203. pmid: 16513943 (Apr. 7, 2006).
84. Seder, R. A. & Ahmed, R. Similarities and Differences in CD4+ and CD8+ Effector and Memory T Cell Generation. *Nature Immunology* **4,** 835–842. ISSN: 1529-2908. pmid: 12942084 (Sept. 2003).

85. Pennock, N. D. *et al.* T Cell Responses: Naive to Memory and Everything in Between. *Advances in Physiology Education* **37,** 273–283. ISSN: 1522-1229. pmid: 24292902 (Dec. 2013).
86. Herberman, R. B., Nunn, M. E. & Lavrin, D. H. Natural Cytotoxic Reactivity of Mouse Lymphoid Cells against Syngeneic Acid Allogeneic Tumors. I. Distribution of Reactivity and Specificity. *International Journal of Cancer* **16,** 216–229. ISSN: 0020-7136. pmid: 50294 (Aug. 15, 1975).
87. Kiessling, R., Klein, E. & Wigzell, H. "Natural" Killer Cells in the Mouse. I. Cytotoxic Cells with Specificity for Mouse Moloney Leukemia Cells. Specificity and Distribution According to Genotype. *European Journal of Immunology* **5,** 112–117. ISSN: 0014-2980. pmid: 1234049 (Feb. 1975).
88. Pross, H. F. & Jondal, M. Cytotoxic Lymphocytes from Normal Donors. A Functional Marker of Human Non-T Lymphocytes. *Clinical and Experimental Immunology* **21,** 226–235. ISSN: 0009-9104. pmid: 810282 (Aug. 1975).
89. Timonen, T., Saksela, E., Ranki, A. & Häyry, P. Fractionation, Morphological and Functional Characterization of Effector Cells Responsible for Human Natural Killer Activity against Cell-Line Targets. *Cellular Immunology* **48,** 133–148. ISSN: 0008-8749. pmid: 509533 (Nov. 1979).
90. Fittje, P. *et al.* HIV-1 Nef-mediated Downregulation of CD155 Results in Viral Restriction by KIR2DL5+ NK Cells. *PLoS pathogens* **18,** e1010572. ISSN: 1553-7374 1553-7366. pmid: 35749424 (June 2022).
91. Lanier, L. L., Le, A. M., Phillips, J. H., Warner, N. L. & Babcock, G. F. Subpopulations of Human Natural Killer Cells Defined by Expression of the Leu-7 (HNK-1) and Leu-11 (NK-15) Antigens. *Journal of Immunology (Baltimore, Md.: 1950)* **131,** 1789–1796. ISSN: 0022-1767. pmid: 6225799 (Oct. 1983).
92. Lanier, L. L., Testi, R., Bindl, J. & Phillips, J. H. Identity of Leu-19 (CD56) Leukocyte Differentiation Antigen and Neural Cell Adhesion Molecule. *The Journal of Experimental Medicine* **169,** 2233–2238. ISSN: 0022-1007. pmid: 2471777 (June 1, 1989).
93. Yu, J., Freud, A. G. & Caligiuri, M. A. Location and Cellular Stages of Natural Killer Cell Development. *Trends in Immunology* **34,** 573–582. ISSN: 1471-4981. pmid: 24055329 (Dec. 2013).
94. Cooper, M. A., Fehniger, T. A. & Caligiuri, M. A. The Biology of Human Natural Killer-Cell Subsets. *Trends in Immunology* **22,** 633–640. ISSN: 1471-4906. pmid: 11698225 (Nov. 2001).
95. Cooper, G. E. *Natural Killer Cell Responses to Influenza A Virus in the Human Lung* PhD thesis (University of Southampton, USA, Dec. 2018). https://eprints.soton.ac.uk/435569/1/GC_Thesis.pdf (2024).
96. Vivier, E. *et al.* Innate or Adaptive Immunity? The Example of Natural Killer Cells. *Science (New York, N.Y.)* **331,** 44–49. ISSN: 1095-9203. pmid: 21212348 (Jan. 7, 2011).

97. Parham, P. & Guethlein, L. A. Genetics of Natural Killer Cells in Human Health, Disease, and Survival. *Annual Review of Immunology* **36,** 519–548. ISSN: 1545-3278. pmid: 29394121 (Apr. 26, 2018).
98. Abel, A. M., Yang, C., Thakar, M. S. & Malarkannan, S. Natural Killer Cells: Development, Maturation, and Clinical Utilization. *Frontiers in Immunology* **9,** 1869. ISSN: 1664-3224. pmid: 30150991 (2018).
99. Vivier, E., Tomasello, E., Baratin, M., Walzer, T. & Ugolini, S. Functions of Natural Killer Cells. *Nature immunology* **9,** 503–510. ISSN: 1529-2908. https://www.nature.com/articles/ni1582#citeas (2023) (2008).
100. Caligiuri, M. A. Human Natural Killer Cells. *Blood* **112,** 461–469. ISSN: 0006-4971. https://doi.org/10.1182/blood-2007-09-077438 (2023) (Aug. 1, 2008).
101. Perera Molligoda Arachchige, A. S. Human NK Cells: From Development to Effector Functions. *Innate Immunity* **27,** 212–229. ISSN: 1753-4267 . pmid: 33761782 (Apr. 2021).
102. Orange, J. S. *et al.* The Mature Activating Natural Killer Cell Immunologic Synapse Is Formed in Distinct Stages. *Proceedings of the National Academy of Sciences of the United States of America* **100,** 14151–14156. ISSN: 0027-8424. pmid: 14612578 (Nov. 25, 2003).
103. Rak, G. D., Mace, E. M., Banerjee, P. P., Svitkina, T. & Orange, J. S. Natural Killer Cell Lytic Granule Secretion Occurs through a Pervasive Actin Network at the Immune Synapse. *PLoS biology* **9,** e1001151. ISSN: 1545-7885. pmid: 21931536 (Sept. 2011).
104. Brown, A. C. N. *et al.* Remodelling of Cortical Actin Where Lytic Granules Dock at Natural Killer Cell Immune Synapses Revealed by Super-Resolution Microscopy. *PLoS biology* **9,** e1001152. ISSN: 1545-7885. pmid: 21931537 (Sept. 2011).
105. Bratke, K., Kuepper, M., Bade, B., Virchow, J. C. J. & Luttmann, W. Differential Expression of Human Granzymes A, B, and K in Natural Killer Cells and during CD8+ T Cell Differentiation in Peripheral Blood. *European journal of immunology* **35,** 2608–2616. ISSN: 0014-2980. pmid: 16106370 (Sept. 2005).
106. Dourmashkin, R. R., Deteix, P., Simone, C. B. & Henkart, P. Electron Microscopic Demonstration of Lesions in Target Cell Membranes Associated with Antibody-Dependent Cellular Cytotoxicity. *Clinical and experimental immunology* **42,** 554–560. ISSN: 0009-9104 1365-2249. pmid: 7214742 (Dec. 1980).
107. Smyth, M. J. *et al.* Activation of NK Cell Cytotoxicity. *Molecular Immunology* **42,** 501–510. ISSN: 0161-5890. pmid: 15607806 (Feb. 2005).
108. Nagata, S. Apoptosis by Death Factor. *Cell* **88,** 355–365. ISSN: 0092-8674. pmid: 9039262 (Feb. 7, 1997).
109. Crowder, R. N. & El-Deiry, W. S. Caspase-8 Regulation of TRAIL-mediated Cell Death. *Experimental Oncology* **34,** 160–164. ISSN: 2312-8852. pmid: 23070000 (Oct. 2012).

110. Pinkoski, M. J. *et al.* Granzyme B-mediated Apoptosis Proceeds Predominantly through a Bcl-2-inhibitable Mitochondrial Pathway. *The Journal of Biological Chemistry* **276,** 12060–12067. ISSN: 0021-9258. pmid: 11278459 (Apr. 13, 2001).
111. Atkinson, E. A. *et al.* Cytotoxic T Lymphocyte-Assisted Suicide. Caspase 3 Activation Is Primarily the Result of the Direct Action of Granzyme B. *The Journal of Biological Chemistry* **273,** 21261–21266. ISSN: 0021-9258. pmid: 9694885 (Aug. 14, 1998).
112. Bhat, R. & Watzl, C. Serial Killing of Tumor Cells by Human Natural Killer Cells–Enhancement by Therapeutic Antibodies. *PloS One* **2,** e326. ISSN: 1932-6203. pmid: 17389917 (Mar. 28, 2007).
113. Khosravi-Far, R. & Esposti, M. D. Death Receptor Signals to Mitochondria. *Cancer Biology & Therapy* **3,** 1051–1057. ISSN: 1538-4047. pmid: 15640619 (Nov. 2004).
114. Alter, G., Malenfant, J. M. & Altfeld, M. CD107a as a Functional Marker for the Identification of Natural Killer Cell Activity. *Journal of Immunological Methods* **294,** 15–22. ISSN: 0022-1759. pmid: 15604012 (Nov. 2004).
115. Fauriat, C., Long, E. O., Ljunggren, H.-G. & Bryceson, Y. T. Regulation of Human NK-cell Cytokine and Chemokine Production by Target Cell Recognition. *Blood* **115,** 2167–2176. ISSN: 1528-0020. pmid: 19965656 (Mar. 18, 2010).
116. Theorell, J. *et al.* Sensitive and Viable Quantification of Inside-out Signals for LFA-1 Activation in Human Cytotoxic Lymphocytes by Flow Cytometry. *Journal of Immunological Methods* **366,** 106–118. ISSN: 1872-7905. pmid: 21295038 (Mar. 7, 2011).
117. Parodi, M. *et al.* Hypoxia Modifies the Transcriptome of Human NK Cells, Modulates Their Immunoregulatory Profile, and Influences NK Cell Subset Migration. *Frontiers in Immunology* **9,** 2358. ISSN: 1664-3224. pmid: 30459756. https://www.ncbi.nlm.nih.gov/pmc/articles/PMC6232835/ (2023) (Oct. 16, 2018).
118. Poli, A. *et al.* CD56bright Natural Killer (NK) Cells: An Important NK Cell Subset. *Immunology* **126,** 458–465. ISSN: 0019-2805. pmid: 19278419. https://www.ncbi.nlm.nih.gov/pmc/articles/PMC2673358/ (2023) (Apr. 2009).
119. Cook, K. D., Waggoner, S. N. & Whitmire, J. K. NK Cells and Their Ability to Modulate T Cells during Virus Infections. *Critical Reviews in Immunology* **34,** 359–388. ISSN: 1040-8401. pmid: 25404045 (2014).
120. Blanchard, D. K., Michelini-Norris, M. B. & Djeu, J. Y. Production of Granulocyte-Macrophage Colony-Stimulating Factor by Large Granular Lymphocytes Stimulated with Candida Albicans: Role in Activation of Human Neutrophil Function. *Blood* **77,** 2259–2265. ISSN: 0006-4971. pmid: 2029583 (May 15, 1991).
121. Van den Bosch, G. *et al.* Granulocyte-Macrophage Colony-Stimulating Factor (GM-CSF) Counteracts the Inhibiting Effect of Monocytes on Natural Killer (NK) Cells. *Clinical and Experimental Immunology* **101,** 515–520. ISSN: 0009-9104. pmid: 7664499 (Sept. 1995).

122. Walzer, T., Dalod, M., Robbins, S. H., Zitvogel, L. & Vivier, E. Natural-Killer Cells and Dendritic Cells: "L'union Fait La Force". *Blood* **106,** 2252–2258. ISSN: 0006-4971. pmid: 15933055 (Oct. 1, 2005).
123. Moffett, A. & Colucci, F. Co-Evolution of NK Receptors and HLA Ligands in Humans Is Driven by Reproduction. *Immunological Reviews* **267,** 283–297. ISSN: 1600-065X. pmid: 26284484 (Sept. 2015).
124. Brias, S. *The Immunoregulatory Role of HLA-F in Human Diseases* PhD thesis (UHH, Hamburg, Oct. 2023). 125 pp. https://ediss.sub.uni-hamburg.de/handle/ediss/10536 (2023).
125. Kruse, Ph., Matta, J., Ugolini, S. & Vivier, E. Natural Cytotoxicity Receptors and Their Ligands. *Immunology and cell biology* **92.** ISSN: 1440-1711 . pmid: 24366519. https://pubmed.ncbi.nlm.nih.gov/24366519/ (2023) (Mar. 2014).
126. Munitz, A. Inhibitory Receptors on Myeloid Cells: New Targets for Therapy? *Pharmacology & Therapeutics* **125,** 128–137. ISSN: 1879-016X. pmid: 19913051 (Jan. 2010).
127. Wang, S. *et al.* Breaking Boundaries: Current Progress of Anticancer NK Cell-Based Drug Development. *Drug Discovery Today* **28,** 103436. ISSN: 1359-6446. https://www.sciencedirect.com/science/article/pii/S135964462200420%2099 (2023) (Feb. 1, 2023).
128. Bryceson, Y. T., March, M. E., Ljunggren, H.-G. & Long, E. O. Synergy among Receptors on Resting NK Cells for the Activation of Natural Cytotoxicity and Cytokine Secretion. *Blood* **107,** 159–166. ISSN: 0006-4971. pmid: 16150947 (Jan. 1, 2006).
129. Forthal, D. N. & Finzi, A. Antibody-Dependent Cellular Cytotoxicity in HIV Infection. *AIDS (London, England)* **32,** 2439–2451. ISSN: 1473-5571 . pmid: 30234611 (Nov. 13, 2018).
130. Dai, H.-S. *et al.* The Fc Domain of Immunoglobulin Is Sufficient to Bridge NK Cells with Virally Infected Cells. *Immunity* **47,** 159–170.e10. ISSN: 1097-4180. pmid: 28723548 (July 18, 2017).
131. Horowitz, A. *et al.* Genetic and Environmental Determinants of Human NK Cell Diversity Revealed by Mass Cytometry. *Science Translational Medicine* **5,** 208ra145. ISSN: 1946-6242. pmid: 24154599 (Oct. 23, 2013).
132. Kärre, K. Natural Killer Cell Recognition of Missing Self. *Nature Immunology* **9,** 477–480. ISSN: 1529-2916. https://www.nature.com/articles/ni0508-477 (2023) (5 May 2008).
133. Kärre, K., Ljunggren, H. G., Piontek, G. & Kiessling, R. Selective Rejection of H-2-deficient Lymphoma Variants Suggests Alternative Immune Defence Strategy. *Nature* **319,** 675–678. ISSN: 0028-0836. pmid: 3951539 (Feb. 20, 1986–26).
134. Moretta, A. *et al.* Receptors for HLA Class-I Molecules in Human Natural Killer Cells. *Annual Review of Immunology* **14,** 619–648. ISSN: 0732-0582. pmid: 8717527 (1996).

135. Karlhofer, F. M., Ribaudo, R. K. & Yokoyama, W. M. MHC Class I Alloantigen Specificity of Ly-49+ IL-2-activated Natural Killer Cells. *Nature* **358,** 66–70. ISSN: 0028-0836. pmid: 1614533 (July 2, 1992).

136. Raulet, D. H. & Guerra, N. Oncogenic Stress Sensed by the Immune System: Role of Natural Killer Cell Receptors. *Nature Reviews. Immunology* **9,** 568–580. ISSN: 1474-1741. pmid: 19629084 (Aug. 2009).

137. Miller-Kittrell, M. & Sparer, T. E. Feeling Manipulated: Cytomegalovirus Immune Manipulation. *Virology Journal* **6,** 1–20. ISSN: 1743-422X . https://virologyj.biomedcentral.com/articles/10.1186/1743-422X-6-4 (2023) (1 Dec. 2009).

138. Garrido, F., Aptsiauri, N., Doorduijn, E. M., Garcia Lora, A. M. & van Hall, T. The Urgent Need to Recover MHC Class I in Cancers for Effective Immunotherapy. *Current Opinion in Immunology. Lymphocyte Development and Activation Tumour Immunology* **39,** 44–51. ISSN: 0952-7915 . https://www.sciencedirect.com/science/article/pii/S095279151500%201739 (2023) (Apr. 1, 2016).

139. Raulet, D. H. & Vance, R. E. Self-Tolerance of Natural Killer Cells. *Nature Reviews. Immunology* **6,** 520–531. ISSN: 1474-1733. pmid: 16799471 (July 2006).

140. Horowitz, A. *et al.* Class I HLA Haplotypes Form Two Schools That Educate NK Cells in Different Ways. *Science Immunology* **1,** eaag1672. ISSN: 2470-9468. pmid: 27868107 (Sept. 2016).

141. Boudreau, J. E. & Hsu, K. C. Natural Killer Cell Education and the Response to Infection and Cancer Therapy: Stay Tuned. *Trends in Immunology* **39,** 222–239. ISSN: 1471-4981. pmid: 29397297 (Mar. 2018).

142. Anfossi, N. *et al.* Human NK Cell Education by Inhibitory Receptors for MHC Class I. *Immunity* **25,** 331–342. ISSN: 1074-7613. pmid: 16901727 (Aug. 2006).

143. Kim, S. *et al.* Licensing of Natural Killer Cells by Host Major Histocompatibility Complex Class I Molecules. *Nature* **436,** 709–713. ISSN: 1476-4687. pmid: 16079848 (Aug. 4, 2005).

144. Fernandez, N. C. *et al.* A Subset of Natural Killer Cells Achieves Self-Tolerance without Expressing Inhibitory Receptors Specific for Self-MHC Molecules. *Blood* **105,** 4416–4423. ISSN: 0006-4971. pmid: 15728129 (June 1, 2005).

145. Stewart, C. A. *et al.* Recognition of Peptide-MHC Class I Complexes by Activating Killer Immunoglobulin-like Receptors. *Proceedings of the National Academy of Sciences of the United States of America* **102,** 13224–13229. ISSN: 0027-8424. pmid: 16141329 (Sept. 13, 2005).

146. Parham, P. MHC Class I Molecules and KIRs in Human History, Health and Survival. *Nature Reviews. Immunology* **5,** 201–214. ISSN: 1474-1733 . pmid: 15719024 (Mar. 2005).

147. Liao, N. S., Bix, M., Zijlstra, M., Jaenisch, R. & Raulet, D. MHC Class I Deficiency: Susceptibility to Natural Killer (NK) Cells and Impaired NK Activity. *Science (New York, N.Y.)* **253,** 199–202. ISSN: 0036-8075. pmid: 1853205 (July 12, 1991).
148. Cichocki, F., Grzywacz, B. & Miller, J. S. Human NK Cell Development: One Road or Many? *Frontiers in Immunology* **10,** 2078. ISSN: 1664-3224 . pmid: 31555287 (2019).
149. Freud, A. G. *et al.* A Human CD34(+) Subset Resides in Lymph Nodes and Differentiates into CD56bright Natural Killer Cells. *Immunity* **22,** 295–304. ISSN: 1074-7613. pmid: 15780987 (Mar. 2005).
150. Chan, A. *et al.* CD56bright Human NK Cells Differentiate into CD56dim Cells: Role of Contact with Peripheral Fibroblasts. *Journal of Immunology (Baltimore, Md.: 1950)* **179,** 89–94. ISSN: 0022-1767. pmid: 17579025 (July 1, 2007).
151. Romagnani, C. *et al.* CD56brightCD16- Killer Ig-like Receptor- NK Cells Display Longer Telomeres and Acquire Features of CD56dim NK Cells upon Activation. *Journal of Immunology (Baltimore, Md.: 1950)* **178,** 4947–4955. ISSN: 0022-1767. pmid: 17404276 (Apr. 15, 2007).
152. Grzywacz, B. *et al.* Natural Killer-Cell Differentiation by Myeloid Progenitors. *Blood* **117,** 3548–3558. ISSN: 1528-0020. pmid: 21173117 (Mar. 31, 2011).
153. Chen, Q. *et al.* Delineation of Natural Killer Cell Differentiation from Myeloid Progenitors in Human. *Scientific Reports* **5,** 15118. ISSN: 2045-2322 . pmid: 26456148 (Oct. 12, 2015).
154. Wu, C. *et al.* Clonal Expansion and Compartmentalized Maintenance of Rhesus Macaque NK Cell Subsets. *Science Immunology* **3,** eaat9781. ISSN: 2470-9468. pmid: 30389798 (Nov. 2, 2018).
155. Björkström, N. K. *et al.* Rapid Expansion and Long-Term Persistence of Elevated NK Cell Numbers in Humans Infected with Hantavirus. *The Journal of Experimental Medicine* **208,** 13–21. ISSN: 1540-9538. pmid: 21173105 (Jan. 17, 2011).
156. O'Leary, J. G., Goodarzi, M., Drayton, D. L. & von Andrian, U. H. T Cell- and B Cell-Independent Adaptive Immunity Mediated by Natural Killer Cells. *Nature Immunology* **7,** 507–516. ISSN: 1529-2908. pmid: 16617337 (May 2006).
157. Paust, S. *et al.* Critical Role for the Chemokine Receptor CXCR6 in NK Cell-Mediated Antigen-Specific Memory of Haptens and Viruses. *Nature Immunology* **11,** 1127–1135. ISSN: 1529-2916. pmid: 20972432 (Dec. 2010).
158. Reeves, R. K. *et al.* Antigen-Specific NK Cell Memory in Rhesus Macaques. *Nature Immunology* **16,** 927–932. ISSN: 1529-2916. pmid: 26193080 (Sept. 2015).
159. Gumá, M. *et al.* Imprint of Human Cytomegalovirus Infection on the NK Cell Receptor Repertoire. *Blood* **104,** 3664–3671. ISSN: 0006-4971. pmid: 15304389 (Dec. 1, 2004).

160. Hammer, Q. *et al.* Peptide-Specific Recognition of Human Cytomegalovirus Strains Controls Adaptive Natural Killer Cells. *Nature Immunology* **19,** 453–463. ISSN: 1529-2916. pmid: 29632329 (May 2018).
161. Béziat, V. *et al.* NK Cell Responses to Cytomegalovirus Infection Lead to Stable Imprints in the Human KIR Repertoire and Involve Activating KIRs. *Blood* **121,** 2678–2688. ISSN: 1528-0020. pmid: 23325834 (Apr. 4, 2013).
162. Rückert, T., Lareau, C. A., Mashreghi, M.-F., Ludwig, L. S. & Romagnani, C. Clonal Expansion and Epigenetic Inheritance of Long-Lasting NK Cell Memory. *Nature Immunology* **23,** 1551–1563. ISSN: 1529-2916. pmid: 36289449 (Nov. 2022).
163. Pahl, J. H. W., Cerwenka, A. & Ni, J. Memory-Like NK Cells: Remembering a Previous Activation by Cytokines and NK Cell Receptors. *Frontiers in Immunology* **9.** ISSN: 1664-3224. https://www.frontiersin.org/articles/10.3389/fimmu.2018.02796 (2023) (2018).
164. Berrien-Elliott, M. M., Wagner, J. A. & Fehniger, T. A. Human Cytokine-Induced Memory-like Natural Killer Cells. *Journal of innate immunity* **7,** 563–571 (2015).
165. Bakhtiyaridovvombaygi, M. *et al.* Cytokine-Induced Memory-Like NK Cells: Emerging Strategy for AML Immunotherapy. *Biomedicine & Pharmacotherapy* **168,** 115718 (2023).
166. Biassoni, R. & Malnati, M. S. Human Natural Killer Receptors, Co-Receptors, and Their Ligands. *Current Protocols in Immunology* **121,** e47. ISSN: 1934-368X. pmid: 30040219 (Apr. 2018).
167. Li, J., Wilhelmy, J. & Davis, M. M. Characterization of KIR+CD8+ Regulatory T Cells in Humans by scRNA- and TCR-seq. *Methods in Molecular Biology (Clifton, N.J.)* **2574,** 41–121. ISSN: 1940-6029. pmid: 36087198 (2022).
168. Uhrberg, M. *et al.* Human Diversity in Killer Cell Inhibitory Receptor Genes. *Immunity* **7,** 753–763. ISSN: 1074-7613. pmid: 9430221 (Dec. 1997).
169. Hölzemer, A., Garcia-Beltran, W. F. & Altfeld, M. Natural Killer Cell Interactions with Classical and Non-Classical Human Leukocyte Antigen Class I in HIV-1 Infection. *Frontiers in Immunology* **8,** 1496. ISSN: 1664-3224. pmid: 29184550 (2017).
170. Carrington, M., Norman, P., Carrington, M. & Norman, P. *The KIR Gene Cluster* (National Center for Biotechnology Information (US), May 28, 2003).
171. Vilches, C. & Parham, P. KIR: Diverse, Rapidly Evolving Receptors of Innate and Adaptive Immunity. *Annual Review of Immunology* **20,** 217–251. ISSN: 0732-0582. pmid: 11861603 (2002).
172. Hsu, K. C., Chida, S., Geraghty, D. E. & Dupont, B. The Killer Cell Immunoglobulin-like Receptor (KIR) Genomic Region: Gene-Order, Haplotypes and Allelic Polymorphism. *Immunological Reviews* **190,** 40–52. ISSN: 0105-2896. pmid: 12493005 (Dec. 2002).

173. Khakoo, S. I. *et al.* Rapid Evolution of NK Cell Receptor Systems Demonstrated by Comparison of Chimpanzees and Humans. *Immunity* **12,** 687–698. ISSN: 1074-7613. pmid: 10894168. https://www.cell.com/immunity/%20%5Clinebreak%20abstract/S1074-7613(00)80219-8 (2023) (June 1, 2000).
174. Parham, P., Norman, P. J., Abi-Rached, L. & Guethlein, L. A. Variable NK Cell Receptors Exemplified by Human KIR3DL1/S1. *Journal of Immunology (Baltimore, Md.: 1950)* **187,** 11–19. ISSN: 1550-6606. pmid: 21690332 (July 1, 2011).
175. Medjouel Khlifi, H., Guia, S., Vivier, E. & Narni-Mancinelli, E. Role of the ITAM-Bearing Receptors Expressed by Natural Killer Cells in Cancer. *Frontiers in Immunology* **13,** 898745. ISSN: 1664-3224. pmid: 35757695 (2022).
176. André, P. *et al.* New Nomenclature for MHC Receptors. *Nature Immunology* **2,** 661. ISSN: 1529-2908. pmid: 11477395 (Aug. 2001).
177. Marsh, S. G. E. *et al.* Killer-Cell Immunoglobulin-like Receptor (KIR) Nomenclature Report, 2002. *Immunogenetics* **55,** 220–226. ISSN: 0093-7711 . pmid: 12838378 (July 2003).
178. Long, E. O., Colonna, M. & Lanier, L. L. Inhibitory MHC Class I Receptors on NK and T Cells: A Standard Nomenclature. *Immunology Today* **17,** 100. ISSN: 0167-5699. pmid: 8808061 (Feb. 1996).
179. Vilches, C., Pando, M. J. & Parham, P. Genes Encoding Human Killer-Cell Ig-like Receptors with D1 and D2 Extracellular Domains All Contain Untranslated Pseudoexons Encoding a Third Ig-like Domain. *Immunogenetics* **51,** 639–646. ISSN: 0093-7711. pmid: 10941835 (July 2000).
180. Olcese, L. *et al.* Human Killer Cell Activatory Receptors for MHC Class I Molecules Are Included in a Multimeric Complex Expressed by Natural Killer Cells. *Journal of Immunology (Baltimore, Md.: 1950)* **158,** 5083–5086. ISSN: 0022-1767. pmid: 9164921 (June 1, 1997).
181. Lanier, L. L., Corliss, B. C., Wu, J., Leong, C. & Phillips, J. H. Immunoreceptor DAP12 Bearing a Tyrosine-Based Activation Motif Is Involved in Activating NK Cells. *Nature* **391,** 703–707. ISSN: 0028-0836. pmid: 9490415 (Feb. 12, 1998).
182. Weiss, A. & Littman, D. R. Signal Transduction by Lymphocyte Antigen Receptors. *Cell* **76,** 263–274. ISSN: 0092-8674. pmid: 8293463 (Jan. 28, 1994).
183. Malissen, B. & Schmitt-Verhulst, A. M. Transmembrane Signalling through the T-cell-receptor-CD3 Complex. *Current Opinion in Immunology* **5,** 324–333. ISSN: 0952-7915. pmid: 8347295 (June 1993).
184. Cosson, P., Lankford, S. P., Bonifacino, J. S. & Klausner, R. D. Membrane Protein Association by Potential Intramembrane Charge Pairs. *Nature* **351,** 414–416. ISSN: 0028-0836. pmid: 1827877 (May 30, 1991).
185. Long, E. O. Negative Signaling by Inhibitory Receptors: The NK Cell Paradigm. *Immunological Reviews* **224,** 70–84. ISSN: 1600-065X. pmid: 18759921 (Aug. 2008).

186. Ono, M., Bolland, S., Tempst, P. & Ravetch, J. V. Role of the Inositol Phosphatase SHIP in Negative Regulation of the Immune System by the Receptor Fc(Gamma)RIIB. *Nature* **383,** 263–266. ISSN: 0028-0836. pmid: 8805703 (Sept. 19, 1996).

187. D'Ambrosio, D. *et al.* Recruitment and Activation of PTP1C in Negative Regulation of Antigen Receptor Signaling by Fc Gamma RIIB1. *Science (New York, N.Y.)* **268,** 293–297. ISSN: 0036-8075. pmid: 7716523 (Apr. 14, 1995).

188. Paulsen, M. & Janssen, O. Pro-and Anti-Apoptotic CD95 Signaling in T Cells. *Cell Communication and Signaling* **9,** 1–9 . https://biosignaling.biomedcentral.com/articles/10.1186/1478-811X-9-7 (2023) (2011).

189. Campbell, K. S. & Colonna, M. DAP12: A Key Accessory Protein for Relaying Signals by Natural Killer Cell Receptors. *The International Journal of Biochemistry & Cell Biology* **31,** 631–636. ISSN: 1357-2725. pmid: 10404635 (June 1999).

190. Hernández-Caselles, T., Miguel, R. C.-S., Ruiz-Alcaraz, A. J. & García- Peñarrubia, P. CD33 (Siglec-3) Inhibitory Function: Role in the NKG2D/DAP10 Activating Pathway. *Journal of Immunology Research* **2019,** 6032141. ISSN: 2314-8861. pmid: 31143782. https://www.ncbi.nlm.nih.gov/pmc/articles/PMC6501159/ (2023) (Apr. 15, 2019).

191. Upshaw, J. L. *et al.* NKG2D-mediated Signaling Requires a DAP10-bound Grb2-Vav1 Intermediate and Phosphatidylinositol-3-Kinase in Human Natural Killer Cells. *Nature Immunology* **7,** 524–532. ISSN: 1529-2908. pmid: 16582911 (May 2006).

192. Stojanovic, A., Correia, M. P. & Cerwenka, A. The NKG2D/NKG2DL Axis in the Crosstalk Between Lymphoid and Myeloid Cells in Health and Disease. *Frontiers in Immunology* **9,** 827. ISSN: 1664-3224. pmid: 29740438 (2018).

193. Latour, S. *et al.* Regulation of SLAM-mediated Signal Transduction by SAP, the X-linked Lymphoproliferative Gene Product. *Nature Immunology* **2,** 681–690. ISSN: 1529-2908. pmid: 11477403 (Aug. 2001).

194. Gonzalez-Galarza, F. F. *et al. Allele Frequency Net Database* Online (Nucleic Acid Research 2020, 2020). http://allelefrequencies.net/kir6002a.asp?kir_locus=&kir_allele1=3DL3&kir_allele2=3DL3*057&kir_selection=&kir_population=&kir_country=&kir_dataset=&kir_region=&kir_ethnic=Caucasoid&kir_study=&kir_order=order_1&kir_sample_size_pattern=equal&kir_sample_size=&kir_sample_year_pattern=equal&kir_sample_year=&kir_digits_pattern=equal&kir_digits=&kir_show= (2023).

195. Stephens, H. A. F. Immunogenetic Surveillance of HIV/AIDS. *Infection, Genetics and Evolution: Journal of Molecular Epidemiology and Evolutionary Genetics in Infectious Diseases* **12,** 1481–1491. ISSN: 1567-7257. pmid: 22575339 (Oct. 2012).

196. Parham, P. *et al.* Nature of Polymorphism in HLA-A, -B, and -C Molecules. *Proceedings of the National Academy of Sciences of the United States of America* **85,** 4005–4009. ISSN: 0027-8424. pmid: 3375250 (June 1988).
197. Howell, W. M., Carter, V. & Clark, B. The HLA System: Immunobiology, HLA Typing, Antibody Screening and Crossmatching Techniques. *Journal of Clinical Pathology* **63,** 387–390. ISSN: 1472-4146. pmid: 20418230 (May 2010).
198. Kulski, J. K., Suzuki, S. & Shiina, T. Human Leukocyte Antigen Super-Locus: Nexus of Genomic Supergenes, SNPs, Indels, Transcripts, and Haplotypes. *Human Genome Variation* **9,** 1–15. ISSN: 2054-345X. https://www.nature.com/articles/s41439-022-00226-5 (2023) (1 Dec. 21, 2022).
199. Wieczorek, M. *et al.* Major Histocompatibility Complex (MHC) Class I and MHC Class II Proteins: Conformational Plasticity in Antigen Presentation. *Frontiers in Immunology* **8.** ISSN: 1664-3224. https://www.frontiersin.org/articles/10.3389/fimmu.2017.00292 (2023) (2017).
200. Shiina, T., Hosomichi, K., Inoko, H. & Kulski, J. K. The HLA Genomic Loci Map: Expression, Interaction, Diversity and Disease. *Journal of Human Genetics* **54,** 15–39. ISSN: 1435-232X. pmid: 19158813 (Jan. 2009).
201. Crux, N. B. & Elahi, S. Human Leukocyte Antigen (HLA) and Immune Regulation: How Do Classical and Non-Classical HLA Alleles Modulate Immune Response to Human Immunodeficiency Virus and Hepatitis C Virus Infections? *Frontiers in Immunology* **8,** 832. ISSN: 1664-3224. pmid: 28769934 (2017).
202. Robinson, J. *et al.* The IPD and IMGT/HLA Database: Allele Variant Databases. *Nucleic Acids Research* **43,** D423–431. ISSN: 1362-4962. pmid: 25414341 (Data base issue Jan. 2015).
203. Robinson, J. *et al.* Distinguishing Functional Polymorphism from Random Variation in the Sequences of >10,000 HLA-A, -B and -C Alleles. *PLoS genetics* **13,** e1006862. ISSN: 1553-7404. pmid: 28650991 (June 2017).
204. Little, A. M. & Parham, P. Polymorphism and Evolution of HLA Class I and II Genes and Molecules. *Reviews in Immunogenetics* **1,** 105–123. ISSN: 1398-1714. pmid: 11256568 (1999).
205. Garcia-Beltran, W. F. *et al.* Open Conformers of HLA-F Are High-Affinity Ligands of the Activating NK-cell Receptor KIR3DS1. *Nature immunology* **17,** 1067–1074. ISSN: 1529-2916 1529-2908. pmid: 27455421 (Sept. 2016).
206. Niehrs, A. & Altfeld, M. Regulation of NK-Cell Function by HLA Class II. *Frontiers in cellular and infection microbiology* **10,** 55. ISSN: 2235-2988 . pmid: 32133304 (2020).
207. Niehrs, A. *et al.* A Subset of HLA-DP Molecules Serve as Ligands for the Natural Cytotoxicity Receptor NKp44. *Nature immunology* **20,** 1129–1137. ISSN: 1529-2916 1529-2908. pmid: 31358998 (Sept. 2019).
208. Rock, K. L., York, I. A. & Goldberg, A. L. Post-Proteasomal Antigen Processing for Major Histocompatibility Complex Class I Presentation. *Nature Immunology* **5,** 670–677. ISSN: 1529-2908. pmid: 15224092 (July 2004).

209. Hämmerling, G. J. & Moreno, J. The Function of the Invariant Chain in Antigen Presentation by MHC Class II Molecules. *Immunology Today* **11,** 337–340. ISSN: 0167-5699. pmid: 1977405 (Oct. 1990).
210. Teyton, L. *et al.* Invariant Chain Distinguishes between the Exogenous and Endogenous Antigen Presentation Pathways. *Nature* **348,** 39–44. ISSN: 0028-0836. pmid: 2234057 (Nov. 1, 1990).
211. Ting, J. P.-Y. & Trowsdale, J. Genetic Control of MHC Class II Expression. *Cell* **109 Suppl,** S21–33. ISSN: 0092-8674. pmid: 11983150 (Apr. 2002).
212. Muhlethaler-Mottet, A., Otten, L. A., Steimle, V. & Mach, B. Expression of MHC Class II Molecules in Different Cellular and Functional Compartments Is Controlled by Differential Usage of Multiple Promoters of the Transactivator CIITA. *The EMBO journal* **16,** 2851–2860. ISSN: 0261-4189. pmid: 9184229 (May 15, 1997).
213. Boyington, J. C., Motyka, S. A., Schuck, P., Brooks, A. G. & Sun, P. D. Crystal Structure of an NK Cell Immunoglobulin-like Receptor in Complex with Its Class I MHC Ligand. *Nature* **405,** 537–543. ISSN: 0028-0836. pmid: 10850706 (June 1, 2000).
214. Stewart-Jones, G. B. E. *et al.* Crystal Structures and KIR3DL1 Recognition of Three Immunodominant Viral Peptides Complexed to HLA-B*2705. *European Journal of Immunology* **35,** 341–351. ISSN: 0014-2980. pmid: 15657948 (Feb. 2005).
215. Fadda, L. *et al.* Common HIV-1 Peptide Variants Mediate Differential Binding of KIR3DL1 to HLA-Bw4 Molecules. *Journal of Virology* **85,** 5970–5974. ISSN: 1098-5514. pmid: 21471246 (June 2011).
216. Sim, M. J. W. *et al.* Canonical and Cross-reactive Binding of NK Cell Inhibitory Receptors to HLA-C Allotypes Is Dictated by Peptides Bound to HLA-C. *Frontiers in Immunology* **8.** ISSN: 1664-3224. https://www.frontiersin.org/articles/10.3389/fimmu.2017.00193 (2023) (2017).
217. Borhis, G. *et al.* A Peptide Antagonist Disrupts NK Cell Inhibitory Synapse Formation. *Journal of Immunology (Baltimore, Md.: 1950)* **190,** 2924–2930. ISSN: 1550-6606. pmid: 23382564 (Mar. 15, 2013).
218. Fadda, L. *et al.* Peptide Antagonism as a Mechanism for NK Cell Activation. *Proceedings of the National Academy of Sciences of the United States of America* **107,** 10160–10165. ISSN: 0027-8424. pmid: 20439706. https://www.ncbi.nlm.nih.gov/pmc/articles/PMC2890497/ (2023) (June 1, 2010).
219. Torkar, M., Norgate, Z., Colonna, M., Trowsdale, J. & Wilson, M. J. Isotypic Variation of Novel Immunoglobulin-like Transcript/Killer Cell Inhibitory Receptor Loci in the Leukocyte Receptor Complex. *European Journal of Immunology* **28,** 3959–3967. ISSN: 0014-2980. pmid: 9862332 (Dec. 1998).
220. Wilson, M. J. *et al.* Plasticity in the Organization and Sequences of Human KIR/ILT Gene Families. *Proceedings of the National Academy of Sciences of the*

United States of America **97,** 4778–4783. ISSN: 0027-8424 . pmid: 10781084 (Apr. 25, 2000).

221. Vendelbosch, S. *et al.* Extensive Variation in Gene Copy Number at the Killer Immunoglobulin-like Receptor Locus in Humans. *PloS One* **8,** e67619. ISSN: 1932-6203. pmid: 23840750 (2013).
222. Hollenbach, J. A., Nocedal, I., Ladner, M. B., Single, R. M. & Trachtenberg, E. A. Killer Cell Immunoglobulin-like Receptor (KIR) Gene Content Variation in the HGDP-CEPH Populations. *Immunogenetics* **64,** 719–737. ISSN: 1432-1211. pmid: 22752190 (Oct. 2012).
223. Leaton, L. A. *et al.* Conservation, Extensive Heterozygosity, and Convergence of Signaling Potential All Indicate a Critical Role for KIR3DL3 in Higher Primates. *Frontiers in Immunology* **10,** 24. ISSN: 1664-3224. pmid: 30745901 (2019).
224. Martin, A. M. *et al.* Comparative Genomic Analysis, Diversity and Evolution of Two KIR Haplotypes A and B. *Gene* **335,** 121–131. ISSN: 0378-1119. pmid: 15194195 (June 23, 2004).
225. Guethlein, L. A., Flodin, L. R., Adams, E. J. & Parham, P. NK Cell Receptors of the Orangutan (Pongo Pygmaeus): A Pivotal Species for Tracking the Coevolution of Killer Cell Ig-Like Receptors with MHC-C1. *The Journal of Immunology* **169,** 220–229. ISSN: 0022-1767. https://doi.org/10.4049/jimmunol.169.1.220 (2023) (July 1, 2002).
226. Hershberger, K. L., Shyam, R., Miura, A. & Letvin, N. L. Diversity of the Killer Cell Ig-Like Receptors of Rhesus Monkeys1 2. *The Journal of Immunology* **166,** 4380–4390. ISSN: 0022-1767. https://doi.org/10.4049/jimmunol.166.7.4380 (2023) (Apr. 1, 2001).
227. Abi-Rached, L. *et al.* A Small, Variable, and Irregular Killer Cell Ig-Like Receptor Locus Accompanies the Absence of MHC-C and MHC-G in Gibbons. *The Journal of Immunology* **184,** 1379–1391. ISSN: 0022-1767. https://doi.org/10.4049/jimmunol.0903016 (2023) (Dec. 21, 2009).
228. Hou, L., Chen, M., Ng, J. & Hurley, C. K. Conserved KIR Allele-Level Haplotypes Are Altered by Microvariation in Individuals with European Ancestry. *Genes and Immunity* **13,** 47–58. ISSN: 1476-5470. pmid: 21796155 (Jan. 2012).
229. Wongfieng, W., Nutalai, R., Jumnainsong, A. & Leelayuwat, C. Quantitative Multiplex Real-Time Reverse Transcriptase-Polymerase Chain Reaction with Fluorescent Probe Detection of Killer Immunoglobulin-Like Receptors, KIR2DL4/3DL3. *Diagnostics (Basel, Switzerland)* **10,** 588. ISSN: 2075-4418. pmid: 32823754 (Aug. 13, 2020).
230. Nutalai, R., Gaudieri, S., Jumnainsong, A. & Leelayuwat, C. Regulation of KIR3DL3 Expression via Mirna. *Genes* **10,** 603. ISSN: 2073-4425. pmid: 31405037 (Aug. 9, 2019).
231. Trompeter, H.-I. *et al.* Three Structurally and Functionally Divergent Kinds of Promoters Regulate Expression of Clonally Distributed Killer Cell Ig-like

Receptors (KIR), of KIR2DL4, and of KIR3DL3. *Journal of Immunology (Baltimore, Md.: 1950)* **174,** 4135–4143. ISSN: 0022-1767. pmid: 15778373 (Apr. 1, 2005).

232. Santourlidis, S. *et al.* Crucial Role of DNA Methylation in Determination of Clonally Distributed Killer Cell Ig-like Receptor Expression Patterns in NK Cells. *Journal of Immunology (Baltimore, Md.: 1950)* **169,** 4253–4261. ISSN: 0022-1767. pmid: 12370356 (Oct. 15, 2002).
233. Li, H., Wright, P. W., McCullen, M. & Anderson, S. K. Characterization of KIR Intermediate Promoters Reveals Four Promoter Types Associated with Distinct Expression Patterns of KIR Subtypes. *Genes & Immunity* **17,** 66–74. ISSN: 1476-5470. https://www.nature.com/articles/gene201556 (2023) (1 Jan. 2016).
234. Jones, D. C., Hiby, S. E., Moffett, A., Trowsdale, J. & Young, N. T. Nature of Allelic Sequence Polymorphism at the KIR3DL3 Locus. *Immunogenetics* **58,** 614–627. ISSN: 0093-7711. pmid: 16823588 (Aug. 2006).
235. Uhrberg, M., Parham, P. & Wernet, P. Definition of Gene Content for Nine Common Group B Haplotypes of the Caucasoid Population: KIR Haplotypes Contain between Seven and Eleven KIR Genes. *Immunogenetics* **54,** 221–229. ISSN: 0093-7711. pmid: 12136333 (July 2002).
236. Swainson, L. A., Mold, J. E., Bajpai, U. D. & McCune, J. M. Expression of the Autoimmune Susceptibility Gene FcRL3 on Human Regulatory T Cells Is Associated with Dysfunction and High Levels of Programmed Cell Death-1. *The Journal of Immunology* **184,** 3639–3647. ISSN: 0022-1767. https://doi.org/10.4049/jimmunol.0903943 (2023) (Apr. 1, 2010).
237. El-Gebali, S. *et al.* The Pfam Protein Families Database in 2019. *Nucleic Acids Research* **47,** D427–D432. ISSN: 1362-4962. pmid: 30357350 (Jan. 8, 2019).
238. Kammerer, U., Kruse, A., Barrientos, G., Arck, P. C. & Blois, S. M. Role of Dendritic Cells in the Regulation of Maternal Immune Responses to the Fetus during Mammalian Gestation. *Immunological Investigations* **37,** 499–533. ISSN: 1532-4311. pmid: 18716936 (2008).
239. Olivares, E. G., Montes, M. J., Oliver, C., Galindo, J. A. & Ruiz, C. Cultured Human Decidual Stromal Cells Express B7-1 (CD80) and B7-2 (CD86) and Stimulate Allogeneic T Cells. *Biology of Reproduction* **57,** 609–615. ISSN: 0006-3363. pmid: 9282998 (Sept. 1997).
240. Lorek, D., Kedzierska, A. E., Slawek, A. & Chelmonska-Soyta, A. Expression of Toll-like Receptors and Costimulatory Molecules in Splenic B Cells in a Normal and Abortion-Prone Murine Pregnancy Model. *American Journal of Reproductive Immunology (New York, N.Y.: 1989)* **82,** e13148. ISSN: 1600-0897. pmid: 31134706 (Aug. 2019).

241. Guleria, I. *et al.* A Critical Role for the Programmed Death Ligand 1 in Fetomaternal Tolerance. *The Journal of Experimental Medicine* **202,** 231–237. ISSN: 0022-1007. pmid: 16027236 (July 18, 2005).
242. Ohno, T. *et al.* The Immune Checkpoint Molecule VISTA Regulates Allergen-Specific Th2-mediated Immune Responses. *International Immunology* **30,** 3–11. ISSN: 1460-2377. pmid: 29267882 (Feb. 3, 2018).
243. Mach, P. *et al.* Changes in the Blood Serum Levels of the Costimulatory Soluble B7-H4 Molecule in Pregnant Women During the Peripartal Phase. *American Journal of Reproductive Immunology (New York, N.Y.: 1989)* **74,** 209–215. ISSN: 1600-0897. pmid: 25907449 (Sept. 2015).
244. Mach, P. *et al.* Soluble B7-H4 Blood Serum Levels Are Elevated in Women at High Risk for Preeclampsia in the First Trimester, as Well as in Patients with Confirmed Preeclampsia. *American Journal of Reproductive Immunology (New York, N.Y.: 1989)* **80,** e12988. ISSN: 1600-0897. pmid: 29797540 (Sept. 2018).
245. Darmochwal-Kolarz, D. *et al.* The Expression of B7-H1 and B7-H4 Co-Stimulatory Molecules on Myeloid and Plasmacytoid Dendritic Cells in Pre-Eclampsia and Normal Pregnancy. *Journal of Reproductive Immunology* **99,** 33–38. ISSN: 1872-7603. pmid: 23773232 (Sept. 2013).
246. Grozdics, E. *et al.* B7 Costimulation and Intracellular Indoleamine-2,3-Dioxygenase (IDO) Expression in Peripheral Blood of Healthy Pregnant and Non-Pregnant Women. *BMC pregnancy and childbirth* **14,** 306. ISSN: 1471-2393. pmid: 25189405 (Sept. 4, 2014).
247. Bolandi, N. *et al.* The Positive and Negative Immunoregulatory Role of B7 Family: Promising Novel Targets in Gastric Cancer Treatment. *International Journal of Molecular Sciences* **22,** 10719. ISSN: 1422-0067. pmid: 34639059 (Oct. 3, 2021).
248. Lens, M., Ferrucci, P. F. & Testori, A. Anti-CTLA4 Monoclonal Antibody Ipilimumab in the Treatment of Metastatic Melanoma: Recent Findings. *Recent Patents on Anti-Cancer Drug Discovery* **3,** 105–113. ISSN: 1574-8928 . pmid: 18537753 (June 2008).
249. Tamura, H. *et al.* Expression of Functional B7-H2 and B7.2 Costimulatory Molecules and Their Prognostic Implications in de Novo Acute Myeloid Leukemia. *Clinical Cancer Research: An Official Journal of the American Association for Cancer Research* **11,** 5708–5717. ISSN: 1078-0432 . pmid: 16115907 (Aug. 15, 2005).
250. Sun, Y. *et al.* B7-H3 and B7-H4 Expression in Non-Small-Cell Lung Cancer. *Lung Cancer (Amsterdam, Netherlands)* **53,** 143–151. ISSN: 0169-5002 . pmid: 16782226 (Aug. 2006).
251. Ingebrigtsen, V. A. *et al.* B7-H3 Expression in Colorectal Cancer: Nuclear Localization Strongly Predicts Poor Outcome in Colon Cancer. *International Journal of Cancer* **131,** 2528–2536. ISSN: 1097-0215. pmid: 22473715 (Dec. 1, 2012).

252. Philips, G. K. & Atkins, M. Therapeutic Uses of Anti-PD-1 and Anti-PD-L1 Antibodies. *International Immunology* **27,** 39–46. ISSN: 1460-2377. pmid: 25323844 (Jan. 2015).

253. Mansh, M. Ipilimumab and Cancer Immunotherapy: A New Hope for Advanced Stage Melanoma. *The Yale Journal of Biology and Medicine* **84,** 381–389. ISSN: 1551-4056. pmid: 22180676 (Dec. 2011).

254. U.S. National Library of Medicine, U. *ClinicalTrial.Gov* (Dec. 22, 2023). https://clinicaltrials.gov/search?term=CTLA-4&viewType=Table&cond=cancer&limit=100&page=1 (2023).

255. Khan, M., Arooj, S. & Wang, H. NK Cell-Based Immune Checkpoint Inhibition. *Frontiers in Immunology* **11,** 167. ISSN: 1664-3224. pmid: 32117298 (2020).

256. Robert, C. A Decade of Immune-Checkpoint Inhibitors in Cancer Therapy. *Nature Communications* **11,** 3801. ISSN: 2041-1723. https://www.nature.com/articles/s41467-020-17670-y (2023) (1 July 30, 2020).

257. Pulanco, M. C., Madsen, A. T., Tanwar, A., Corrigan, D. T. & Zang, X. Recent Advancements in the B7/CD28 Immune Checkpoint Families: New Biology and Clinical Therapeutic Strategies. *Cellular & Molecular Immunology* **20,** 694–713. ISSN: 2042-0226. https://www.nature.com/articles/s41423-023-01019-8 (2023) (7 July 2023).

258. Lian, B. *et al.* IBI310 Monotherapy or in Combination with Sintilimab in Patients with Advanced Melanoma: An Open-Label Phase Ia/1b Study. *Journal of Clinical Oncology* **38,** e15111–e15111. ISSN: 0732-183X. https://ascopubs.org/doi/10.1200/JCO.2020.38.15_suppl.e15111 (2023) (May 2020).

259. Gao, X. *et al.* Safety and Antitumour Activity of Cadonilimab, an Anti-PD-1/CTLA-4 Bispecific Antibody, for Patients with Advanced Solid Tumours (COMPASSION-03): A Multicentre, Open-Label, Phase 1b/2 Trial. *The Lancet. Oncology* **24,** 1134–1146. ISSN: 1474-5488. pmid: 37797632 (Oct. 2023).

260. Wilky, B. A. *et al.* Phase I Open-Label, Ascending Dose Trial of AGEN1884, an Anti-CTLA-4 Monoclonal Antibody, in Advanced Solid Malignancies: Dose Selection for Combination with PD-1 Blockade. *Journal of Clinical Oncology* **36,** 3075–3075. ISSN: 0732-183X. https://ascopubs.org/doi/10.1200/JCO.2018.36.15_suppl.3075 (2023) (15_suppl May 20, 2018).

261. Friedman, C. *et al.* 393 First-in-human Phase 1/2a Study of the Novel Non-fucosylated Anti–CTLA-4 Monoclonal Antibody BMS-986218 ± Nivolumab in Advanced Solid Tumors: Initial Phase 1 Results. *Journal for ImmunoTherapy of Cancer* **8.** ISSN: 2051-1426. https://jitc.bmj.com/content/8/Suppl_3/A239.1 (2023) (Suppl 3 Nov. 1, 2020).

262. Gay, C. L. *et al.* Clinical Trial of the Anti-PD-L1 Antibody BMS-936559 in HIV-1 Infected Participants on Suppressive Antiretroviral Therapy. *The Journal of Infectious Diseases* **215,** 1725–1733. ISSN: 1537-6613. pmid: 28431010 (June 1, 2017).

263. Engelhardt, J. *et al.* Abstract 4552: Preclinical Characterization of BMS-986218, a Novel Nonfucosylated Anti–CTLA-4 Antibody Designed to Enhance Antitumor Activity. *Cancer Research* **80,** 4552. ISSN: 0008-5472. https://doi.org/10.1158/1538-7445.AM2020-4552 (2023) (16_Supplement Aug. 15, 2020).
264. Collins, J. M. & Gulley, J. L. Product Review: Avelumab, an Anti-PD-L1 Antibody. *Human Vaccines & Immunotherapeutics* **15,** 891–908. ISSN: 2164-554X. pmid: 30481100 (2019).
265. Desai, J. *et al.* Abstract CT253: Preliminary Safety and Efficacy Data of BGB-A333, an Anti-PD-L1 Monoclonal Antibody, Alone and in Combination with Tislelizumab in Patients with Advanced Solid Tumors. *Cancer Research* **80,** CT253. ISSN: 0008-5472. https://doi.org/10.1158/1538-7445.AM2020-CT253 (2023) (16_Supplement Aug. 15, 2020).
266. Myint, H. *et al.* 748 A Phase 1/2, Open-Label, Dose-Escalation, Safety and Tolerability Study of NC762 in Subjects with Advanced or Metastatic Solid Tumors. *Journal for ImmunoTherapy of Cancer* **10.** ISSN: 2051-1426. https://jitc.bmj.com/content/10/Suppl_2/A781 (2023) (Suppl 2 Nov. 1, 2022).
267. Koopman, L. *et al.* 863 In Vitro and in Vivo Studies Establish DuoBody®-CD3xB7H4 as a Novel Drug Candidate for the Treatment of Solid Cancers. *Journal for ImmunoTherapy of Cancer* **9.** ISSN: 2051-1426. https://jitc.bmj.com/content/9/Suppl_2/A904 (2023) (Suppl 2 Nov. 1, 2021).
268. Park, K. *et al.* Abstract 4246: ABL103, A Novel T-cell Engaging Bispecific Antibody, Exhibits Potent in Vitro and Vivo Antitumor Activity and Low Toxicity via B7-H4 Dependent 4-1BB Activation in Tumor Microenvironment. *Cancer Research* **82,** 4246. ISSN: 0008-5472. https://doi.org/10.1158/1538-7445.AM2022-4246 (2023) (12_Supplement June 15, 2022).
269. Wu, J. *et al.* 381O First-in-human/Phase I Trial of HS-20089, a B7-H4 ADC, in Patients with Advanced Solid Tumors. *Annals of Oncology* **34,** S336. ISSN: 0923-7534, 1569-8041. https://www.annalsofoncology.org/article/S0923-7534(23)01394-7/fulltext (2023) (Oct. 1, 2023).
270. Sachdev, J. C. *et al.* Phase 1a/1b Study of First-in-Class B7-H4 Antibody, FPA 150, as Monotherapy in Patients with Advanced Solid Tumors. *Journal of Clinical Oncology* **37,** 2529–2529. ISSN: 0732-183X. https://ascopubs.org/doi/abs/10.1200/JCO.2019.37.15_suppl.2529 (2023) (15_suppl May 20, 2019).
271. Wainberg, Z. A. *et al.* 1198P - FPA150 (B7-H4 Antibody) Phase I Update in Advanced Solid Tumours: Monotherapy and in Combination with Pembrolizumab. *Annals of Oncology. Abstract Book of the 44th ESMO Congress (ESMO 2019) 27 September – 1 October 2019, Barcelona, Spain* **30,** v489. ISSN: 0923-7534. https://www.sciencedirect.com/science/article/pii/S0923753419594108 (2023) (Oct. 1, 2019).

272. Patnaik, A., Lakhani, N. J., Xu, P., Nazarenko, N. N. & Call, J. A. Phase 1 Study of SGN-B7H4V, a Novel, Investigational Vedotin Antibody–Drug Conjugate Directed to B7-H4, in Patients with Advanced Solid Tumors (SGNB7H4V-001, Trial in Progress). *Journal of Clinical Oncology* **40,** TPS3155–TPS3155. ISSN: 0732-183X. https://ascopubs.org/doi/abs/10.1200/JCO.2022.40.16_suppl.TPS3155 (2023) (June 2022).

273. Shilts, J. *et al.* A Physical Wiring Diagram for the Human Immune System. *Nature* **608,** 397–404. ISSN: 1476-4687. pmid: 35922511 (Aug. 2022).

274. Huang, X. *et al.* VISTA: An Immune Regulatory Protein Checking Tumor and Immune Cells in Cancer Immunotherapy. *Journal of Hematology & Oncology* **13,** 83. ISSN: 1756-8722. pmid: 32600443 (June 29, 2020).

275. Falchook, G. S. *et al.* A First-in-Human Phase I Dose-Escalation Trial of the B7-H6/CD3 T-cell Engager BI 765049 ± Ezabenlimab (BI 754091) in Patients with Advanced Solid Tumors Expressing B7-H6. *Journal of Clinical Oncology* **40,** TPS3175–TPS3175. ISSN: 0732-183X. https://ascopubs.org/doi/abs/10.1200/JCO.2022.40.16_suppl.TPS3175 (2023) (June 2022).

276. BioMed, H. *HBM1020 in Advanced Solid Tumor - Clinical Trials Registry - ICH GCP* ClinicalTrials.gov. https://ichgcp.net/clinical-trials-registry/NCT05824663 (2023).

277. Lamb, M. *et al.* 489 NPX267, a First-in-Class Monoclonal Antibody Targeting KIR3DL3, Blocks HHLA2-mediated Immunosuppression and Potentiates T and NK Cell-Mediated Antitumor Immunity. *Journal for ImmunoTherapy of Cancer* **10.** ISSN: 2051-1426. https://jitc.bmj.com/content/10/Suppl_2/A510 (2023) (Nov. 1, 2022).

278. Naing, A. *et al.* 633 A Phase 1a/1b, Dose-Escalation/Dose-Expansion Study of NPX267 in Subjects with Solid Tumors Known to Express HHLA2. *Journal for ImmunoTherapy of Cancer* **11.** ISSN: 2051-1426. https://jitc.bmj.com/content/11/Suppl_1/A723 (2023) (Nov. 1, 2023).

279. Janakiram, M. *et al.* The Third Group of the B7-CD28 Immune Checkpoint Family: HHLA2, TMIGD2, B7x, and B7-H3. *Immunological reviews* **276,** 26–39. ISSN: 1600-065X 0105-2896. pmid: 28258693 (Mar. 2017).

280. Ahangar, N. K. *et al.* The Regulatory Cross-Talk between microRNAs and Novel Members of the B7 Family in Human Diseases: A Scoping Review. *International Journal of Molecular Sciences* **22,** 2652. ISSN: 1422-0067. pmid: 33800752 (Mar. 6, 2021).

281. Wang, B., Ran, Z., Liu, M. & Ou, Y. Prognostic Significance of Potential Immune Checkpoint Member HHLA2 in Human Tumors: A Comprehensive Analysis. *Frontiers in Immunology* **10,** 1573. ISSN: 1664-3224. pmid: 31379814 (2019).

282. Janakiram, M., Chinai, J. M., Zhao, A., Sparano, J. A. & Zang, X. HHLA2 and TMIGD2: New Immunotherapeutic Targets of the B7 and CD28 Families. *Oncoimmunology* **4,** e1026534. ISSN: 2162-4011. pmid: 26405587 (Aug. 2015).

283. Wei, L., Tang, L., Chang, H., Huo, S. & Li, Y. HHLA2 Overexpression Is a Novel Biomarker of Malignant Status and Poor Prognosis in Gastric Cancer. *Human Cell* **33,** 116–122. ISSN: 1749-0774. pmid: 31552567 (Jan. 2020).
284. Ying, H., Xu, J., Zhang, X., Liang, T. & Bai, X. Human Endogenous Retrovirus-H Long Terminal Repeat-Associating 2: The next Immune Checkpoint for Antitumour Therapy. *EBioMedicine* **79,** 103987. ISSN: 2352-3964. pmid: 35439678 (May 2022).
285. Koirala, P. *et al.* HHLA2, a Member of the B7 Family, Is Expressed in Human Osteosarcoma and Is Associated with Metastases and Worse Survival. *Scientific Reports* **6,** 31154. ISSN: 2045-2322. pmid: 27531281 (Aug. 17, 2016).
286. Chen, D. *et al.* Upregulated Immune Checkpoint HHLA2 in Clear Cell Renal Cell Carcinoma: A Novel Prognostic Biomarker and Potential Therapeutic Target. *Journal of Medical Genetics* **56,** 43–49. ISSN: 1468-6244. pmid: 29967134 (Jan. 2019).
287. Zhu, Y. *et al.* B7-H5 Costimulates Human T Cells via CD28H. *Nature Communications* **4,** 2043. ISSN: 2041-1723. https://www.nature.com/articles/ncomms3043 (2023) (1 June 19, 2013).
288. Zhuang, X. & Long, E. O. CD28 Homolog Is a Strong Activator of Natural Killer Cells for Lysis of B7H7+ Tumor Cells. *Cancer Immunology Research* **7,** 939–951. ISSN: 2326-6074. pmid: 31018957 (June 2019).
289. Biotechne. *Kd B7-H7 CD28H* Dec. 21, 2023. https://www.bio-techne.com/reagents/proteins/b7-h7-protein (2023).
290. Rieder, S. A. *et al.* B7-H7 (HHLA2) Inhibits T-cell Activation and Proliferation in the Presence of TCR and CD28 Signaling. *Cellular & Molecular Immunology* **18,** 1503–1511. ISSN: 2042-0226. https://www.nature.com/articles/s41423-020-0361-7 (2023) (6 June 2021).
291. Guo, H. *et al.* HHLA2 Activates the JAK/STAT Signaling Pathway by Binding to TMIGD2 in Hepatocellular Carcinoma Cells. *Inflammation* **45,** 1585–1599. ISSN: 1573-2576. pmid: 35175496 (Aug. 2022).
292. Maruthamuthu, S. *et al.* Individualized Constellation of Killer Cell Immunoglobulin-Like Receptors and Cognate HLA Class I Ligands That Controls Natural Killer Cell Antiviral Immunity Predisposes COVID-19. *Frontiers in genetics* **13,** 845474. ISSN: 1664-8021. pmid: 35273641 (2022).
293. Britannica, T. E. o. E. Human Body. *Encyclopedia Britannica.* https://www.britannica.com/science/human-body. (2023) (June 14, 2023).
294. Benjamini, Y. & Hochberg, Y. Controlling the False Discovery Rate: A Practical and Powerful Approach to Multiple Testing. *Journal of the Royal Statistical Society: Series B (Methodological)* **57,** 289–300. ISSN: 0035-9246. https://doi.org/10.1111/j.2517-6161.1995.tb02031.x (2023) (Jan. 1, 1995).
295. Vollmers, S., Lobermeyer, A. & Körner, C. The New Kid on the Block: HLA-C, a Key Regulator of Natural Killer Cells in Viral Immunity. *Cells* **10.** ISSN: 2073-4409. pmid: 34831331 (Nov. 10, 2021).

296. Beelen, N. A., Ehlers, F. A. I., Bos, G. M. J. & Wieten, L. Inhibitory Receptors for HLA Class I as Immune Checkpoints for Natural Killer Cell-Mediated Antibody-Dependent Cellular Cytotoxicity in Cancer Immunotherapy. *Cancer immunology, immunotherapy : CII* **72,** 797–804. ISSN: 1432-0851 0340-7004. pmid: 36261539 (Apr. 2023).

297. Hou, L. *et al.* Seventeen Novel Alleles Add to the Already Extensive KIR3DL3 Diversity. *Tissue Antigens* **70,** 449–454. https://onlinelibrary.wiley.com/doi/abs/10.1111/j.1399-0039.2007.00930.x (2007).

298. Britten, C. M. *et al.* The Use of HLA-A*0201-Transfected K562 as Standard Antigen-Presenting Cells for CD8(+) T Lymphocytes in IFN-gamma ELISPOT Assays. *Journal of immunological methods* **259,** 95–110. ISSN: 0022-1759. pmid: 11730845 (Jan. 1, 2002).

299. Garson, D., Dokhélar, M. C., Wakasugi, H., Mishal, Z. & Tursz, T. HLA Class-I and Class-II Antigen Expression by Human Leukemic K562 Cells and by Burkitt-K562 Hybrids: Modulation by Differentiation Inducers and Interferon. *Experimental hematology* **13,** 885–890. ISSN: 0301-472X . pmid: 3930277 (Oct. 1985).

300. ATCC. *NK-92MI* Nov. 2, 2023. https://www.atcc.org/products/crl-2408 (2023).

301. Kelly, A. & Trowsdale, J. Introduction: MHC/KIR and Governance of Specificity. *Immunogenetics* **69,** 481–488. ISSN: 1432-1211 . pmid: 28695288 (Aug. 2017).

302. D'Silva, S. Z., Singh, M. & Pinto, A. S. NK Cell Defects: Implication in Acute Myeloid Leukemia. *Frontiers in Immunology* **14,** 1112059. ISSN: 1664-3224. pmid: 37228595 (2023).

303. Dębska-Zielkowska, J. *et al.* KIR Receptors as Key Regulators of NK Cells Activity in Health and Disease. *Cells* **10,** 1777. ISSN: 2073-4409. pmid: 34359951 (July 14, 2021).

304. Kulkarni, S., Martin, M. P. & Carrington, M. The Yin and Yang of HLA and KIR in Human Disease. *Seminars in Immunology* **20,** 343–352. ISSN: 1044-5323. pmid: 18635379 (Dec. 2008).

305. Khakoo, S. I. *et al.* HLA and NK Cell Inhibitory Receptor Genes in Resolving Hepatitis C Virus Infection. *Science (New York, N.Y.)* **305,** 872–874. ISSN: 1095-9203. pmid: 15297676 (Aug. 6, 2004).

306. Martin, M. P. *et al.* Epistatic Interaction between KIR3DS1 and HLA-B Delays the Progression to AIDS. *Nature Genetics* **31,** 429–434. ISSN: 1061-4036. pmid: 12134147 (Aug. 2002).

307. Kiessling, R. *et al.* Killer Cells: A Functional Comparison between Natural, Immune T-cell and Antibody-Dependent in Vitro Systems. *The Journal of Experimental Medicine* **143,** 772–780. ISSN: 0022-1007. pmid: 1082915. https://www.ncbi.nlm.nih.gov/pmc/articles/PMC2190156/ (2023) (Apr. 1, 1976).

308. Orange, J. S. Natural Killer Cell Deficiency. *The Journal of Allergy and Clinical Immunology* **132,** 515–525. ISSN: 1097-6825. pmid: 23993353 (Sept. 2013).
309. Mace, E. M. & Orange, J. S. Emerging Insights into Human Health and NK Cell Biology from the Study of NK Cell Deficiencies. *Immunological Reviews* **287,** 202–225. ISSN: 1600-065X. pmid: 30565241 (Jan. 2019).
310. Vargas-Hernández, A. & Forbes, L. R. The Impact of Immunodeficiency on NK Cell Maturation and Function. *Current Allergy and Asthma Reports* **19,** 2. ISSN: 1534-6315. pmid: 30661124 (Jan. 19, 2019).
311. McCusker, C., Upton, J. & Warrington, R. Primary Immunodeficiency. *Allergy, Asthma, and Clinical Immunology: Official Journal of the Canadian Society of Allergy and Clinical Immunology* **14,** 61. ISSN: 1710-1484. pmid: 30275850 (Suppl 2 2018).
312. Ozdemir, O. Primary Immunodeficiency Diseases in the Newborn. *Northern Clinics of Istanbul* **8,** 405–413. ISSN: 2148-4902. pmid: 34585079. https://www.ncbi.nlm.nih.gov/pmc/articles/PMC8430363/ (2024) (Aug. 20, 2021).
313. Bucciol, G. & Meyts, I. Recent Advances in Primary Immunodeficiency: From Molecular Diagnosis to Treatment. *F1000Research* **9,** F1000 Faculty Rev–194. ISSN: 2046-1402. pmid: 32226610 (2020).
314. Devonshire, A. L. & Makhija, M. Approach to Primary Immunodeficiency. *Allergy and Asthma Proceedings* **40,** 465–469. ISSN: 1539-6304. pmid: 31690396 (Nov. 1, 2019).
315. Amaya-Uribe, L., Rojas, M., Azizi, G., Anaya, J.-M. & Gershwin, M. E. Primary Immunodeficiency and Autoimmunity: A Comprehensive Review. *Journal of Autoimmunity* **99,** 52–72. ISSN: 1095-9157. pmid: 30795880 (May 2019).
316. Ballow, M., Sánchez-Ramón, S. & Walter, J. E. Secondary Immune Deficiency and Primary Immune Deficiency Crossovers: Hematological Malignancies and Autoimmune Diseases. *Frontiers in Immunology* **13,** 928062. ISSN: 1664-3224. pmid: 35924244 (2022).
317. Korthauer, K. *et al.* A Practical Guide to Methods Controlling False Discoveries in Computational Biology. *Genome biology* **20,** 118. ISSN: 1474-760X 1474-7596. pmid: 31164141 (June 4, 2019).
318. Krzywinski, M. & Altman, N. Comparing Samples—Part II. *Nature Methods* **11,** 355–356. ISSN: 1548-7105. https://doi.org/10.1038/nmeth.2900 (Apr. 1, 2014).
319. Noble, W. S. How Does Multiple Testing Correction Work? *Nature biotechnology* **27,** 1135–1137. ISSN: 1546-1696 1087-0156. pmid: 20010596 (Dec. 2009).
320. Schreurs, R. R. C. E. *et al.* Quantitative Comparison of Human Intestinal Mononuclear Leukocyte Isolation Techniques for Flow Cytometric Analyses. *Journal of immunological methods* **445,** 45–52. ISSN: 1872-7905 0022-1759. pmid: 28274838 (June 2017).

321. Jung, J. M. *et al.* KIR3DS1 Directs NK Cell-Mediated Protection against Human Adenovirus Infections. *Science immunology* **6,** eabe2942. ISSN: 2470-9468. pmid: 34533978 (Sept. 17, 2021).
322. Chapel, A. *et al.* Peptide-Specific Engagement of the Activating NK Cell Receptor KIR2DS1. *Scientific reports* **7,** 2414. ISSN: 2045-2322. pmid: 28546555 (May 25, 2017).
323. Sino Biologicals, U. *B7-1 (CD80)* https://www.sinobiological.com/recombinant-proteins/human-b7-1-10698-h08h-b (2023).
324. Sino Biologicals, U. *B7-2 (CD86)* https://www.sinobiological.com/recombinant-proteins/human-cd86-10699-h08h-b (2023).
325. Sino Biologicals, U. *B7-DC (PD-L2)* https://www.sinobiological.com/recombinant-proteins/human-pd-l2-10292-h08h-b (2023).
326. Sino Biologicals, U. *B7-H1 (PD-L1)* https://www.sinobiological.com/recombinant-proteins/human-pd-l1-10084-h08h-b (2023).
327. Sino Biologicals, U. *B7-H2 (ICOSLG)* https://www.sinobiological.com/recombinant-proteins/human-icos-ligand-11559-h08h-b (2023).
328. Sino Biologicals, U. *B7-H3* https://www.sinobiological.com/recombinant-proteins/human-b7-h3-11188-h08h-b (2023).
329. Sino Biologicals, U. *B7-H4 (VTCN1)* https://www.sinobiological.com/recombinant-proteins/human-b7-h4-10738-h08h-b (2023).
330. Sino Biologicals, U. *B7-H5 (VISTA)* https://www.sinobiological.com/recombinant-proteins/human-vista-13482-h08h (2023).
331. Sino Biologicals, U. *B7-H6 (NCR3LG1)* https://www.sinobiological.com/recombinant-proteins/human-b7-h6-16140-h08h-b (2023).
332. Sino Biologicals, U. *B7-H7 (HHLA2)* https://www.sinobiological.com/recombinant-proteins/human-hhla2-16139-h08h-b (2023).
333. Narni-Mancinelli, E. *et al.* Complement Factor P Is a Ligand for the Natural Killer Cell-Activating Receptor NKp46. *Science immunology* **2,** eaam9628. ISSN: 2470-9468. pmid: 28480349 (Apr. 28, 2017).
334. Graef, T. *et al.* KIR2DS4 Is a Product of Gene Conversion with KIR3DL2 That Introduced Specificity for HLA-A*11 While Diminishing Avidity for HLA-C. *The Journal of experimental medicine* **206,** 2557–2572. ISSN: 1540-9538 0022-1007. pmid: 19858347 (Oct. 26, 2009).
335. Hansasuta, P. *et al.* Recognition of HLA-A3 and HLA-A11 by KIR3DL2 Is Peptide-Specific. *European journal of immunology* **34,** 1673–1679. ISSN: 0014-2980. pmid: 15162437 (June 2004).
336. Di Bona, D. *et al.* KIR2DL3 and the KIR Ligand Groups HLA-A-Bw4 and HLA-C2 Predict the Outcome of Hepatitis B Virus Infection. *Journal of viral hepatitis* **24,** 768–775. ISSN: 1365-2893 1352-0504. pmid: 28211154 (Sept. 2017).
337. Zhen, J. X. *et al.* KIR3DL1 and HLA-Bw4 Interaction Showed a Favorable Role in Patients with Myelodysplastic Syndromes in Chinese Southern Han. *BioMed*

research international **2020,** 6215435. ISSN: 2314-6141 2314-6133. pmid: 32420357 (2020).

338. Moesta, A. K. *et al.* Synergistic Polymorphism at Two Positions Distal to the Ligand-Binding Site Makes KIR2DL2 a Stronger Receptor for HLA-C than KIR2DL3. *Journal of immunology (Baltimore, Md. : 1950)* **180,** 3969–3979. ISSN: 0022-1767. pmid: 18322206 (Mar. 15, 2008).
339. Rajagopalan, S. & Long, E. O. A Human Histocompatibility Leukocyte Antigen (HLA)-G-specific Receptor Expressed on All Natural Killer Cells. *The Journal of experimental medicine* **189,** 1093–1100. ISSN: 0022-1007 1540-9538. pmid: 10190900 (Apr. 5, 1999).
340. Greenwald, R. J., Freeman, G. J. & Sharpe, A. H. The B7 Family Revisited. *Annual review of immunology* **23,** 515–548. ISSN: 0732-0582. pmid: 15771580 (2005).
341. Linsley, P. S. *et al.* CTLA-4 Is a Second Receptor for the B Cell Activation Antigen B7. *The Journal of experimental medicine* **174,** 561–569. ISSN: 0022-1007 1540-9538. pmid: 1714933 (Sept. 1, 1991).
342. Boussiotis, V. A. *et al.* Activated Human B Lymphocytes Express Three CTLA-4 Counterreceptors That Costimulate T-cell Activation. *Proceedings of the National Academy of Sciences of the United States of America* **90,** 11059–11063. ISSN: 0027-8424 1091-6490. pmid: 7504293 (Dec. 1, 1993).
343. Linsley, P. S. *et al.* Human B7-1 (CD80) and B7-2 (CD86) Bind with Similar Avidities but Distinct Kinetics to CD28 and CTLA-4 Receptors. *Immunity* **1,** 793–801. ISSN: 1074-7613. pmid: 7534620 (Dec. 1994).
344. Wang, S. *et al.* Costimulation of T Cells by B7-H2, a B7-like Molecule That Binds ICOS. *Blood* **96,** 2808–2813. ISSN: 0006-4971. pmid: 11023515 (Oct. 15, 2000).
345. Husain, B. *et al.* A Platform for Extracellular Interactome Discovery Identifies Novel Functional Binding Partners for the Immune Receptors B7-H3/CD276 and PVR/CD155. *Molecular & cellular proteomics : MCP* **18,** 2310–2323. ISSN: 1535-9484 1535-9476. pmid: 31308249 (Nov. 2019).
346. Tseng, S. Y. *et al.* B7-DC, a New Dendritic Cell Molecule with Potent Costimulatory Properties for T Cells. *The Journal of experimental medicine* **193,** 839–846. ISSN: 0022-1007 1540-9538. pmid: 11283156 (Apr. 2, 2001).
347. Freeman, G. J. *et al.* Engagement of the PD-1 Immunoinhibitory Receptor by a Novel B7 Family Member Leads to Negative Regulation of Lymphocyte Activation. *The Journal of experimental medicine* **192,** 1027–1034. ISSN: 0022-1007 1540-9538. pmid: 11015443 (Oct. 2, 2000).
348. Latchman, Y. *et al.* PD-L2 Is a Second Ligand for PD-1 and Inhibits T Cell Activation. *Nature immunology* **2,** 261–268. ISSN: 1529-2908. pmid: 11224527 (Mar. 2001).
349. Johnston, R. J. *et al.* VISTA Is an Acidic pH-selective Ligand for PSGL-1. *Nature* **574,** 565–570. ISSN: 1476-4687 0028-0836. pmid: 31645726 (Oct. 2019).

350. Ulmer, A. J., Scholz, W., Ernst, M., Brandt, E. & Flad, H. D. Isolation and Subfractionation of Human Peripheral Blood Mononuclear Cells (PBMC) by Density Gradient Centrifugation on Percoll. *Immunobiology* **166,** 238–250. ISSN: 0171-2985. pmid: 6329947 (May 1984).

351. Inc, B.-R. *Bio-Rad TC20 Automated Cell Counter* https://www.bio-rad.com/de-de/product/tc20-automated-cell-counter?ID=M7FBG34VY (2023).

352. Dieffenbach, C. W. & Dveksler, G. S. *PCR Primer: A Laboratory Manual.* ISBN: 0-87969-653-2 (Cold Spring Harbor Laboratory Press, 2003).

353. Hutchison, C. A. *et al.* Design and Synthesis of a Minimal Bacterial Genome. *Science* **351,** aad6253. https://www.science.org/doi/abs/10.1126/science.aad6253 (2016).

354. Bergmans, H. E., van Die, I. M. & Hoekstra, W. P. Transformation in Escherichia Coli: Stages in the Process. *Journal of bacteriology* **146,** 564–570. ISSN: 0021-9193 1098-5530. pmid: 7012133 (May 1981).

355. Cohen, S. N., Chang, A. C. & Hsu, L. Nonchromosomal Antibiotic Resistance in Bacteria: Genetic Transformation of Escherichia Coli by R-factor DNA. *Proceedings of the National Academy of Sciences of the United States of America* **69,** 2110–2114. ISSN: 0027-8424. pmid: 4559594 (Aug. 1972).

356. Wood, E. J. Molecular Cloning. A Laboratory Manual by T Maniatis, E F Fritsch and J Sambrook. Pp 545. Cold Spring Harbor Laboratory, New York. 1982. $48 ISBN 0-87969-136-0. *Biochemical Education* **11,** 82–82. ISSN: 1879-1468. https://onlinelibrary.wiley.com/doi/abs/10.1016/0307-4412%2883%2990068-7 (2023) (1983).

357. Qiagen. *HiSpeed Plasmid Maxi Kit (EN)* https://www.qiagen.com/us/resources/resourcedetail?id=52d67294-f2d7-4181-a532-7ea147b28b36&lang=en (2023).

358. Qiagen. *QIAquick Gel Extraction Kit and QIAquick PCR & Gel Cleanup Kit - (EN)* https://www.qiagen.com/us/resources/resourcedetail?id=a72e2c07-7816-436f-b920-98a0ede5159a&lang=en (2023).

359. NEB New England Biolabs, U. *NEB Restriction Enzyme Double Digestion Protocol* https://nebcloner.neb.com/#!/protocol/re/double/NotI-HF,EcoRI-HF (2023).

360. NEB New England Biolabs, U. *NEBuilder HiFi DNA Assembly Reaction Protocol* https://international.neb.com/protocols/2014/11/26/nebuilder-hifi-dna-assembly-reaction-protocol (2023).

361. Thermo Fisher Scientific, U. *One Shot™ Stbl3™ Chemisch Kompetente E. Coli* https://www.thermofisher.com/order/catalog/product/C737303 (2023).

362. Thomas, S., Maynard, N. D. & Gill, J. DNA Library Construction Using Gibson Assembly®. *Nature Methods* **12,** i–ii. ISSN: 1548-7091. https://www.nature.com/articles/nmeth.f.384 (2023) (2015).

363. Thermo Fisher Scientific, U. *Thermo Fisher Scientific GeneArt Gene Synthesis* https://www.thermofisher.com/de/de/home/life-science/cloning/gene-synthesis/geneart-gene-synthesis.html (2023).
364. Bio, T. *Advantage®-HF 2 PCR Kit User Manual* 2006. https://www.takarabio.com/documents/User%20Manual/PT3317/PT3317-1.pdf (2023).
365. Agilent, U. *QuikChange Primer Design Manual* https://www.agilent.com/store/primerDesignProgram.jsp (2023).
366. Agilent, U. *QuikChange II Site-Directed Mutagenesis Kit* https://www.agilent.com/cs/library/usermanuals/public/200523.pdf (2023).
367. Kalidasan, V. *et al.* A Guide in Lentiviral Vector Production for Hard-to- Transfect Cells, Using Cardiac-Derived c-Kit Expressing Cells as a Model System. *Scientific Reports* **11,** 19265. ISSN: 2045-2322. https://www.ncbi.nlm.nih.gov/pmc/articles/PMC8478948/ (2021).
368. Thermo Fisher Scientific, U. *TRANSFECTION PROTOCOL Lipofectamin 3000* https://assets.thermofisher.com/TFS-Assets/BID/manuals/lipofectamine3000-mcf10a-protocol.pdf (2023).
369. Holmberg, A. *et al.* The Biotin-Streptavidin Interaction Can Be Reversibly Broken Using Water at Elevated Temperatures. *Electrophoresis* **26,** 501–510. ISSN: 0173-0835. pmid: 15690449 (Feb. 2005).
370. NIH, U. *Tetramerization* https://tetramer.yerkes.emory.edu/support/protocols#10 (2023).
371. McKinnon, K. M. Flow Cytometry: An Overview. *Current protocols in immunology* **120,** 5.1.1–5.1.11. ISSN: 1934-368X 1934-3671 . pmid: 29512141 (Feb. 21, 2018).
372. Adan, A., Alizada, G., Kiraz, Y., Baran, Y. & Nalbant, A. Flow Cytometry: Basic Principles and Applications. *Critical reviews in biotechnology* **37,** 163–176. ISSN: 1549-7801 0738-8551. pmid: 26767547 (Mar. 2017).
373. Maciorowski, Z., Chattopadhyay, P. K. & Jain, P. Basic Multicolor Flow Cytometry. *Current protocols in immunology* **117,** 5.4.1–5.4.38. ISSN: 1934-368X 1934-3671. pmid: 28369683 (Apr. 3, 2017).
374. Verschoor, C. P., Lelic, A., Bramson, J. L. & Bowdish, D. M. E. An Introduction to Automated Flow Cytometry Gating Tools and Their Implementation. *Frontiers in immunology* **6,** 380. ISSN: 1664-3224. pmid: 26284066 (2015).
375. Austin Suthanthiraraj, P. P. & Graves, S. W. Fluidics. *Current protocols in cytometry* **Chapter 1,** 1.2.1–1.2.14. ISSN: 1934-9300 1934-9297. pmid: 23835801 (July 2013).
376. Eisert, W. G. High Resolution Optics Combined with High Spatial Reproducibility in Flow. *Cytometry* **1,** 254–259. ISSN: 0196-4763. pmid: 7021108 (Jan. 1981).
377. Duesedau, A. *LSR Fortessa* July 28, 2023. https://www.leibniz-liv.de/en/research/technologies/flow-cytometryfacs/device-information/ (2023).

378. Bergquist, P. L., Hardiman, E. M., Ferrari, B. C. & Winsley, T. Applications of Flow Cytometry in Environmental Microbiology and Biotechnology. *Extremophiles : life under extreme conditions* **13,** 389–401. ISSN: 1433-4909 1431-0651. pmid: 19301090 (May 2009).
379. Manohar, S. M., Shah, P. & Nair, A. Flow Cytometry: Principles, Applications and Recent Advances. *Bioanalysis* **13,** 181–198. ISSN: 1757-6199 1757-6180. pmid: 33543666 (Feb. 2021).
380. Berg, E. A. & Fishman, J. B. Labeling Antibodies. *Cold Spring Harbor protocols* **2020,** 099242. ISSN: 1559-6095. pmid: 32611784 (July 1, 2020).
381. Pang, K. *et al.* Advanced Flow Cytometry for Biomedical Applications. *Journal of biophotonics* **16,** e202300135. ISSN: 1864-0648 1864-063X. pmid: 37263969 (Sept. 2023).
382. Zola, H. *et al.* CD Molecules 2006–Human Cell Differentiation Molecules. *Journal of immunological methods* **319,** 1–5. ISSN: 0022-1759. pmid: 17174972 (Jan. 2007).
383. Wilson, D. J., Smith, T. F. & Ilstrup, D. M. Comparison of Iodine- and Fluorescein-Labeled Monoclonal Antibodies for Detection of Chlamydia Trachomatis Inclusions in Cells Grown in Glass Vials. *Diagnostic microbiology and infectious disease* **2,** 17–22. ISSN: 0732-8893. pmid: 6399479 (Jan. 1984).
384. Tidman, N. *et al.* Delineation of Human Thymocyte Differentiation Pathways Utilizing Double-Staining Techniques with Monoclonal Antibodies. *Clinical and experimental immunology* **45,** 457–467. ISSN: 0009-9104 1365-2249 . pmid: 6461444 (Sept. 1981).
385. Poli, V., Di Gioia, M. & Zanoni, I. Quantitative Cytofluorimetric Analysis of Mouse Neutrophil Extracellular Traps. *STAR protocols* **4,** 102372. ISSN: 2666-1667. pmid: 37352106 (June 22, 2023).
386. Kalfeist, L. *et al.* Simultaneous Isolation of CD45 Tumor-Infiltrating Lymphocytes, Tumor Cells, and Associated Fibroblasts from Murine Breast Tumor Model by MACS. *STAR protocols* **4,** 101951. ISSN: 2666-1667. pmid: 36856770 (Jan. 18, 2023).
387. Andersen, M. N., Al-Karradi, S. N. H., Kragstrup, T. W. & Hokland, M. Elimination of Erroneous Results in Flow Cytometry Caused by Antibody Binding to Fc Receptors on Human Monocytes and Macrophages. *Cytometry. Part A : the journal of the International Society for Analytical Cytology* **89,** 1001–1009. ISSN: 1552-4930 1552-4922. pmid: 27731950 (Nov. 2016).
388. BioLegend. *Human TruStain FcX™ (Fc Receptor Blocking Solution)* https://www.biolegend.com/en-us/products/human-trustain-fcx-fc-receptor-blocking-solution-6462?pdf=true&displayInline=true&leftRightMargin=15&topBottomMargin=15&filename=Human%20TruStain%20FcX%E2%84%A2%20(Fc%20Receptor%20Blocking%20Solution).pdf&v=20230701123045 (2023).
389. Thermo Fisher Scientific, U. *LIVE/DEAD Fixable Dead Cell Stains Protocol* https://www.thermofisher.com/de/de/home/references/protocols/cell

-and-tissue-analysis/protocols/live-dead-fixable-dead-cell-stains.html (2023).

390. BD Biosciences, U. *Anti-Mouse, Anti-Rat, Anti-Rat/Hamster Ig, /Negative Control Compensation Particles Set Protocol* https://www.bdbiosciences.com/en-us/products/reagents/flow-cytometry-reagents/research-reagents/compensation-beads (2023).
391. Cheung, M. *et al.* Current Trends in Flow Cytometry Automated Data Analysis Software. *Cytometry. Part A : the journal of the International Society for Analytical Cytology* **99,** 1007–1021. ISSN: 1552-4930 1552-4922. pmid: 33606354 (Oct. 2021).
392. Wong, P., Wagner, J. A., Berrien-Elliott, M. M., Schappe, T. & Fehniger, T. A. Flow Cytometry-Based Ex Vivo Murine NK Cell Cytotoxicity Assay. *STAR protocols* **2,** 100262. ISSN: 2666-1667. pmid: 33490978 (Mar. 19, 2021).
393. Thermo Fisher Scientific, U. *Protocol CellTrace™ Cell Proliferation Kits* https://www.thermofisher.com/document-connect/document-connect.html?url=https://assets.thermofisher.com/TFS-Assets%2FLSG%2Fmanuals%2FMAN0002595_CellTrace_Cell_Proliferation_Kits_UG.pdf (2023).
394. Li, Y. *et al.* KIR3DL3-HHLA2 and TMIGD2-HHLA2 Pathways: The Dual Role of HHLA2 in Immune Responses and Its Potential Therapeutic Approach for Cancer Immunotherapy. *Journal of advanced research* **47,** 137–150. ISSN: 2090-1224 2090-1232. pmid: 35933091 (May 2023).
395. Pham-Gia, T. & Hung, T. The Mean and Median Absolute Deviations. *Mathematical and Computer Modelling* **34,** 921–936. ISSN: 0895-7177. https://www.sciencedirect.com/science/article/pii/S0895717701001091 (2001).
396. Peterson, C. & Miller, A. Mode, Median, and Mean as Optimal Strategies. *Journal of Experimental Psychology* **68,** 363–367. ISSN: 0022-1015(Print) (1964).
397. Rice, T. K., Schork, N. J. & Rao, D. C. Methods for Handling Multiple Testing. *Advances in genetics* **60,** 293–308. ISSN: 0065-2660. pmid: 18358325 (2008).
398. Glickman, M. E., Rao, S. R. & Schultz, M. R. False Discovery Rate Control Is a Recommended Alternative to Bonferroni-type Adjustments in Health Studies. *Journal of clinical epidemiology* **67,** 850–857. ISSN: 1878-5921 0895-4356. pmid: 24831050 (Aug. 2014).
399. Lai, Y. A Statistical Method for the Conservative Adjustment of False Discovery Rate (q-Value). *BMC bioinformatics* **18,** 69. ISSN: 1471-2105. pmid: 28361675 (Mar. 14, 2017).
400. Benjamini, Y., Krieger, A. M. & Yekutieli, D. Adaptive Linear Step-up Procedures That Control the False Discovery Rate. *Biometrika* **93,** 491–507. ISSN: 0006-3444. https://doi.org/10.1093/biomet/93.3.491 (2023) (Sept. 1, 2006).
401. Ignatiadis, N., Klaus, B., Zaugg, J. B. & Huber, W. Data-Driven Hypothesis Weighting Increases Detection Power in Genome-Scale Multiple Testing. *Nature methods* **13,** 577–580. ISSN: 1548-7105 1548-7091. pmid: 27240256 (July 2016).

402. Boca, S. M. & Leek, J. T. A Direct Approach to Estimating False Discovery Rates Conditional on Covariates. *PeerJ* **6,** e6035. ISSN: 2167-8359 . pmid: 30581661 (2018).
403. Cai, T. T. & Sun, W. Simultaneous Testing of Grouped Hypotheses: Finding Needles in Multiple Haystacks. *Journal of the American Statistical Association* **104,** 1467–1481. ISSN: 01621459. JSTOR: 40592354. http://www.jstor.org/stable/40592354 (2009).
404. Lei, L. & Fithian, W. AdaPT: An Interactive Procedure for Multiple Testing with Side Information. *Journal of the Royal Statistical Society Series B: Statistical Methodology* **80,** 649–679. ISSN: 1369-7412 (2018).
405. Scott, J. G., Kelly, R. C., Smith, M. A., Zhou, P. & Kass, R. E. False Discovery Rate Regression: An Application to Neural Synchrony Detection in Primary Visual Cortex. *Journal of the American Statistical Association* **110,** 459–471. ISSN: 0162-1459 (2015).
406. Stephens, M. False Discovery Rates: A New Deal. *Biostatistics (Oxford, England)* **18,** 275–294. ISSN: 1468-4357 1465-4644. pmid: 27756721 (Apr. 1, 2017).
407. Murray, M. H. & Blume, J. D. FDRestimation: Flexible False Discovery Rate Computation in R. *F1000Research* **10,** 441. ISSN: 2046-1402. pmid: 34956625 (2021).
408. Prism, G. *Analysis Checklist: Friedman's Test* https://www.graphpad.com/guides/prism/latest/statistics/stat_checklist_friedman.htm (2023).
409. Universität Hamburg Studienbüro für Biologie, U. A. *Eidesstattliche Versicherung* online, Jan. 26, 2024. https://www.biologie.uni-hamburg.de/studium/promotion/promotion-2018/_download-dateien/eidesstattliche-versicherung-declaration-on-oath.pdf (2024).

Declaration of authorship

Decleration under oath:

I hereby declare, on oath, that I have written the present dissertation by my own and have not used other than the acknowledged resources and aids [409].

Versicherung an Eides statt:

Hiermit erkläre ich an Eides statt, dass ich die vorliegende Dissertationsschrift selbst verfasst und keine anderen als die angegebenen Quellen und Hilfsmittel benutzt habe [409].

Signature:

Hamburg, Date: 16.02.2024

A Appendix

A.1 Plasmid sequences for cell line transductions

A.1.1 NCBI blast of KIR3DL3*001,*003 and *009

The following results for sequence similarities were obtained for the nucleotide sequences of KIR3DL3 allotypes *001, *003 and *009. The sequence homology of the nucleotide sequence of KIR3DL3*001 and KIR3DL3*003 are 100 % and therefore the sequences for the extracellular receptor domain identical (Figure A.1). Furthermore, the sequence homology of the nucleotide sequence of KIR3DL3*001 and KIR3DL3 *009 are 100 % and therefore the sequences for the extracellular receptor domain identical (Figure A.2).

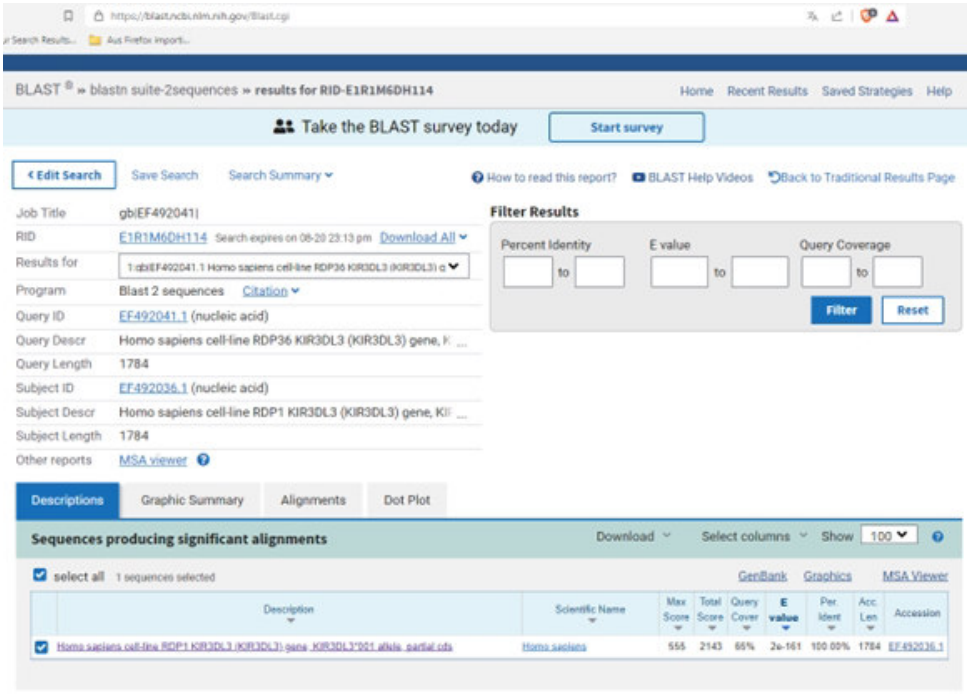

FIGURE A.1: NCBI blast of the UniProt KIR3DL3 allotypes *001 and *003. The sequence homology of the nucleotide sequence of KIR3DL3*001 and KIR3DL3*003 are 100 % and therefore the sequences for the extracellular receptor domain identical.

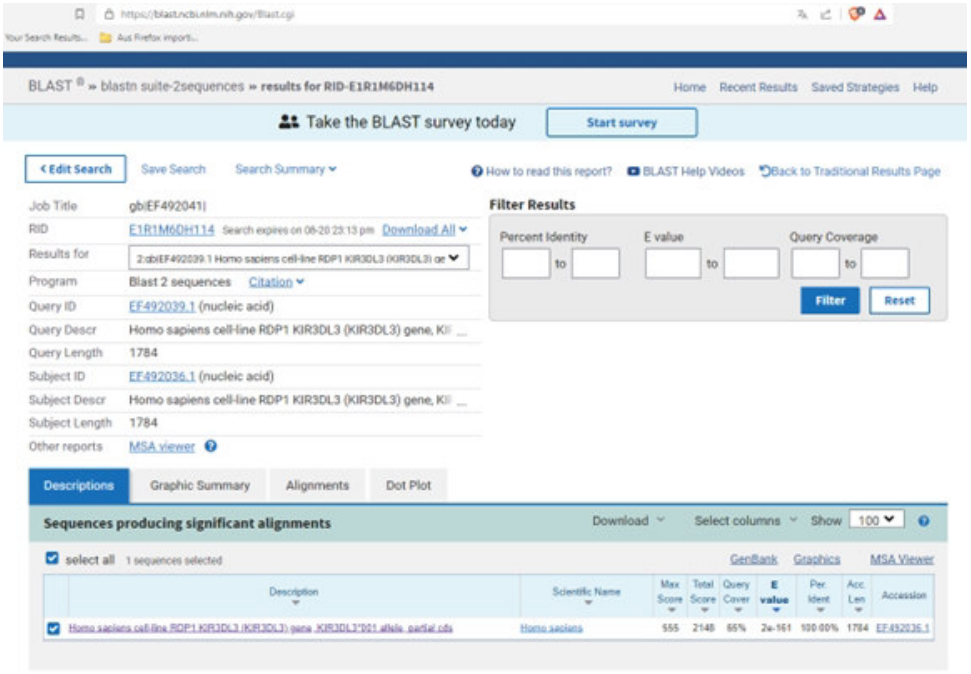

FIGURE A.2: NCBI blast of the UniProt KIR3DL3 allotypes *001 and *009. The sequence homology of the nucleotide sequence of KIR3DL3*001 and KIR3DL3*009 are 100 % and therefore the sequences for the extracellular receptor domain identical.

A.1.2 β2m-KO-Jurkat KIR3DL3*001 sequence

The following sequence of KIR3DL3*001 of the UniProt database ID Q8N743 was used for plasmid generation:

CCG GGG GGG ATC TAT TTC CGG TGA ATT CTC TAG AGC CAC CAT GAG CCT GAT GGT GGT GTT TCT ATG GCC TGC GTG GGA TTC TTC CTG CTG GAA GGA CCT TGG CCT CAC GTT GGC GGA CAG GAC AAG CCT TTT CTG TCT GCC TGG CCT GGC ACC GTG GTG TCT GAA GGA CAG CAT GTG ACC CTG CAG TGC AGA AGC AGA CTG GGC TTC AAC GAG TTC AGC CTG AGC AAA GAG GAC GGC ATG CCT GTG CCT GAG CTG TAC AAC CGG ATC TTC CGG AAC AGC TTC CTG ATG GGC CCT GTG ACA CCA GCT CAC GCC GGC ACC TAC AGA TGC TGT TCT TCT CAC CCT CAC AGC CCC ACA GGC TGG AGC GCA CCT TCT AAT CCC GTG GTC ATC ATG GTC ACC GGC GTG CAC AGA AAG CCT AGC CTG CTT CAT CCC GGA CCT CTG GTC AAG TCT GGC GAG ACA GTG ATT CTG CAG TGT TGG AGC GAC GTC CGC TTC GAG AGA TTC CTG CTG CAC AGA GAG GGA ATC ACC GAG GAT CCA CTG AGA CTG ATC GGC CAG CTG CAC GAT GCC GGC AGC CAA GTG AAT TAC AGC ATG GGC CCA ATG ACA CCC GCA CTG GCC GGC ACA TAT AGA TGT TTC GGC AGC GTG ACC CAT CTG CCT TAC GAG CTG TCT GCC CCT AGC GAC CCT CTG GAT ATC GTG GTC GTG GGC CTG TAC GGC AAG CCT AGT CTT TCT GCT CAG CCT GGA CCT ACA GTG CAG GCC GGC GAA AAT GTG ACA

CTG AGC TGC TCC AGC AGA AGC CTG TTC GAC ATC TAC CAC CTG TCC AGA GAA GCC GAA GCC GGC GAA CTG AGA CTT ACC GCT GTG CTG AGA GTG AAC GGC ACC TTC CAG GCC AAC TTT CAC ACT GGG ACC AGT GAC ACA CGG CGG CAA CTA TCG GTG CTT CGG CAG CTT TAG AGC CCT GCC TCA TGC TTG GAG CGA TCC CTC TGA TCC TCT GCC TGT GCC GTG ACC GGC AAC AGC AGA AAT CTG CAC GTG CTG ATC GGA ACC AGC GTC GTG ATC ATC CCC TTC GCT ATC CTG CTG TTT TTC CTG CTG AGG GTC AAG TTC AGC CGC AGC GCT GAT GCC CCT GCA TAT CAG CAG GGA CAG AAC CAG CTG TAT AAC GAG CTG AAC CTG GGG CGC AGA GAA GAG TAC GAC GTG CTG GAC AAG AGA AGG CAG GGA CCC CTG AGA TGG GCG GAA AGC CCC AGA GAA GAA AGA ACC CTC AAG AGG GAC TGT ACA ATG AGC TGC AAA AGG ACA AGA TGG CCG AGG CCT ACA GCG AGA TCG GAA TGA AGG GCG AAC GCA GAA GAG GAA AGG GCC ACG ACG GAC TGT ATC AGG GCC TGA GCA CAG CCA CCA AGG ACA CCT ATG ATG CCC TGC ACA TGC AGG GCC CTG CCA CCT AGA GCG GCC GCG GAT CCC GCC CCT CTC CCT

In the translated version:

MSL MVV SMA CVG FFL LEG PWP HVG GQD KPF LSA WPG TVV EGQ HVT LQC RSR LGF NEF SLS KED GMP VPE LYN RIF RNS FL MGP VTP AHA GTY RCC SSH PHS PTG WSA PSN PVV IMV TGV HRK PSL LAH PGP LVK SGE TVI LQC WSD VRF ERF LLH REG ITD PLR LIG QLH DAG SQV NYS MGP MTP ALA GTY RCF GSV THL PYE LSA PSD PLD IVV VGL YGK PSL SAQ PGP TVQ AGE NVT LSC SSR SLF DIY HLS REA EAG ELR LTA VLR VNG TFQ ANF PLG PVT HGG NYS RCF GSF RAL PHA WSD PSD PLP VSV TGN RNLHVL IGT SVV IIP FAI LLF LLH RWC ANK KNA VVM DQE PAG NRT VNR EDS DEQ DPE VTY AQL NHC VFT QRK ITR PSQ RPK TTP TDS TV

Signalpeptid, Extracellular domain, Transmembrane domain, Cytoplasmic Domain

Of the shown sequence above the signal peptide, extracellular and transmembrane domain were fused with the CD3ζ chain to the following sequence:

ATG AGC CTG ATG GTG GTG AGC ATG GCG TGC GTG GGC TTT TTT CTG CTG GAA GGC CCG TGG CCG CAT GTG GGC GGC CAG GAT AAA CCG TTT CTG AGC GCG TGG CCG GGC ACC GTG GTG GAA GGC CAG CAT GTG ACC CTG CAG TGC CGC AGC CGC CTG GGC TTT AAC GAA TTT AGC CTG AGC AAA GAA GAT GGC ATG CCG GTG CCG GAA CTG TAT AAC CGC ATT TTT CGC AAC AGC TTT CTG ATG GGC CCG GTG ACC CCG GCG CAT GCG GGC ACC TAT CGC TGC TGC AGC AGC CAT CCG CAT AGC CCG ACC GGC TGG AGC GCG CCG AGC AAC CCG GTG GTG ATT ATG GTG ACC GGC GTG CAT CGC AAA CCG AGC CTG CTG GCG CAT CCG GGC CCG CTG GTG AAA AGC GGC GAA ACC GTG ATT CTG CAG TGC TGG AGC GAT GTG CGC TTT GAA CGC TTT CTG CTG CAT CGC GAA GGC ATT ACC GAA GAT CCG CTG CGC

CTG ATT GGC CAG CTG CAT GAT GCG GGC AGC CAG GTG AAC TAT AGC
ATG GGC CCG ATG ACC CCG GCG CTG GCG GGC ACC TAT CGC TGC TTT
GGC AGC GTG ACC CAT CTG CCG TAT GAA CTG AGC GCG CCG AGC GAT
CCG CTG GAT ATT GTG GTG GTG GGC CTG TAT GGC AAA CCG AGC CTG
AGC GCG CAG CCG GGC CCG ACC GTG CAG GCG GGC GAA AAC GTG ACC
CTG AGC TGC AGC AGC CGC AGC CTG TTT GAT ATT TAT CAT CTG AGC
CGC GAA GCG GAA GCG GGC GAA CTG CGC CTG ACC GCG GTG CTG
CGC GTG AAC GGC ACC TTT CAG GCG AAC TTT CCG CTG GGC CCG
GTG ACC CAT GGC GGC AAC TAT CGC TGC TTT GGC AGC TTT CGC GCG
CTG CCG CAT GCG TGG AGC GAT CCG AGC GAT CCG CTG CCG GTG AGC
GTG ACC GGC AAC CGC AAC CTG CAT GTG CTG ATT GGC ACC AGC GTG
GTG ATT ATT CCG TTT GCG ATT CTG CTG TTT TTT CTG CTG CGC GTG
AAA TTT AGC CGC AGC GCG GAT GCG CCG GCG TAT CAG CAG GGC CAG
AAC CAG CTG TAT AAC GAA CTG AAC CTG GGC CGC CGC GAA GAA TAT
GAT GTG CTG GAT AAA CGC CGC GGC CGC GAT CCG GAA ATG GGC GGC
AAA CCG CAG CGC CGC AAA AAC CCG CAG GAA GGC CTG TAT AAC GAA
CTG CAG AAA GAT AAA ATG GCG GAA GCG TAT AGC GAA ATT GGC ATG
AAA GGC GAA CGC CGC CGC AAA GGC GGC CAT GAT GGC CTG TAT CAG
GGC CTG AGC ACC GCG ACC AAA GAT ACC TAT GAT GCG CTG CAT ATG
CAG GCG CTG CCG CCG CGC

In the translated version:

MSL MVV SMAC VGFF LLE GPW PHV GGQ DKP FLS AWP GTV VEG QHV
TLQ CRS RLG FNE FSL SKE DGM PVP ELY NRIF RNS FLM GPV TPA HAG
TYR CCS SHP HSP TGW SAP SNP VVI MVT GVH RKP SLL AHP GPL VKS
GET VIL QCW SDV RFE RFL LHR EGI TED PLR LIG QLH DAG SQV NYS
MGP MTP ALA GTY RCF GSV THL PYE LSA PSD PLD IVV VGL YGK PSL
SAQ PGP TVQ AGE NVT LSC SSR SLF DIY HLS REA EAG ELR LTA VLR VNG
TFQ ANF PLG PVT HGG NYR CFG SFR ALP HAW SDP SDP LPV SVT GNR
NLH VLI GTS VVI IPF AIL LFF LLR VKF SRS ADA PAY QQG QNQ LYN ELN
LGR REE YDV LDK RRG RDP EMG GKP QRR KNP QEG LYN ELQ KDK MAE
AYS EIG MKG ERR RKG GHD GLY QGL STA TKD TYD ALH MQA LPP R

Signalpeptid, Extracellular domain, Transmembrane domain, CD3ζ domain

A.1.3 *β*2m-KO-Jurkat KIR2DL5*001 sequence

The following sequence of KIR2DL5*001 was used by Fittje *et al.* to generate the plasmid / *β*2m-KO-Jurkat KIR2DL5 cell line [90]:

CCG GGG GGG GAT CTA TTT CGG TGA ATT CGC CAC CAT GTC ACT GAT
GGT GAT CTC CAT GGC GTG TGT AGG CTT CTT CCT TCT CCA GGG TGC
GTG GAC TCA CGA GGA GGT CAG GAT AAA CCA CTG TTG TCT GCA TGG
CCC AGT GCC GTT GTC CCG CGA GGA GGT CAT GTA ACA CTT CTC TGC

CGA AGC AGA CTT GGA TTT ACA ATT TTT AGC TTG TAT AAA GAG GAT GGT GTT CCT GTG CCC GAG CTC TAT AAC AAG ATA TTC TGG AAA TCT ATT TTT GAT GGG GCC AGT GAC TCC AGC TCA CGC AGG AAC TTA CCG CTG CAG GGG CTC TCA TCC TAG ATC ACC TAT CG

In the translated version:

MSL MVI SMA CVG FLL QGA WTH EGG QDK PLL SAW PSA VVP RGG HVT LLC RSR LGF TIF SLY EDG VPV PEL YNK IFW KSI ILM GPV TPA HAG TYR CRG SHP RSP IEW SAP SNP LVI VVT GLF GKP SLS AQP GPT VRT GEN VTS LCS SRS FDM YHL SRE GRA HEP RLP AVP SVN GTF QAD FPL GPA THG GTY TCF GSL HDS PYE WSD PLL SVS VTG NSS SSS SPS PTE PSS KTG IRR HLHILI GTS VAI ILF IIL LFF FLL RVK FSR SAD APA YQQ GQN QLY NEL NLG RRE EYD VLD KRR GRD PEM GGK PQR RKN PQE GLY NEL QKD KMA EAY SEI GMK GER RRG KGH DGL YQG LST ATK DTY DAL HMQ ALP PR

Signalpeptid, Extracellular domain, Transmembrane domain, CD3ζ domain

A.1.4 β2m-KO-Jurkat KIR3DL1*001 sequence

The following sequence of KIR3DL1*001 was used by Dr. Wilfredo Garcia-Beltran *et al.* to generate the plasmid / β2m-KO-Jurkat KIR3DL1 cell line [205]:

ATG AGC CTG ATG GTG GTG AGC ATG GCC TGC GTG GGC CTG TTC CTG GTG CAG AGG GCC GGC CCC CAC ATG GGC GGC CAG GAC AAG CCC TTC CTG AGC GCC TGG CCC AGC GCC GTG GTG CCC AGG GCG GCC ACG TGA CCC TGA GGT GCC ACT ACA GGC ACA GGT TCA ACA ACT TCA TGC TGT ACA AGG AGG ACA GGA TCC ACA TCC CCA TCT TCC ACG GGC AGG ATC TTC CAG GAG AGC TTC AAC ATG AGC CCC GTG ACC ACC GCC CAC GCC GGC AAC TAC ACC TGC AGG GGC AGC CAC CCC CAC AGC CCC ACC GGC TGG AGC GCC CCC AGC AAC CCC CGT GGT GAT CAT GGT GAC CGG CAA CCA CAG GAA GCC CAG CCT GCT GGC CCA CCC CGG CCC CCC TGG TGA AGA GCG GCG AGA GGG TGA TCC TGC AGT GCT GGA GCG ACA TCA TGT TCG AGC ACT TCT TCC TGC ACA AGG AGG GCA TCA GCA AGG ACC CCC AGC AGG CTG GTG GGC CAG ATC CAC GAC GGC GTG AGC AAG GCC AAC TTC AGC ATC GGC CCCC CCA TGA TGC TGG CCC TGG CCG GCA CCT ACA GGT GCT ACG GCA GCG TGA CCC ACA CCA CCC TAC CAG CTG AGC GCC CCC AGC GAC CCC CTG GAC ATC GTG GTG ACC GGC CCC TAC GAG AAG CCC AGC CTG AGC GCC CCA GCC CGG CCC CA AGG TGC AGG CCG GCG AGA GCG TGA CCC TGA GCT GCA GCA GCAG GAG CAG CTA CGA CAT GTA CCA CCT GAG CAG GGA GGG CGG CGC CCA CGA GAG GAG GCT GCC CGC CGT GAG GAA GGT GAA CAG GAC CTT CCA GGC CGA CTT CCC CTT GGG CCC CGC CAC CCA CGG CGG CAC CTA CAG GGT GCT TCG GCA GCT TCA GGC ACA GCC CCT ACG AGA GCG ACC CCA GCG ACC CCC TGC TGG TGA GCG TGA CCG GCA ACC CCA GCA GCAG CTG GCC

CAG CCC CAC CGA GCC CAG CAG CAAG AGC GGC AAC CCC AGG CAC CTG CAC ATC CTG ATC GGC ACC AGC GTG GTG ATC ATC CTG TTC ATC CTG CTG CTG TTC CTT GCT GCA CCT GTG GAG GGT GAA GTT CAG CAG GAG CGC CGA CGC CCC CGC TAC CAG CAG GGC CAG AAC CAG CTG TAC AAC GAG CTG AAC CTG GGC AGG AGG GAG TAC GAC GTG CTG GAC AAG AGG AGG GGC AGG GAC CCC GAG ATG GGC GGC AAG CCC CAG AGG AGG AAG AAC CCC CAG GAG GGC CTG TAC AAC GAG CTG CAG AAG GAC AAG ATG GCC GAG GCC TAC AGC GAG ATC GGC ATG AAG GGC GAG AGG AGG AGG GGC AAG GGC CAC GAC GGC CTG TAC CAG GGC CTG AGC ACC GCC ACC AAG GAC ACC TAC GAC GCC CTG CAC ATG CAG GCC CTG CCC CCA GG

In the translated version:

MSL MVV SMA CVG LFL VQR AGP HMG GQD KPF LSA WPS AVV PRG GHV TLR CHY RHR FNN FML YKE DRI HIP IFH GRI FQE SFN MSP VTT AHA GNY TCR GSH PHS PTG WSA PSN PVV IMV TGN HRK PSL LAH PGP LVK SGE RVI LQC WSD IMF EHF FLH KEG ISK DPS RLV GQI HDG VSK ANF SIG PPM MLA LAG TYR CYG SVT HTT PYQ LSA PSD PLD IVV TGP YEK PSL SAQ PGP KVQ AGE SVT LSC SSR SSY DMY HLS REG GAH ERR LPA VRK VNR TFQ ADF PLG PAT HGG TYR CFG SFR HSP YES DPS DPL LVS VTG NPS SSW PSP TEP SSK SGN PRH LHI LIG TSV VII LFI LLL FFL LHL WRVK FSR SAD APA YQQ GQN QLY NEL NLG RRE EYD VLD KRR GRD PEM GGK PQR RKN PQE GLY NEL QKD KMA EAY SEI GMK GER RRG KGH DGL YQG LST ATK DTY DAL HMQ ALP PR

Signalpeptid, Extracellular domain, Transmembrane domain, CD3ζ domain

A.1.5 β2m-KO-Jurkat KIR3DL2*001 sequence

The following sequence of KIR3DL2*001 was used by Dr. Wilfredo Garcia-Beltran *et al.* to generate the plasmid / β2m-KO-Jurkat KIR3DL2 cell line [205]:

ATG TCG CTC ACG GTC GTC AGC ATG GCG TGC GTT GGG TTC TTC TTG CTG CAG GGG GCC TGG CCA CTC ATG GGT GGT CAG GAC AAA CCC TTC CTG TCT GCC CGG CCC AGC ACT GTG GTG CCT CGA GGA GGA CAC GTG GCT CTT CAG TGT CAC TAT CGT CGT GGG TTT AAC AAT TTC ATG CTG TAC AAA GAA GAC AGA AGC CAC GTT CCC ATC TTC CAC GGC AGA ATA TTC CAG GAG AGC TTC ATC ATG GGC CCT GTG ACC CCA GCA CAT GCA GGG ACC TAC AGA TGT CGG GGT TCA CGC CCA CAC TCC CTC ACT GGG TGG TCG GCA CCC AGC AAC CCC CTG GTG ATC ATG GTC ACA GGA AAC CAC AGA AAA CCT TCC CTC CTG GCC CAC CCA GGG CCC CTG CTG AAA TCA GGA GAG ACA GTC ATC CTG CAA TGT TGG TCA GAT GTC ATG TTT GAG CAC TTC TTT CTG CAC AGA GAG GGG ATC TCT GAG GAC CCC TCA CGC CTC GTT GGA CAG ATC CAT GAT GGG GTC TCC AAG GCC AAC TTC

TCC ATC GGT CCC TTG ATG CCT GTC CTT GCA GGA ACC TAC AGA TGT
TAT GGT TCT GTT CCT CAC TCC CCC TAT CAG TTG TCA GCT CCC AGT
GAC CCC CTG GAC ATC GTG ATC ACA GGT CTA TAT GAG AAA CCT TCT
CTC TCA GCC CAG CAG GGC CCC ACG GTT CAG GCA GGA GAG AAC GTG
ACC TTG TCC TGT AGC TCC TGG AGC TCC TAT GAC ATC TAC CAT CTG
TCC AGG GAA GGG GAG GCC CAT GAA CGT AGG CTC CGT GCA GTG
CCC AAG GTC AAC AGA ACA TTC CAG GCA GAC TTT CCT CTG GGC CCT
GCC ACC CAC GGA GGG ACC TAC AGA TGC TTC GGC TCT TTC CGT GCC
CTG CCC TGC GTG TGG TCA AAC TCA AGT GAC CCA CTG CTT GTT TCT
GTC ACA GGA AAC CCT TCA AGT AGT TGG CCT TCA CCC ACA GAA CCA
AGC TCC AAA TCT GGT ATC TGC AGA CAC CTG CAT GTT CTG ATT GGG
ACC TCA GTG GTC ATC TTC CTC TTC ATC CTC CTC CTC TTC TTT CTC
CTT TAT CGC GTG AAA TTT AGC CGC AGC GCG GAT GCG CCG GCG TAT
CAG CAG GGC CAG AAC CAG CTG TAT AAC GAA CTG AAC CTG GGC CGC
CGC GAA GAA TAT GAT GTG CTG GAT AAA CGC CGC GGC CGC GAT CCG
GAA ATG GGC GGC AAA CCG CAG CGC CGC AAA AAC CCG CAG GAA GGC
CTG TAT AAC GAA CTG CAG AAA GAT AAA ATG GCG GAA GCG TAT AGC
GAA ATT GGC ATG AAA GGC GAA CGC CGC CGC GGC AAA GGC CAT GAT
GGC CTG TAT CAG GGC CTG AGC ACC GCG ACC AAA GAT ACC TAT GAT
GCG CTG CAT ATG CAG GCG CTG CCG CCG CGC TAA

In the translated version:

MSL TVV SMA CVG FFL LQG AWP LMG GQD KPF LSA RPS TVV PRG GHV
ALQ CHY RRG FNN FML YKE DRS HVP IFH GRI FQE SFI MGP VTP AHA
GTY RCR GSR PHS LTG WSA PSN PLV IMV TGN HRK PSL LAH PGP LLK
SGE TVI LQC WSD VMF EHF FLH REG ISE DPS RLV GQI HDG VSK ANF SIG
PLM PVL AGT YRC YGS VPH SPY QLS APS DPL DIV ITG LYE KPS LSA QPG
PTV QAG ENV TLS CSS WSS YDI YHL SRE GEA HER RLR AVP KVN RTF
QAD FPL GPA THG GTY RCF GSF RAL PCV WSN SSD PLL VSV TGN PSS
SWP SPT EPS SKS GIC RHL HVL IGT SVV IFL FIL LLF FLL Y RVK FSR SAD
APA YQQ GQN QLY NEL NLG RRE EYD VLD KRR GRD PEM GGK PQR RKN
PQE GLY NEL QKD KMA EAY SEI GMK GER RRG KGH DGL YQG LST ATK
DTY DAL HMQ ALP PR

Signalpeptid, Extracellular domain, Transmembrane domain, CD3ζ domain

A.1.6 β2m-KO-Jurkat KIR2DS4*001 sequence

The following sequence of KIR2DS4*001 was used by Dr. Wilfredo Garcia-Beltran *et al.* to generate the plasmid / β2m-KO-Jurkat KIR2DS4 cell line [205]:

ATG TCG CTC ACG GTC GTC AGC ATG GCG TGC GTT GGG TTC TTC TTG
CTG CAG GGG GCC TGG CCA CTC ATG GGT GGT CAG GAC AAA CCC TTC
CTG TCT GCC CGG CCC AGC ACT GTG GTG CCT CGA GGA GGA CAC GTG

GCT CTT CAG TGT CAC TAT CGT CGT GGG TTT AAC AAT TTC ATG CTG
TAC AAA GAA GAC AGA AGC CAC GTT CCC ATC TTC CAC GGC AGA ATA
TTC CAG GAG AGC TTC ATC ATG GGC CCT GTG ACC CCA GCA CAT GCA
GGG ACC TAC AGA TGT CGG GGT TCA CGC CCA CAC TCC CTC ACT GGG
TGG TCG GCA CCC AGC AAC CCC CTG GTG ATC ATG GTC ACA GGA AAC
CAC AGA AAA CCT TCC CTC CTG GCC CAC CCA GGG CCC CTG CTG AAA
TCA GGA GAG ACA GTC ATC CTG CAA TGT TGG TCA GAT GTC ATG TTT
GAG CAC TTC TTT CTG CAC AGA GAG GGG ATC TCT GAG GAC CCC TCA
CGC CTC GTT GGA CAG ATC CAT GAT GGG GTC TCC AAG GCC AAC TTC
TCC ATC GGT CCC TTG ATG CCT GTC CTT GCA GGA ACC TAC AGA TGT
TAT GGT TCT GTT CCT CAC TCC CCC TAT CAG TTG TCA GCT CCC AGT
GAC CCC CTG GAC ATC GTG ATC ACA GGT CTA TAT GAG AAA CCT TCT
CTC TCA GCC CAG CAG GGC CCC ACG GTT CAG GCA GGA GAG AAC GTG
ACC TTG TCC TGT AGC TCC TGG AGC TCC TAT GAC ATC TAC CAT CTG
TCC AGG GAA GGG GAG GCC CAT GAA CGT AGG CTC CGT GCA GTG
CCC AAG GTC AAC AGA ACA TTC CAG GCA GAC TTT CCT CTG GGC CCT
GCC ACC CAC GGA GGG ACC TAC AGA TGC TTC GGC TCT TTC CGT GCC
CTG CCC TGC GTG TGG TCA AAC TCA AGT GAC CCA CTG CTT GTT TCT
GTC ACA GGA AAC CCT TCA AGT AGT TGG CCT TCA CCC ACA GAA CCA
AGC TCC AAA TCT GGT ATC TGC AGA CAC CTG CAT GTT CTG ATT GGG
ACC TCA GTG GTC ATC TTC CTC TTC ATC CTC CTC CTC TTC TTT CTC
CTT TAT CGC GTG AAA TTT AGC CGC AGC GCG GAT GCG CCG GCG TAT
CAG CAG GGC CAG AAC CAG CTG TAT AAC GAA CTG AAC CTG GGC CGC
CGC GAA GAA TAT GAT GTG CTG GAT AAA CGC CGC GGC CGC GAT CCG
GAA ATG GGC GGC AAA CCG CAG CGC CGC AAA AAC CCG CAG GAA GGC
CTG TAT AAC GAA CTG CAG AAA GAT AAA ATG GCG GAA GCG TAT AGC
GAA ATT GGC ATG AAA GGC GAA CGC CGC CGC GGC AAA GGC CAT GAT
GGC CTG TAT CAG GGC CTG AGC ACC GCG ACC AAA GAT ACC TAT GAT
GCG CTG CAT ATG CAG GCG CTG CCG CCG CGC TAA

In the translated version:

MSL TVV SMA CVG FFL LQG AWP QEG VHR KPS FLA LPG HLV KSE ETV
ILQ CWS DVM FEH FLL HRE GKF NNT LHL IGE HHD GVS KAN FSI GPM
MPV LAG TYR CYG SVP HSP YQL SAP SDP LDM VII GLY EKP SLS AQPG
PTV QAG ENV TLS CSS RSS YDM YHL SRE GEA HER RLP AVR SIN GTF
QAD FPL GPA THG GTY RCF GSF RDA PYE WSN SSD PLL VSV TGN PSN
SWP SPT EPS SKT GNP R HL HVL IGT SVV KIP FTI LLF FLL RVK FSR SAD
APA YQQ GQN QLY NEL NLG RRE EYD VLD KRR GRD PEM GGK PQR RKN
PQE GLY NEL QKD KMA EAY SEI GMK GER RRG KGH DGL YQG LST ATK
DTY DAL HMQ ALP PR

Signalpeptid, Extracellular domain, Transmembrane domain, CD3ζ domain

A.1.7 UniProt Blast B7-H7*001 and *002

The following result for protein sequence similarities were obtained for the B7-H7 allotypes *001 and *002. As the protein sequences show a homology of 100 % they are identical. B7-H7 allotype *001 was used for K562 cell line transduction (Figure A.3).

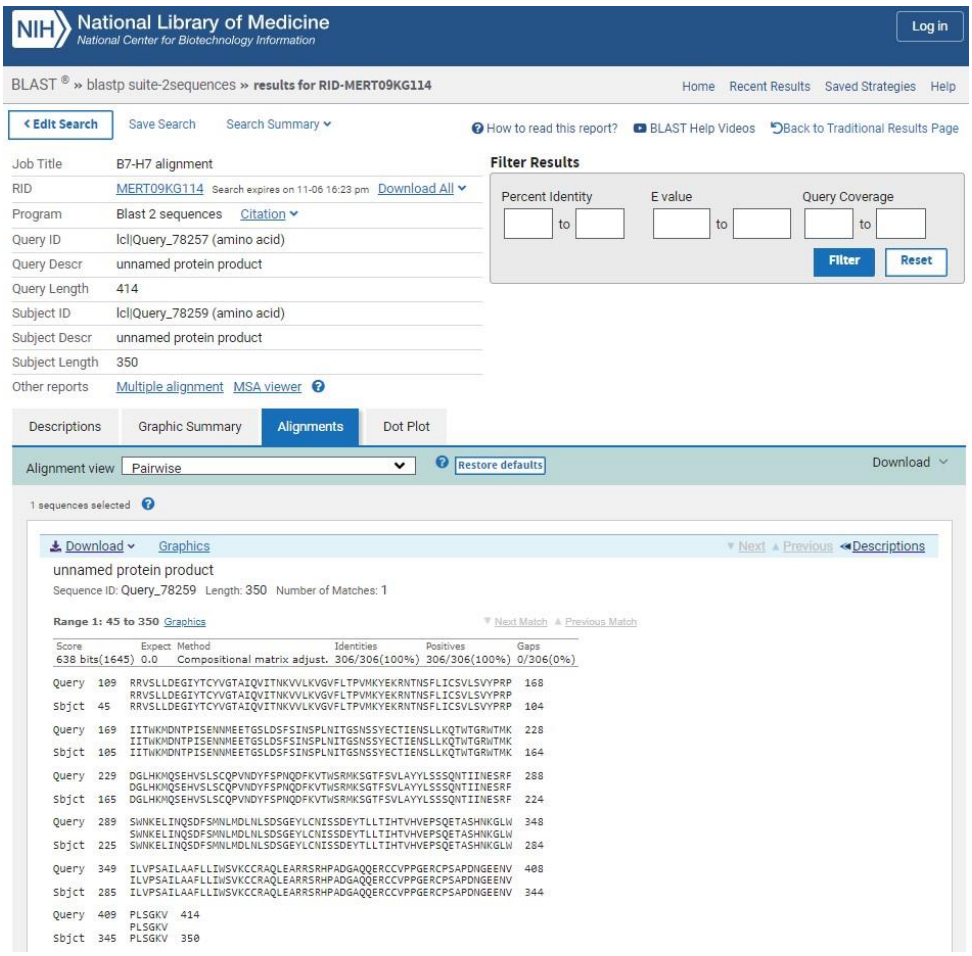

FIGURE A.3: NCBI blast of the UniProt B7-H7 allotypes *001 and *002. The sequence homology of the B7-H7*001 and B7-H7*002 are 100 % and therefore the sequences identical.

A.1.8 K562.B7-H7 sequence

The following sequence of B7-H7 with UniPort ID Q9UM44 was used for plasmid generation:

GAA TTC TCT AGA GCC ACC ATG AAG GCA CAG ACA GCA CTG TCT TTC TTC CCA TTC TCA TAA CAT CTC TAG TGG ATC TCA AGG CAT ATT CCC TTT GCT TTC TTC ATT TGT TCC TAT GAA TGA ACA AAT CGT CAT TGG AAG ACT TGA TGA AGA TAT AAT TCT CCC TTC ATT TGA GAG GGG ATC CGA AGT CGT AAT ACA CTG GAA GTA TCA AGA TAG CTA TAA GGT TCA CAG TTA CTA CAA AGG CAG TGA CCA TTT GGA AAG CCA AGA TCC CAG ATA TGC AAA CAG GAC ATC CCT TTT TCT ATA ATG AGA TTC AAA ATG

GGA ATG CGT CGC TAT TTT TCA GAA GAG TAA GCC TTC TGG ACG AAG GAA TTT ACA CCT GCT ATG TAG GAA CAG CAA TTC AAG TGA TTA CAA ACA AAG TGG TGC TAA AGG TGG GAG TTT TCT CAC ACC CGT GAT GAA GTA TGA AAA GAG GAA CAC AAA CAG CTT CTT AAT ATG CAG CGT GTT AAG TGT TTA TCC TCG TCC AAT TAT CAC GTG GAA AAT GGA CAA CAC ACC TAT CTC TGA AAA CAA CAT GGA AGA AAC AGG GTC TTT GGA TTC TTT TTC TAT TAA CAG CCC ACT GAA TAT TAC AGG ATC AAA TTC ATC TTA TGA ATG TAC AAT TGA AAA TTC ACT GCT GAA GCA AAC ATG GAC AGG GCG CTG GAC GAT GAA AGA TGG CCT TCA TAA AAT GCA AAG TGA ACA CGT TTC ACT CTC ATG TCA ACC TGT AAT GAT TAT TTT TCA CCA AAC CAA GAC TTC AAA GTT ACT TGG TCC AGA ATG AAA AGT GGG ACT TTC TCT GTC CTG GCT TAC TAT CTG AGC TCC TCA CAA AAT ACA ATT ATC AAT GAA TCC CGA TTC TCA TGG AAC AAA GAG CTG ATA AAC CAG AGT GAC TTC TCT ATG AAT TTG ATG GAT CTT AAT CTT TCA GAC AGT GGG GAA TAT TTA TGC AAT ATT TTC TCG GAT GAA TAT ACT TTA CTT ACC ATC CAC ACA GTG CAT GTA GAA CCG AGC CAA GAA ACA GCT CCC ATA ACA AAG GCT TAT GGA TTT TGG TGC CCT CTG CGA TTT GGC AGC TTT TCT GCT GAT TTG GAG CGT AAA ATG TTG CAG AGC CCA GCT AGA AGC CAG GAG GAG CAG ACA CCC TGC TGA TGG AGC CCA ACA AGA AAG ATG TTG TGT CCC TCC TGG TGA GCG CTG TCC AGT GCA CCC GAT AAT GGC GAA GAA AAT GTG CCT CTT TCA GGA AAA GTA TAG

In the translated version:

MKA QTA LSF FLI LIT SLS GSQ GIF PLA FFI YVP MNE QIV IGR LDE DII LPS SFE RGS EVV IHW KYQ DSY KVH SYY KGS DHL ESQ DPR YAN RTS LFY NEI QNG NAS LFF RRV SLL DEG IYT CYV GTA IQV ITN KVV LKV GVF LTP VMK YEK RNT NSF LIC SVL SVY PRP IIT WKM DNT PIS ENN MEE TGS LDS FSI NSP LNI TSN SSY ECT IEN SLL KQT WTG RWT MKD GLH KMQ SEH VSL SCQ PVN DYF SPN QDF KVT WSR MKS GTF SVL AYY LSS SQN TII NES RFS WNK ELI NQS DFS MNL MDL NLS DSG EYL CNI SSD EYT LLT IHT VHV EPS QET ASH NKGLWI LVP SAI LAA FLL IWS VKC CRA QLE ARR SRH PAD GAQQ ERC CVP PGE RCP SAP DNG EEN VPL SGK V

Signalpeptid, Extracellular domain, Transmembrane domain, Cytoplasmic Domain

A.2 R code for statistical analyses and tests

A.2.1 R code for the B7 protein KIR-Fc fusion construct protein screen analysis

A.2.1.1 B7 bead coating

```
##################################################
###### Nils Dominik Lonken
###### Analysis of B7-KIR-Fc screen B7 bead coating controls
###### Dissertation: The B7 protein family as ligands
###### for KIRs
###### 10.11.2023
##################################################

rm(list=ls())

install.packages("FDRestimation")
library("FDRestimation")


#Data frame with all values
df <- structure(list(Protein = c("Biotin", "B7_1", "B7_2",
"B7_Dc", "B7-H1", "B7-H2",
"B7-H3", "B7-H4", "B7-H5", "B7-H6", "B7-H7"),
Biotin1 = c(260380, 936, 353, 42.4, 55.2, 51.4, 41.3, 51.4,
-10.3, 59.1, 436),
Biotin2 = c(261647, 1230, 228, 55.2, 53.9, 55.2, 41.5, 55.2,
29.5, 59.1, 436),
Biotin3 = c(261647, 1270, 275, 48.8, 53.9, 53.9, 42.9, 55.2,
37.2, 59.1, 435),
Biotin4 = c(NA, 998, 755, 43.6,NA,  42.4, 47.5, 50.1,
48.8, 56.5, 450),
Biotin5 = c(NA, 1206, 742, 42.4, NA,51.4, 47.5, 50.1,
48.8, 57.8, 448),
Biotin6 = c(NA, 1558, 587, 50.1, NA, 51.4, 44.9, 47.5,
46.2, 56.5, 451),
Mab1 = c(1109, 8138, 2597, 26196, 20666, 32099, 6241, 15455,
60.4, 6866, 2202),
Mab2 = c(981, 8018, 3426, 26321, 20764, 25580, 4817, 15135,
11800, 6602, 2388),
Mab3 = c(891, 4207, 4313, 26828, 20764, 26637, 1918, 15241,
16154, 2998, 1696),
Mab4 = c(NA, 13144, 5713, 25157, 14349, 34663, 10248, 20042,
```

```
21512, 4692, 2123),
Mab5 = c(NA, 12993, 6821, 25157, 13764, 36459, 10271, 20137,
21614, 4721, 2297),
Mab6 = c(NA, 12815, 6792, 25641, 8658, 35336, 10248, 19854,
14483, 8794, 2202)),
class = "data.frame", row.names = c("1", "2",
"3", "4", "5", "6", "7", "8", "9", "10", "11"))
df

#removal of biotin from data frame as less values
df_no_biotin= df[-1,]
df_no_biotin

#seperate wilcoxon test for biotin
wilcox.test(unlist(df[1, 2:7]),
            unlist(df[1, 8:13]))$p.value

#replacement of NA from B7-H1 with median
median_B7_H1=median(df[5,2],df[5,3],df[5,4])
df_no_biotin[is.na (df_no_biotin)] <- median_B7_H1
df_no_biotin

#as the samples are timly replicates the samples are paired
#and not normally distributed as only two repetitions were
#made--> paired Wilcoxon test per row
a_biotin=wilcox.test(unlist(df_no_biotin[1, 2:7]),
                     unlist(df_no_biotin[1, 8:13]),
                     paired = TRUE, exact = TRUE,
                     correct = TRUE,
                     conf.int = TRUE)$p.value
p_paired <- apply(df_no_biotin[, 2:13], 1,
                  function(x) wilcox.test(x[1:6],
                  x[7:12], paired = TRUE, exact = FALSE,
                  correct = TRUE)$p.value)
p_paired_combined<-c(a_biotin,p_paired)
p_paired_combined

#adjust p-values according to FDR 5%
results=p.fdr(pvalues = p_paired_combined,
      zvalues = "two.sided",
      threshold = 0.05,
      adjust.method = "BH",
```

```
        BY.corr = "positive",
        just.fdr = FALSE,
        default.odds = 1,
        estim.method = "set.pi0",
        set.pi0 = 1,
        hist.breaks = "scott",
        ties.method = "max",
        sort.results = FALSE,
        na.rm = TRUE
)
results

#overview
df_combined=df
df_combined$adjusted_p_values<-results[["Results Matrix"]]
                                      [["Adjusted p-values"]]
df_combined
```

A.2.1.2 HLA bead coating

```
##################################################
###### Nils Dominik Lonken
###### Analysis of B7-KIR-Fc screen HLA controls
###### Dissertation: The B7 protein family as ligands
###### for KIRs
###### 20.11.2023
##################################################

rm(list=ls())

install.packages("FDRestimation")
library("FDRestimation")

#Data frame with all values
df <- structure(list(Protein = c("HLA-A", "HLA-B", "HLA-C",
"HLA-F", "HLA-G", "B7-H6", "B7-H7", "CD155"),
Biotin1 = c(55.2, 281, 47.5, 47.5, 55.2, 60.4, 463, 56.5),
Biotin2 = c(55.2, 83.5, 48.8, 48.8, 55.2, 59.1, 463, 59.1),
Biotin3 = c(55.2, 82.2, 55.2, 55.2, 55.2, 60.4, 464, 60.4),
Biotin4 = c(55.2, 44.9, 51.4, 51.4, 55.2, 57.8, 465, 56.5),
Biotin5 = c(55.2, 10.3, 43.6, 43.6, 55.2, 56.5, 467, 60.4),
Biotin6 = c(56.5, 42.4, 52.6, 52.6, 56.5, 60.4, 464, 59.1),
Mab1 = c(15527, 7957, 15277, 8010, 11507, 5912, 1953, 25337),
```

```
Mab2 = c(15819, 7430, 13892, 6488, 4882, 2033, 1946, 25763),
Mab3 = c(15819, 8081, 14822, 9555, 8373, 3420, 1972, 27085),
Mab4 = c(15819, 7714, 13956, 6516, 4903, 3246, 2021, 28207),
Mab5 = c(15819, 7957, 14754, 9620, 8411, 3319, 1832, 22027),
Mab6 = c(15600, 5951, 15312, 8010, 11534, 3299, 1798,
        22132)),
class = "data.frame", row.names = c("1", "2",
"3", "4", "5", "6", "7", "8"))
df

#as the samples are timly replicates the samples are paired
#and not normally distributed as only one measurement was
#made--> paired Wilcoxon test per row
p_paired <- apply(df[, 2:13], 1, function(x)
                    wilcox.test(x[1:6], x[7:12],
                  paired = TRUE, exact = FALSE,
                  correct = TRUE)$p.value)
p_paired

#adjust p-values according to FDR 5%
results=p.fdr(pvalues = p_paired,
       zvalues = "two.sided",
       threshold = 0.05,
       adjust.method = "BH",
       BY.corr = "positive",
       just.fdr = FALSE,
       default.odds = 1,
       estim.method = "set.pi0",
       set.pi0 = 1,
       hist.breaks = "scott",
       ties.method = "max",
       sort.results = FALSE,
       na.rm = TRUE
)
results
#overview
df_combined=df
df_combined$adjusted_p_values<-results[["Results Matrix"]]
                                [["Adjusted p-values"]]
df_combined
```

A.2.1.3 B7 protein functionality

```
#########################################################
###### Nils Dominik Lonken
###### Analysis of B7–KIR–Fc screen B7 protein functionality
###### controls
###### Dissertation: The B7 protein family as ligands
###### for KIRs
###### 20.11.2023
#########################################################

rm(list=ls())

install.packages("FDRestimation")
library("FDRestimation")

#Data frame with all values
df <- structure(list(Protein = c("B7_1", "B7_2", "B7_Dc",
"B7–H1", "B7–H2", "B7–H3", "B7–H5", "B7–H6", "B7–H7"),
Biotin1 = c(772, 772, 183, 183, 212, 523, 183, 210, 228),
Biotin2 = c(770, 770, 182, 182, 204, 507, 186, 210, 227),
Biotin3 = c(830, 830, 183, 183, 204, 371, 186, 195, 228),
Biotin4 = c(837, 837, 182, 182, 205, 367, 184, 195, 228),
Biotin5 = c(817, 817, 185, 185, 204, 600, 183, 193, 228),
Biotin6 = c(700, 700, 183, 183, 205, 644, 183, 192, 226),
Mab1 = c(4462, 1754, 5865, 6995, 9146, 3212, 185, 6318,
            1254),
Mab2 = c(4435, 1788, 4176, 8322, 8179, 1493, 184, 6318,
            874),
Mab3 = c(3769, 2083, 3717, 8261, 8703, 1126, 183, 7224,
            1016),
Mab4 = c(4761, 3959, 9541, 8447, 7900, 1029, 185, 7224,
            1036),
Mab5 = c(3746, 2514, 4176, 8364, 8118, 3204, 185, 7206,
            987),
Mab6 = c(3126, 2466, 9541, 8468, 7369, 3165, 184, 6541,
            1016)),
class = "data.frame", row.names = c("1", "2",
"3", "4", "5", "6", "7", "8", "9"))
df

#as the samples are timly replicates the samples are paired
#and not normally distributed as only two repetitions were
```

```
#made --> paired Wilcoxon test per row
p_paired <- apply(df[, 2:13], 1, function(x)
                    wilcox.test(x[1:6], x[7:12],
                    paired = TRUE, exact = FALSE,
                    correct = TRUE)$p.value)
p_paired

#adjust p-values according to FDR 5%
result=p.fdr(pvalues = p_paired,
       zvalues = "two.sided",
       threshold = 0.05,
       adjust.method = "BH",
       BY.corr = "positive",
       just.fdr = FALSE,
       default.odds = 1,
       estim.method = "set.pi0",
       set.pi0 = 1,
       hist.breaks = "scott",
       ties.method = "max",
       sort.results = FALSE,
       na.rm = TRUE
)

#overview
df_combined=df
df_combined$adjusted_p_values<-result[["Results Matrix"]]
                                    [["Adjusted p-values"]]
df_combined
```

A.2.1.4 Fc protein functionality

```
#########################################################
###### Nils Dominik Lonken
###### Analysis of B7-KIR-Fc screen Fc protein
###### functionality controls
###### Dissertation: The B7 protein family as ligands
###### for KIRs
###### 22.11.2023
#########################################################

rm(list=ls())

#install.packages("FDRestimation")
```

```
library("FDRestimation")

#Data frame with all values
df <- structure(list(Protein = c("KIR2DL1", "KIR2DL2",
"KIR2DL3", "KIR2DL4", "KIR2DL5", "KIR2DS4", "KIR3DL1",
"KIR3DL2", "KIR3DL3", "KIR3DS1", "NKp30", "NKp46"),
Biotin1 = c(64.6, 60.5, 65.8, 65.8, 67.5, 444, 63.4, 62.3,
76.7, 63.4, 63.4, 62.8),
Biotin2 = c(61.1, 64.6, 63.4, 65.2, 65.2, 445, 67.5, 62.3,
76.7, 68.7, NA, 62.8),
Biotin3 = c(59.9, 65.8, 66.3, 65.8, 65.8, 443, 68.7, 62.3,
75, 62.8, NA, 70.4),
Mab1 = c(23965, 19763, 19811, 1472, 1475, 2795, 36620,
36891, 7704, 28512, 23293, 19334),
Mab2 = c(24319, 19811, 37073, 1468, 1475, 2769, 36620,
36800, 12656, 20299, NA, 19571),
Mab3 = c(19666, 19859, 1472, 1481, 1478, 2743, 36710,
36891, 17613, 20399, NA, 19523)),
class = "data.frame", row.names = c("1", "2",
"3", "4", "5", "6", "7", "8", "9", "10", "11", "12"))
df

#replacement of NA from NKp30 with median
median_NKp30_biotin=median(df[11,2])
df['Biotin2'][is.na(df['Biotin2'])]<- median_NKp30_biotin
df['Biotin3'][is.na(df['Biotin3'])]<- median_NKp30_biotin
median_NKp30_mab=median(df[11,5])
df['Mab2'][is.na(df['Mab2'])]<- median_NKp30_mab
df['Mab3'][is.na(df['Mab3'])]<- median_NKp30_mab
df

#as the samples are only one replicates the samples are
#not paired and not normally distributed -->
#Wilcoxon test per row
p_paired <- apply(df[, 2:6], 1, function(x)
            wilcox.test(x[1:3], x[4:6],
                  paired = FALSE, exact = FALSE,
                  correct = TRUE)$p.value)
p_paired

#adjust p-values according to FDR 5%
results=p.fdr(pvalues = p_paired,
```

```
        zvalues = "two.sided",
        threshold = 0.05,
        adjust.method = "BH",
        BY.corr = "positive",
        just.fdr = FALSE,
        default.odds = 1,
        estim.method = "set.pi0",
        set.pi0 = 1,
        hist.breaks = "scott",
        ties.method = "max",
        sort.results = FALSE,
        na.rm = TRUE
)

#overview
df_combined=df
df_combined$adjusted_p_values<-results[["Results Matrix"]]
                                      [["Adjusted p-values"]]
df_combined


#Simulation to test whether results with bigger n would
#have been statistically significant. Assuming a normal
#distribution around MdFI and MAD.

#collection of Median and MAD for all KIR in Table
df_median_MAD <- structure(list(Protein = c("KIR2DL1",
"KIR2DL2", "KIR2DL3", "KIR2DL4", "KIR2DL5", "KIR2DS4",
"KIR3DL1", "KIR3DL2", "KIR3DL3", "KIR3DS1", "NKp30",
"NKp46"),
              Dist_Values=rep(3,each=12),
              Median_biotin = c(61.10, 64.60, 65.80, 65.80,
              65.80, 444.00, 67.50, 62.30, 76.70, 63.40,
              63.40, 62.80),
              MAD_biotin = c(1.20, 1.20, 0.50, 0.60, 0.60,
              1.00, 4.70, 0.00, 1.70, 0.60, 0.50, 4.50),
              Median_mab = c(23965.00, 19811.00, 19811.00,
              1472.00, 1475.00, 2769.00, 36620.00,
              36891.00, 12656.00, 20399.00, 23293.00,
              9523.00),
              MAD_mab = c(354.00, 48.00, 17262.00, 4.00,
              3.00, 26.00, 30.00, 5.30, 4952.00, 100.00,
```

```
            24.50, 48.00)),
            class = "data.frame", row.names = c("1", "2",
                                                "3", "4",
                                                "5", "6",
                                                "7", "8",
                                                "9", "10",
                                                "11", "12"))
df_median_MAD

#Generating normally distributed values around measured MdFI
#with sd of MAD for each row

#values for biotin measures
normalise_biotin <- apply(df_median_MAD[,-1], 1,
function(x) rnorm(x[1], mean=x[2], sd=x[3]))
normalise_biotin
trans_normalise_biotin<-t(normalise_biotin)
trans_normalise_biotin

#values for Fc measures
normalise_Fc <- apply(df_median_MAD[,-1], 1,
function(x) rnorm(x[1], mean=x[4], sd=x[5]))
normalise_Fc
trans_normalise_Fc<-t(normalise_Fc)
trans_normalise_Fc

#New df with modulated values
df_modulated <- structure(list(Protein = c("KIR2DL1",
"KIR2DL2", "KIR2DL3", "KIR2DL4", "KIR2DL5",
"KIR2DS4", "KIR3DL1", "KIR3DL2", "KIR3DL3", "KIR3DS1",
"NKp30", "NKp46"),
                      Biotin1 = c(64.6, 60.5, 65.8, 65.8,
                      67.5, 444, 63.4, 62.3, 76.7, 63.4,
                      63.4, 62.8),
                      Biotin2 = c(61.1, 64.6, 63.4, 65.2,
                      65.2, 445, 67.5, 62.3, 76.7, 68.7,
                      NA, 62.8),
                      Biotin3 = c(59.9, 65.8, 66.3, 65.8,
                      65.8, 443, 68.7, 62.3, 75, 62.8,
                      NA, 70.4),
                      Biotin4 = trans_normalise_biotin[,1],
                      Biotin5 = trans_normalise_biotin[,2],
```

```
                    Biotin6 = trans_normalise_biotin[,3],
                    Mab1 = c(23965, 19763,
                    19811, 1472, 1475, 2795, 36620, 36891,
                    7704, 28512, 23293, 19334),
                    Mab2 = c(24319, 19811,
                    37073, 1468, 1475, 2769, 36620, 36800,
                    12656, 20299, NA, 19571),
                    Mab3 = c(19666, 19859,
                    1472, 1481, 1478, 2743, 36710, 36891,
                    17613, 20399, NA, 19523),
                    Mab4 = trans_normalise_Fc[,1],
                    Mab5 = trans_normalise_Fc[,2],
                    Mab6 = trans_normalise_Fc[,3]),
                class = "data.frame", row.names = c("1", "2",
                                                    "3", "4",
                                                    "5", "6",
                                                    "7", "8",
                                                    "9",
                                                    "10",
                                                    "11",
                                                    "12"))
df_modulated

#replacement of NA from NKp30 with median
median_NKp30_biotin=median(df_modulated[11,2])
df_modulated['Biotin2'][is.na(df_modulated['Biotin2'])]<-
median_NKp30_biotin
df_modulated['Biotin3'][is.na(df_modulated['Biotin3'])]<-
median_NKp30_biotin
median_NKp30_mab=median(df_modulated[11,8])
df_modulated['Mab2'][is.na(df_modulated['Mab2'])]<-
median_NKp30_mab
df_modulated['Mab3'][is.na(df_modulated['Mab3'])]<-
median_NKp30_mab
df_modulated


#as the samples are timely replicates the samples are
#paired and not normally distributed as only two
#repetitions were made--> paired Wilcoxon test per row
p_paired <- apply(df_modulated[, 2:13], 1,
function(x) wilcox.test(x[1:6], x[7:12], paired = TRUE,
```

```
exact = FALSE, correct = TRUE)$p.value)
p_paired


#adjust p-values according to FDR 5%
results=p.fdr(pvalues = p_paired,
              zvalues = "two.sided",
              threshold = 0.05,
              adjust.method = "BH",
              BY.corr = "positive",
              just.fdr = FALSE,
              default.odds = 1,
              estim.method = "set.pi0",
              set.pi0 = 1,
              hist.breaks = "scott",
              ties.method = "max",
              sort.results = FALSE,
              na.rm = TRUE
)

#overview
df_combined=df_modulated
df_combined$adjusted_p_values<-results[["Results Matrix"]]
[["Adjusted p-values"]]
df_combined
```

A.2.1.5 B7 protein KIR-Fc fusion construct protein screen

```
##################################################
###### Nils Dominik Lonken
###### Analysis of B7-KIR-Fc screen
###### Dissertation: The B7 protein family as ligands
###### for KIRs
###### 10.11.2023
##########################################################

#Analysis of NKp30 data
NKp30_B7_H6_2nd_only<-c(79.8, 116, 89.5, 84.3, 75.8, 69.8)
NKp30_B7_H6_Fc<-c(2893, 2803, 2837, 1345, 1609, 1382)
data_NKp30_B7_H6<-data.frame(NKp30_B7_H6_2nd_only,
                             NKp30_B7_H6_Fc)

#as the samples are timly replicates the samples are paired
```

```
#and not normally distributed as only two repetitions were
#made--> paired Wilcoxon test

wilcox.test(data_NKp30_B7_H6$NKp30_B7_H6_2nd_only,
            data_NKp30_B7_H6$NKp30_B7_H6_Fc,
            paired = TRUE, exact = TRUE,
            correct = TRUE, conf.int = TRUE)

#Analysis of KIR3DL2 data
KIR3DL2_B7_H1_2nd_only<-c(97.1, 96.3, 97.1, 101, 99.1, 99.1)
KIR3DL2_B7_H1_Fc<-c(116, 118, 122, 1601, 1563, 2190)
data_KIR3DL2_B7_H1<-data.frame(KIR3DL2_B7_H1_2nd_only,
                               KIR3DL2_B7_H1_Fc)

#as the samples are timly replicates the samples are paired
#and not normally distributed as only two repetitions were
#made--> paired Wilcoxon test

wilcox.test(data_KIR3DL2_B7_H1$KIR3DL2_B7_H1_2nd_only,
            data_KIR3DL2_B7_H1$KIR3DL2_B7_H1_Fc,
            paired = TRUE, exact = TRUE, correct = TRUE,
            conf.int = TRUE)

#Analysis of KIR3DL3 data
KIR3DL3_B7_H7_2nd_only<-c(66, 56.2, 59.9, 61.4, 62.3, 61.4)
KIR3DL3_B7_H7_Fc<-c(7687, 12666, 17589, 168, 143, 257)
data_KIR3DL3_B7_H7<-data.frame(KIR3DL3_B7_H7_2nd_only,
                               KIR3DL3_B7_H7_Fc)

#as the samples are timly replicates the samples are paired
#and not normally distributed as only two repetitions were
#made--> paired Wilcoxon test

wilcox.test(data_KIR3DL3_B7_H7$KIR3DL3_B7_H7_2nd_only,
            data_KIR3DL3_B7_H7$KIR3DL3_B7_H7_Fc,
            paired = TRUE, exact = TRUE, correct = TRUE,
            conf.int = TRUE)
```

A.2.2 R code for the β2m-KO-Jurkat KIR3DL2 and B7-H1-Fc fusion construct protein binding assay analysis

```
#####################################################
###### Nils Dominik Lonken
###### Analysis of B7-H1 Fc vs. KIR3DL2 binding assay
###### Dissertation: The B7 protein family as ligands
###### for KIRs
###### 20.11.2023
#############################################################

rm(list=ls())

#install.packages("FDRestimation")
library("FDRestimation")

##Expression testing
#Statistical significance expression level KIR2DS4
KIR2DS4_Iso<-c(0.48,    0.05, 0.00)
KIR2DS4_mab<-c(92.00,   96.10,  79.80)
data_KIR2DS4<-data.frame(KIR2DS4_Iso, KIR2DS4_mab)

#as the samples are timely replicates the samples are paired
#and not normally distributed as only three repetitions were
#made--> paired Wilcoxon test
wilcox.test(data_KIR2DS4$KIR2DS4_Iso,
data_KIR2DS4$KIR2DS4_mab, paired = TRUE, exact = TRUE,
correct = TRUE, conf.int = TRUE)

#Statistical significance expression level KIR3DL2
KIR3DL2_Iso<-c(0.70, 0.02, 0.07)
KIR3DL2_mab<-c(42.30, 34.90, 20.3)
data_KIR3DL2<-data.frame(KIR3DL2_Iso, KIR3DL2_mab)

#as the samples are timely replicates the samples are paired
#and not normally distributed as only three repetitions were
#made--> paired Wilcoxon test
wilcox.test(data_KIR3DL2$KIR3DL2_Iso,
data_KIR3DL2$KIR3DL2_mab, paired = TRUE, exact = TRUE,
correct = TRUE, conf.int = TRUE)
```

```
##B7–H1 Fc test
#Data frame with all values
df <- data.frame(Measurement = rep(1:9, times=3),
                 Cell_Line = rep(c("Beta2KO", "KIR2DS4",
                 "KIR3DL2"), each=9),
                 Score = c(21.3, 18.7, 16.7, 30.7, 20.2,
                 24.7, 18.5, 20.5, 23.3, 102, 30.7,
                 30.7, 28.5, 30.1, 29.8, 44, 34.6, 37.8,
                 19.6, 21.1, 24.5, 28.9, 25.6, 26.7,
                 23.8, 27.8, 30.1))
df

#as the samples are timely replicates of the same samples,
#they are paired and not normally distributed as only
#three repetitions were made. As one compares three groups
#with each other Friedman test Post hoc analysis with
#pairwise wilcoxon tests adjusted for multiple testing
#with Benjamini & Hochberg method
friedman.test(y=df$Score, groups=df$Cell_Line,
blocks=df$Measurement)
Overall_result_of_Friedmantest<-friedman.test(y=df$Score,
groups=df$Cell_Line, blocks=df$Measurement)$p.value
Overall_result_of_Friedmantest

pairwise_comparison<-pairwise.wilcox.test(df$Score,
            df$Cell_Line, exact=FALSE, p.adj = "BH")
pairwise_comparison

#result overview
results<-cbind(pairwise_comparison[["p.value"]],
Overall_result_of_Friedmantest)
results
```

A.2.3 R code for the β2m-KO-Jurkat KIR3DL3 and B7-H7-Fc fusion construct protein binding assay analysis

A.2.3.1 R code for the β2m-KO-Jurkat KIR3DL3 and B7-H7-Fc fusion construct protein binding assay - KIR Expression

```
#########################################################
####### Nils Dominik Lonken
####### Analysis of KIR3DL3 expression
```

```
###### Dissertation: The B7 protein family as ligands
###### for KIRs
###### 20.11.2023
#############################################################

rm(list=ls())

#install.packages("FDRestimation")
library("FDRestimation")

##Expression testing
#Statistical significance expression level KIR2DS4
KIR3DL3_Iso<-c(0.02, NA, NA)
KIR3DL3_mab<-c(36.7, 37.8, 51.1)
data_KI3DL3<-data.frame(KIR3DL3_Iso, KIR3DL3_mab)

#as the samples are timely replicates the samples are paired
#and not normally distributed as only three repetitions were
#made--> paired Wilcoxon test
wilcox.test(data_KI3DL3$KIR3DL3_Iso,data_KI3DL3$KIR3DL3_mab,
            paired = TRUE, exact = TRUE,
            correct = TRUE, conf.int = TRUE)
```

A.2.3.2 R code for the β2m-KO-Jurkat KIR3DL3 and B7-H7-Fc fusion construct protein binding assay - Assay

```
#####################################################
###### Nils Dominik Lonken
###### Analysis of B7-H7 Fc vs. KIR3DL3 binding assay
###### Dissertation: The B7 protein family as ligands
###### for KIRs
###### 21.11.2023
#############################################################

rm(list=ls())

install.packages("FDRestimation")
library("FDRestimation")

##KIR Expression testing
#Statistical significance expression level KIR2DL5
KIR2DL5_Iso<-c(0.10, 0.02, 1.73)
KIR2DL5_mab<-c(17.50, 0.01, 44.10, 7.63, 3.32E-05, 62.70)
```

```
data_KIR2DL5<-data.frame(KIR2DL5_Iso, KIR2DL5_mab)

#as the samples are timely replicates the samples are paired
#and not normally distributed as only three repetitions were
#made--> paired Wilcoxon test
wilcox.test(data_KIR2DL5$KIR2DL5_Iso,
data_KIR2DL5$KIR2DL5_mab, paired = TRUE,
            exact = TRUE, correct = TRUE, conf.int = TRUE)

#Statistical significance expression level KIR3DL1
KIR3DL1_Iso<-c(0.05, 0.02, 0.22)
KIR3DL1_mab<-c(12.30, 0.11, 62.40, 8.88, 0.09, 62.80)
data_KIR3DL1<-data.frame(KIR3DL1_Iso, KIR3DL1_mab)

#as the samples are timely replicates the samples are paired
#and not normally distributed as only three repetitions were
#made--> paired Wilcoxon test
wilcox.test(data_KIR3DL1$KIR3DL1_Iso,
data_KIR3DL1$KIR3DL1_mab, paired = TRUE,
            exact = TRUE, correct = TRUE, conf.int = TRUE)

#Statistical significance expression level KIR3DL3
KIR3DL3_Iso<-c(0.02, 0.02, 0.04)
KIR3DL3_mab<-c(93.30, 52.70, 50.40, 86.90, 39.60, 47.80)
data_KIR3DL3<-data.frame(KIR3DL3_Iso, KIR3DL3_mab)

#as the samples are timely replicates the samples are paired
#and not normally distributed as only three repetitions were
#made--> paired Wilcoxon test
wilcox.test(data_KIR3DL3$KIR3DL3_Iso,
data_KIR3DL3$KIR3DL3_mab, paired = TRUE,
            exact = TRUE, correct = TRUE, conf.int = TRUE)

##B7-H7 Fc test
#Data frame with all values
df <- data.frame(Measurement = rep(1:9, times=4),
                 Cell_Line = rep(c("Beta2KO", "KIR2DL5",
                 "KIR3DL1", "KIR3DL3"), each=9),
                 Score = c(217, 211, 215, 388, 408, 400, 245,
                 248, 255, NA, 280, 320, 531, 519, 527, 442,
                 394, 361, 259, 268, 271, 486, 485, 473, 336,
                 277, 314, 802, 930, 1068, 612, 1012, 1189,
```

```
                    4976, 5262, 6428))
df

#as the samples are timely replicates of the same samples,
#they are paired and not normally distributed as only
#three repetitions were made.
#As one compares four groups with each other Friedman test
#Post hoc analysis with pairwise wilcoxon tests adjusted for
#multiple testing with Benjamini & Hochberg method
friedman.test(y=df$Score, groups=df$Cell_Line,
blocks=df$Measurement)
Overall_result_of_Friedmantest<-friedman.test(y=df$Score,
groups=df$Cell_Line, blocks=df$Measurement)$p.value
Overall_result_of_Friedmantest

pairwise_comparison<-pairwise.wilcox.test(df$Score,
            df$Cell_Line, exact=FALSE, p.adj = "BH")
pairwise_comparison

#result overview
results<-cbind(pairwise_comparison[["p.value"]],
Overall_result_of_Friedmantest)
results
```

A.2.4 R code for the β2m-KO-Jurkat KIR3DL3 B7-H7 protein reporter cell assay analysis

```
##################################################
###### Nils Dominik Lonken
###### Analysis of B7-H7 vs. KIR3DL3 reporter cell assay
###### Dissertation: The B7 protein family as ligands
###### for KIRs
###### 21.11.2023
##################################################

rm(list=ls())

install.packages("FDRestimation")
library("FDRestimation")

##KIR Expression testing
#Statistical significance expression level KIR2DL5
KIR2DL5_Iso<-c(2.29)
```

```
KIR2DL5_mab<-c(41.40, 35.70, 21.20, 40.80, 37.80, 25.20,
39.80, 34.70, 24.80)
data_KIR2DL5<-data.frame(KIR2DL5_Iso, KIR2DL5_mab)

#as the samples are timely replicates the samples are paired
#and not normally distributed as only three repetitions
#were made--> paired Wilcoxon test
wilcox.test(data_KIR2DL5$KIR2DL5_Iso,
data_KIR2DL5$KIR2DL5_mab, paired = TRUE, exact = TRUE,
correct = TRUE, conf.int = TRUE)

#Statistical significance expression level KIR3DL1
KIR3DL1_Iso<-c(8.19)
KIR3DL1_mab<-c(29.20, 43.90, 36.90, 33.60, 37.10, 36.30,
39.00, 46.30, 29.90)
data_KIR3DL1<-data.frame(KIR3DL1_Iso, KIR3DL1_mab)

#as the samples are timely replicates the samples are paired
#and not normally distributed as only three repetitions
#were made--> paired Wilcoxon test
wilcox.test(data_KIR3DL1$KIR3DL1_Iso,
data_KIR3DL1$KIR3DL1_mab, paired = TRUE, exact = TRUE,
correct = TRUE, conf.int = TRUE)

#Statistical significance expression level KIR3DL3
KIR3DL3_Iso<-c(3.66)
KIR3DL3_mab<-c(2.01, 46.80, 14.50, 49.90, 45.90, 5.31,
47.90, 32.30, 26.00)
data_KIR3DL3<-data.frame(KIR3DL3_Iso, KIR3DL3_mab)

#as the samples are timely replicates the samples are paired
#and not normally distributed as only three repetitions
#were made--> paired Wilcoxon test
wilcox.test(data_KIR3DL3$KIR3DL3_Iso,
data_KIR3DL3$KIR3DL3_mab, paired = TRUE, exact = TRUE,
correct = TRUE, conf.int = TRUE)


##Reporter cell assay test
#data frame with all values
df <- data.frame(Measurement = rep(1:9, times=12),
                 Cell_Line = rep(c("Beta2KO", "KIR2DL5",
```

```
                    "KIR3DL1", "KIR3DL3"), each=27),
                    Condition = rep(rep(c("Medium", "Mab",
                    "B7–H7"), timestamp=3),each=9),
                    Score = c(318, 294, 291, 250, 301, 301, 250,
                    251, 271, 288, 282, 422, 299, 298, 288, 271,
                    276, 246, 403, 406, 457, 285, 291, 303, 294,
                    295, 294,
                              286, 250, 253, 269, 271, 303, 287,
                   358, 354, 693, 597, 587, 1194, 1326, 1062,
                   1289, 1728, 1543, 254, 265, 254, 326, 273,
                   288, 357, 347, 344,
                              298, 289, 281, 268, 277, 290, 255,
                   268, 272, 791, 755, 541, 1211, 1558, 1476,
                   555, 467, 1031, 282, 280, 282, 291, 278, 282,
                   279, 243, 263,
                              513, 272, 272, 318, 292, 316, 304,
                   272, 258, 464, 516, 496, 1376, 1014, 1059,
                   6381, 1660, 1602, 498, 503, 493, 1504, 943,
                   1067, 1186, 1569, 1197))
df

##as the samples are timely replicates of the same samples,
##they are paired and not normally distributed as only three
##repetitions were made. As one compares three groups with
##each other Friedman test post-hoc analysis with pairwise
##wilcoxon tests adjusted for multiple testing with
##Benjamini & Hochberg method

##first test within the cell lines whether difference
##between medium, mab, B7–H7

##Beta2KO
#get data from original frame
df_Beta2KO<-df[df$Cell_Line=="Beta2KO",]
df_Beta2KO

friedman.test(y=df_Beta2KO$Score,
                   groups=df_Beta2KO$Condition,
                   blocks=df_Beta2KO$Measurement)
Overall_result_of_Friedmantest_df_Beta2KO<-
friedman.test(y=df_Beta2KO$Score,
                   groups=df_Beta2KO$Condition,
```

```
                blocks=df_Beta2KO$Measurement)$p.value
Overall_result_of_Friedmantest_df_Beta2KO

pairwise_comparison_df_Beta2KO<-
pairwise.wilcox.test(df_Beta2KO$Score, df_Beta2KO$Condition,
                     exact=FALSE, p.adj = "BH")
pairwise_comparison_df_Beta2KO

#result overview Beta2KO
results_df_Beta2KO<-cbind(
pairwise_comparison_df_Beta2KO[["p.value"]],
Overall_result_of_Friedmantest_df_Beta2KO)
results_df_Beta2KO


##KIR2DL5
#get data from original frame
df_KIR2DL5<-df[df$Cell_Line=="KIR2DL5",]
df_KIR2DL5

friedman.test(y=df_KIR2DL5$Score,
                groups=df_KIR2DL5$Condition,
                blocks=df_KIR2DL5$Measurement)
Overall_result_of_Friedmantest_df_KIR2DL5<-
friedman.test(y=df_KIR2DL5$Score,
                groups=df_KIR2DL5$Condition,
                blocks=df_KIR2DL5$Measurement)$p.value
Overall_result_of_Friedmantest_df_KIR2DL5

pairwise_comparison_df_KIR2DL5<-
pairwise.wilcox.test(df_KIR2DL5$Score, df_KIR2DL5$Condition,
                     exact=FALSE, p.adj = "BH")
pairwise_comparison_df_KIR2DL5

#result overview KIR2DL5
results_df_KIR2DL5<-cbind(
pairwise_comparison_df_KIR2DL5[["p.value"]],
Overall_result_of_Friedmantest_df_KIR2DL5)
results_df_KIR2DL5

##KIR3DL1
#get data from original frame
```

```
df_KIR3DL1<-df[df$Cell_Line=="KIR3DL1",]
df_KIR3DL1

friedman.test(y=df_KIR3DL1$Score,
              groups=df_KIR3DL1$Condition,
              blocks=df_KIR3DL1$Measurement)
Overall_result_of_Friedmantest_df_KIR3DL1<-
friedman.test(y=df_KIR3DL1$Score,
              groups=df_KIR3DL1$Condition,
              blocks=df_KIR3DL1$Measurement)$p.value
Overall_result_of_Friedmantest_df_KIR3DL1

pairwise_comparison_df_KIR3DL1<-
pairwise.wilcox.test(df_KIR3DL1$Score, df_KIR3DL1$Condition,
                     exact=FALSE, p.adj = "BH")
pairwise_comparison_df_KIR3DL1

#result overview KIR3DL1
results_df_KIR3DL1<-cbind(
pairwise_comparison_df_KIR3DL1[["p.value"]],
Overall_result_of_Friedmantest_df_KIR3DL1)
results_df_KIR3DL1

##KIR3DL3
#get data from original frame
df_KIR3DL3<-df[df$Cell_Line=="KIR3DL3",]
df_KIR3DL3

friedman.test(y=df_KIR3DL3$Score,
              groups=df_KIR3DL3$Condition,
              blocks=df_KIR3DL3$Measurement)
Overall_result_of_Friedmantest_df_KIR3DL3<-
friedman.test(y=df_KIR3DL3$Score,
              groups=df_KIR3DL3$Condition,
              blocks=df_KIR3DL3$Measurement)$p.value
Overall_result_of_Friedmantest_df_KIR3DL3

pairwise_comparison_df_KIR3DL3<-
pairwise.wilcox.test(df_KIR3DL3$Score, df_KIR3DL3$Condition,
                     exact=FALSE, p.adj = "BH")
pairwise_comparison_df_KIR3DL3
```

```
#result overview KIR3DL3
results_df_KIR3DL3<-cbind(
pairwise_comparison_df_KIR3DL3[["p.value"]],
Overall_result_of_Friedmantest_df_KIR3DL3)
results_df_KIR3DL3

##as the samples are timely replicates of the same samples,
##they are paired and not normally distributed as only
##three repetitions were made. As one compares three
##groups with each other Friedman test post-hoc analysis
##with pairwise wilcoxon tests adjusted for multiple testing
##with Benjamini & Hochberg method

##Now test between all B7-H7 treated groups B7-H7
##B7-H7
df_B7_H7<-df[df$Condition=="B7-H7",]
df_B7_H7

friedman.test(y=df_B7_H7$Score,
                groups=df_B7_H7$Cell_Line,
                blocks=df_B7_H7$Measurement)
Overall_result_of_Friedmantest_df_B7_H7<-
friedman.test(y=df_B7_H7$Score,
                groups=df_B7_H7$Cell_Line,
                blocks=df_B7_H7$Measurement)$p.value
Overall_result_of_Friedmantest_df_B7_H7

pairwise_comparison_df_B7_H7<-
pairwise.wilcox.test(df_B7_H7$Score, df_B7_H7$Cell_Line,
exact=FALSE, p.adj = "BH")
pairwise_comparison_df_B7_H7

#result overview KIR3DL3
results_df_B7_H7<-cbind(
pairwise_comparison_df_B7_H7[["p.value"]],
Overall_result_of_Friedmantest_df_B7_H7)
results_df_B7_H7
```

A.2.5 R code for the NK cell killing assay and its inhibition analysis

A.2.5.1 R code for the NK cell killing assay and its inhibition analysis - B7-H7 Expression

```
################################################
###### Nils Dominik Lonken
###### Analysis of B7-H7 expression
###### Dissertation: The B7 protein family as ligands
###### for KIRs
###### 20.11.2023
################################################################

##Expression testing
#Statistical significance expression level KIR2DS4
B7_H7_Iso<-c(0.0, NA, NA)
B7_H7_mab<-c(72.4,      70.8,    80.1)
data_B7_H7<-data.frame(B7_H7_Iso, B7_H7_mab)

#as the samples are timely replicates the samples are paired
#and not normally distributed as only three repetitions were
#made--> paired Wilcoxon test
wilcox.test(data_B7_H7$B7_H7_Iso,data_B7_H7$B7_H7_mab,
            paired = TRUE, exact = TRUE,
            correct = TRUE, conf.int = TRUE)
```

A.2.5.2 R code for the NK cell killing assay and its inhibition analysis - Assay

```
################################################
###### Nils Dominik Lonken
###### Analysis of NK cell killing assay
###### Dissertation: The B7 protein family as ligands
###### for KIRs
###### 21.11.2023
################################################################

rm(list=ls())

install.packages("FDRestimation")
library("FDRestimation")

##B7-H7 Expression testing
#Statistical significance expression level B7-H7
```

```
#on K562.B7-H7
B7_H7_Iso<-c(1.56, 1.62, 1.91)
B7_H7_mab<-c(98.60, 93.00, 85.00, 98.70, 95.70, 95.20,
             97.80, 97.00, 77.40)
data_B7_H7<-data.frame(B7_H7_Iso, B7_H7_mab)

#as the samples are timely replicates the samples are paired
#and not normally distributed as only three repetitions were
#made--> paired Wilcoxon test
wilcox.test(data_B7_H7$B7_H7_Iso,data_B7_H7$B7_H7_mab,
            paired = TRUE, exact = TRUE, correct = TRUE,
            conf.int = TRUE)


##KIR3DL3 Expression testing
#Statistical significance expression level KIR3DL3
#on NK-92MI
KIR3DL3_Iso<-c(0.39, 0.76, 1.92)
KIR3DL3_mab<-c(39.60, 33.30, 81.60, 53.30, 34.70, 78.10,
               35.60, 37.50, 73.30)
data_KIR3DL3<-data.frame(KIR3DL3_Iso, KIR3DL3_mab)

#as the samples are timely replicates the samples are paired
#and not normally distributed as only three repetitions were
#made--> paired Wilcoxon test
wilcox.test(data_KIR3DL3$KIR3DL3_Iso,
            data_KIR3DL3$KIR3DL3_mab,
            paired = TRUE, exact = TRUE, correct = TRUE,
            conf.int = TRUE)


######## WITHOUT B7-H7 Blocking Mab #############
#Data frame with all values for the experiments with B7-H7
#blocking Antibody
df_without_mab <- data.frame(Measurement = rep(1:9, times=3),
        Condition = rep(c("Only", "E:T 5:1","E:T 3:1",
                          "E:T 1:1", "E:T 1:3", "E:T 1:5"),
                          each=9),
        Score = c(1.048321638, 1.138369375, 0.813308987,
                  1.045766745, 0.997657623, 0.956575632,
                  1.027145853, 0.99341981, 0.979434337,
                  1.023413506, 1.046246998, 0.906882376,
```

```
                    0.928969875, 0.873840691, 0.894206347,
                    0.319665937, 0.603546535, 0.638310985,
                    0.979432966, 1.002269106, 0.885104362,
                    0.920053018, 0.897060197, 0.837504869,
                    0.319046943, 0.294824821, 0.331298225,
                    0.763067245, 0.896892905, 0.814156602,
                    0.757678922, 0.73991122, 0.764982625,
                    0.286389635, 0.288566844, 0.28946437,
                    0.817127643, 0.685097531, 0.78435624,
                    0.678497633, 0.704255241, 0.676250953,
                    0.280283569, 0.28390872, 0.290017072,
                    0.778131191, 0.829752181, 0.771438328,
                    0.583727983, 0.647508079, 0.604566673,
                    0.308093639, 0.294509942, 0.296539267))
df_without_mab

#as the samples are timely replicates of the same samples,
#they are paired and not normally distributed as only
#three repetitions were made. As one compares three groups
#with each other Friedman test post-hoc analysis with
#pairwise wilcoxon tests adjusted for multiple testing
#with Benjamini & Hochberg method
friedman.test(y=df_without_mab$Score,
              groups=df_without_mab$Condition,
              blocks=df_without_mab$Measurement)
Overall_result_of_Friedmantest_without_mab<-
friedman.test(y=df_without_mab$Score,
                groups=df_without_mab$Condition,
                blocks=df_without_mab$Measurement)$p.value
Overall_result_of_Friedmantest_without_mab

pairwise_comparison_without_mab<-
pairwise.wilcox.test(df_without_mab$Score,
                     df_without_mab$Condition, exact=FALSE,
                                          p.adj = "BH")
pairwise_comparison_without_mab

#result overview
results_without_mab<-cbind(
         pairwise_comparison_without_mab["p.value"],
          Overall_result_of_Friedmantest_without_mab)
results_without_mab
```

```
######## WITH B7-H7 Blocking Mab ##############
#Data frame with all values for the experiments with B7-H7
#blocking Antibody
df_with_mab <- data.frame(Measurement = rep(1:9, times=3),
            Condition = rep(c("Only", "E:T 5:1","E:T 3:1",
                              "E:T 1:1", "E:T 1:3",
                              "E:T 1:5"), each=9),
            Score = c(1.048321638, 1.138369375, 0.813308987,
                      1.045766745, 0.997657623, 0.956575632,
                      1.027145853, 0.99341981, 0.979434337,
                      0.770572516, 0.610205401, 0.629562192,
                      2.805552561, 2.807413205, 2.772806577,
                      0.978772018, 1.138241126, 1.014256646,
                      0.667826866, 0.781991194, 72.56465028,
                      3.183586243, 2.921205957, 3.546938813,
                      0.873753561, 0.884744172, 0.816882028,
                      1.517609584, 1.368759679, 1.134512034,
                      3.610606518, 2.996868701, 4.008327516,
                      1.465115287, 1.379776307, 1.629817867,
                      1.590207701, 1.948347151, 1.923692497,
                      3.768229167, 3.943854407, 3.936158771,
                      1.270694237, 1.72365037,  1.69766212,
                      2.602158057, 2.543005112, 3.019136731,
                      4.101426446, 3.751594826, 4.575007007,
                      1.366765347, 1.402473756, 1.384677254))
df_with_mab

#as the samples are timely replicates of the same samples,
#they are paired and not normally distributed as only
#three repetitions were made. As one compares three groups
#with each other Friedman test post-hoc analysis with
#pairwise wilcoxon tests adjusted for multiple testing
#with Benjamini & Hochberg method
friedman.test(y=df_with_mab$Score,
              groups=df_with_mab$Condition,
              blocks=df_with_mab$Measurement)
Overall_result_of_Friedmantest_with_mab<-
        friedman.test(y=df_with_mab$Score,
                  groups=df_with_mab$Condition,
                  blocks=df_with_mab$Measurement)$p.value
```

```
Overall_result_of_Friedmantest_with_mab

pairwise_comparison_with_mab<-
        pairwise.wilcox.test(df_with_mab$Score,
                    df_with_mab$Condition, exact=FALSE,
                    p.adj = "BH")
pairwise_comparison_with_mab

#result overview
results_with_mab<-cbind(
    pairwise_comparison_with_mab[["p.value"]],
    Overall_result_of_Friedmantest_with_mab)
results_with_mab
```

A.2.6 R code for the KIR3DL3 and B7-H7 screen in cell systems analysis

A.2.6.1 R code for the KIR3DL3 expression on NK cells derived from PBMCs analysis

```
##################################################
###### Nils Dominik Lonken
###### Analysis of KIR3DL3 on NK cell subsets
###### Dissertation: The B7 protein family as ligands
###### for KIRs
###### 21.11.2023
##########################################################

rm(list=ls())

#install.packages("FDRestimation")
library("FDRestimation")

##KIR Expression testing
#Statistical significance expression level KIR3DL3 day 0
KIR3DL3_0_Iso<-c(0.43)
KIR3DL3_0_mab<-c(64.4, 42.5, 52.8)
data_KIR3DL3_0<-data.frame(KIR3DL3_0_Iso, KIR3DL3_0_mab)

#as the samples are timely replicates the samples are
#paired and not normally distributed as only three
#repetitions were made--> paired Wilcoxon test
wilcox.test(data_KIR3DL3_0$KIR3DL3_0_Iso,KIR3DL3_0_mab,
```

```
            paired = TRUE, exact = TRUE, correct = TRUE,
            conf.int = TRUE)

#Statistical significance expression level KIR3DL3 day 3
KIR3DL3_3_Iso<-c(0.01)
KIR3DL3_3_mab<-c(22.7, 12.5)
data_KIR3DL3_3<-data.frame(KIR3DL3_3_Iso, KIR3DL3_3_mab)

#as the samples are timely replicates the samples are
#paired and not normally distributed as only three
#repetitions were made--> paired Wilcoxon test
wilcox.test(data_KIR3DL3_3$KIR3DL3_3_Iso,KIR3DL3_3_mab,
            paired = TRUE, exact = TRUE, correct = TRUE,
            conf.int = TRUE)

#Statistical significance expression level KIR3DL3 day 7
KIR3DL3_7_Iso<-c(0.17)
KIR3DL3_7_mab<-c(51.13, 18.33, 62.90)
data_KIR3DL3_7<-data.frame(KIR3DL3_7_Iso, KIR3DL3_7_mab)

#as the samples are timely replicates the samples are
#paired and not normally distributed as only three
#repetitions were made--> paired Wilcoxon test
wilcox.test(data_KIR3DL3_7$KIR3DL3_7_Iso,KIR3DL3_7_mab,
            paired = TRUE, exact = TRUE, correct = TRUE,
            conf.int = TRUE)


##KIR3DL3 in NK cells screen test
#data frame with all values
df <- data.frame(Time_point=rep(c("Day 0", "Day 3", "Day 7"),
                                each=126),
                 Donor = rep(rep(c("Donor 224", "Donor 322",
                                   "Donor 326", "Donor 285",
                                  "Donor 286", "Donor 303"),
                                  each=3), times=21),
                 Condition = rep(rep(c("KIR3DL3",
                 "KIR3DL3/NKp30","KIR3DL3/NKp44",
                 "KIR3DL3/NKp46","KIR3DL3/NKG2A",
                 "KIR3DL3/NKG2C", "KIR3DL3/NKG2D"),
                 each=18), times=3),
                 Measurement = rep(1:3, times=126),
```

```
  Experiment_number= rep(1:18, times=21),
  Score= c(0.07, 0.12, 0.055, 0.81, 0.55,
  0.49, 0.48, 0.62, 0.93, 1.97, 3.03,
  2.03, 1.69, 2.35, 2.63, 0.87, 1.19,
  1.22, 2.31, 2.79, 2.67, 0.72, 0.68,
  0.86, 1.19, 1.71, 1.75, 11.4, 14.2,
  10.8, 9.48, 10.6, 12.4, 6.48, 7.73,
  7.68, 1.54, 1.36, 1.58, 1.66, 1.53,
  1.89, 0.97, 1.3, 1.47, 7.69, 11.1,
  8.35, 3.88, 5.71, 6.44, 2.54, 3.28,
  2.97, 2.17, 2.55, 2.4, 1.28, 1.11,
  1.43, 1.21, 1.45, 1.92, 9.01, 10.2,
  7.34, 6.62, 6.91, 8.79, 3.77, 4.78,
  4.53, 0.35, 0.59, 0.66, 3.39, 3.73,
  4.1, 3.6, 4.72, 7.61, 10.7, 12.4,
  10.2, 7.09, 9.24, 10.9, 4.35, 5.07,
  5.21, 0.7, 1.01, 1.09, 1.29, 1.41,
  1.58, 1.11, 1.92, 2.33, 2.87, 3.42,
  2.55, 1.89, 2.52, 3.33, 1.7, 1.89,
  2.17, 0.21, 0.36, 0.16, 3.99, 5.07,
  5.36, 3.26, 4.13, 6.4, 12.6, 14.2,
  11.1, 8.73, 10.6, 12.2, 5.54, 6.7,
  6.77,
 0.18, 0.17, 0.29, NA, 0.056, 0.047,
 0.063, 0.16, 0.043, 1.62, 1.52, 1.72,
 2.53, 2.74, 2.63, 1.44, 1.22, 1.4,
NA, NA, NA, NA, 2.19, 3.34, 2.5,
 2.81, 3.45, 7.7, 9.12, 9.25, 7.28,
 8.42, 6.79, 6.91, 4.48, 5.94, NA, NA,
NA, NA, 2.15, 2.46, 1.75, 2.18, 2.6,
 4.37, 6.27, 6.06, 4.45, 5.33, 4.2,
 4.71, 2.78, 3.77, NA, NA, NA, NA,
 0.77, 0.99, 1.44, 1.13, 2.05, 6.1,
 6.28, 6.74, 5.89, 6.21, 5.7, 3.41,
 2.3, 3.17, NA, NA, NA, NA, 0.8,
 1.02, 1.28, 1.36, 2.05, 1.83, 3.1,
 3.01, 2.8, 3.32, 2.5, 3.18, 2.05,
 2.7, NA, NA, NA, NA, 0.72, 1.02, 1,
 1.04, 1.79, 1.15, 1.37, 1.7, 1.01,
 1.19, 0.97, 1.94, 1.37, 1.69, NA, NA,
NA, NA, 1.2, 2.02, 1.35, 1.83, 2.3,
 6.86, 6.39, 7.13, 6.07, 6.63, 6.12,
```

```
                    4.18, 2.6, 3.62,
                    0, 0, 0, 0.00387, 0, 0, 0.66, 0.63,
                    0.64, 0.75, 0.75, 0.88, 0.59, 0.44,
                    0.67, 0.37, 0.34, 0.27, 0.018,
                    0.00539, 0.009, 0.00387, 0.014, 0,
                    2.3, 2.16, 2.4, 2.47, 3.83, 2.5,
                    1.73, 1.23, 2.75, 1.98, 2.23, 1.24,
                    0.19, 0.17, 0.2, 0.41, 0.31, 0.47,
                    5.69, 6.27, 6.23, 3.69, 5.17, 3.68,
                    3.68, 3.36, 5.29, 3.07, 3.17, 2.35,
                    0.00447, 0, 0.003, 0.078, 0.027,
                    0.028, 2.68, 2.81, 2.93, 2.38, 3.07,
                    2.46, 2.58, 2.27, 3.83, 1.47, 1.48,
                    1.13, 0.018, 0.011, 0.003, 0, 0, 0,
                    1.74, 1.7, 1.73, 1.78, 2.55, 1.79,
                    1.72, 1.53, 2.68, 1.34, 1.37, 0.85,
                    0.00447, 0.011, 0, 0, 0, 0, 0.88,
                    0.74, 0.8, 0.33, 0.31, 0.38, 0.37,
                    0.32, 0.47, 0.25, 0.24, 0.19, 0, 0,
                    0, 0.012, 0.00467, 0, 2.44, 2.36,
                    2.5, 4.22, 5.16, 4, 3.42, 3.06, 5.02,
                    3.21, 3.02, 2.24))
df


##as the samples are timely replicates of the same samples,
##they are paired and not normally distributed as only
##three repetitions were made.
##As one compares seven groups with each other Friedman test
##Post hoc analysis with pairwise wilcoxon tests adjusted
##for multiple testing with Benjamini & Hochberg method

##test within days whether difference between NK cell
##receptor combinations
##day 0
#get data from original frame
df_day0<-df[df$Time_point=="Day 0",]
df_day0

friedman.test(y=df_day0$Score, groups=df_day0$Condition,
blocks=df_day0$Experiment_number)
Overall_result_of_Friedmantest_df_day0<-
```

```
friedman.test(y=df_day0$Score, groups=df_day0$Condition,
                blocks=df_day0$Experiment_number)$p.value
Overall_result_of_Friedmantest_df_day0

pairwise_comparison_df_day0<-
pairwise.wilcox.test(df_day0$Score, df_day0$Condition,
exact=FALSE, p.adj = "BH")
pairwise_comparison_df_day0

#result overview day 0
results_df_day0<-cbind(
pairwise_comparison_df_day0[["p.value"]],
Overall_result_of_Friedmantest_df_day0)
results_df_day0


##day 3
#get data from original frame
df_day3<-df[df$Time_point=="Day 3",]
df_day3

friedman.test(y=df_day3$Score, groups=df_day3$Condition,
blocks=df_day3$Experiment_number)
Overall_result_of_Friedmantest_df_day3<-
friedman.test(y=df_day3$Score, groups=df_day3$Condition,
blocks=df_day3$Experiment_number)$p.value
Overall_result_of_Friedmantest_df_day3

pairwise_comparison_df_day3<-
pairwise.wilcox.test(df_day3$Score, df_day3$Condition,
exact=FALSE, p.adj = "BH")
pairwise_comparison_df_day3

#result overview day 3
results_df_day3<-cbind(
pairwise_comparison_df_day3[["p.value"]],
Overall_result_of_Friedmantest_df_day3)
results_df_day3


##day 7
#get data from original frame
```

```
df_day7<-df[df$Time_point=="Day 7",]
df_day7

friedman.test(y=df_day7$Score, groups=df_day7$Condition,
blocks=df_day7$Experiment_number)
Overall_result_of_Friedmantest_df_day7<-
friedman.test(y=df_day7$Score,
groups=df_day7$Condition,
blocks=df_day7$Experiment_number)$p.value
Overall_result_of_Friedmantest_df_day7

pairwise_comparison_df_day7<-
pairwise.wilcox.test(df_day7$Score, df_day7$Condition,
exact=FALSE, p.adj = "BH")
pairwise_comparison_df_day7

#result overview day 7
results_df_day7<-cbind(
pairwise_comparison_df_day7[["p.value"]],
Overall_result_of_Friedmantest_df_day7)
results_df_day7

##Test for tendency of downregulation of receptor on
##cell surface
#install.packages("ggplot2")
#installed.packages("ggcorplot")
#install.packages("ggpubr")
library(ggpubr)
library(ggplot2)
library(ggcorrplot)

#scatter plot and linear regression for different receptors
#over time change of days as discrete time points to
#continous data
df_scatter_plot <- df[,-1]
df_scatter_plot <- cbind(
df_scatter_plot,c(rep(c(0, 3, 7),
each=126)))
df_scatter_plot
colnames(df_scatter_plot) <- c(
"Donor", "Condition", "Measurement",
"Experiment_number", "Score", "Day")
```

```
df_scatter_plot

df_scatter_plot_pdf<-ggplot(df_scatter_plot,
aes(x=Day, y=Score, shape=Condition, color=Condition)) +
  geom_point() + ylab("Frequency of parent [%]") +
  xlab("Days after isolation")+
  scale_x_continuous(breaks=seq(0,7,1))+
  geom_smooth(aes(x = as.numeric(Day), y = Score,
  fill=Condition), method = "lm", formula = y~x)+
  scale_shape_manual(values=c(1:7)) +
  scale_color_brewer(palette="Dark2") +
  ggtitle("KIR3DL3 expression on NK cells
            derived from PBMCs") +
  theme_classic() +
  guides(color=guide_legend(override.aes=list(fill=NA))) +
  theme(plot.title = element_text(lineheight=.8,
  face="bold", hjust=0.5),
        axis.title = element_text(face="bold"))+
  stat_regline_equation(label.x =
  c(4.5,4.5,4.5,4.5,4.5,4.5,4.5),
                        label.y =
  c(12,13.5,15, 16.5, 18, 19.5, 21),
    aes(label =  paste(..eq.label.., ..adj.rr.label..,
    sep = "~~~~")), formula=y~x,size=3)
df_scatter_plot_pdf
```

A.2.6.2 R code for the KIR3DL3 expression on $\gamma\delta$, CD4 and CD8 T cells analysis

```
##################################################
###### Nils Dominik Lonken
###### Analysis of KIR3DL3 on T cell subsets
###### Dissertation: The B7 protein family as ligands
###### for KIRs
###### 21.11.2023
##################################################

rm(list=ls())

#install.packages("FDRestimation")
library("FDRestimation")

##KIR Expression testing
```

```
#Statistical significance expression level KIR3DL3
KIR3DL3_Iso<-c(NA,NA,NA,2.17,NA,NA, 4.83,NA,NA)
KIR3DL3_mab<-c(54.9, 72.3, 16.7, 1.2, 1.34, 1.31,
                3.65, 4.2, 2.92)
data_KIR3DL3<-data.frame(KIR3DL3_Iso, KIR3DL3_mab)

#as the samples are timely replicates the samples are paired
#and not normally distributed as only three repetitions
#were made--> paired Wilcoxon test
wilcox.test(data_KIR3DL3$KIR3DL3_Iso,KIR3DL3_mab,
            paired = TRUE, exact = TRUE,
            correct = TRUE, conf.int = TRUE)

##KIR3DL3 in T cells screen test
#data frame with all values
df <- data.frame(Condition= rep(c("Isotype", "KIR3DL3",
                "KIR3DL3", "KIR3DL3"),times=27),
                 Donor = rep(rep(c("Donor 101",
                 "Donor 108","Donor 195", "Donor 218",
                 "Donor 224", "Donor 248", "Donor 262",
                 "Donor 322", "Donor 326"),
                                 each=12)),
                 Subpopulation = rep(rep(c("CD4", "CD8",
                 "Gamma Delta"), each=4),
                 times=9),
                 Measurment= rep(1:4, times=27),
                 Score= c(1.24, 1.64, 0.98, 1.63,
                          2.56, 2.96, 2.13, 5.36,
                          4.62, 11.1, 0, 0,

                          0.82, 0.56, 0.48, 0.75,
                          5.36, 2.88, 1.68, 4.23,
                          27.3, 25, 0, 0,

                          0.38, 2.02, 3.37, 1.23,
                          0.63, 3.8, 6.68, 4.54,
                          33.3, 33.3, 100, 80,

                          0.00997, 2.9, 2.79, 1.45,
                          0.075, 1.39, 0.38, 3.47,
                          17, 49.5, 78.8, 47.9,
```

```
                                3.63, 0.25, 0.03, 0.18,
                                1.22, 0.67, 0.53, 0.53,
                                0, 0, 0, 7.32,

                                0.033, 0.51, 0.4, 0.47,
                                0.042, 1.01, 0.87, 0.65,
                                33.9, 45.4, 55, 45,

                                0.018, 1.01, 1.51, 1.04,
                                0.031, 1.28, 1.54, 1.22,
                                7.11, 30.2, 40.3, 28.9,

                                0.7, 0.17, 0.04, 0.13,
                                1.37, 0.36, 0.09, 0.18,
                                0, 0, 0, 0,

                                0.17, 0.43, 1.04, 0.29,
                                0.36, 0.43, 0.3, 0.24,
                                0, 0, 0, 0))
df


##test within population difference between T cell and
##isotype control
##Analysis of CD4
df_CD4<-df[df$Subpopulation=="CD4",]
df_CD4

CD4_Iso<-c(1.24, 0.82, 0.38, 0.00997, 3.63, 0.033, 0.018,
           0.7, 0.17)
CD4_mab<-c(1.64, 0.98, 1.63, 0.56, 0.48, 0.75, 2.02, 3.37,
           1.23, 2.9, 2.79, 1.45, 0.25, 0.03, 0.18, 0.51,
           0.4, 0.47, 1.01, 1.51, 1.04, 0.17, 0.04, 0.13,
           0.43, 1.04, 0.29)

#not paired as each value comes from other biological
#individual not normally distributed as only nine
#repetitions were made--> Wilcoxon test

wilcox.test(CD4_Iso,CD4_mab, paired = FALSE, exact = FALSE,
           correct = TRUE, conf.int = TRUE)
```

```
##Analysis of CD8
df_CD8<-df[df$Subpopulation=="CD8",]
df_CD8

CD8_Iso<-c(2.56, 5.36, 0.63, 0.075, 1.22, 0.042, 0.031,
           1.37, 0.36)
CD8_mab<-c(2.96, 2.13, 5.36, 2.88, 1.68, 4.23, 3.8,
           6.68, 4.54, 1.39, 0.38, 3.47, 0.67, 0.53,
           0.53, 1.01, 0.87, 0.65, 1.28, 1.54, 1.22,
           0.36, 0.09, 0.18, 0.43, 0.3, 0.24)

#not paired as each value comes from other biological
#individual not normally distributed as only nine
#repetitions were made--> Wilcoxon test

wilcox.test(CD8_Iso,CD8_mab, paired = FALSE, exact = FALSE,
           correct = TRUE, conf.int = TRUE)


##Analysis of Gamma Delta
df_gammadelta<-df[df$Subpopulation=="Gammadelta",]
df_gammadelta

gammadelta_Iso<-c(4.62, 27.3, 33.3, 17, 0, 33.9, 7.11, 0, 0)
gammadelta_mab<-c(11.1, 0, 0, 25, 0, 0, 33.3, 100, 80, 49.5,
                  78.8, 47.9, 0, 0, 7.32, 45.4, 55, 45,
                  30.2, 40.3, 28.9, 0, 0, 0, 0, 0, 0)

#not paired as each value comes from other biological
#individual not normally distributed as only nine
#repetitions were made--> Wilcoxon test

wilcox.test(gammadelta_Iso,gammadelta_mab, paired = FALSE,
           exact = FALSE, correct = TRUE,
           conf.int = TRUE)
```

A.2.6.3 R code for the B7-H7 expression on monocytes/macrophages and B cells analysis

```
#####################################################
####### Nils Dominik Lonken
####### Analysis of B7-H7 on PBMCs
```

```
###### Dissertation: The B7 protein family as ligands
###### for KIRs
###### 27.01.2027
#############################################################

rm(list=ls())

#install.packages("FDRestimation")
library("FDRestimation")

##B7-H7 Expression testing monocytes/macrophages
#Statistical significance expression level B7-H7
B7_H7_Iso_Mono<-c(0, NA, NA, 0, NA, NA, 3.40, NA, NA,
                  6.23, NA, NA)
B7_H7_mab_Mono<-c(28.10, 12.00, 19.80, 29.60, 9.89, 6.28,
                  18.80, 13.30, 19.80, 35.30, 30.00, 38.50)
data_B7_H7_Mono<-data.frame(B7_H7_Iso_Mono, B7_H7_mab_Mono)

#as the samples are timely replicates the samples are paired
#and not normally distributed as only three repetitions
#were made--> paired Wilcoxon test
wilcox.test(data_B7_H7_Mono$B7_H7_Iso_Mono,B7_H7_mab_Mono,
            paired = FALSE, exact = TRUE,
            correct = TRUE, conf.int = TRUE)

##B7-H7 Expression testing B Cells
#Statistical significance expression level B7-H7
B7_H7_Iso_bcell<-c(96.6, NA, NA, 96.6, NA, NA, 0, NA, NA,
                   0, NA, NA)
B7_H7_mab_bcell<-c(3.58, 0, 2.07, 1.14, 1.09, 0.51, 0.25,
                   0, 0.28, 0, 0.65, 0.76)
data_B7_H7_bcell<-data.frame(B7_H7_Iso_bcell,
                             B7_H7_mab_bcell)

#as the samples are timely replicates the samples are paired
#and not normally distributed as only three repetitions
#were made--> paired Wilcoxon test
wilcox.test(data_B7_H7_bcell$B7_H7_Iso_bcell,
            B7_H7_mab_bcell,
            paired = FALSE, exact = TRUE,
            correct = TRUE, conf.int = TRUE)
```

A.2.6.4 R code for the KIR3DL3 and B7-H7 expression on adult IEL gut samples analysis

```
#########################################################
###### Nils Dominik Lonken
###### Analysis of KIR3DL3 and B7-H7 on gut samples
###### Dissertation: The B7 protein family as ligands
###### for KIRs
###### 21.11.2023
#########################################################

rm(list=ls())

#install.packages("FDRestimation")
library("FDRestimation")

##KIR Expression testing
#Statistical significance expression level KIR3DL3
KIR3DL3_Iso<-c(7.87,NA,NA, 29.6,NA,NA)
KIR3DL3_mab<-c(9.30, 13.60,      8.92, 30.10, 37.20, 30.50)
data_KIR3DL3<-data.frame(KIR3DL3_Iso, KIR3DL3_mab)

#as the samples are timely replicates the samples are paired
#and not normally distributed as only three repetitions were
#made--> paired Wilcoxon test
wilcox.test(data_KIR3DL3$KIR3DL3_Iso,KIR3DL3_mab,
            paired = TRUE, exact = TRUE,
            correct = TRUE, conf.int = TRUE)



##B7-H7 Expression testing
#Statistical significance expression level B7-H7
B7_H7_Iso<-c(0, NA, NA, 0.41, NA, NA, 4.28, NA, NA)
B7_H7_mab<-c(96.30, 96.40, NA, 89.70, 89.30, 92.60,
             52.00, 58.00, 65.00)
data_B7_H7<-data.frame(B7_H7_Iso, B7_H7_mab)

#as the samples are timely replicates the samples are paired
#and not normally distributed as only three repetitions were
#made--> paired Wilcoxon test
wilcox.test(data_B7_H7$B7_H7_Iso,B7_H7_mab, paired = TRUE,
            exact = TRUE, correct = TRUE, conf.int = TRUE)
```

```
############################
##KIR3DL3 in gut samples test compared to isotype control

##Analysis of CD4
CD4_KIR3DL3_Iso<-c(57.6, 13.3, 1.48, 13.4, 0, 0, 0)
CD4_KIR3DL3_mab<-c(31.1, 29.6, 23.7, 27.3, 36.4, 11.8,
                   10.3, 6.47, 15.5, 7.76, 11.6, 6.49,
                   0, 0, 0, 6.45, 0, 5.88, 0, 20, 0)

#not paired as each value comes from other biological
#individual not normally distributed as only seven
#repetitions were made--> Wilcoxon test

wilcox.test(CD4_KIR3DL3_Iso,CD4_KIR3DL3_mab,
            paired = FALSE, exact = FALSE,
            correct = TRUE, conf.int = TRUE)


##Analysis of CD8
CD8_KIR3DL3_Iso<-c(10, 6.67, 1.09, 11.6, 0, 0.17, 0.02)
CD8_KIR3DL3_mab<-c(33.3, 50, 33.3, 13.8, 21.90, 11.9, 9.24,
                   8.63, 13.9, 11.6, 13.6, 11.1, 0.88, 0.79,
                   7.93, 9.07, 7.55, 9.29, 2.68, 2.51, 2.21)

#not paired as each value comes from other biological
#individual not normally distributed as only seven
#repetitions were made--> Wilcoxon test

wilcox.test(CD8_KIR3DL3_Iso,CD8_KIR3DL3_mab,
            paired = FALSE, exact = FALSE,
            correct = TRUE, conf.int = TRUE)


##Analysis of Epithelial cells
Epithelial_KIR3DL3_Iso<-c(38.6, 8.27, 12, 27.3, 0, 13.9, 0.18)
Epithelial_KIR3DL3_mab<-c(19.5, 20.3, 19.2, 38.6, 42, 22.1,
                          29.3, 20.4, 34.3, 37.6, 40.1,
                          23.8, 3.77, 3.33, 17.7, 14.9,
                          15, 15, 6.61, 24.8, 5.17)

#not paired as each value comes from other biological
```

```
#individual not normally distributed as only seven
#repetitions were made--> Wilcoxon test

wilcox.test(Epithelial_KIR3DL3_Iso,Epithelial_KIR3DL3_mab,
            paired = FALSE, exact = FALSE,
            correct = TRUE, conf.int = TRUE)

##Analysis of NK cells
NK_KIR3DL3_Iso<-c(42.8, 15.9, 24.2, 42.6, 0, 17.6, 0.78)
NK_KIR3DL3_mab<-c(7.35, 5.79, 7.36, 59.1, 66.6, 27.3, 45.7,
                  35, 46.4, 50.5, 48.9, 26.6, 9.40, 7.85,
                  35.6, 25.3, 24.1, 25.5, 19.8, 35.0,
                  15.4)

#not paired as each value comes from other biological
#individual not normally distributed as only seven
#repetitions were made--> Wilcoxon test

wilcox.test(NK_KIR3DL3_Iso,NK_KIR3DL3_mab,
            paired = FALSE, exact = FALSE,
            correct = TRUE, conf.int = TRUE)



############################
##B7-H7 in gut samples test compared to isotype control

##Analysis of CD4
CD4_B7_H7_Iso<-c(39.1, 13, 0.99, 8.28, 0, 0, 0)
CD4_B7_H7_mab<-c(85.6, 81.6, 89.8, 9.09, 15.2, 11.8, 1.24,
                 1.26, 1.56, 2.16, 4.13, 3.9, 0, 0, 0,
                 0, 0, 0, 0, 0, 0)

#not paired as each value comes from other biological
#individual not normally distributed as only seven
#repetitions were made--> Wilcoxon test

wilcox.test(CD4_B7_H7_Iso,CD4_B7_H7_mab,
            paired = FALSE, exact = FALSE,
            correct = TRUE, conf.int = TRUE)
```

```
##Analysis of CD8
CD8_B7_H7_Iso<-c(0, 4.17, 0.39, 14.1, 0, 0, 0.01)
CD8_B7_H7_mab<-c(0, 60, 66.7, 17.2, 9.38, 1.49, 0.45, 0.65,
                 0.98, 5.34, 6.01, 2.96, 0, 0, 1.02,
                 0.07, 0, 0, 0.02, 0.06, 0.01)

#not paired as each value comes from other biological
#individual not normally distributed as only seven
#repetitions were made--> Wilcoxon test

wilcox.test(CD8_B7_H7_Iso,CD8_B7_H7_mab,
            paired = FALSE, exact = FALSE,
            correct = TRUE, conf.int = TRUE)

##Analysis of Epithelial cells
Epithelial_B7_H7_Iso<-c(13.9, 19.5, 8.23, 39.2, 0, 0, 0.15)
Epithelial_B7_H7_mab<-c(65.1, 64.9, 72.5, 22, 29.7, 21.6,
                        18.4, 21.9, 21.7, 27.9, 31.8,
                        28.8, 0.44, 0.58, 0.17, 0.02, 0.02,
                        0.0000948, 0.24, 0.31, 0.12)

#not paired as each value comes from other biological
#individual not normally distributed as only seven
#repetitions were made--> Wilcoxon test

wilcox.test(Epithelial_B7_H7_Iso,Epithelial_B7_H7_mab,
            paired = FALSE, exact = FALSE,
            correct = TRUE, conf.int = TRUE)

##Analysis of NK cells
NK_B7_H7_Iso<-c(17.1, 24, 12.3, 58.8, 0, 0.02, 0.72)
NK_B7_H7_mab<-c(35.4, 39.8, 39.9, 27.8, 41.7, 30.4, 25.2,
                30.3, 30.4, 44.8, 46.2, 39.4, 1.50, 0.65,
                0.93, 0.05, 0.03, 0.04, 0.85, 0.62, 0.70)

#not paired as each value comes from other biological
#individual not normally distributed as only seven
#repetitions were made--> Wilcoxon test

wilcox.test(NK_B7_H7_Iso,NK_B7_H7_mab,
            paired = FALSE, exact = FALSE,
            correct = TRUE, conf.int = TRUE)
```